

# Mechanically flexible crystals of cadmium(II) coordination polymers

---

Pisačić, Mateja

Doctoral thesis / Disertacija

2022

*Degree Grantor / Ustanova koja je dodijelila akademski / stručni stupanj:* **University of Zagreb, Faculty of Science / Sveučilište u Zagrebu, Prirodoslovno-matematički fakultet**

*Permanent link / Trajna poveznica:* <https://urn.nsk.hr/urn:nbn:hr:217:204762>

*Rights / Prava:* [In copyright](#) / [Zaštićeno autorskim pravom.](#)

*Download date / Datum preuzimanja:* **2024-04-25**



*Repository / Repozitorij:*

[Repository of the Faculty of Science - University of Zagreb](#)





University of Zagreb  
FACULTY OF SCIENCE

Mateja Pisačić

**MECHANICALLY FLEXIBLE CRYSTALS  
OF CADMIUM(II) COORDINATION  
POLYMERS**

DOCTORAL THESIS

Supervisor:  
Assoc. Prof. Marijana Đaković

Zagreb, 2022



Sveučilište u Zagrebu  
PRIRODOSLOVNO-MATEMATIČKI FAKULTET

Mateja Pisačić

**KRISTALI KOORDINACIJSKIH POLIMERA  
KADMIJA(II) S MEHANIČKI POTAKNUTIM  
FLEKSIBILNIM ODZIVOM**

DOKTORSKI RAD

Mentor:  
Izv. prof. dr. sc. Marijana Đaković

Zagreb, 2022.

This doctoral thesis was made at the University of Zagreb, Faculty of Science, Department of Chemistry, under the supervision of Marijana Đaković, Associate Professor, as a part of the Doctoral Program in Chemistry at the University of Zagreb, Faculty of Science, Department of Chemistry.

This doctoral thesis has been fully supported by the Croatian Science Foundation under project “From form to function: Mechanically flexible crystalline materials with controllable responses“ (IP-2019-04-1242).



## Acknowledgements

*I am grateful to my dear mentor Assoc. Prof. Marijana Đaković, for giving me the opportunity to join her group and enter the exciting world of crystallography. I am thankful for all the help, guidance, kind words and encouragement she provided, for believing in me even when I did not, for numerous opportunities to learn, and all the challenges she put in front of me which enabled my personal and professional growth. **Thank you!***

*I am thankful to reviewers, Prof. Biserka Prugovečki, Prof. Davor Kovačević and Dr. Ana Šantić for their effort, time and all the help.*

*I also thank Assoc. Prof. Ivana Biljan who helped me to perform AFM measurements and Assist. Prof. Ivan Kodrin for performing calculations, which upgraded this work to a higher level. I am grateful for the friendship, conversations, and support they are constantly providing.*

*I am thankful to Prof. Željka Soldin for always providing rational solutions and for every kind word.*

*I would like to thank my dear Barbara for being a true friend from the very first moment we met, for always giving her honest opinion, for convincing me to do fun things, for all the help, laughter and priceless memories. B, thank you for always being by my side.*

*I am thankful to Mladen for all the answers to a million questions I asked, comforting words, hilarious comments and for always being there and keeping my back.*

*To Ozana, for all the positive energy she brought to our group. Most of all, I am thankful for all the patience, understanding, and for always selflessly offering help and stepping in when it was needed the most.*

*To Marko, for all our conversations, jokes and good mood which made our lab work fun, and, most importantly, for his amazing ability to crystallize almost anything.*

*To Philipp, who taught me it is important to be thankful for little things in life. I am very much grateful for knowing him, for all the support and kindness he gives me although he is far away.*

*To my dear friends, Ana, Petra, Marija, Snježana, Patricija, Nikolina, Ivana, Katarina, Darko, Marta, Helena, Michele, and all the other friends and colleagues, for many fruitful discussions and priceless memories.*

*To my dear friend Ana, who is like a sister to me. I am extremely happy to have her in my life.*

*And at the end, I am deeply indebted to my family for their unconditional love which was a real wind in the back during this all time. Especially to my dear parents Marijanka and Siniša, for being there for me at any time, for caring, helping and patiently supporting me in every step.*

*To my sisters Vjera and Maja, for always being my best friends, my reality check and for knowing that I can always count on them.*

*I am extremely grateful for my little sunshine, nephew Leonardo, who keeps filling my days with joy.*

*I am grateful to my grandparents for every kind word that went directly from their loving hearts, for every warm look, comforting hug, and for always being my greatest support.*

## Contents

<b>ABSTRACT .....</b>	<b>VII</b>
<b>SAŽETAK.....</b>	<b>VIII</b>
<b>§ 1. INTRODUCTION .....</b>	<b>9</b>
1.1. Dynamic effects in crystalline materials .....	10
1.2. Photosalient and thermosalient crystals .....	11
1.3. Mechanically induced dynamic behaviour .....	13
1.3.1. Mechanically deformable organic molecular crystals .....	15
1.3.1.1. Plastic responses .....	15
1.3.1.2. Elastic responses .....	18
1.3.1.1. Superelasticity, ferroelasticity, superplasticity .....	20
1.3.2. Mechanically bendable metal-organic molecular crystals .....	22
1.4. Perspectives on application of adaptable molecular crystals.....	28
1.5. Hypothesis and objectives of the research .....	30
<b>§ 2. SCIENTIFIC PAPERS.....</b>	<b>31</b>
Scientific article I .....	32
Scientific article II.....	42
Scientific article III .....	53
<b>§ 3. DISCUSSION .....</b>	<b>64</b>
3.1. One-dimensional coordination polymers with ligands bearing halogen functionalities for targeting the flexible response .....	66
3.2. Modulating the crystalline mechanical responses through cyano functionality .....	82
<b>§ 4. CONCLUSIONS AND OUTLOOK.....</b>	<b>92</b>
<b>§ 5. LIST OF ABBREVIATIONS AND SYMBOLS.....</b>	<b>95</b>
<b>§ 6. REFERENCES.....</b>	<b>96</b>
<b>§ 7. CURRICULUM VITAE.....</b>	<b>IX</b>
<b>PROŠIRENI SAŽETAK.....</b>	<b>XVI</b>



University of Zagreb  
Faculty of Science  
**Department of Chemistry**

Doctoral Thesis

## ABSTRACT

### MECHANICALLY FLEXIBLE CRYSTALS OF CADMIUM(II) COORDINATION POLYMERS

Mateja Pisačić  
Horvatovac 102a, 10 000 Zagreb, Croatia

Mechanically responsive crystals have recently attracted the attention of a wide scientific community, but the origin of this remarkable crystal behaviour is still unclear. This thesis provides a systematic study of mechanically induced crystal flexibility on a series of one-dimensional crystalline cadmium(II) coordination polymers, which provided a valuable dataset of different structural architectures, morphologies, and an unexpectedly wide range of variable mechanical responses. A detailed and systematic correlation of the structural features and mechanical responses using advanced experimental and computational methods, provided a deeper insight into the origin and mechanism of mechanically induced flexibility. It was shown that the relative strength and directionality of intermolecular interactions are one of the key parameters in delivering a specific mechanical response. Thorough research emphasized further importance of the direction-dependent responses, and obtained results provided a fruitful avenue of potential practical applications.

(94 pages, 28 figures, 2 tables, 102 references, original in English)

Thesis deposited in Central Chemical Library, Horvatovac 102a, Zagreb, Croatia and National and University Library, Hrvatske bratske zajednice 4, Zagreb, Croatia.

Keywords: coordination polymers / flexible crystals / intermolecular interactions / mechanically induced response

Supervisor: Dr. Marijana Đaković, Associate Professor, Faculty of Science, Zagreb

Thesis accepted: November 2<sup>nd</sup>, 2022

Reviewers:

1. Dr. Biserka Prugovečki, Full Professor, Faculty of Science, Zagreb
2. Dr. Davor Kovačević, Full Professor, Faculty of Science, Zagreb
3. Dr. Ana Šantić, Senior Research Associate, Ruđer Bošković Institute, Zagreb



Sveučilište u Zagrebu  
Prirodoslovno-matematički fakultet  
**Kemijski odsjek**

Doktorski rad

## SAŽETAK

### KRISTALI KOORDINACIJSKIH POLIMERA KADMIJA(II) S MEHANIČKI POTAKNUTIM FLEKSIBILNIM ODZIVOM

Mateja Pisačić  
Horvatovac 102a, 10 000 Zagreb, Hrvatska

Iako su u posljednje vrijeme kristali s mehaničkim odzivom privukli znatnu pažnju šire znanstvene zajednice, još uvijek nije jasno koje je strukturno porijeklo ovog izvanrednog ponašanja kristala. U okviru ovog doktorskog rada provedeno je sustavno istraživanje mehanički inducirane fleksibilnosti kristala na nizu jednodimenzijskih koordinacijskih polimera kadmija(II), koji su pružili mnoštvo različitih strukturnih arhitektura, morfologija i neočekivano širok raspon raznovrsnih mehaničkih odgovora. Detaljna i sustavna korelacija strukturnih značajki i mehaničkih odziva, korištenjem naprednih eksperimentalnih i računalnih metoda, omogućila je dublji uvid u podrijetlo i mehanizam mehanički izazvane fleksibilnosti. Utvrđeno je da su relativna jakost i usmjerenost međumolekulskih interakcija jedan od ključnih parametara koji određuju vrstu i stupanj mehaničkog odgovora. Rezultati provedenog istraživanja naglasili su važnost smjera primjene mehaničke sile u ostvarivanju specifičnih odgovora kristala, čime je istaknut širok spektar potencijalne primjene kristala u dizajnu novih, naprednih materijala.

(94 stranice, 28 slika, 2 tablice, 102 literaturna navoda, jezik izvornika: engleski)

Rad je pohranjen u Središnjoj kemijskoj knjižnici, Horvatovac 102a, Zagreb i Nacionalnoj i sveučilišnoj knjižnici, Hrvatske bratske zajednice 4, Zagreb.

Ključne riječi: fleksibilni kristali / koordinacijski polimeri / međumolekulske interakcije / mehanički potaknut odziv

Mentor: izv. prof. dr. sc. Marijana Đaković, PMF, Zagreb

Rad prihvaćen: 2. studenoga 2022.

Ocjenitelji:

1. prof. dr. sc. Biserka Prugovečki, PMF, Zagreb
2. prof. dr. sc. Davor Kovačević, PMF, Zagreb
3. dr. sc. Ana Šantić, v. zn. sur., IRB, Zagreb

## § 1. INTRODUCTION

*“A material is a crystal if it has an essentially sharp diffraction pattern.*

*A solid is a crystal if its atoms, ions, and/or molecules form, on average, a long-range ordered arrangement.”<sup>1</sup>*

Although being highly ordered and widely investigated for a long time, crystalline solids have been mostly neglected as a material of choice when it comes to practical application due to their unflattering mechanical properties. Most of all, being commonly perceived as static, hard, severely fragile, and prone to breakage upon application of even the smallest mechanical stress, crystals were often compared to a chemical cemetery. However, that perception started to dramatically change during the past few decades, with the serendipitous finding of crystals capable of performing a plethora of different dynamic movements such as jumping, bending, crawling, and even exploding when subjected to external thermal, light or mechanical stimuli.<sup>2,3</sup>

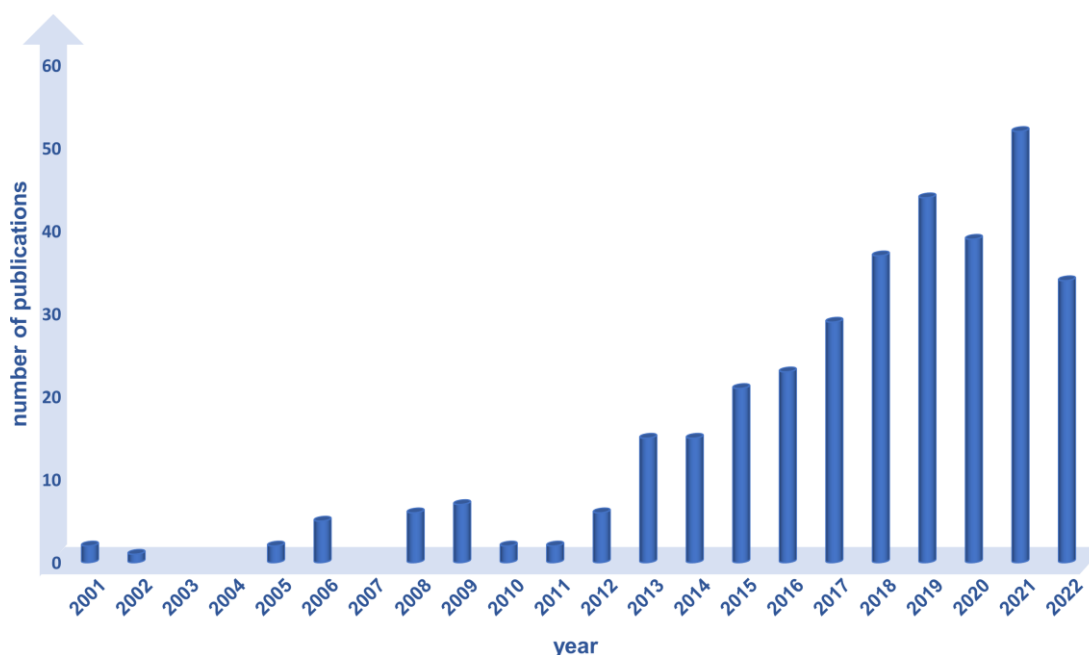


**Figure 1.** The number of published papers describing mechanically responsive crystals, according to Web of Science (September 20<sup>th</sup>, 2022).

Since the first literature report on the stimuli-induced dynamic behaviour of crystals, the growing interest of the scientific community in a new subfield of the solid-state chemistry was

observed, which was reflected in a substantial increase in the number of published papers on this phenomenon (Figure 1). This relatively newly observed property of crystals overcame the obstacle of crystals not being compliant and thus provided a whole new avenue of crystals' potential yet to be discovered. However, to get to the point where mechanically bendable crystals will become a material of choice, a thorough structure–mechanical property correlation must be made (Figure 2), as the underlying structural features that enable this amazing mechanical behaviour are still not clear.

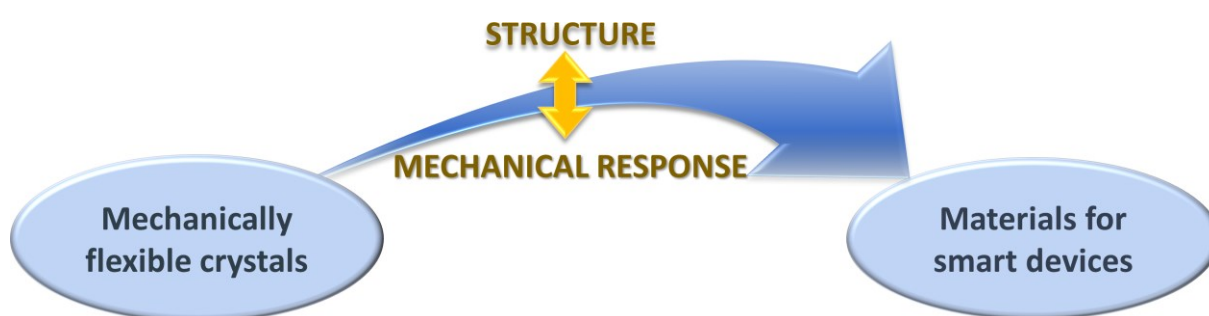


**Figure 2.** The importance of structure–mechanical response correlation for considering mechanically compliant crystals as materials for their implementation in smart devices.

### 1.1. Dynamic effects in crystalline materials

The discovery of unusual mechanical properties of crystals has encouraged scientists worldwide to study these systems in detail what consequently stimulated development of a new research direction in materials science – crystal adaptronics.<sup>4</sup> When exposed to the external stimuli such as heat, light or mechanical force, crystals can display dynamic effects which can be either slow, such as bending, twisting, curling, elongation, contraction, or crawling, or fast and abrupt which are frequently manifested as crystal jumping, flipping, fragmenting, and even exploding (Figure 3).<sup>2,3</sup> During the application of the stimuli, different types of processes take part in the crystal which consequently stimulates the development of stress in the crystal. It was found that the main determinator of a certain type of the macroscopic event is the stress accumulation period. If the stress is released immediately after, or almost simultaneously with the stimuli application (i.e., the stress accumulation period is short), slow and controlled, reversible, or

irreversible deformation happens. On the other hand, long stress accumulation period leads to a sudden release of a large amount of energy, which is often followed by crystal disintegration.

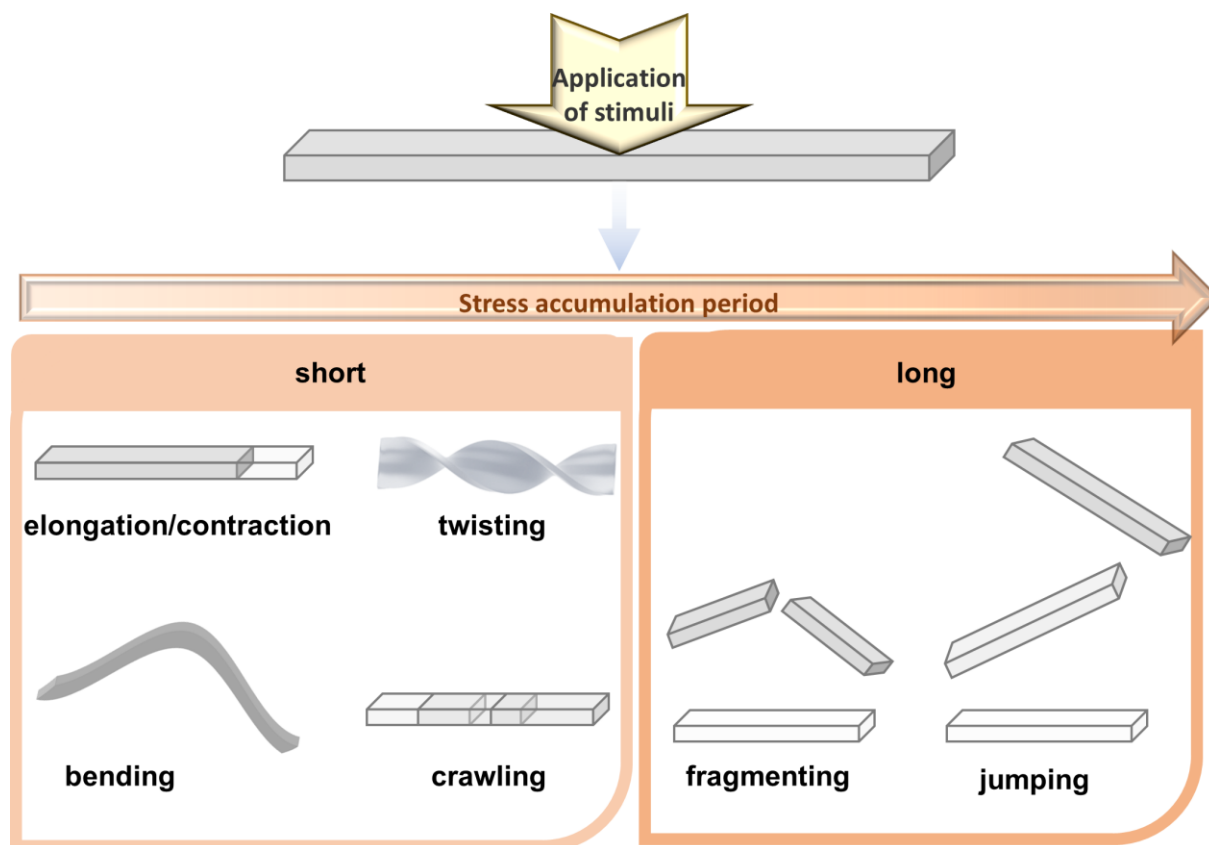


**Figure 3.** Types of the observed macroscopic crystal responses according to the stress accumulation time.

## 1.2. Photosalient and thermosalient crystals

The first examples of crystals with dynamic properties emerged about 50 years ago.<sup>56</sup> Since then, this research topic has moved to the forefront of research in the solid-state chemistry, already delivering some conclusions about the origin of the dynamic behaviour. When illuminated, or exposed to a temperature change, crystals undergo structural transformation because of the stimuli initiated chemical reactions or phase transformations in the crystal. The non-uniform distribution of a daughter (product) phase in a mother crystal (usually from the part of the crystal where the illumination started) causes the development of the stress and strain inside the crystal. The relaxation of the stress can be either slow or fast, leading to diverse macroscopically observed phenomena.<sup>2</sup>



These impressive capabilities of converting light or heat into mechanical work were reported for a number of organic, metal-organic, and inorganic crystalline compounds. Most of the responsive molecular crystals were found to undergo different kinds of isomerization,<sup>7–10</sup> dimerization,<sup>11,12</sup> cycloadditions,<sup>13</sup> phase transformations,<sup>17</sup> etc. which facilitated the dynamic behaviour.

Azo- and imine compounds were found to be of particular interest for investigating these phenomena since the *cis*–*trans* isomerization causes severe structural perturbations on a molecular level, which consequently manifest macroscopically with impressive movements. There are plenty of examples of crystalline compounds containing these functionalities that display reversible and irreversible bending movements when exposed to light and heat.<sup>7–10</sup> One particularly interesting example is the light-induced crawling of the 3,3'-dimethylazobenzene crystals on the glass surface. When simultaneously exposed to the ultraviolet (365 nm) and visible (465 nm) light from different directions (used wavelengths correspond to the wavelengths that induce *trans*→*cis* and *cis*→*trans* isomerization, respectively), crystals display amoeboid directional movement from UV towards the VIS light.<sup>14</sup> Light-induced conversion between *cis* and *trans* isomers, followed by melting and crystallization, respectively, is the main driving force of the observed creeping motion.

One of the most studied cases of a photoreactive metal-containing crystalline matter are the crystals of a cobalt(III) complex, [Co(NH<sub>3</sub>)<sub>5</sub>(NO<sub>2</sub>)](Cl)(NO<sub>3</sub>), which show a variety of different mechanical motions. If crystallized as thin needles, and exposed to UV light, crystals bend, because of the nitro to nitrito isomerization.<sup>15</sup> However, their original shape can be recovered completely with thermal treatment which induces the reversible reaction (i.e., nitrito to nitro re-isomerization). These bending processes were recently also quantified by experimental determining of the produced bending strain in a crystal and compared with a mathematical model.<sup>16</sup> On the other hand, if crystallized in a block-like morphology, crystals do not bend upon irradiation with a moderately strong UV light but display a rather more dramatic mechanical effect: they hop vigorously, propel, or dislocate on the base. Moreover, by increasing the excitation power, the mechanical effects become even more violent with crystal fragmentation and even explosion.

The amazing jumping of crystals can also be achieved with a thermal stimulus, which is shown on an example of the anticholinergic agent, oxitropium bromide.<sup>17</sup> While heating the crystals, a highly anisotropic change in the cell volume is observed which is accompanied by a

conformational change of the oxitropium cation, which is the reason behind the severe crystal jumping motion.

Even though still being relatively rarely found, crystals showing multi-stimuli dynamic behaviour emerged, therefore providing the avenue for the potential development of multistimuli-receptive actuators.<sup>18,19</sup> One of the most recent examples of the multisalient crystal's behaviour is the crystal of Pb(II) one-dimensional polymer,  $[\text{Pb}(\text{SCN})_2(2\text{F-spy})_2]$  (2F-spy = 2-fluoro-4'-styrylpyridine), which shows the ability to concurrently respond to light, heat and mechanical force. Although it is known that the jumping events are facilitated by  $[2 + 2]$  cycloaddition of photoreactive ligands, and macroscopic jumping, bending, and splitting of the crystals were observed during both heating and cooling cycles because of reversible phase transition, it is not quite clear which structural features enable mechanically induced bending.

### 1.3. Mechanically induced dynamic behaviour

Recently, it has been observed that molecular crystals can adapt even to the application of pure mechanical force, therefore showing a resemblance to the behaviour of soft matter. As opposed to the thermosalient and photosalient crystals, for which it is known that chemical reactions or phase transformations facilitate dynamic behaviour, it is not yet clear which structural features enable the mechanically induced flexible responses. However, most of the mechanically responsive molecular crystals are of organic composition and possess a 'short' crystallographic axis which consequently determines them to be mostly found in an elongated morphology, i.e. needle-like shapes.

Moreover, several types of mechanically induced responses can be observed (Figure 4). While some compliant crystals adapt by showing the reversible deformation, i.e., deform upon stress application and regain their original shape once the force is removed, others remain irreversibly deformed even after the removal of the mechanical force, with the latter deformation being the dominant one observed amongst organic molecular crystals. Irreversibly deformable crystals could further be divided into two subgroups, crystals displaying shearing deformation and ferroelasticity, and those being plastically bendable, while reversibly deformable crystals can display elastic bending and superelastic deformation. Superelasticity and ferroelasticity are special types of deformation where a crystal deforms when being exposed to mechanical stress, with a deformation resembling shearing, however crystals can regain their

initial, undeformed shape, either by removing the impact of the mechanical force, or by applying the mechanical stress in opposite direction. During the superelastic and ferroelastic response, crystals undergo either phase transformation or twinning, therefore clearly differentiating these phenomena from the other mechanically induced responses.

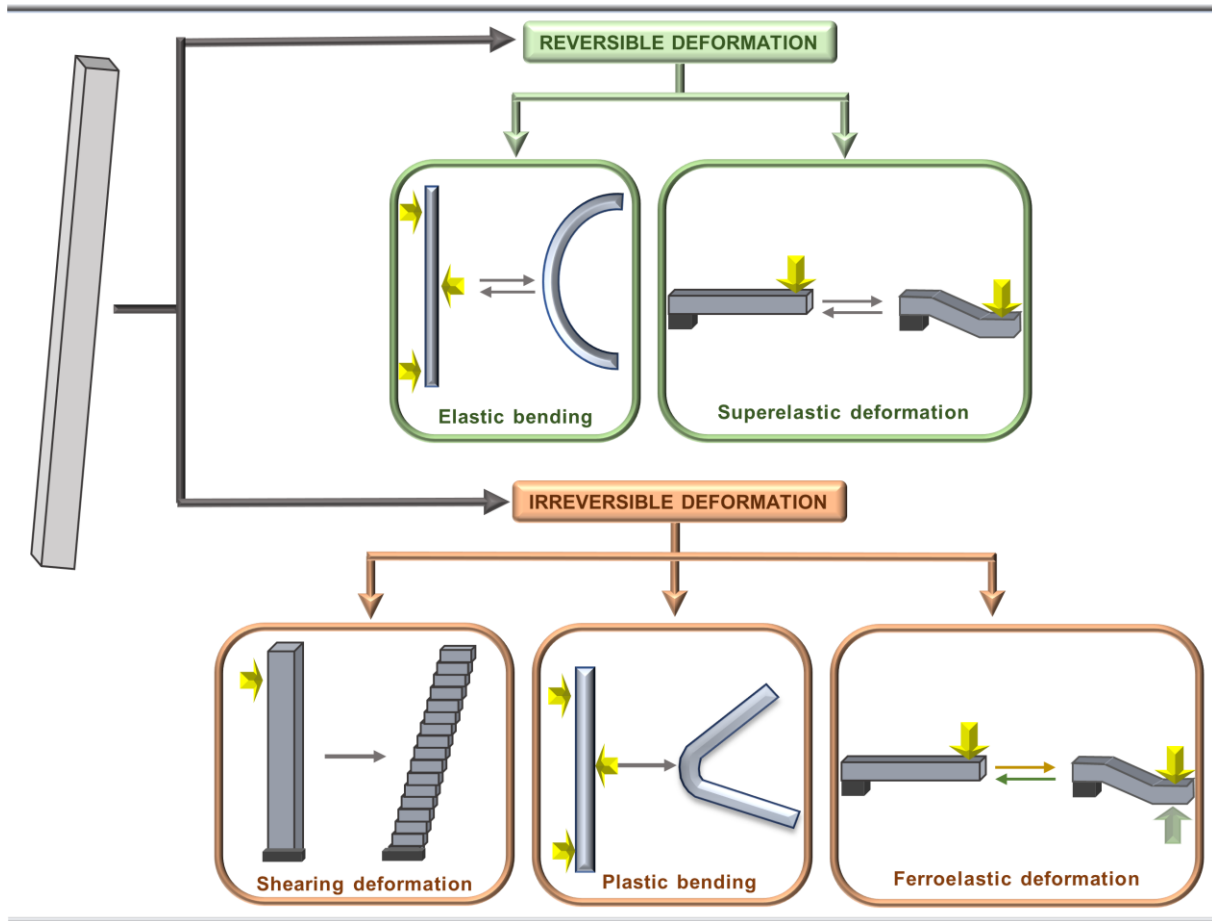


**Figure 4.** Types of the mechanically induced responses.

All listed mechanical responses could be observed either when the mechanical force is applied in only one direction, therefore classifying those crystals as one-dimensionally (1D) responsive or in two or more orthogonal directions, classifying those as two-dimensionally (2D) or multi-dimensionally responsive.

### 1.3.1. Mechanically deformable organic molecular crystals

#### 1.3.1.1. Plastic responses

First reports on mechanosalient organic crystals date back to the beginning of the 21<sup>st</sup> century when an overview of two types of irreversible deformation was given; shear deformation (Figure 5a) and plastic bendability (Figure 5b).<sup>20–24</sup> When exposed to shear stress, crystal undergoes a shear deformation upon which sheared layers do not change volume or orientation. A crystal is considered to display plastic bending if it bends during the force application but does not regain its original shape with the removal of the mechanical force. By examining the crystal structures of these compliant molecular crystals, a few common structural properties could be observed and pointed out. Firstly, all crystals that displayed these kinds of behaviour upon application of the mechanical force had a short ‘4 Å’ crystallographic axis. However, it was found that possessing ‘4 Å’ crystallographic axis was not the only prerequisite that needed to be fulfilled that a crystal can display adaptive properties. The anisotropic distribution of intermolecular interactions, i.e. the existence of areas characterized by weak intermolecular interactions orthogonal to the areas of strong supramolecular interactions, was found to be one of the important structural features present in the adaptable crystalline solids. The regions of the weak intermolecular interactions were considered responsible for the crystal’s ability to comply during the force application.

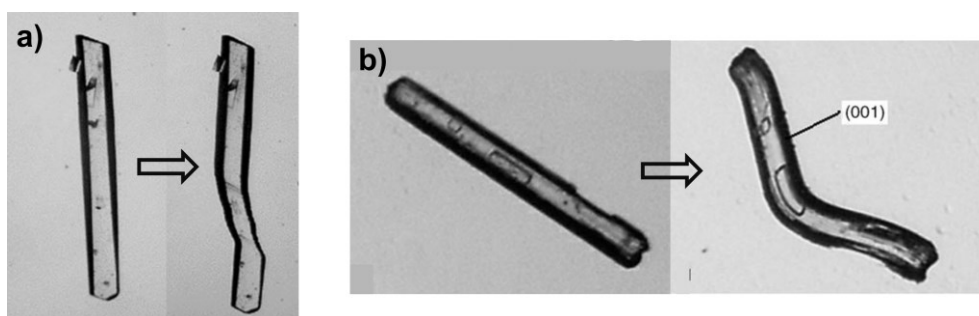


**Figure 5.** a) Shear deformation of 1,3,5-trichloro-2,4,6-triiodobenzene, b) plastic bending of hexachlorobenzene. The images were adopted from reference 23 and modified.

A few years later, detailed inspection of a stress-compliant, exceptionally plastically bendable crystal of hexachlorobenzene (Figure 6a), using a combination of various experimental techniques, gave an insight into the origin of plastic responsiveness.<sup>25</sup> It was

thereby revealed that upon plastic bending, the crystal surface (which is flat while the crystal is undeformed) becomes striated, with the discrete layers of approximately 3.2  $\mu\text{m}$  in size. The crystal domains, composed of hexachlorobenzene molecules mutually held by relatively strong  $\pi$ -interactions, slide over each other during the force application, which was accompanied by breakage and restoration of relatively weaker  $\text{Cl}\cdots\text{Cl}$  halogen contacts (Figure 6c). These are the areas of weak interactions, the so-called slip planes.

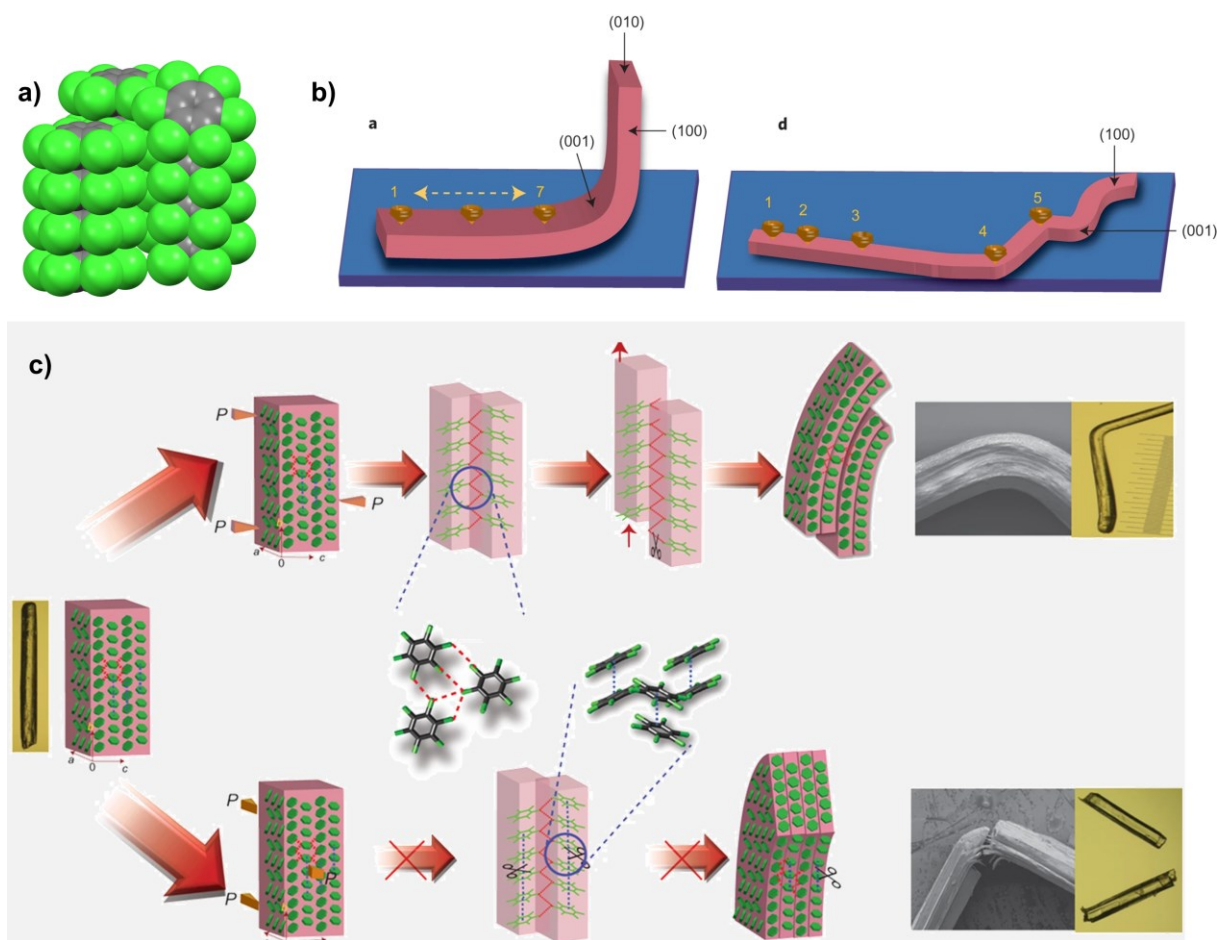


**Figure 6.** Plastically bendable crystal of hexachlorobenzene; a) structure b) nanoindentation experiment c) structural features and bending consequences. The images were adopted from reference 25 and modified.

Raman and IR spectroscopy together with microfocus diffraction experiments have shown that with bending no loss of long-range arrangement was observed, but only minor changes in the dimensions of the unit cell on the outer and inner arcs of the bent crystals. During bending,

the external layer of the crystal extends, while the inner part slightly contracts, to preserve the crystal integrity. Nanoindentation experiments have shown that plastic bending of crystals leads to "softening" of the crystals on the bent part which was confirmed with the reduction of the elastic modulus and hardness compared to an undeformed, straight crystal, due to decreased density, increased mosaicity, and packing imperfections (Figure 6b).

The slip-plane model was, and still is, widely accepted as the most possible mechanism of plastic bendability in organic molecular crystals and is demonstrated in a large number of literature reports describing irreversibly deformable compounds.<sup>26–45</sup>

The slippage mechanism was also experimentally confirmed on an example of rod-shaped crystals of *N*-(4-ethynylphenyl)-3-fluoro-4-(trifluoromethyl) benzamide.<sup>42</sup> By mapping out the structural features in the cross-section of a bent part of the crystal using micro-focus X-ray diffraction, it was determined that there was no perceptible change in the structure during plastic bending, i.e. no noteworthy changes in the unit cell parameters were observed. Therefore, the domains inside the crystal, composed of building blocks mutually connected *via* strong intermolecular interactions, simply slide over each other during bending without experiencing any type of deformation or harm.

Besides being able to be plastically bent in one or two directions, it was found that some organic molecular crystals can show even more magnificent mechanical responses such as ductility, and malleability, which makes them more alike to metals.<sup>46</sup> Isomorphous crystals of two globular molecules of aminoboranes,  $\text{BH}_3\text{N}(\text{CH}_3)_3$  and  $\text{BF}_3\text{N}(\text{CH}_3)_3$ , which crystalize in a high symmetry space group ( $R3m$ ), can be stretched, elongated, compressed, thinned, coiled, or twisted (Figure 7), i.e., these crystals can be deformed in any way possible (showing 3D plasticity), without losing the long-range order (only going through the phase transformation). In fact, if two pieces of a crystal are pushed together using mechanical force, they fuse and stick together (as metals do when subjected to high temperature), showing also self-healing ability. Moreover, nanoindentation measurements revealed that these crystals are even softer than plastically bendable crystals. These crystals, with extraordinary mechanical properties, are classified as *plastic crystals* (which should clearly be differentiated from the term *plastically bendable crystals*). On the other hand, crystals of a similar molecule,  $\text{BH}_3\text{NH}(\text{CH}_3)_2$ , show the ability to be plastically bent over only one set of bending faces, i.e., 1D plastic bendability, even though these crystals have similar values of a (high) globularity (which is the proportion between the Hirshfield surface area and the area of a sphere of an equal volume) and (low)

asphericity (the measure of anisotropy of an object) as the plastic ones. Therefore, the origin of the extreme pliability of the plastic crystals was ascribed to crystal structure features, mostly intermolecular interactions. The strong dihydrogen interaction achieved in the crystal structure of the 1D plastically bendable crystal,  $\text{BH}_3\text{NH}(\text{CH}_3)_2$ , prevents molecular rotations and limits the number of slip planes to one, while in plastic crystals, many slip planes are observed due to the presence of solely weak intermolecular interactions, which also enable molecular rotations.

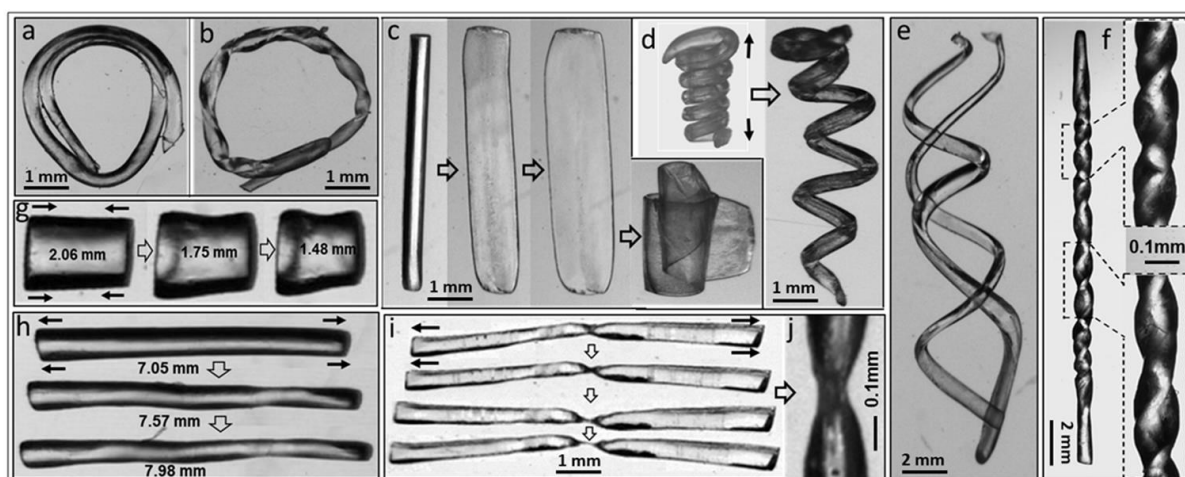


**Figure 7.** Mechanical responses of aminoboranes: a) coiling, b) twisting, c) thinning, d) crystalline spring e) double helix, f) twisting, g) compression, h) stretching, i) necking, j) necking – enlarged. The images were adopted from reference 46 and modified.

#### 1.3.1.2. Elastic responses

Elastic bendability is relatively rarely observed amongst organic crystals. The first example of the reversible crystals' deformation was reported back in 2012 when the elastically bendable co-crystal of caffeine with 4-chloro-3-nitrobenzoic acid and methanol (1:1:1) was described (Figure 8).<sup>47</sup> Crystal could be repeatedly bent many times without being broken (Figure 8b), as long as it was bent below a certain radius, and no perceptible difference in the “ease” of bending was noticed when bending the crystal either at room or lower ( $-100\text{ }^{\circ}\text{C}$ ) temperature. Moreover, it was observed that the crystal retains long-range order, even in its bent shape, however, substantial broadening of the peaks was noticed (Figure 8c). The inspection of crystal packing suggested an approximately isotropic arrangement in which the structural features are

interlocked and thus prevent sliding of the molecular layers over each other, could be the main reason behind the high elastic bendability of this crystalline material.

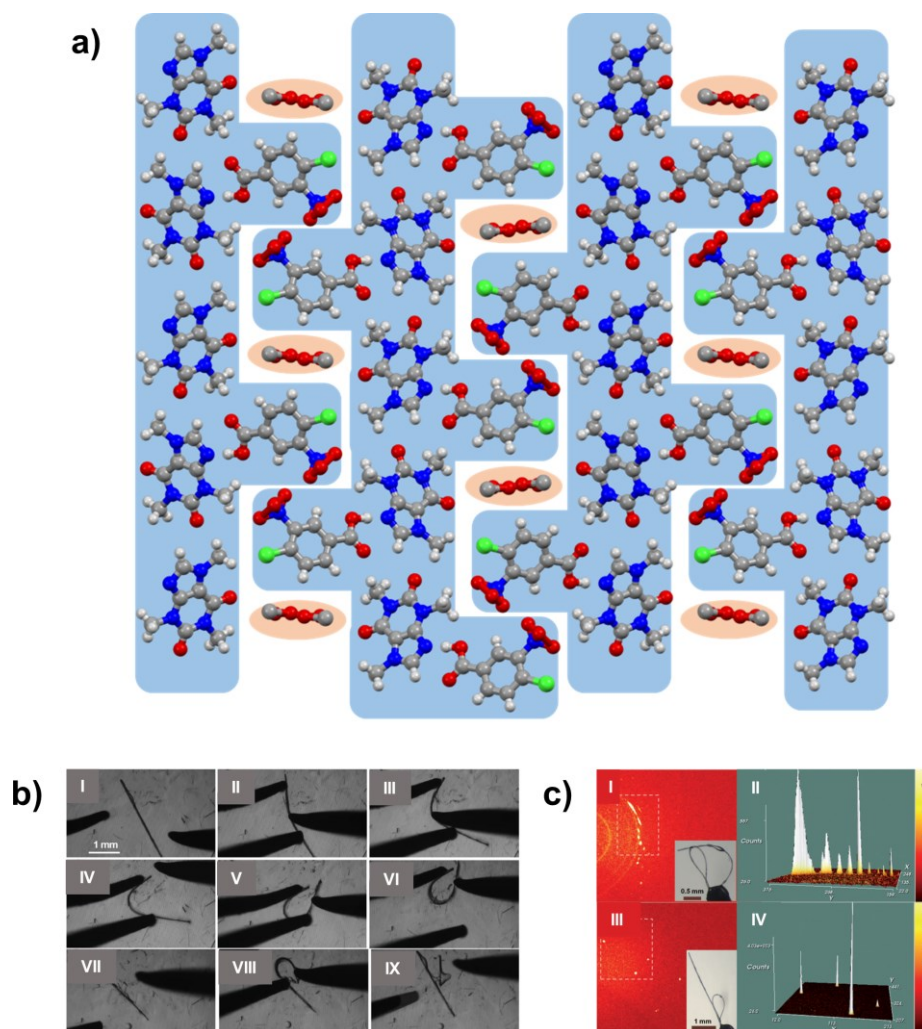


**Figure 8.** a) Crystal packing of a co-crystal of caffeine with 4-chloro-3-nitrobenzoic acid and methanol in comb-like tapes (blue shades, with methanol molecules which are highlighted in pale orange). b) Mechanically induced response of the co-crystal. c) Diffraction patterns of a bent (up) and straight (down) crystal. Images b) and c) were taken from reference 47 and adjusted.

Moreover, methanol molecules present in the so-called “mobile solvent channels”, and intermolecular interactions which are achieved with methanol molecules in the crystal packing, were also found to be one of the key features responsible for equipping this co-crystal with flexible properties (Figure 8a). It was observed that removing the solvent from the structure (by



heating the crystal up to 60 °C), did not affect the crystallinity of the sample, however, the crystal ability to elastically bend was lost, i.e., the crystal became brittle. The molecular dynamics simulations showed that the loss of methanol caused a large rearrangement of structure, and a drying process introduced defects, which might be the reason for the brittleness of the crystals.<sup>48</sup> A similar effect of the importance of solvent molecules was also observed for achieving the plastic bendability, where hydrated forms of two zwitterionic drugs, Pregabalin and Gabapentin, exhibit mechanically induced plasticity, while anhydrous forms remain brittle.<sup>40</sup>

Many other reports followed this research, and some common structural features in most of the elastically adaptable crystals were observed. It was suggested that avoiding the existence of the slip planes, i.e. achieving the nearly isotropic crystal packing, together with interlocked structure, should ensure the elastic response. These prerequisites were achieved in the highly elastic crystals of 4-bromo-3-chlorophenol, which contained hydrogen and halogen bonding of comparable strength in different directions.<sup>26</sup> Moreover, in a series of reversibly flexible halogenated N-benzylideneanilines, weak and dispersive interactions, namely halogen bonds, acting as structural buffers, and corrugated (i.e., interlocked) packing patterns, were found to be responsible for elastic behaviour.<sup>49</sup> Similar structural characteristics were observed also in the crystals of 2,6-dichlorobenzylidene-4-fluoro-3-nitroaniline,<sup>50</sup> and in the series of the elastically bendable co-crystals comprised of heterocyclic bases with halogenated aromatic acids,<sup>51–53</sup> where the co-crystallization was employed as a strategy for achieving the isotropic crystal packing thus enabling the desired elastic responses.

Moreover, it was found that elastically flexible crystals can display a large variety of additional interesting properties such as magnetic, optical and electric, what makes them suitable for future application in pharmaceutical,<sup>54</sup> luminescent, semiconducting,<sup>55</sup> and optical waveguiding purposes.<sup>56,57</sup>

#### *1.3.1.3. Superelasticity, ferroelasticity, superplasticity*

A special kind of the reversible mechanically induced crystal deformation, superelasticity (a so-called crystal-to-crystal transformation pseudo-elasticity), typically observed for metal alloys and ceramics,<sup>58–61</sup> with the NiTi<sub>2</sub> (nickel-titanium alloys) being the most prominent and widely used representatives, was recently also found to be a feature of some organic crystals.<sup>62–66</sup> The main difference between the elastic and superelastic

deformation is that superelasticity is accompanied either by martensitic transformations or “mechanical twinning” while those structural events are not observed during the elastic bending. In case of martensitic transformations, the crystal structure of the stress-induced domain and initial (mother) domain are of different phases, while in the case of “mechanical twinning” stress-induced domain and mother domain are of the same phase. Regaining the original, undeformed shape of a superelastically deformed crystal can be accomplished by simply removing the mechanical stress or heating.<sup>65</sup> If the superelastically deformed crystal regains its original shape upon heating, then it also shows a shape-memory effect. Superelastically deformed crystalline solids by martensitic transformations recover their initial shape by diffusionless single-crystal-to-single-crystal transformation.

Takamizawa and co-workers reported the first example of the superelasticity of the organic crystal of tereftalamide, what they termed organosuperelasticity.<sup>62</sup> The application of shear stress on the (010) face of the straight crystal, induced a deformation with a concurrent generation of another, daughter crystal phase with a sharp boundary across the crystal specimen between the two phases (Figure 9). By removal of the mechanical stress, the crystal readily regained its original shape. The crystal displayed high durability and reproducibility, by enduring more than 100 loading–unloading cycles, without suffering any wear or fatigue. That revelation was followed by many examples of the superelastic behaviour, facilitated by molecular twinning,<sup>63,67,68</sup> and those with shape memory effects.<sup>65</sup>

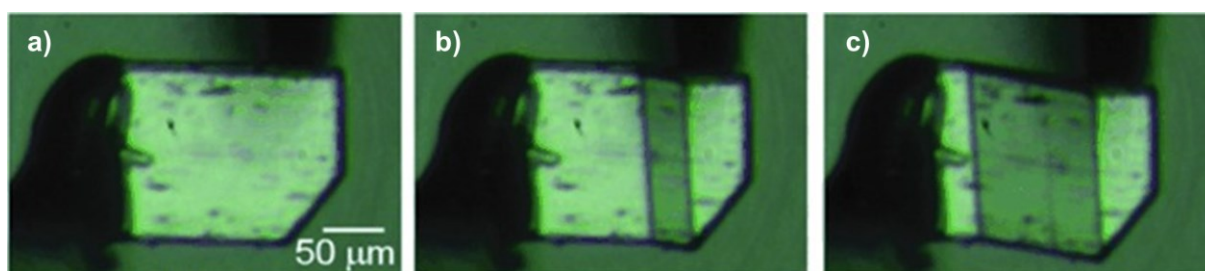


**Figure 9.** Superelastic response of tereftalamide. a) Undeformed crystal, b-c) superelastically deformed crystal with clear distinction between the mother domain (lighter part of the crystal), and a daughter domain (darker part of the crystal). The image was adopted from the reference 62 and adjusted.

It was recently determined that crystal can simultaneously display superelastic and superplastic properties.<sup>69</sup> When a shear stress is applied to a crystal of *N,N'*-dimethyl-4-nitroalanine in [100] direction, crystal displays an exceptional superplastic deformation, caused

either by slipping or twinning mechanism. On the other hand, when applying shear stress in the [201] direction, crystal displays superelastic deformation by twinning, and regains its original shape by removal of the impactor.

Ferroelasticity, similarly to the superelastic deformation, emerged as stress-induced deformation associated with a reorientation process. By removal of the stress, the crystal remains deformed, with the volume unchanged. The initial, undeformed shape can be obtained simply by applying the stress in an opposite direction. The first example of the ferroelastic crystal by twinning was reported for the crystal of 5-chloro-2-nitroalanine.<sup>70</sup> The crystal deformation was followed by mechanical twinning at a room temperature, by applying the shear force on (101) upon which a daughter twin phase appeared in between two original mother domains. The deformation remained even after the removal of the impactor. However, the straight, undeformed shape was completely recovered by application of the shear stress in an opposite direction, i.e., perpendicular to ( $\bar{1}0\bar{1}$ ). The crystal displayed deformation of an exceptional strain of 115.9%, which was the highest known amongst the reported materials that show deformation upon twinning, therefore indicating the potential utilization of this material as a mechanical damping agent. A number of other crystals displaying ferroelastic behaviour were reported in the last few years,<sup>71</sup> undoubtedly paving the way towards their wider potential applications.

### 1.3.2. Mechanically bendable metal-organic molecular crystals

Although the field of crystal dynamics is evolving rapidly, there is still a limited number of the stress compliant crystals of metal-organic compounds. In fact, the first examples of metal-containing crystals displaying the mechanically induced responses were reported only four years ago, when, almost simultaneously, two research groups presented their discoveries on this matter. Clegg and McMurtrie reported the first example of the zero-dimensional elastically flexible crystalline material, a long-known bis(2,4-pentanedionato)copper(II),  $[\text{Cu}(\text{acac})_2]$  (Figure 10a),<sup>72</sup> while Đaković *et al.* reported series of elastically bendable crystals of one-dimensional polymers of cadmium(II) halides with halopyrazine ligands.<sup>73</sup>

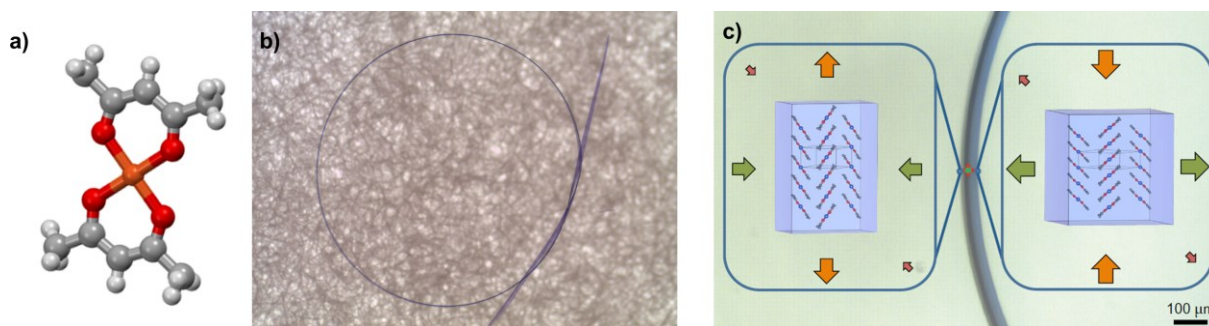


**Figure 10.** a) Molecular structure of  $[\text{Cu}(\text{acac})_2]$ , b) elastically bent crystal of  $[\text{Cu}(\text{acac})_2]$ , c) the crystal structure of  $[\text{Cu}(\text{acac})_2]$  on the outer (left) and inner (right) arc of a bent crystal. Images b) and c) adopted and adjusted according to reference 72.

The plate-like crystals of  $[\text{Cu}(\text{acac})_2]$ , although having the crystal structure that resembles the structures of most plastically bendable organic molecular crystals, with anisotropic distribution of structural features, do not display plastic bending but exceptional elastic responsiveness (Figure 10b). The crystal structure of  $[\text{Cu}(\text{acac})_2]$  is characterized with strong  $\pi$ -interactions and  $\text{Cu} \cdots \pi$  interactions in one direction (direction of the elongation of the crystal itself) and only weak dispersive interactions in other directions. Crystals can be extensively, repeatedly, elastically bent and twisted, while at the same time retaining their crystal identity. Tensile tests revealed an amazing ability of crystals to endure the stretching deformation up to 4.4% before breakage, with the tensile elastic modulus of around 210–550 MPa, such as soft organic polymer, polyethylene. On the other hand, nanoindentation experiments pointed out the directional difference in hardness and elastic modulus; the face of larger dimensions (101) was found to be mechanically softer and more elastic than the face of smaller dimensions (10 $\bar{1}$ ), what was reflected in approximately two times smaller values of hardness and Young's moduli. Moreover, three-point bending tests confirmed the soft nature of these crystals with Young's modulus value of 2–8 GPa, i.e., the same order of magnitude as nylon.

Microfocus X-ray diffraction experiments allowed the determination of the crystal structure throughout the cross-section of a bent crystal, at the equidistant points of 5  $\mu\text{m}$ , which thereby revealed the molecular movements that enable outstanding flexible response.<sup>72,74</sup> The results demonstrated that the [010] axis (that runs in the direction of the crystal elongation) is significantly elongated (1.5%) on the outer loop of the crystal, and compressed at the inner loop (1.9%). Moreover, the opposite trends were observed for the other two directions of the crystal

with the  $[10\bar{1}]$  direction being the least affected. Overall differences in the crystal dimensions for the inner to the outer loop for each direction are: 3.4%  $[010]$ , 3.0%  $[101]$  and 0.7%  $[10\bar{1}]$ . Moreover, it was found that during the bending process the interplanar distances between the discrete  $[\text{Cu}(\text{acac})_2]$  molecules do not change, but the molecules reversibly rotate as a response to mechanical stress, therefore allowing the compression on the inner, and concurrent expansion on the outer arc of the bent crystal, with the slight changes in the unit cell dimensions (Figure 10c).

Soon after that, a first report on mechanically flexible one-dimensional crystalline coordination polymers of cadmium(II) halides with halopyrazine ligands was published, where a group of seven isostructural crystals delivering elastic flexure as a response to outer stress was described.<sup>73</sup> All crystals showed 2D elastic response, however, surprisingly, the extent of elasticity differed amongst compounds, what was also shown with quantification of the responses by calculating the bending strain value ( $\varepsilon$ ) using Euler-Bernoulli equation, considering pure bending without shear component. Therefore, these seven compounds were divided into three subgroups regarding the elastic bendability – highly ( $\varepsilon \approx 1\%$ ), moderately ( $\varepsilon \approx 0.6\%$ ), and slightly ( $\varepsilon \approx 0.4\%$ ) elastically bendable. Moreover, some common structural characteristics were present amongst each group. Firstly, interlocking of the structural features was found to be one of the key factors responsible for determining the observed type of the mechanical response – the elastic bending, as interweaving prevents sliding of the adjacent domains, and therefore eliminates the possibility for the plastic response. Intermolecular interactions, hydrogen, and halogen bonds were found to be responsible for achieving different degrees of elastic bendability. The existence of the continuous intermolecular interactions of the comparable strength in the directions orthogonal to the direction of the elongation of a crystal itself was found to facilitate the high elasticity. On the other hand, in crystal structures of the slightly bendable crystalline compounds, the influence of the hydrogen bond interactions diminishes, while only isolated halogen bond interactions become predominantly present. Therefore, with the introduction of slight structural changes at a molecular level by altering either halide anion in a bridging or halogen atom on the ligand, it was possible to fine-tune the crystals' ability to bend elastically.

After these reports, several other examples of mechanically induced flexibility of crystalline materials emerged, predominantly describing polymeric crystalline compounds. The first example of a plastically bendable metal-containing molecular crystal was the 2D polymer

of the potassium salt of 4-*n*-hexyloxybenzoic acid.<sup>75</sup> The 2D polymeric structures close pack *via* van der Waals interactions between the methyl groups of the hexyl chains resulting in a slip planes system, which facilitates the irreversible deformation, therefore going in line with the observations for the structural prerequisites observed in purely organic systems. Moreover, upon performing repeatedly bending-unbending cycles, crystals tend to exfoliate, again, most probably due to existence of areas of very weak interactions in the crystal structure.

Next example of the plastically bendable metal-organic crystals was reported for 1D coordination polymer of  $[\text{ZnCl}_2(3,5\text{-Cl}_2\text{py})_2]_n$ ,<sup>76</sup> which was structurally very similar to the elastically bendable coordination polymers of Cd(II) with halopyrazine ligands.

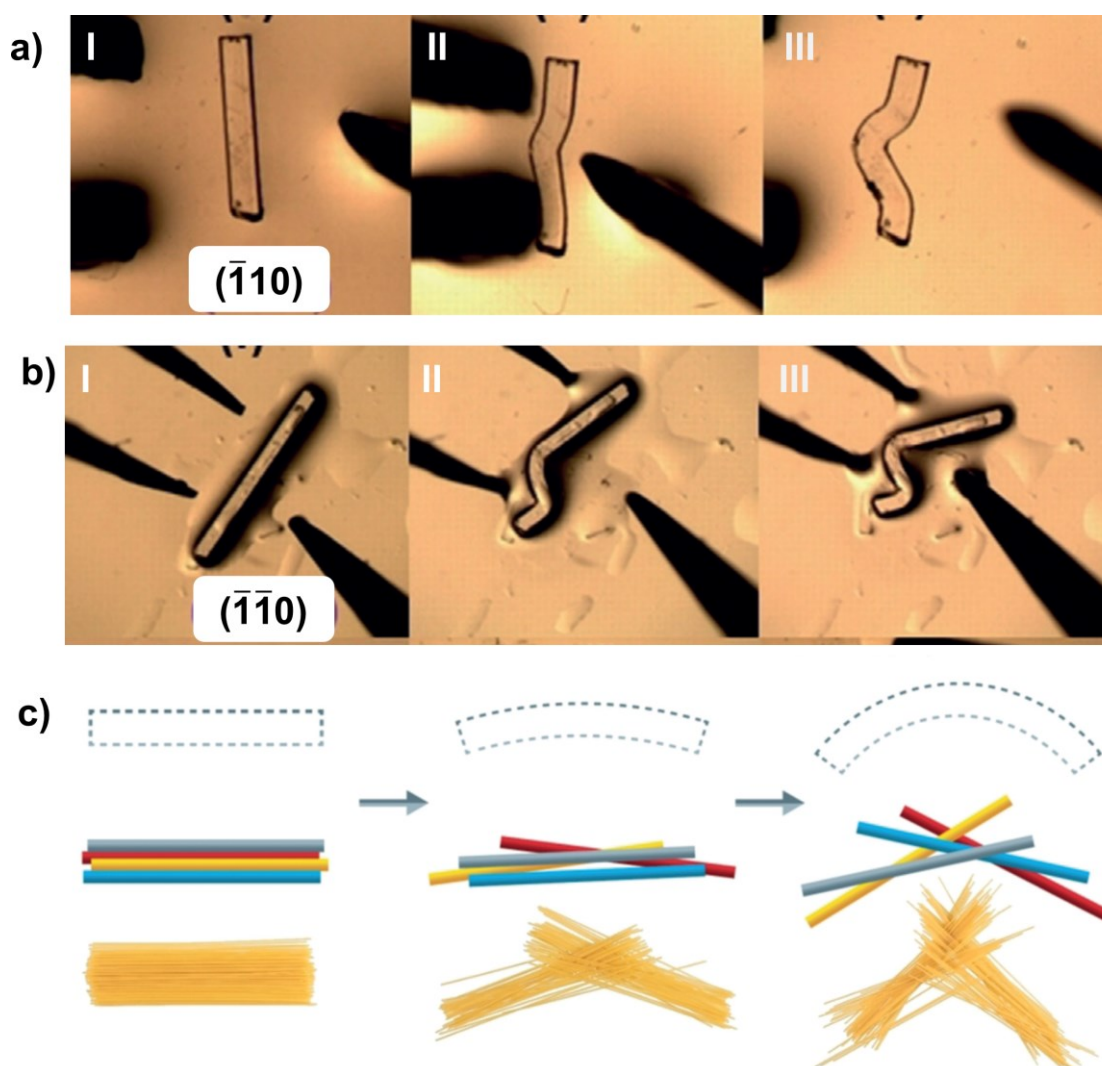


**Figure 11.** Crystals of  $[\text{ZnCl}_2(3,5\text{-Cl}_2\text{py})_2]_n$  displaying plastic bending as a response to application of mechanical force on a)  $(\bar{1}10)$  and b)  $(\bar{1}\bar{1}0)$  crystal faces. c) Proposed “spaghetti model” for plastic bendability. The images were adopted from the reference 76 and adjusted.

However, despite the structural resemblance, the crystals displayed a distinctively different mechanical response – plastic bending when the mechanical force is applied to the dominant crystal faces (Figure 11a, b). Moreover, no noticeable presence of the slip planes was observed, what was found to be the main structural characteristic of most plastically bendable organic crystals. However, the existence of exclusively weak intermolecular interactions throughout the whole structure was observed. Therefore, the authors proposed the so-called “spaghetti model” for plastic bending (Figure 11c), where one-dimensional polymers during application of the mechanical force move, and become interwoven, thus facilitating the irreversible deformation. Moreover, it was shown that at smaller deformation extents crystal structure remains untacked, however, inducing more deformation leads to failure of the crystal structure, and an increase in the polycrystalline phase. Moreover, the results demonstrated that during the bending, stress accumulates in between the one-dimensional polymeric chains, not within the chain.

Crystals of another one-dimensional coordination polymer,  $[\text{PbBr}_2(3\text{F-spy})_2]_n$  (3F-spy, 3-fluoro-4'-styrylpyridine), displayed a mechanically induced 1D highly elastic response ( $\varepsilon \approx 1.3\%$ ), i.e. these crystals of a plate-like morphology showed the reversible deformation when impacted on the faces of the larger dimensions, while broke upon stress application to the faces of smaller dimensions.<sup>77</sup> The structural background behind this behaviour lies in anisotropic crystal packing with the interlocking of structural features and presence of interactions strong enough to enable the restoration of the pristine crystal's shape upon withdrawal of the stress. Interestingly, these crystals displayed dynamic behaviour even when being irradiated, therefore presenting an example of the multi-stimuli responsive crystalline material.

Similar coordination polymer of Pb(II),  $[\text{Pb}(\text{SCN})_2(2\text{F-spy})_2]$  (2F-spy = 2-fluoro-4'-styrylpyridine), displayed even more magnificent multi-stimuli dynamic effects.<sup>19</sup> These crystals show an amazing ability of displaying concurrent mechanical responsiveness to thermal, light and mechanical stimuli. While heating/cooling cycles initiate jumping, bending, and splitting events as a consequence of thermal isomerisation, UV illumination of the crystals causes more pronounced effects, i.e., exploding, that is a result of  $[2 + 2]$  cycloaddition of 2F-spy ligands. Moreover, upon application of the mechanical force on the pair of faces of larger dimensions the crystals respond with a reversible bending motion, i.e., 1D elasticity ( $\varepsilon \approx 0.8\%$ ). Neighbouring corrugated 1D polymeric chains, interconnected by  $\pi$ - and  $\text{C-H}\cdots\text{F}$  interactions, form a 2D supramolecular architecture in the crystallographic *ab* plane. The main reason behind the adaptive crystalline property lies in the flexibility of the  $\text{Pb}_3(\text{SCN})_3$  units which, together

with the presence of the C–H $\cdots$ H–C and C–H $\cdots$ S interactions between the chains, helps in amortizing the stress which develops during the stress application, and enables the crystals to respond elastically.

Recently, Shi et al. described three multi-stimuli responsive triple-helix uranyl-organic 1D coordination polymers that are capable of exhibiting mechanical stress and temperature actuated dynamic behaviour.<sup>78</sup> Interestingly, these crystals undergo stress-induced elastic flexure to a high deformation extent and regain their original shape once the mechanical force is removed without introducing any harm to a crystal during the bending process. Moreover, nanoindentation experiments revealed relatively low hardness ( $H \approx 0.6$  GPa), and high values of the elastic modulus ( $E > 10$  GPa), thus clearly indicating an important role of mutually stabilized helical strands in allowing the crystals to withstand high amounts of stress caused by bending and preserving their crystal integrity. Anisotropic interchain intermolecular interactions, on the other hand, prevent domains within the crystal from sliding during the stress application, therefore disabling the plastic deformation. Tensile tests coupled with X-ray diffraction experiments revealed the importance of the spring-like extension and contraction behaviour of the 1D coordination polymers in achieving the high elasticity of this type of crystalline compounds.

Moreover, relatively recently, crystals of a discrete Ni(II) coordination compound, [Ni(salophen)] ( $\text{H}_2\text{salophen} = \text{N,N'-bis(salicylidene)-o-phenylenediamine}$ ), displaying unprecedented one-dimensional elastic response of the highest extent observed so far ( $\epsilon > 10\%$ ) were reported. Freshly crystalized, plate-like crystals, responded elastically to mechanical stress, whilst delaminating to the tiny fibres, which also displayed an amazing mechanically stimulated elasticity.<sup>79</sup> The X-ray diffraction experiments revealed that the crystal structure of the [Ni(salophen)] comprises a 1D assemblies of slip-stacked discrete molecules mutually connected via Ni $\cdots\pi$  and C $\cdots$ O interactions along the [100] direction. These 1D stacks are held with hydrogen bonds and C–H $\cdots\pi$  intermolecular interactions. The computational studies, together with the structural observations, suggested that overall intermolecular interactions are responsible for preventing gliding of the adjacent 1D slabs, thus allowing the elastic response of the crystals.

The latest paper on stress compliant coordination compounds described a group of five isostructural single crystals of a discrete tetrahedral Zn(II) complexes ( $[\text{Zn}(\text{SCN})_2(\text{L})_2]$ , L = 4-methylpyridine, 4-ethylpyridine, 4-isopropylpyridine, 4-*tert*-butylpyridine or



isonicotinamide).<sup>80</sup> It was found that with a careful manipulation of the intermolecular interactions through a deliberate choice of pyridine ligands, a specific macroscopic response can be accomplished. While in the elastically bendable crystals of  $[\text{Zn}(\text{SCN})_2(4\text{-methylpyridine})_2]$  and  $[\text{Zn}(\text{SCN})_2(\text{isonicotinamide})_2]$  intermolecular interactions were strong enough to withstand the stress and allow the crystal to spring back after being bent, choice of the more bulky and flexible ligands (with ethyl, isopropyl and *tert*-butyl substituents) weakened the interactions, whilst consequently producing the slip planes in the packing and endowed crystals with plasticity as a response to the mechanical stress.

#### 1.4. Perspectives on application of adaptable molecular crystals

Although widely investigated, crystals are still in principle neglected as a material of choice in engineering and design of novel and advanced materials, mainly because of their brittle nature. However, the newly discovered adaptive property of crystalline materials is firmly paving a new way in emerging technologies, promoting the crystals as a new set of advanced, soft, flexible, lightweight, and mostly environmentally benign materials. The mechanical properties of pharmaceutical ingredients are particularly important and the mechanically adaptable crystals, especially those displaying plastic bending,<sup>35,81,82</sup> showed to be extremely appropriate for tabletability process, as excellent ability of plastic bending facilitates compression properties. Furthermore, compliant pharmaceutical crystals, both plastically and elastically bendable ones,<sup>54</sup> could be the candidates for design of smart microdevices for potential biomedical applications.

Due to their long-range ordered structures, softness, and a high refractive index, crystals impose as ideal candidates for being the next generation optical waveguides. Their abilities of light conductivity, both passive and active have been studied thoroughly in the last few years. More recent research displayed an excellent optical and light transduction properties of the crystals showing also dynamic responses to the external stimuli such as mechanical stress,<sup>55,56,83–89</sup> or light.<sup>90</sup> Combining the mechanical flexibility with the optical properties gives the opportunity to develop crystal-based micro optoelectronic smart devices.

Besides the optical transduction, flexible crystals were also found to be able to conduct electrical energy. Simultaneous existence of high electrical conductivity and flexibility in crystals is highly desirable, however, hardly achievable. Crystals of 9,10-

bis(phenylethynyl)anthracene radical cation in addition to displaying an excessive elastic responsiveness, show the ability to transduce electrical energy, in both undeformed and severely bent shape, without any significant loss in the conductance capability.<sup>91</sup>

A great potential of the responsive crystalline materials for possible actuating applications was also recognized.

## 1.5. Hypothesis and objectives of the research

Four hypotheses were made to fulfil this research's main objective, which is to determine which structural features must be present in the crystals of coordination polymers to equip them with the flexibility, in particular of a desired type and degree of elasticity, to the applied mechanical stimulus.

- H1. The existence of areas of very weak interactions in the crystal (disperse and weak hydrogen and/or halogen interactions) parallel to the direction of elongation of the 1D polymer chain, i.e., the direction of elongation of the crystal itself, the so-called sliding planes, will allow plastic deformation of the crystal.
- H2. Intermolecular interactions (stronger hydrogen and/or halogen interactions) of equal strength in the directions orthogonal to the direction of elongation of the 1D polymer chain, will allow an elastic response.
- H3. The degree of elastic flexibility of crystals can be controlled by fine-tuning the intermolecular interactions.
- H4. Bending of crystals leads to small structural changes at the molecular level that consequently lead to changes in macroscopic properties (e.g., thermal properties, etc.)

## § 2. SCIENTIFIC PAPERS

This work is based on the three published scientific papers listed in the Table 1.

Table 1. List of the publications

Publication reference	Citing bases	Category	Quartile	Impact factor
<b>M. Pisačić</b> , I. Biljan, I. Kodrin, N. Popov, Ž. Soldin, M. Đaković, Elucidating the Origins of a Range of Diverse Flexible Responses in Crystalline Coordination Polymers. <i>Chem. Mater.</i> <b>33</b> (2021) 3660–3668.	CCC WoSCC Scopus	Chemistry	Q1	10.508
<b>M. Pisačić</b> , I. Kodrin, I. Biljan, M. Đaković, Exploring the diversity of elastic responses of crystalline cadmium(II) coordination polymers: from elastic towards plastic and brittle responses. <i>CrystEngComm</i> <b>23</b> (2021) 7072–7080.	CCC WoSCC Scopus	Chemistry	Q1	3.756
<b>M. Pisačić</b> , I. Kodrin, A. Trninić, M. Đaković, Two-Dimensional Anisotropic Flexibility of Mechanically Responsive Crystalline Cadmium(II) Coordination Polymers. <i>Chem. Mater.</i> <b>34</b> (2022) 2439–2448.	CCC WoSCC Scopus	Chemistry	Q1	10.508

# I

## Elucidating the Origins of a Range of Diverse Flexible Responses in Crystalline Coordination Polymers

Mateja Pisačič, Ivana Biljan, Ivan Kodrin, Nina Popov, Željka Soldin, Marijana Đaković

*Chem. Mater.* **33** (2021) 3660–3668

### Author contributions:

**M.P.** and M.Đ. conceived the research and wrote the paper with input from all authors; **M.P.** and N.P. performed the synthesis and crystallization experiments; **M.P.** and M.Đ. performed diffraction experiments; I.B. and **M.P.** performed AFM measurements; I.K. performed computational studies and analyzed the data; Ž.S. performed thermal measurements and analyzed the data.

# Elucidating the Origins of a Range of Diverse Flexible Responses in Crystalline Coordination Polymers

Mateja Pisačič, Ivana Biljan, Ivan Kodrin, Nina Popov, Željka Soldin, and Marijana Đaković\*



Cite This: *Chem. Mater.* 2021, 33, 3660–3668



Read Online

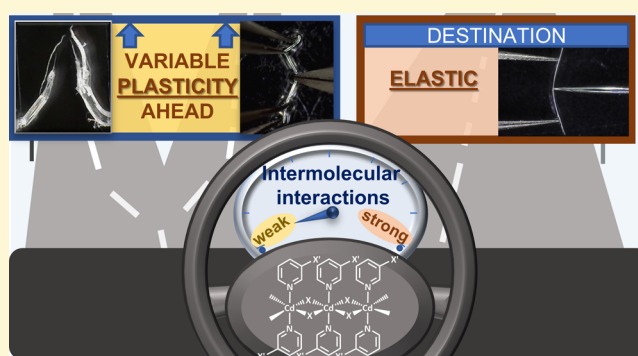
ACCESS |

Metrics & More

Article Recommendations

Supporting Information

**ABSTRACT:** The mechanical adaptability of a family of six one-dimensional crystalline coordination polymers (CPs) of cadmium ( $[\text{CdX}_2(3\text{-X'py})_2]_n$ ; 1: X = Br, X' = Cl, 2: X = I, X' = Cl, 3: X = I, X' = Br, 4: X = Cl, X' = I, 5: X = Br, X' = I, and 6: X, X' = I) to applied external force was examined, and a plethora of flexible responses was noticed. While two of the six CPs (4 and 6) were slightly elastic, the remaining four CPs (1–3 and 5) presented variable plastic deformation; three of these (1–3) displayed exceptional crystal flow, and one (2) demonstrated unprecedented ductility of crystalline metal–organic material. The feature was examined by theory and custom-designed experiments, and it was shown that specific and directional intermolecular interactions are not only the most influential structural feature in determining the type of mechanical responses (i.e., elastic vs plastic), with interlocking of adjacent molecules playing only a supportive role, but also an unavoidable tool for dialing-in a diversity of plastic responses in Cd(II) coordination polymers.



## INTRODUCTION

The ability to adapt to external mechanical stimuli with precise and predictable responses is still relatively rare among molecular crystals.<sup>1–4</sup> Endowing crystalline materials with such features enables a range of advanced practical applications in, e.g., flexible electronics<sup>5</sup> and magnetic<sup>6</sup> or optoelectronic devices.<sup>7,8</sup> Crystalline coordination polymers (CPs) are, due to their tunable magnetic and electronic properties, of particular interest in this context, but unfortunately, only a handful of such compounds have been found to display elastic<sup>9,10</sup> or plastic<sup>11–13</sup> flexibility in response to external mechanical pressure.

Recently, we discovered a family of Cd(II) coordination polymers<sup>9</sup> that, in addition to exhibiting exceptional elastic flexibility, displays a different extent of elasticity in response to applied mechanical force. They can, in fact, be bent extensively, moderately, or only slightly, with full recovery of the initial crystal shape prior to being fractured, and two structural features, interlocking coupled with specific intermolecular interactions, were found to be crucial for imparting this remarkable elastic behavior. This insight brought us to a new family of structures, all comprising a 1-D spine, with the aim to elucidate the relative role and importance of the two features (structural interlocking and intermolecular interactions) in furnishing coordination polymers with more controllable and predictable mechanical properties.

Against this background, we selected cadmium(II) halides for building the 1-D spine, in combination with 3-chloropyridine (3-Clpy), 3-bromopyridine (3-Brpy), and 3-

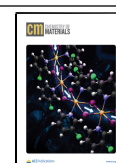
iodopyridine (3-Ipy) ligands that would ensure an octahedral geometry at each cadmium(II) center while also allowing us to systematically probe the structural influence of intermolecular interactions, namely, hydrogen and halogen bonds, on the subsequent mechanical behavior.

A survey of *Cambridge Structural Database* (CSD)<sup>14</sup> found six CPs with the desired molecular formula  $[\text{CdX}_2(3\text{-X'py})_2]_n$  (X = Cl, Br, I, X' = Cl, Br),<sup>15</sup> while calculated BFDH crystal morphologies<sup>16–18</sup> indicated that all the crystals could be expected to satisfy a critical prerequisite for mechanical flexibility, a needlelike appearance (see the [Supporting Information](#)). We prepared crystals of required morphology and sufficient quality of  $[\text{CdBr}_2(3\text{-Clpy})_2]_n$  (1),  $[\text{CdI}_2(3\text{-Clpy})_2]_n$  (2), and  $[\text{CdI}_2(3\text{-Brpy})_2]_n$  (3), and these were further complemented with three new compounds,  $[\text{CdCl}_2(3\text{-Ipy})_2]_n$  (4),  $[\text{CdBr}_2(3\text{-Ipy})_2]_n$  (5), and  $[\text{CdI}_2(3\text{-Ipy})_2]_n$  (6). This set of materials offers a diverse data set for examining crystal responsiveness to applied mechanical force and for rationalizing those responses in the context of morphological, structural, and mechanical features. To get to the mechanical behavior of our crystalline CPs and back to structural

Received: February 14, 2021

Revised: April 23, 2021

Published: May 6, 2021



influences of intermolecular interactions on those responses, we performed a highly integrated approach using both theory and experiment. Crystal responsiveness was examined via a variety of custom-designed experiments complemented by extensive crystallographic considerations, atomic force microscopy, and theoretical studies.

## RESULTS AND DISCUSSION

**Examining Mechanical Responses.** A careful inspection of the crystal morphology showed that crystals of 1–6, despite all being needle-shaped, can be categorized into two subgroups: those with two pairs of potential bending faces (faces parallel to the elongation of the crystal) equally developed (1–3 and 6) and those with noticeably different ones (4 and 5) (Figure 1).

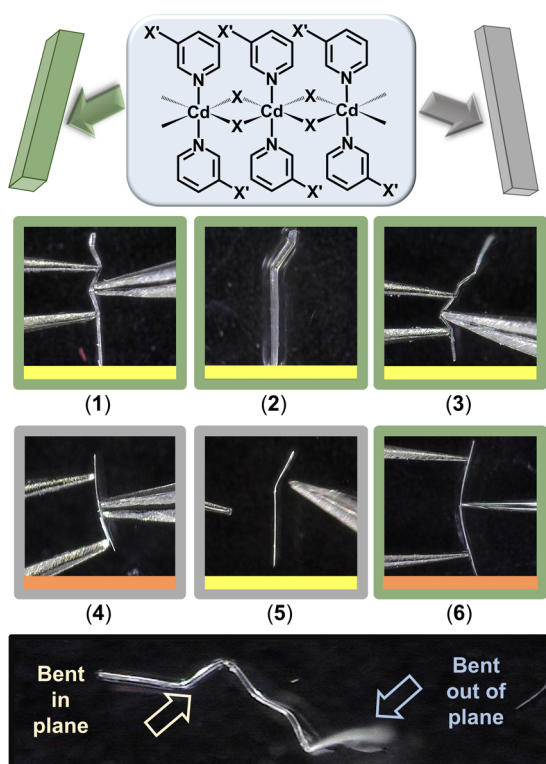


**Figure 1.** Crystals of 1–6 classified into two groups: those with equally developed bending faces (green picture borders, 1–3 and 6) and those with very elongated platelike morphology (gray picture borders, 4–5). In both groups, plastic (yellow inner line, 1–3 and 5) and elastic (orange inner line, 4 and 6) responses to applied mechanical force were observed.

Examining the mechanical behavior revealed that crystals of 1–3 were not elastically flexible but instead displayed plastic deformation. More interestingly, they also showed distinct differences in responses related to the ease with which crystals were bent, something that has not yet been reported for crystalline coordination polymers. While crystals of 2 were the most easily deformable ones (Movie S2; they were even difficult to handle due to pronounced compliance), crystals of 1 and 3 exhibited noticeable elasticity prior to presenting solely plastic deformation. When they (1 and 3) were bent just slightly, their initial shape could be recovered to some extent, but once bent more extensively, they were exclusively plastic (Movies S1 and S3). Such behavior of plastically deformable

crystals, i.e., different compliance in response to applied external force, has hitherto not been reported for metal–organic materials but only for globular organic substances.<sup>19</sup> Moreover, for all the crystals (1–3), no differences in responses were noticed when force was applied on two pairs of bending faces ((011)/(0–1–1) and (0–11)/(01–1); Figures S13, S15, and S17). This means that they can be categorized as 2-D (two-directional) plastically bendable.

In contrast to 1–3, crystals of 6, despite having the same morphology, responded differently. They were in fact elastic (i.e., showing complete crystal shape recovery upon removal of the applied pressure), and they snapped instantly once bent past the critical radius, without noticeable plasticity at any part of the crystal (Movie S6). To eliminate any influence of crystal dimensions, i.e., thickness and/or length, on the ability of crystals to elastically bend, the bending strain ( $\epsilon$ ) was calculated,<sup>20</sup> and it was  $\epsilon \approx 0.4\%$  for all examined samples of 6 (Table S6). Similarly to 1–3, no perceptible difference in crystal response was noticed when bent over two sets of bending faces, which classified 6 as 2-D elastically bendable.

Crystals of 4 and 5, in contrast to 1–3 and 6, presented two distinctively different pairs of potential bending faces (crystal faces (010)/(0–10) and (001)/(00–1)), thus more closely resembling an elongated platelike rather than acicular shape (Figures S18 and S21). Crystals of 4 and 5, although having almost identical morphology and crystal packing, responded differently from each other. Once placed on their larger faces (4:(100); 5:(010)) and applying force on the smaller ones, both crystals readily cracked and broke. However, when bending was probed over the smaller faces (4, 5:(001)) (i.e., the force applied on the larger ones), 4 was slightly elastic ( $\epsilon \approx 0.3\%$ ), while 5 was purely plastically deformable (Figure 1; Figures S19, S20, and S22); this means that they can be classified as 1-D (one-directional) elastically and 1-D plastically flexible, respectively (Movies S4 and S5).

**Elucidating Diverse Plastic Responses.** The remarkable difference in plastic behavior observed for 1–3 was further examined to get an insight into the mechanism controlling those properties, and several interesting features came into focus.<sup>4</sup>

During the application of mechanical force, all the samples (1–3), regardless of the ease with which they were deformed, displayed substantial sliding of the crystal itself over the tips of metal supporters. The crystals just smoothly slid over two metal supporters while the force was applied by a metal needle (impactor) in a modified three-point bending experiment (Figure 1; Movies S1–S3), thus more closely resembling a behavior of a living creature or soft matter rather than a regular metal–organic crystalline material. Moreover, if additional supporters were added on both sides, simulating a five-point bending experiment (Figure 2b),<sup>21</sup> the crystals were still smoothly sliding and passing between the supporters (Movies S7 and S8, Figure 2b). Despite a complex (wavy) path that each crystal end needed to follow while passing between the pair of supporters, once pulled out, both ends immediately straightened out, similar to a metal wire in a straightening process (i.e., the process of pulling a wire through a set of roller supporters placed on both sides of the wire).<sup>22</sup>

A careful (visual) inspection of the crystal flow further suggested that, due to pulling, the crystal might be even slightly elongated during the experiment. To shed light on the observation, the experiment was additionally adjusted; the crystals (1–3) were mounted with both ends fixed, and the



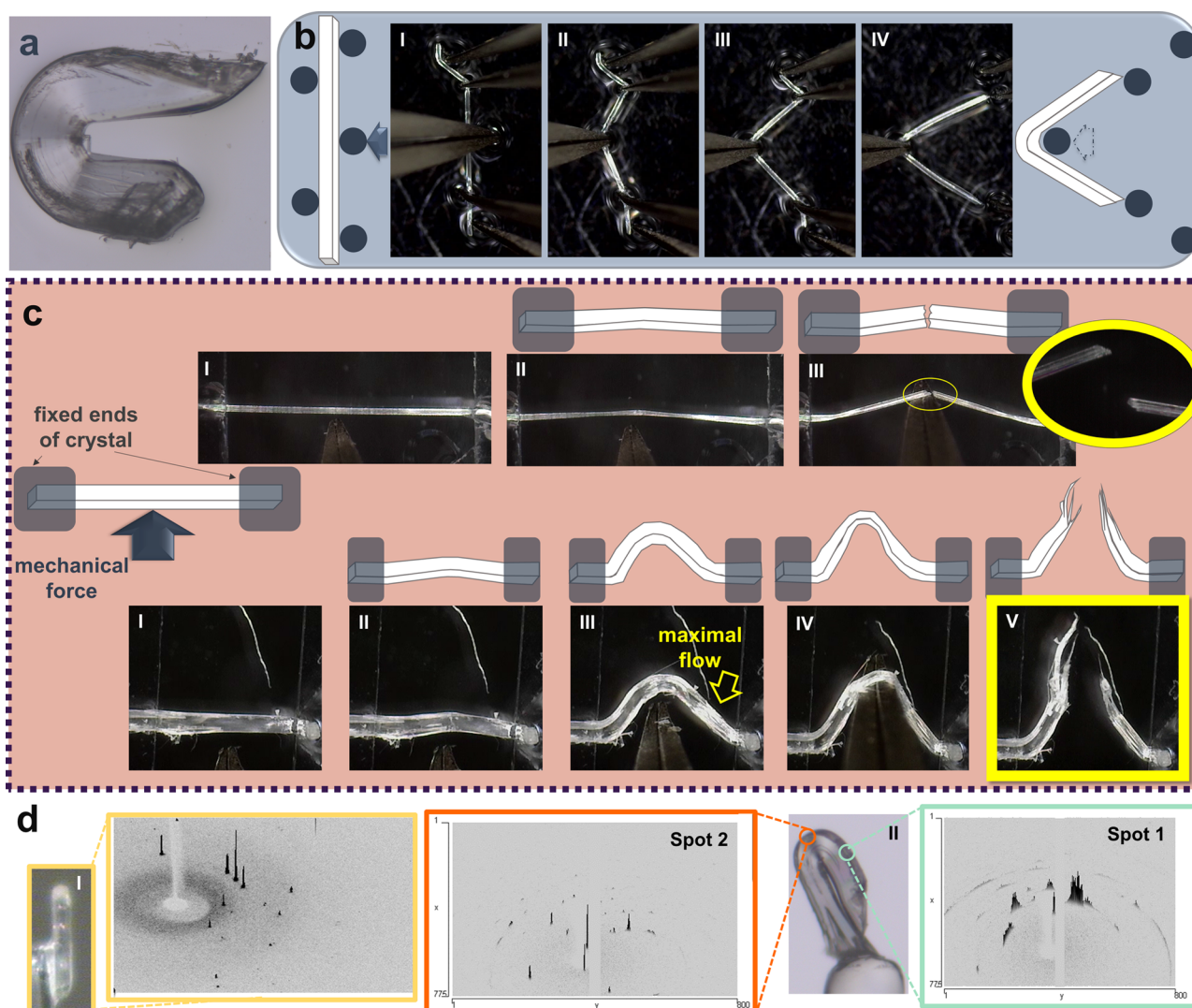


**Figure 2.** (a) U-shaped crystal of **2** with fully preserved transparency upon plastic deformation. (b) Pulling a crystal through two sets of metal supporters, positioned on each side of an impactor (a pair of tweezers with curved ends coupled), simulating a modified five-point bending experiment. Two ends of the crystals immediately straighten out while being pulled out of the supporters. (c) Different plastic flow of material (**1** and **3**, top; **2**, bottom) during application of force orthogonal to the direction of the straight, undeformed crystal, resulting in slight (**1** and **3**) and pronounced (**2**) elongation of the crystal. While **1** and **3** presented a typical brittle breakage, **2** displayed a continuous thinning of the material, ending up with thin fibers, some of even approximately nano dimensions. (d) Diffraction peaks of (I) undeformed crystal and (II) two spots on a U-shaped crystal of **2**. A substantial azimuthal elongation of Bragg peaks was noticed at the lateral point (spot 1), while only a slight broadening of Bragg peaks was noticed at the U-turn spot (spot 2), pointing at the significant slippage of adjacent domains over each other only at lateral regions of the crystal upon plastic deformation (each domain having a preserved unit cell of the undeformed crystal).

force was applied perpendicular to the crystals (Figure 2c; for details, see the experimental part).

The crystals of **1** and **3** indeed displayed a slight elongation (Figure 2c, top). The distance the impactor moved before the crystals cracked and broke was in all cases in the range of 80–100  $\mu\text{m}$ ; also, the crystals displayed a typical brittle breakage similar to the breakage of elastic crystals (Figure 2c, top, III; Movies S9 and S12). No noticeable difference in the behavior of **1** and **3** was observed. On the other hand, crystals of **2** showed a substantially larger elongation that was observed in the essentially longer distance the impactor moved, i.e., approximately 500–550  $\mu\text{m}$  (**2**) vs 80–100  $\mu\text{m}$  (**1** and **3**). Moreover, the crystals of **2** displayed a continuous plastic deformation, being steadily thinned out before they finally presented complete discontinuation of the material (Movie S10).

To demonstrate the effect more clearly and to examine the origin of this observation, the process was repeated on thicker crystals of **2** (Figure 2a and Figure 2c, bottom). It was clearly visible (Movie S11) that the application of the force was causing continuous movement of the neighboring domains over each other within the crystal. The phenomenon resulted in a plastic flow of the polymeric crystalline material that resembled a plastic flow of a typical high-symmetry ductile material.<sup>23,24</sup> Interestingly, in all cases, sliding of neighboring domains initiated (and was most pronouncedly noticed) at lateral regions and not at the point of the force application (Figure 2c III, bottom). Once initiated, sliding of the neighboring domains continued, with clearly visible thinning out of a crystal with the force application and progression of material's flow, ending up in tiny fibers of almost nano dimensions. This exceptional plastic flow, which was observed



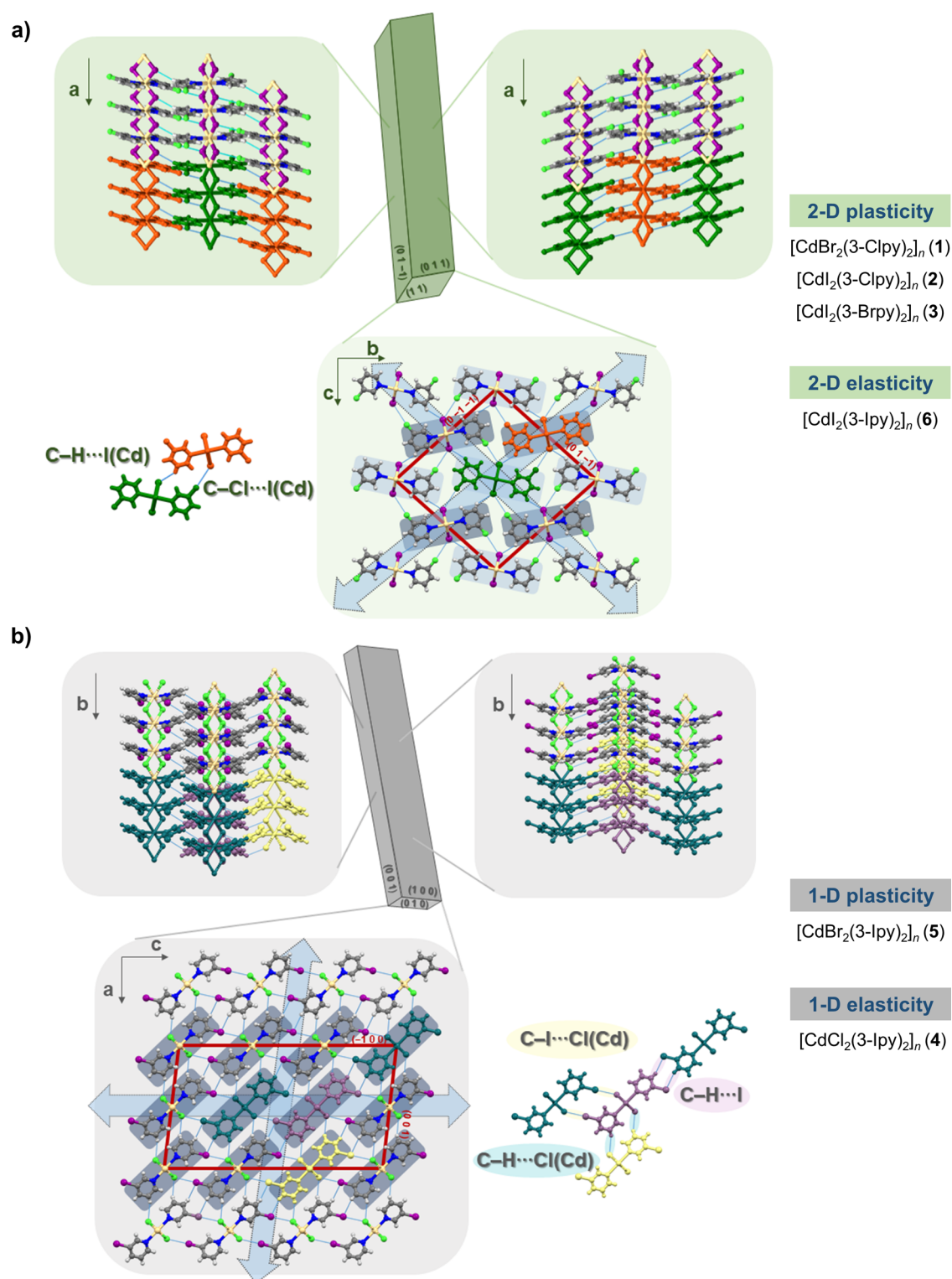


**Figure 3.** Crystal packing of 2 (a) and 4 (b). In 2, 1-D polymeric chains are arranged in a parallel fashion along the *b* axis and an antiparallel fashion along the *c* crystallographic axis, resulting in an almost identical structural arrangement in two bending directions (indicated by blue double-arrows) that in turn made the crystals 2-D mechanically responsive. In 4, along both crystallographic directions, *a* and *c*, 1-D polymeric chains are organized in a parallel fashion, resulting in substantially different structural arrangements in two (potential) bending directions (blue double-arrows) that in turn made the crystals 1-D mechanically responsive. Both plastic and elastic flexibilities are observed in 2-D and 1-D responsive crystals. Crystal packings of 1, 3, and 6 resemble 2, while 5 is similar to 4.

only for crystals of 2, indicated the weakest intermolecular interactions in 2 (in comparison to 1 and 3) parallel to bending face that in turn allowed this unprecedented, long-range sliding of adjacent polymeric regions within the crystal.

**Microfocus SCXRD.** To confirm the visually observed phenomenon, the crystals of 2 in their bent form were inspected by microfocus single-crystal X-ray diffraction (Figure 2d). Thicker crystals were selected, bent (using a modified

three-point bending procedure), and mounted on a glass fiber. Despite being excessively bent, making a U-turn, in all inspected cases, the crystals fully retained their initial transparency (Figure 2a,d; Movie S13), suggesting an ideal sliding of adjacent domains (viz., no visible cracks within the crystal).

Two spots on the bent crystal were selected, a spot on a lateral region (spot 1, green; Figure 2d, right) and a spot on a region of the maximal crystal curvature (spot 2, red; Figure 2d, center), and the Bragg peaks were examined. Surprisingly, at spot 2, Bragg peaks did not show any substantial peak broadening and changes of the unit cell parameters in comparison to the undeformed crystal.<sup>25</sup> On the other hand, a pronounced azimuthal elongation of Bragg peaks (known as asterisms) was observed at spot 1. Asterisms, typically noticed on plastically deformed metals<sup>26</sup> or perovskite-type oxides (e.g., strontium titanate),<sup>27</sup> are generally a result of tilts of mesoscopic, relatively defect-poor crystalline regions bounded by structural dislocations. The more pronounced the azimuthal elongation is, the larger the number of small crystalline domains, with the preserved unit cell of undeformed crystal, slightly tilted to each other. Substantially pronounced asterisms in 2, spanning an azimuth angle of up to approximately 60°, confirmed the significant slippage of neighboring domains at lateral regions, also visible on the crystal edges of a bent crystal (Figures 2a and 2d).

**Analysis of Structural Characteristics.** Regardless of different morphologies and different directionalities of mechanical responses of the two subgroups, 2-D bendable (1–3 and 6) and 1-D bendable (4–5) crystals, within each group, both types of crystal flexibility (viz., plastic and elastic) were observed (Figure 3). This prompted us to examine crystal structures more closely to identify the key structural features for determining different mechanical responses.

Crystal structure determination of three newly prepared compounds, 4–6, revealed that, analogously to 1–3, 1-D polymeric CdX<sub>2</sub> chains were formed. Octahedrally coordinated Cd(II) centers were bridged by halide ions and additionally decorated with two *trans*-oriented 3-halopyridine ligands. The main difference between the six structures arises from the relative orientation of the 1-D chains in the overall supra-molecular architecture.

Compounds 1–3 and 6 are isostructural with polymeric chains organized in a parallel fashion along the longest crystallographic axis (the *b* axis) and in an antiparallel fashion along the shorter *c* axis (Figure 3a and Figure S2). In contrast, 4 and 5 (which display near-identical crystal packing) have polymeric chains arranged in parallel in both crystallographic directions perpendicular to the elongation of the crystal (*a* and *c* (4); *b* and *c* (5)) (Figure 3b and Figure S3). In addition to the somewhat different interlocking of adjacent molecules, this makes the main difference between the two groups of CPs (1–3 and 6, and 4–5).

To elucidate the differences in directionality of flexible properties (viz., 1-D vs 2-D bending), a more detailed inspection of structural features parallel/orthogonal to two bending faces (indicated by blue double-arrows, Figure 3) was performed. It revealed virtually the same arrangement of 1-D polymeric chains in both directions for 2-D (1–3 and 6) and a distinctly different one for 1-D bendable crystals (4–5). This, in turn, ensured isotropy of structural features (1-D building blocks and intermolecular interactions) for 2-D (1–3 and 6) and anisotropy of structural organization in the two indicated

directions for 1-D bendable crystals (4–5). This unequivocally provided a clear relation between crystal packing (an)isotropy in the plane orthogonal to the elongation of the crystal and directionality of mechanical responsiveness (2-D vs 1-D).

On the other hand, the rationalization of different responses (plastic vs elastic) among each group, as well as the different compliance of plastically deformable crystals 1–3, was less obvious and could only be correlated with subtle differences of specific and directional interactions within each group of virtually the same structures (1–3 and 6, and 4–5).

Irrespective of morphology and flexible responses, all structures (1–6) rely on relatively weak C–X...X'(Cd) halogen and C–H...X'(Cd) hydrogen bonds (Tables S3 and S4). A detailed analysis of intermolecular interactions for 2-D bendable crystals (1–3 and 6) revealed halogen bonds as the most influential noncovalent force (assessed on the normalized distances between respective donor/acceptor sites,  $R_{\text{HX}}$  vs  $R_{\text{X1X2}}$ ).<sup>b,28,29</sup> The contacts are found to be among the least influential ones (the largest  $R_{\text{X1X2}}$  values) for the most responsive crystals (2) and the most influential ones for the elastic crystals (6), while in 1 and 3, the contacts are found to be of intermediate importance ( $R_{\text{X1X2}}$ : 1.01 (1), 1.02 (2), 0.98 (3), and 0.96 (6)).

In contrast, the mechanical behavior of 1-D bendable crystals (4 and 5) seems to be mainly controlled by hydrogen bonds. The anisotropic crystal packing (orthogonal to the elongation of the crystal) is produced by 2-D halogen bonded layers parallel to the bending faces (i.e., larger crystal face; Figure 3, bottom) and regions of very weak hydrogen bonds in between. While halogen bonds in two structures are of equal importance ( $R_{\text{X1X2}}$  = 0.92, 4 and 5), hydrogen bonds revealed a noticeable difference ( $R_{\text{HX}}$ : 1.02–1.03 (4) and 1.04–1.06 (5)), being slightly more influential in elastically (4) than in plastically bendable crystals (5). This implies that even such small differences are sufficient enough to control the nature and difference in crystal responsiveness.

**Computational Studies.** To complement the findings based on purely structural considerations and to identify the regions of the weakest interactions within the crystal (the regions regarded as those that allow slippage of adjacent domains over each other), we calculated pairwise interaction energies for all double pairs of adjacent molecular fragments (green–red pairs, Figure 4a; each double pair linked by a different set of intermolecular interactions, for simplicity depicted as C1–C3 and D1–D3; for details, see the Supporting Information).

For 2-D and 1-D responsive crystals, two (C1 and D1) and four distinct double pairs (C2, C3, D2, and D3) of molecular fragments are identified, respectively, and these were classified according to spreading the region of intermolecular interactions (Figure 4a): (i) parallel to crystal faces (C1–C3; red dotted lines) or (ii) slanted to them (D1–D3; blue dotted lines). Interactions spreading parallel to crystal faces (C-type) are notably weaker in both groups (i.e., 2-D and 1-D) than those spreading in other directions (D-type), thus being regarded as the “weakest” link in the crystal structure, prone to allow slippage of adjacent domains. Interestingly, the same interactions (C-type) were also found to be the weakest ones in elastically flexible crystals (6 and 4) but were slightly more influential than in their plastically deformable congeners (with a slight exception of C2-type interactions in 5, which are the topic of our next paper currently in preparation). Considering the overall strength of interactions in directions orthogonal to

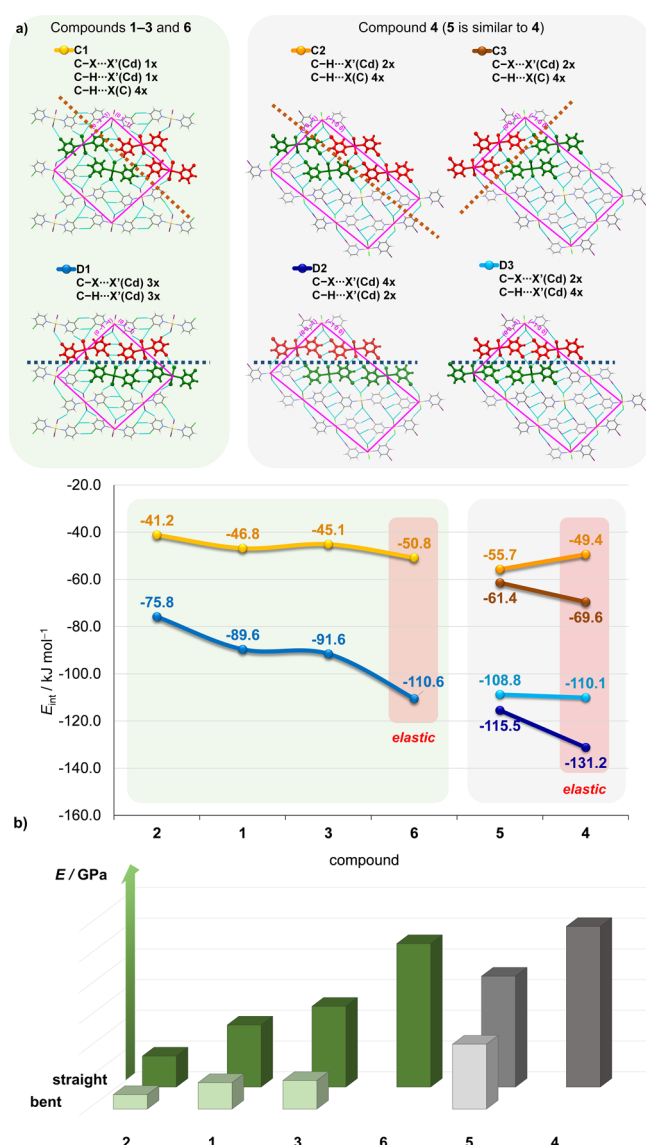


**Figure 4.** (a, top) Pairs of molecular fragments (green–red) identified in the crystal structures of 1–6; 2-D (left) and 1-D (right) responsive crystals, with dotted lines indicating the regions of intermolecular interactions being parallel/orthogonal to crystal faces (red dotted lines; upper) and slanted (blue dotted line; lower). (a, bottom) The M06-2X/DGDZVP interaction energies calculated for the different types of molecular interactions (C1–C3 and D1–D3) between neighboring molecular fragments in 1–6 (more details in the Supporting Information). (b) Young's moduli determined for 2-D (1–3 and 6; green) and 1-D (4–5; gray) responsive crystals on straight (darker colors) and bent crystals (lighter colors).

the elongation of the crystal (both C- and D-type interactions), these were always stronger for elastically (6 and 4) than for plastically deformable crystals (1–3 and 5), following our observation on deformability of crystals. This may suggest that for inducing a specific crystal response, an interplay of interactions orthogonal to the direction of elongation of the crystal might have a supportive role.

**Atomic Force Microscopy (AFM).** To correlate the mechanical responses observed on the macroscopic level with the microscopic-level crystals' properties, we measured Young's modulus for each sample using AFM (for details, see the Supporting Information) (Figure 4b). All six samples (1–

6) were probed in their original shape, while plastically deformable crystals were also probed at the kink in their bent form (Figure 5); only faces orthogonal to bending faces were

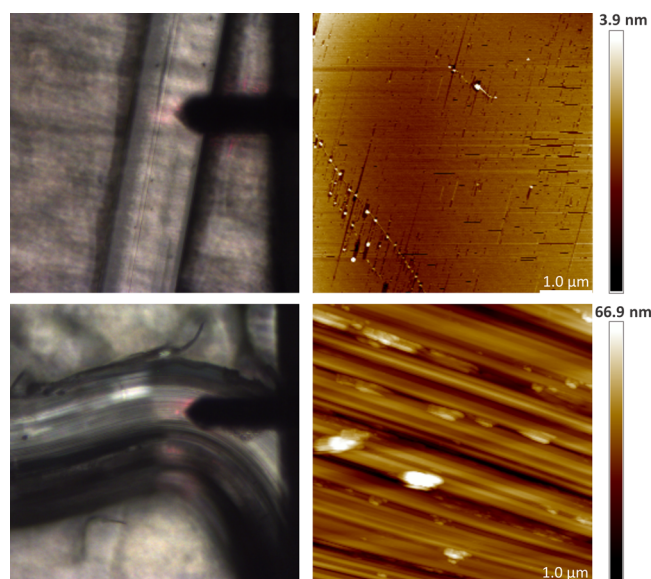


**Figure 5.** Morphology and surface texture visualized by optical microscopy and AFM of the straight (top) and bent (bottom) crystal of 1.

examined. The Young's moduli, determined for the crystals in their original form, showed noticeably larger values for elastically flexible crystals (4: 5.23 GPa and 6: 4.67 GPa) than for plastically deformable ones (1: 2.02 GPa, 2: 1.01 GPa, 3: 2.63 GPa, and 5: 3.61 GPa), irrespective of the organization of 1-D building units in their crystal structures (i.e., 1–3 and 6 vs 4–5). This implies that crystals of CPs, capable of responding plastically, are generally less stiff than their elastically flexible counterparts. This is consistent with what has been observed for organic molecular solids.<sup>30</sup> Moreover, the elastic moduli also correlated well with the slight differences in compliance observed for the three isostructural plastically deformable samples (the most compliant substance displayed the smallest values of the elastic modulus, while the least compliant ones displayed larger values), supporting our rationalization of the observed mechanical responses on a purely structural basis (i.e., the normalized distances between the donor/acceptor sites in the respective intermolecular interactions).

The Young's moduli on the bent crystals were somewhat smaller than the ones determined on their initial shapes (1: 0.86 GPa, 2: 0.47 GPa, 3: 0.93 GPa, and 5: 2.11 GPa), indicating a slight "softening" of the crystals at the kink.<sup>31,c</sup> In addition, the crystal surfaces (orthogonal to the bending faces) were inspected with AFM both before and after the plastic deformation was induced (1–3 and 5). It showed that surfaces at the bent region became striated after bending (Figure 5), with distinctive ridges of thickness of approximately 0.2  $\mu$ m running parallel to the bending face. This indicates spatial segregation of neighboring domains as a consequence of weakening of intermolecular interactions between the layers caused apparently by slippage of those layers over each other during bending.



## CONCLUSIONS

Having a closely related family of cadmium(II) coordination polymers that offers us a diverse data set of crystal responsiveness (from variable plasticity to slight elastic responses), we were able to rationalize the observed differences in mechanical adaptability against a backdrop of a variety of structural, morphological, and energy features. Moreover, the exceptional crystal flow and ductility of our samples, which have hitherto not been reported for metal–organic crystalline substances, prompted us to elucidate the origin of such behavior.

Our results clearly demonstrate that, irrelevant of the type of crystal responses (*viz.*, elastic or plastic) or extent of plastic deformability, with remarkable ductility of crystalline samples as the extreme case, the mechanical responses are primarily governed by the relative importance of specific and directional interactions rather than the interlocking of neighboring molecules (that may play only a supportive role). Only slight differences in the strength and influence of intermolecular interactions proved sufficient to control a plethora of different responses, from exceptional ductility, over regularly observed plasticity to even slight elasticity of coordination polymers. By attaining this level of understanding, we hope to be able to precisely engineer mechanical responses for a range of coordination polymers using a hypothesis-driven bottom-up approach that makes them available for advanced practical applications.

## EXPERIMENTAL SECTION

**Growing Crystals.** An aqueous solution of cadmium(II) salt ( $\text{CdX}_2$ , 1 equiv) was carefully added to a test tube and layered with 1 mL of ethanol, which was further layered with an ethanol solution of a ligand (2 equiv). White needlelike crystals were harvested after a few weeks.

**A Modified Three-Point Bending Experiment.** Mechanical responses of 1–6 to applied external force were investigated via a modified three-point bending procedure (see Supporting Information, Figure S11). A selected needlelike crystal was immersed in a small amount of paratone oil placed on a microscope slide (to prevent crystal damage by the metal accessories), and the force was applied by a metal needle while the crystal was supported by a pair of tweezers from the opposite side. The experiment was repeated for each complex (1–6) on several crystals from at least five different batches.

**Ductility Testing.** The crystals (1–3) were mounted with both ends fixed, and the force was applied orthogonal to the direction of the crystal elongation. To eliminate any impact of either a medium (*i.e.*, oil) or the surface–crystal friction, the crystals were held in air during the experiment (ends fixed to glass supporters). For all the experiments, the crystals of approximately the same thickness ( $\approx 30 \mu\text{m}$ ) were selected, while a constant effective length of the crystals was ensured by keeping the same distance between supporters. The force was then applied in a controlled fashion by moving the metal impactor (*i.e.*, tweezers with the curved ends coupled) at regular increments ( $15 \mu\text{m}$ ) and the same velocity ( $100 \mu\text{m/s}$ ).

**PXRD.** X-ray powder diffraction experiments were performed on a Philips PW 1850 diffractometer with  $\text{Cu K}\alpha$  radiation, a voltage of 40 kV, and a current of 40 mA. The patterns were collected in the angle region between  $5$  and  $50^\circ$  ( $2\theta$ ) with a step size of  $0.02^\circ$ .

**SCXRD.** Data collections (4–6) were carried out on an Oxford Diffraction Xcalibur four-circle kappa geometry single-crystal diffractometer with a Sapphire 3 CCD detector using a graphite monochromated  $\text{Mo K}\alpha$  ( $\lambda = 0.71073 \text{ \AA}$ ) radiation and applying the CrysAlisPro Software system<sup>32</sup> at  $296(2) \text{ K}$ . Data reduction, including absorption correction, was done by the CrysAlisPro program. The structures were solved by SHELXT<sup>33</sup> and refined by the SHELXL program.<sup>34</sup>

**Microfocus SCXRD.** Crystals of 2 (approximately  $2 \text{ mm}$  in length and  $400 \mu\text{m}$  in diameter) were mounted on a glass fiber in a bent form, and data collections were performed on an XtaLAB Synergy-S Dualflex diffractometer with a PhotonJet (Mo) microfocus X-ray source (FWHM  $150 \mu\text{m}$ ) and HyPix-6000HE hybrid photon counting (HPC) X-ray area detector.

**TG/DSC.** TG analysis was performed using a simultaneous TGA-DSC analyzer (Mettler-Toledo TGA/DSC 3+). DSC was performed on a Mettler-Toledo DSC823e. For each plastically deformable sample (1, 2, 3, and 5), two measurements were performed: on straight and randomly bent crystals. The crystals were placed in Al pans ( $40 \mu\text{L}$ ) and heated in flowing nitrogen ( $120 \text{ mL/min}$ ) from RT up to  $300^\circ\text{C}$  at a rate of  $10^\circ\text{C/min}$ .

**Computational Details.** DFT study was performed on the X-ray determined geometries of compounds 1–6 in Gaussian 16.<sup>35</sup> All C–H bond lengths were normalized, and single-point calculations were performed at the M06-2X/DGDZVP level of theory, which performs very well for the calculation of halogen-bond strengths among DFT methods with small basis sets.<sup>36</sup> Each adjacent 1-D polymeric chain was modeled as a neutral molecule composed of three octahedrally coordinated Cd(II) centers, and pairwise interaction energies were calculated and corrected by basis set superposition errors (BSSE) according to the counterpoise method of Boys and Bernardi.<sup>37,38</sup> All the calculated values are divided by 3 to obtain the normalized interaction energies per one metal center.

**AFM.** AFM topography and mechanical measurements were performed at RT on a commercial MultiMode8 AFM (Bruker). NCHV-A silicon probes (resonance frequency:  $320 \text{ kHz}$  and spring constant:  $42 \text{ N/m}$ ) were used to obtain the height images and to determine the mechanical properties of straight and bent crystals.

## ASSOCIATED CONTENT

### Supporting Information

The Supporting Information is available free of charge at <https://pubs.acs.org/doi/10.1021/acs.chemmater.1c00539>.

Synthetic procedures for the preparation of compounds 1–6; SCXRD results; PXRD results; DSC and TGA analysis; results of crystal bending experiments; results of AFM topography and mechanical measurements; and DFT study of intermolecular interactions (PDF)

Plastic deformation of 1 (AVI)

Plastic deformation of 2 (AVI)

Plastic deformation of 3 (AVI)

Elastic deformation of 4 (AVI)

Plastic deformation of 5 (AVI)

Elastic deformation of 6 (AVI)

Modified five-point bending experiment of 3 (AVI)

Modified five-point bending experiment of 1 (AVI)

Ductility testing of 1 accelerated  $4.5\times$  (AVI)

Ductility testing of 2 thin accelerated  $4.5\times$  (AVI)

Ductility testing of 2 thick accelerated  $4.5\times$  (AVI)

Ductility testing of 3 accelerated  $3.5\times$  (AVI)

Transparency of 2 after plastic deformation (AVI)

## AUTHOR INFORMATION

### Corresponding Author

Marijana Đaković – Department of Chemistry, Faculty of Science, University of Zagreb, 10000 Zagreb, Croatia;  
✉ [orcid.org/0000-0001-6789-6399](https://orcid.org/0000-0001-6789-6399); Email: [mdjakovic@chem.pmf.hr](mailto:mdjakovic@chem.pmf.hr)

### Authors

Mateja PISAČIĆ – Department of Chemistry, Faculty of Science, University of Zagreb, 10000 Zagreb, Croatia

Ivana Biljan – Department of Chemistry, Faculty of Science, University of Zagreb, 10000 Zagreb, Croatia; [orcid.org/0000-0002-0650-1063](https://orcid.org/0000-0002-0650-1063)

Ivan Kodrin – Department of Chemistry, Faculty of Science, University of Zagreb, 10000 Zagreb, Croatia

Nina Popov – Ruđer Bošković Institute, 10000 Zagreb, Croatia

Željka Soldin – Department of Chemistry, Faculty of Science, University of Zagreb, 10000 Zagreb, Croatia; [orcid.org/0000-0003-4206-8209](https://orcid.org/0000-0003-4206-8209)

Complete contact information is available at:

<https://pubs.acs.org/10.1021/acs.chemmater.1c00539>

## Author Contributions

M.P. and M.Đ. conceived the research and wrote the paper with input from all authors; M.P. and N.P. performed the synthesis and crystallization experiments; M.P. and M.Đ. performed diffraction experiments; I.B. and M.P. performed AFM measurements; I.K. performed computational studies and analyzed the data; and Ž.S. performed thermal measurements and analyzed the data. All authors have given approval to the final version of the manuscript.

## Funding

Croatian Science Foundation, IP-2019-04-1242.

## Notes

The authors declare no competing financial interest.

## ACKNOWLEDGMENTS

This work has been fully supported by the Croatian Science Foundation under Project IP-2019-04-1242. The support of project CluK co-financed by the Croatian Government and the European Union through the European Regional Development Fund—Competitiveness and Cohesion Operational Programme (Grant KK.01.1.1.02.0016) is acknowledged. M.P. and M.Đ. are grateful to Marin Lukas and Damjan Pelc for fruitful discussions.

## ADDITIONAL NOTES

<sup>a</sup>Crystals of **5**, although plastically responsive, did not present sliding of crystalline material.

<sup>b</sup>No trend in hydrogen-bond distances with respect to the acceptor ability of metal-bound halides was observed (i.e.,  $D-H\cdots Cl-M \geq D-H\cdots Br-M > D-H\cdots I-M$ ; see refs 28. and 29, suggesting that the hydrogen bond only has a supportive rather than structure-determining role, while an analogous trend for halogen bonding was clearly recognized. For more details on normalized distances, see the [Supporting Information](#).

<sup>c</sup>The "softening" of bent crystals was also reflected on the decomposition temperatures. For all bent crystals, they were lower (by 2–8 °C) in comparison with the crystals in their original shape, indicating a noticeable decrease in thermal stability as a consequence of induced plastic deformation (see the [Supporting Information](#)).

## REFERENCES

- (1) Ahmed, E.; Karothu, D. P.; Naumov, P. Crystal Adaptronics: Mechanically Reconfigurable Elastic and Superelastic Molecular Crystals. *Angew. Chem., Int. Ed.* **2018**, *57*, 8837.
- (2) Dey, S.; Das, S.; Bhunia, S.; Chowdhury, R.; Mondal, A.; Bhattacharya, B.; Devarapalli, R.; Yasuda, N.; Moriwaki, T.; Mandal, K.; Mukherjee, G. D.; Reddy, C. M. Mechanically Interlocked

Architecture Aids an Ultra-Stiff and Ultra-Hard Elastically Bendable Cocrystal. *Nat. Commun.* **2019**, *10*, 3711.

(3) Kakkar, S.; Bhattacharya, B.; Reddy, C. M.; Ghosh, S. Tuning mechanical behaviour by controlling the structure of a series of theophylline co-crystals. *CrystEngComm* **2018**, *20*, 1101.

(4) Alimi, L. O.; Lama, P.; Smith, V. J.; Barbour, L. J. Hand-Twistable Plastically Deformable Crystals of a Rigid Small Organic Molecule. *Chem. Commun.* **2018**, *54*, 2994–2997.

(5) Wang, Y.; Sun, L.; Wang, C.; Yang, F.; Ren, X.; Zhang, X.; Dong, H.; Hu, W. Organic Crystalline Materials in Flexible Electronics. *Chem. Soc. Rev.* **2019**, *48*, 1492–1530.

(6) Kenny, E. P.; Jacko, A. C.; Powell, B. J. Mechanomagnetism in Elastic Crystals: Insights from  $[Cu(acac)_2]$ . *Angew. Chem., Int. Ed.* **2019**, *58*, 15082–15088.

(7) Annadhasan, M.; Agrawal, A. R.; Bhunia, S.; Pradeep, V. V.; Zade, S. S.; Kazantsev, M. S.; Konstantinov, V. G.; Dominskiy, D. I.; Bruevich, V. V.; Postnikov, V. A.; Luponosov, Y. N.; Tafeenko, V. A.; Surin, N. M.; Ponomarenko, S. A.; Parashchuk, D. Y. Highly Bendable Luminescent Semiconducting Organic Single Crystal. *Synth. Met.* **2017**, *232*, 60.

(8) Das, S.; Mondal, A.; Reddy, C. M. Harnessing Molecular Rotations in Plastic Crystals: A Holistic View for Crystal Engineering of Adaptive Soft Materials. *Chem. Soc. Rev.* **2020**, *49*, 8878.

(9) Đaković, M.; Borovina, M.; Pisičić, M.; Aakeröy, C. B.; Soldin, Ž.; Kukovec, B.-M.; Kodrin, I. Mechanically Responsive Crystalline Coordination Polymers with Controllable Elasticity. *Angew. Chem., Int. Ed.* **2018**, *57*, 14801.

(10) Mei, L.; An, S.; Hu, K.; Wang, L.; Yu, J.; Huang, Z.; Kong, X.; Xia, C.; Chai, Z.; Shi, W. Molecular Spring-like Triple-Helix Coordination Polymers as Dual-Stress and Thermally Responsive Crystalline Metal–Organic Materials. *Angew. Chem., Int. Ed.* **2020**, *59*, 16061.

(11) Nath, N. K.; Gupta, P.; Hazarika, P. J.; Deka, N.; Mukherjee, A.; Dutta, G. K. Plastically Deformable and Exfoliating Molecular Crystals of a 2-D Coordination Polymer and Its Ligand. *Cryst. Growth Des.* **2019**, *19*, 6033.

(12) Bhattacharya, B.; Michalchuk, A. A. L.; Silbernagl, D.; Rautenberg, M.; Schmid, T.; Feiler, T.; Reimann, K.; Ghalgaoui, A.; Sturm, H.; Paulus, B.; Emmerling, F. A Mechanistic Perspective on Plastically Flexible Coordination Polymers. *Angew. Chem., Int. Ed.* **2020**, *59*, 5557–5561. ; *Angew. Chem.*, **2020**, *132*, 5602.

(13) Liu, X.; Michalchuk, A. A. L.; Bhattacharya, B.; Emmerling, F.; Pulham, C. R. Reversibility in a Plastically Flexible Coordination Polymer Crystal: A High-Pressure Study. [chemrxiv.org](https://chemrxiv.org), submitted: September 29, 2020, URL: <https://doi.org/10.26434/chemrxiv.13022606> (accessed: 2021-02-10)

(14) Groom, C. R.; Bruno, I. J.; Lightfoot, M. P.; Ward, S. C. The Cambridge Structural Database. *Acta Cryst.* **2016**, *72*, 171–179.

(15) Hu, C.; Li, Q.; Englert, U. Structural Trends in One and Two Dimensional Coordination Polymers of Cadmium(II) with Halide Bridges and Pyridine-Type Ligands. *CrystEngComm* **2003**, *5*, 519.

(16) Bravais, A. *Études Crystallographiques*; Gauthier-Villars: Paris, 1866, p 194–264.

(17) Freidel, G. Études Sur la loi de Bravais. *Bull. Soc. Fr. Mineral.* **1907**, *30*, 326.

(18) Donnay, J. D. H.; Harker, D. A new law of crystal morphology extending the Law of Bravais. *Am. Mineral.* **1937**, *22*, 463.

(19) Mondal, A.; Bhattacharya, B.; Das, S.; Bhunia, S.; Chowdhury, R.; Dey, S.; Reddy, C. M. Metal-like Ductility in Organic Plastic Crystals: Role of Molecular Shape and Dihydrogen Bonding Interactions in Aminoboranes. *Angew. Chem., Int. Ed.* **2020**, *59*, 10971–10980.

(20) Timoshenko, S. *Strength of materials Part 1*; D. Van Nostrand Company: New York, 1940, p 88–127.

(21) Ma, L.; Ma, H.; Liu, Z.; Chen, S. Theoretical Analysis of Five-Point Bending and Springback for Preforming Process of ERW Pipe FFX Forming. *Math. Probl. Eng.* **2019**, 1703739.

- (22) Nastran, M.; Kuzman, K. Stabilisation of Mechanical Properties of the Wire by Roller Straightening. *J. Mater. Process. Technol.* **2002**, 125-126, 711–719.
- (23) Hom, C. L.; McMeeking, R. M. Plastic Flow in Ductile Materials Containing a Cubic Array of Rigid Spheres. *Int. J. Plast.* **1991**, 7, 255.
- (24) Hertzberg, R. W.; Vinvi, R. P.; Hertzberg, J. L. *Deformation and Fracture Mechanics of Engineering Materials*; J. Wiley & Sons, 5<sup>th</sup> Ed., 2013, p 63–142.
- (25) Commins, P.; Karothu, D. P.; Naumov, P. Is a Bent Crystal Still a Single Crystal? *Angew. Chem., Int. Ed.* **2019**, 58, 10052–10060.
- (26) Gay, P.; Honeycombe, R. W. K. X-ray asterisms from deformed crystals. *Proc. Phys. Soc. A.* **1951**, 64, 844.
- (27) Hameed, S.; Pelc, D.; Anderson, Z. W.; Klein, A.; Spieker, R. J.; Lukas, M.; Liu, Y.; Krongstad, M. J.; Osborn, R.; Leighton, C.; Fernandes, R. M.; Greven, M. Enhanced Superconductivity in Plastically Deformed Strontium Titanate. [arXiv.org](https://arxiv.org/abs/2005.00514), submitted: May 1, 2020, URL: [arxiv.org/abs/2005.00514](https://arxiv.org/abs/2005.00514) (accessed 2021-02-10)
- (28) Lommerse, J. P. M.; Stone, A. J.; Taylor, R.; Allen, F. H. The Nature and Geometry of Intermolecular Interactions between Halogens and Oxygen or Nitrogen. *J. Am. Chem. Soc.* **1996**, 118, 3108.
- (29) Brammer, L.; Bruton, E. A.; Sherwood, P. Fluoride Ligands Exhibit Marked Departures from the Hydrogen Bond Acceptor Behavior of Their heavier Halogen Congeners. *New J. Chem.* **1999**, 23, 965.
- (30) Cappuccino, C.; Catalao, L.; Marin, F.; Dushaq, G.; Raj, G.; Rasras, M.; Rezgui, R.; Zambianchi, M.; Melucci, M.; Naumov, P.; Maini, L. Structure–Mechanical Relationships in Polymorphs of an Organic Semiconductor (C4-NT3N). *Cryst. Growth & Des.* **2020**, 20, 884.
- (31) Panda, M. K.; Ghosh, S.; Yasuda, N.; Moriwaki, T.; Mukherjee, G. D.; Reddy, C. M.; Naumov, P. Spatially Resolved Analysis of Short-Range Structure Perturbations in a Plastically Bent Molecular Crystal. *Nat. Chem.* **2015**, 7, 65.
- (32) *CrysAlisPRO*, Oxford Diffraction/Agilent Technologies UK Ltd, Yarnton, England.
- (33) Sheldrick, G. M. SHELXT— Integrated Space-Group and Crystal-Structure Determination. *Acta Crystallogr.* **2015**, 71, 3.
- (34) Sheldrick, G. M. A Short History of ShelX. *Acta Crystallogr.* **2008**, A64, 112.
- (35) Frisch, M. J.; Trucks, G. W.; Schlegel, H. B.; Scuseria, G. E.; Robb, M. A.; Cheeseman, J. R.; Scalmani, G.; Barone, V.; Petersson, G. A.; Nakatsuji, H.; Li, X.; Caricato, M.; Marenich, A. V.; Bloino, J.; Janesko, B. G.; Gomperts, R.; Mennucci, B.; Hratchian, H. P.; Ortiz, J. V.; Izmaylov, A. F.; Sonnenberg, J. L.; Williams-Young, D.; Ding, F.; Lipparini, F.; Egidi, F.; Goings, J.; Peng, B.; Petrone, A.; Henderson, T.; Ranasinghe, D.; Zakrzewski, V. G.; Gao, J.; Rega, N.; Zheng, G.; Liang, W.; Hada, M.; Ehara, M.; Toyota, K.; Fukuda, R.; Hasegawa, J.; Ishida, M.; Nakajima, T.; Honda, Y.; Kitao, O.; Nakai, H.; Vreven, T.; Throssell, K.; Montgomery, J. A., Jr.; Peralta, J. E.; Ogliaro, F.; Bearpark, M. J.; Heyd, J. J.; Brothers, E. N.; Kudin, K. N.; Staroverov, V. N.; Keith, T. A.; Kobayashi, R.; Normand, J.; Raghavachari, K.; Rendell, A. P.; Burant, J. C.; Iyengar, S. S.; Tomasi, J.; Cossi, M.; Millam, J. M.; Klene, M.; Adamo, C.; Cammi, R.; Ochterski, J. W.; Martin, R. L.; Morokuma, K.; Farkas, O.; Foresman, J. B.; Fox, D. J. *Gaussian 16*, Revision C.01, Gaussian, Inc.: Wallingford CT, 2016.
- (36) Siiskonen, A.; Priimagi, A. Benchmarking DFT methods with small basis sets for the calculation of halogen-bond strengths. *J. Mol. Model.* **2017**, 23, 50.
- (37) Boys, S. F.; Bernardi, F. The calculation of small molecular interactions by the differences of separate total energies. Some procedures with reduced errors. *Mol. Phys.* **1970**, 19, 553.
- (38) Simon, S.; Duran, M.; Dannenberg, J. J. How does basis set superposition error change the potential surfaces for hydrogen bonded dimers? *J. Chem. Phys.* **1996**, 105, 11024–11031.

## II

### Exploring the diversity of elastic responses of crystalline cadmium(II) coordination polymers: from elastic towards plastic and brittle responses

Mateja Pisačić, Ivan Kodrin, Ivana Biljan, Marijana Đaković

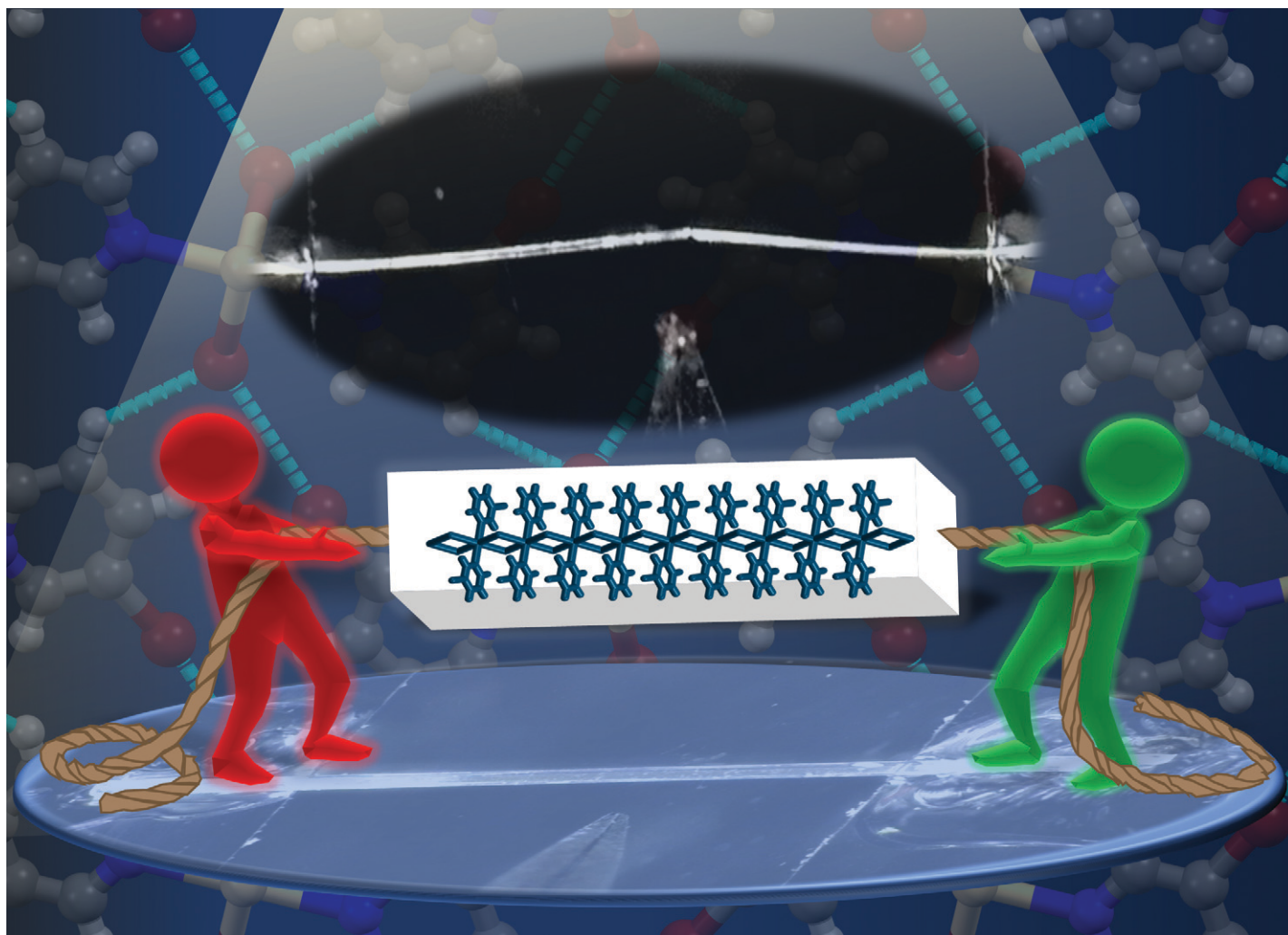
*CrystEngComm* **23** (2021) 7072–7080

*Reproduced with permission from CrystEngComm 2021, 23,7072-7080. Published by The Royal Society of Chemistry.*

#### Author contributions:

**M. P.** and **M. Đ.** conceived the research and wrote the paper with the input of all authors; **M. P.** performed the synthesis, crystallization experiments, and mechanical measurements; **I. B.** and **M. P.** performed the AFM measurements; **I. K.** performed computational studies and analysed the data.





Showcasing research from Professor Đaković's laboratory,  
Department of Chemistry, Faculty of Science, University of  
Zagreb, Zagreb, Croatia.

Exploring the diversity of elastic responses of crystalline  
cadmium(II) coordination polymers: from elastic towards  
plastic and brittle responses

Exploring the origins of mechanically induced  
responsiveness of crystalline coordination polymers by  
employing a multidisciplinary approach, combining both,  
theory and experiments, with the aim to examine potential  
avenues for bottom-up design of metal-containing  
crystalline solids with *a priori* determined mechanical output.

As featured in:



See Marijana Đaković *et al.*,  
*CrystEngComm*, 2021, **23**, 7072.





Cite this: *CrystEngComm*, 2021, 23, 7072

# Exploring the diversity of elastic responses of crystalline cadmium(II) coordination polymers: from elastic towards plastic and brittle responses†

Mateja Pisačić,  Ivan Kodrin,  Ivana Biljan and Marijana Đaković \*

The ability of one-dimensional crystalline coordination polymers of cadmium(II), namely  $[\text{CdCl}_2(3\text{-Clpy})_2]_n$  (**1**),  $[\text{CdCl}_2(3\text{-Brpy})_2]_n$  (**2**), and  $[\text{CdBr}_2(3\text{-Brpy})_2]_n$  (**3**) (3-Clpy = 3-chloropyridine; 3-Brpy = 3-bromopyridine), to adapt to mechanical stimuli was examined and differences in elastic responses were observed. Crystals of **1** and **3** showed similar behaviour with substantial elastic responses to external mechanical force followed by slight plasticity close to the breakage point, where these responses were classified as *elastic*→*plastic*. On the other hand, crystals of **2** were found to be less adaptable to mechanical stimuli, displaying only a slight elastic response with a typical brittle breakage. Crystals were further examined by atomic force microscopy while structural features were explored by theoretical methods. The rationalization of the observed mechanical properties in the context of interaction energies and Young's moduli revealed that the stronger interactions are reflected in the larger Young's modulus values, which in turn made the crystals stiffer and consequently less adaptable to external mechanical stimuli.

Received 16th June 2021,  
Accepted 6th September 2021

DOI: 10.1039/d1ce00797a

rsc.li/crystengcomm

## Introduction

The adaptability of crystalline solids to external stimuli has recently attracted widespread attention due to their great potential for application in emerging technologies, *i.e.* tissue engineering,<sup>1</sup> flexible electronics,<sup>2</sup> optical waveguides,<sup>3,4</sup> wearable technologies,<sup>5</sup> *etc.*<sup>6–8</sup> However, for practical application and implementation of mechanically responsive materials in smart devices we need to be in a position to control their responses with high accuracy, and for this purpose a deep understanding of the underlying principles leading to a targeted response is a necessity.

The rationale behind flexible behaviour, *i.e.* elastic *vs.* plastic, in organic crystalline solids has been well documented.<sup>9–31</sup> It was established that columnar molecular arrangement with substantial anisotropy of intermolecular interactions (*viz.* one strong direction along the column, and the other two directions being weaker) resulting in slip planes is a prerequisite for plastic behaviour,<sup>10–23</sup> while near-isotropy of crystal packing with interlocking of structural features is crucial for the elastic flexibility of organic molecular solids.<sup>22–31</sup> In contrast, the number of mechanically responsive metal-organic crystalline solids is

still limited, and the rationale behind their flexible behaviour is not yet quite understood. For the only flexible 0-D metal-organic complex,  $[\text{Cu}(\text{acac})_2]_n$ ,<sup>32</sup> a significant anisotropy (relatively strong  $\pi$ -interaction in one direction and only weak interactions in others) with no interlocking was found crucial for its elastic behaviour.

On the other hand, crystalline one-dimensional (1-D) coordination polymers (CPs), in addition to their unique and tunable properties (*i.e.* magnetic and electronic),<sup>33</sup> emerged as ideal model systems for exploring structural prerequisites for the delivery of a specific mechanical response due to the pre-organization of molecular subunits into structurally rigid 1-D building blocks. In the first report on flexible 1-D CPs,  $[\text{CdX}_2(\text{X}'\text{-pz})_2]_n$  (X-pz = halopyrazine, X' = Cl, Br, I), we have shown that the isotropy of intermolecular interactions (orthogonal to the elongation of 1-D building units) together with molecular interlocking was crucial for imparting elastic flexibility to crystalline 1-D CPs, but also that the extent of elastic bending could be controlled by altering the importance of non-covalent interactions in the structure.<sup>34</sup> Similar structural features were also observed in another elastically flexible 1-D coordination polymer of Pb(II), namely  $[\text{PbBr}_2(3\text{F-spy})_2]_n$  (3F-spy = 3-fluoro-4'-styrylpyridine).<sup>35</sup> On the other hand, for a plastically deformable 1-D coordination polymer,  $[\text{ZnCl}_2(3,5\text{-Cl}_2\text{py})_2]_n$ , a new 'spaghetti' model was proposed as substantial interlocking with no slip planes was present in the crystal structure.<sup>36</sup>

Recently, for crystals of a family of isostructural coordination polymers of Cd(II) we have reported both plastic

Department of Chemistry, Faculty of Science, University of Zagreb, Horvatovac 102a, Zagreb, Croatia. E-mail: mdjakovic@chem.pmf.hr

† Electronic supplementary information (ESI) available. See DOI: 10.1039/d1ce00797a

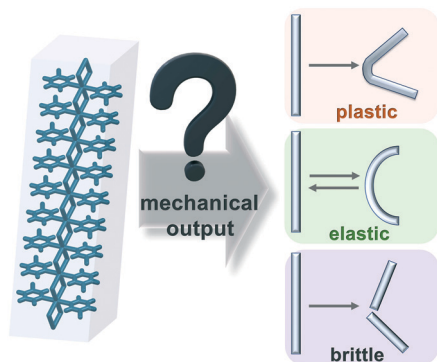


Fig. 1 Possible mechanical output of the 1-D coordination polymers of cadmium(II) upon application of external mechanical stimuli.

and elastic flexibility.<sup>37</sup> The observation prompted us to point at the intermolecular forces as the key feature for controlling flexible responses of CPs to external mechanical stimuli. In addition, pronounced differences in plasticity, with exceptional crystal deformability and ductility, were also observed for crystals from the same family of coordination polymers, leaving slight differences in the strength and geometry of intermolecular interactions as the only features for controlling crystal pliability.

To provide a deeper understanding of the relevance of crystal packing and/or intermolecular interactions in furnishing coordination polymers with a specific mechanical response (Fig. 1), herewith we focus on closely related coordination polymers of cadmium(II). With the aim to complement our previous observation, we put additional effort into growing crystals, and eventually we were lucky to deliver crystals of required quality and intended needle-shaped morphology for an additional three CPs of cadmium(II) from the same series,<sup>37</sup> namely  $[\text{CdCl}_2(3\text{-Clpy})_2]_n$  (**1**),  $[\text{CdCl}_2(3\text{-Brpy})_2]_n$  (**2**), and  $[\text{CdBr}_2(3\text{-Brpy})_2]_n$  (**3**) (3-Clpy = 3-chloropyridine; 3-Brpy = 3-bromopyridine).<sup>38</sup> Unexpectedly, additional variability in mechanical responses was noticed which we present herein.

## Results and discussion

Acicular crystals **1–3** were grown by a liquid diffusion technique (for details see the ESI†), and crystals of sufficient quality (including length and thickness) for testing mechanical responses were harvested after a few weeks.

### Crystal packing features

The crystal structures of **1–3**, firstly reported by Hu and Englert,<sup>38</sup> are isostructural with each other, and crystallize in the monoclinic space group  $P2_1/c$ , thus presenting a suitable data set for testing mechanical responsiveness and correlating this with slight differences in the importance and geometry of intermolecular interactions. The 1-D polymeric building units, constructed from the Cd-halide structural spines (halide = Cl, Br) and equipped with 3-halopyridine ligands (3-Clpy, 3-Brpy) in the axial positions, are organized in a parallel fashion along the crystallographic *b* axis and an

antiparallel fashion along the *c* axis (Fig. 2 bottom and S1†). In the two directions, two sets of intermolecular interactions dominate the crystal packing; along the *b* axis the  $\text{C3-H2}\cdots\text{X}$  ( $\text{X} = \text{Cl}$  or  $\text{Br}$ ) hydrogen bonds link the neighbouring polymeric units, whilst along the crystallographic *c* axis the 1-D chains are mutually connected *via*  $\text{C-X}\cdots\text{X}'\text{-Cd}$  halogen bonds and supported by  $\text{C4-H3}\cdots\text{X-Cd}$  and  $\text{C5-H4}\cdots\text{X-C}$  hydrogen bonds.

On the other hand, a closer inspection of the crystal packing (**1–3**) in the directions perpendicular to the potential bending faces (*i.e.* the crystal faces that are parallel to the elongation of the polymeric chains,  $011/0\bar{1}\bar{1}$  and  $0\bar{1}\bar{1}/011$ ) revealed an almost identical arrangement of the polymeric units and intermolecular interactions (indicated by pale-orange double arrows, Fig. 2). This consequently resulted in two sets of equally developed potential bending faces (Fig. 2 and S2, S4 and S6†).

### Examining mechanical flexibility

The mechanical properties of **1–3** were examined *via* a modified three-point bending procedure. For this purpose, several crystals (*i.e.* at least ten crystals) of each compound (**1–3**) were extracted from a few different batches. Selected crystals were immersed in paratone oil to avoid damage by metalware during the application of the force. Each crystal was supported by a pair of metal tweezers from one side, while the mechanical force was applied by using a metal needle from the opposite one. The experiment revealed that crystals of all three materials (**1–3**) could be bent repeatedly without gaining any visible damage as long as the maximal crystal curvature was not exceeded. Once the crystals were bent over the “critical radius”, they broke. In addition, the experiment clearly showed distinctly different flexibility for crystals of **1** and **3**, and crystals of **2**. While crystals of **1** and **3** could be bent pronouncedly, the crystals of **2** tolerated the application of the force to a substantially smaller extent (Fig. 3 movies 1–3). To confirm the observation and to eliminate any impact of the crystal dimensions (*i.e.* length and thickness) on crystal bending, the extent of elastic responses was quantified using the Euler-Bernoulli equation and expressed as bending strain,  $\epsilon$ .<sup>39</sup> For each sample, ten representative measurements along with the average bending strain values are presented in Tables S3–S5 in the ESI† (see also Fig. S3, S5 and S7). The calculated bending strain was found to be the smallest for **2** ( $\epsilon = 0.47\%$ ) and somewhat larger for **1** and **3** (**1**:  $\epsilon = 0.71\%$ , **3**:  $\epsilon = 0.59\%$ ), indicating the least adaptability of **2** to applied external mechanical force. Moreover, for all three materials, the crystals displayed no noticeable difference in elasticity regardless of the pairs of prominent crystal faces ( $011/0\bar{1}\bar{1}$  or  $0\bar{1}\bar{1}/011$ ) to which the mechanical force was exerted, indicating that they are two-directionally (2-D) flexible crystals.

Despite the fact that all three materials (**1–3**) were elastic, another clear difference between the crystals of **1** and **3** *vs.* crystals of **2** was observed, and it was noticeable just close to the point of crystal breakage. Although all the crystals **1–3** showed purely elastic responses at a smaller curvature, the

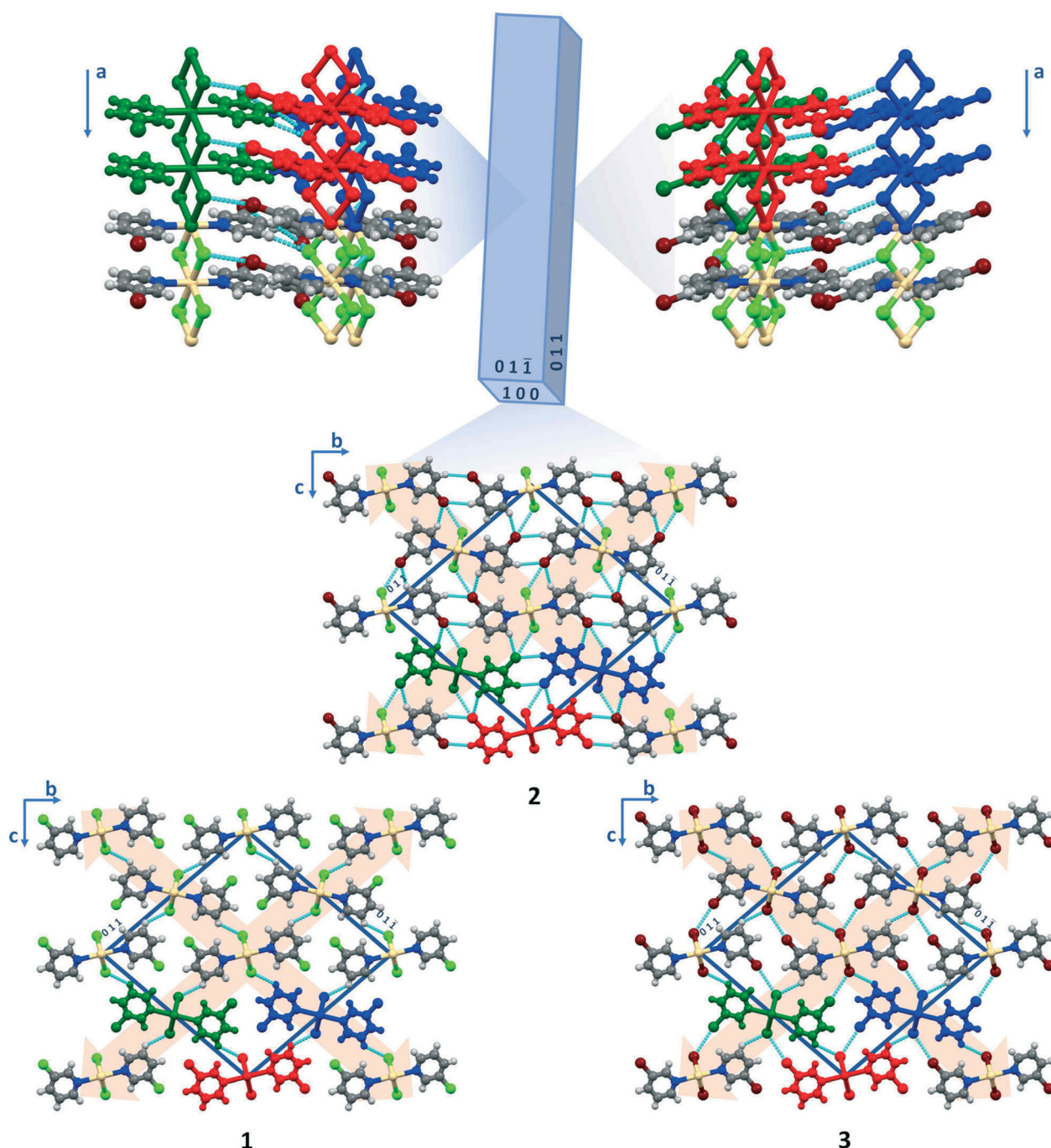


Fig. 2 Crystal packing of 2 (top), 1 (bottom left) and 3 (bottom right). Intermolecular interactions that are shorter than the sum of van der Waals radii are coloured light blue. In all three compounds, 1-D polymeric chains are arranged in a parallel fashion along the  $b$  axis and in an antiparallel fashion along the  $c$  crystallographic axis, resulting in almost identical structural arrangement in (potential) bending directions (indicated by pale orange double-arrows, bottom/middle rows) that in turn made the crystals two-directionally (2-D) mechanically responsive.

crystals of 1 and 3 displayed a slight plastic deformation only close to the breakage point (Fig. 3 bottom left/bottom right; movies 1 and 3) that was further displayed in slightly plastically deformed crystal ends after crystal breakage (Fig. 3 movies 1 and 3 and S4 and S8<sup>†</sup>). Therefore, we categorized the crystals of 1 and 3 as borderline cases of elastically flexible crystals, *i.e.* displaying *elastic*→*plastic* behaviour. On the other hand, crystals of 2 did not go through

any plastic regime during bending; broken parts of the crystal were straight, without any visible permanent deformation (Fig. 3 bottom middle; movie 2 and S6<sup>†</sup>); they display a slightly elastic response with a typical brittle breakage.

To further examine the difference in the adaptability of 1–3 to external mechanical force and to shed light on the observation, additional experiments were set. The crystals were mounted with both ends fixed and the force was applied



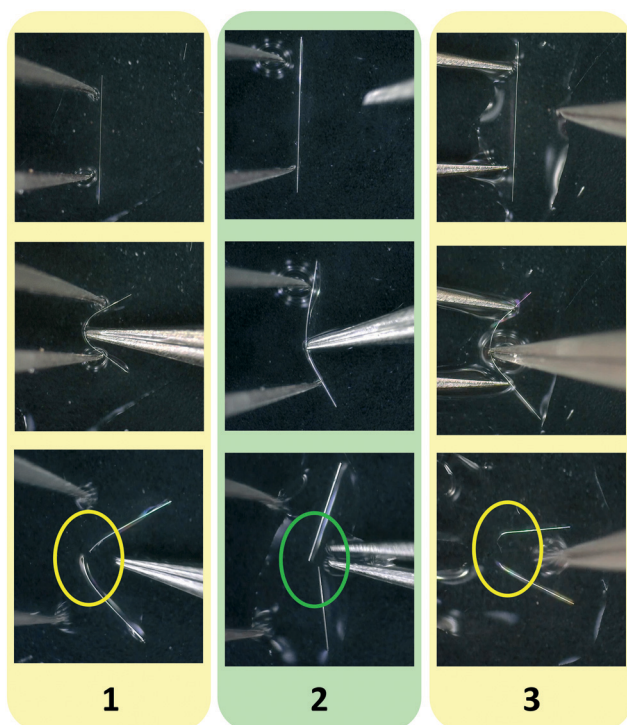


Fig. 3 Comparison of crystals 1–3 displaying brittle (green oval) and slightly plastically deformed (yellow ovals) crystal ends after breakage.

perpendicular to the direction of the largest crystal dimension. The crystal ends were glued to the glass supports to hold the crystals in air during the whole experiment, thus eliminating any impact of the medium (*i.e.* oil) or the surface–crystal friction. Several crystals of each material (1–3) of approx. the same length and thickness were selected, mounted, and the mechanical force was applied in a controlled fashion, by moving the pair of tweezers (with both ends kept together) at regular increments and constant velocity. All the crystals (1–3) showed typical elasticity at relatively small distances travelled by the tips of the metal tweezers (distance  $h$ , Fig. 4); the crystals slightly elongated upon the application of the force and returned to their initial shape and length once the force was removed (movies 4–6). Here as well, 1 and 3 displayed better adaptability to the external force than 2, tolerating a larger distance (*i.e.* ‘critical distance’,  $h$ ) travelled by the tweezers’ tips prior to crystal breakage (movies 4 and 6). But once the ‘critical distance’ was exceeded, the crystals broke with a noticeable elongation of the crystals of 1 and 3 (Fig. 4 bottom left and bottom right), while any elongation of the crystals of 2 was not observed upon crystal breakage (Fig. 4 bottom middle; movie 5).

### Atomic force microscopy

To provide further details on the observed differences in the flexible responses of 1–3 (*i.e.* *elastic*→*plastic* vs. slight elasticity with a typical brittle breakage), and to examine if there is any correlation between the mechanical responses and crystals’

properties at a microscopic level, we performed atomic force microscopy (AFM) experiments. Crystals (1–3) in their original, straight shape were glued on the metal discs and probed with the AFM tip on their dominant faces (*i.e.* faces parallel to the elongation of the crystal). The Young’s moduli were obtained, and are tabulated in Table S6† and presented in Fig. 5 and 6c.

Interestingly, even such small differences in compliances, as observed for our samples, were clearly reflected in their Young’s modulus values. The crystals of 2, the material that showed the least adaptability to applied external mechanical pressure and without going through any plastic regime prior to crystal breakage (*i.e.* being slightly elastic and presenting a typical brittle breakage) displayed the largest value of Young’s modulus, 9.50 GPa, thus confirming the highest degree of stiffness of all the three tested samples. On the other hand, the crystals of 1 and 3 that were more elastically bendable to the applied mechanical force, displaying a minor, but clearly observed plastic regime close to the breakage point (*i.e.* displaying *elastic*→*plastic* behaviour), presented lower Young’s modulus values, 3.58 GPa (1) and 4.55 GPa (3), being softer than 2. Moreover, a tendency towards a negative correlation between Young’s moduli and calculated bending strain for the three samples (1–3) was also clearly noticed (Fig. 5).

### Computational studies

To gain deeper insight into the origin of the observed variations in responses to the external mechanical force of the three examined isostructural materials 1–3 and to rationalize the difference in their mechanical behaviour within the interaction energy framework, DFT calculations were performed. To identify the regions comprising the weakest supramolecular links, as these were recently considered as regions that might govern mechanical responses of crystalline coordination polymers, in particular plastic responses,<sup>9,40</sup> we calculated the interaction energies between adjacent molecular fragments for 1–3.

For calculation of the interaction energies, two models were considered, a simpler one comprising single pairs, Fig. 6a, and a somewhat more complex one involving double pairs of adjacent molecular fragments (1–3), Fig. 6b. For both models, two molecular pairs were identified (red–green pairs, as presented in Fig. 6a and b), each involving a different set of intermolecular interactions (labelled as **A** and **B** in the single-pair model, and **C** and **D** in the double-pair model).‡ Since the selection of molecular fragments consequently determines the regions comprising intermolecular interactions of interest

‡ In the single-pair model, each 1-D coordination polymer (taken as an electroneutral finite molecule made of three Cd(II) centres) interacts with only one closest neighbour, thus constructing a molecular pair (red–green; Fig. 5a) for which the interaction energy was then calculated. Two single pairs were identified and referred to as **A** and **B**. In the double pair model, two interacting fragments (red and green) are each comprised of one pair of 1-D coordination polymers (two green and two red molecules). The two double pairs are labelled as **C** and **D**.

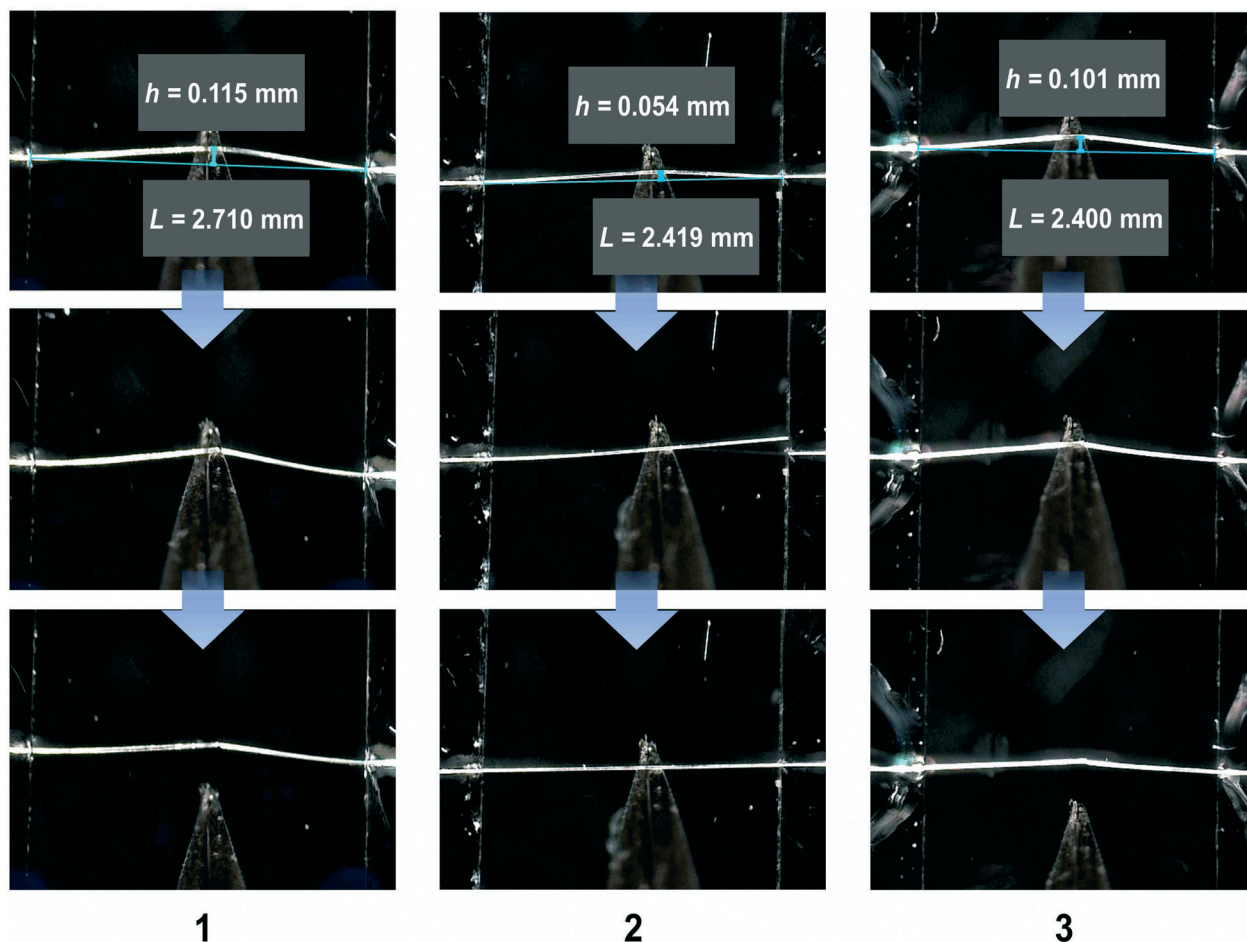


**Fig. 4** Different elasticity of 1–3. The crystals, with two ends glued on the glass holders, were kept in air while the force was applied perpendicular to the direction of the longest crystal dimension. All three materials displayed noticeable elasticity of crystals upon application of the force, being fairly prominent in 1 and 3.

(depicted as dotted lines; single-pair model: red/green, double-pair model: orange/blue), we have calculated the interaction energies for all four selected pairs. The interaction energies for the two single pairs and two double pairs in 1–3 and I–IV are presented in the diagrams in Fig. 6a and b (bottom), respectively.

Of all four regions (single pairs and double pairs; A–D), only C defines the region of intermolecular interactions that spreads parallel/perpendicular to the crystal faces, thus being the region of utmost interest. The other three regions (A, B, D) present regions slanted to crystal faces, consequently having only a supportive role. While A and D describe the same region, with D only comprising an extended set of the same intermolecular interaction as A (subsequently reflected in an analogous trend of the interaction energies), B is ruled out (and not taken into further consideration) as it does not represent an outspread region of intermolecular interactions solely (it, in fact, comprises molecular building units/fragments in the adjacent layers).

Focusing on the regions C and A/D in 1–3, it is clearly visible that the material with the least adaptable crystals to external mechanical force (2), *i.e.* the smallest bending strain

value ( $\varepsilon = 0.47\%$ ), displays the strongest interaction energies for both regions under consideration. On the other hand, the materials that are more adaptable to external pressure (1:  $\varepsilon = 0.71\%$ ; 3:  $\varepsilon = 0.59\%$ ), which display a plastic regime close to the breakage point, have visibly smaller calculated interaction energies (C and A/D). Moreover, the adaptability to external force (expressed in the bending strain,  $\varepsilon$ ) and the calculated interaction energies for the three CPs (1–3) reflect a strongly negative correlation (Fig. 6).

Furthermore, the stronger interaction energies are also reflected in the larger values of Young's moduli ( $E$ ), making the crystals stiffer and consequently less tolerant to the application of the external force.

### The bending strain–stiffness interaction energy correlation

To shed more light on the observed variability in mechanical responsiveness of 1–3 and to gain a deeper understanding of the overall phenomenon of mechanically stimulated adaptability of CPs, we compared the mechanical behaviour of 1–3 with the behaviour of an additional four recently published isostructural CPs (labelled as I–IV, Fig. 6).<sup>37</sup>

## CrystEngComm

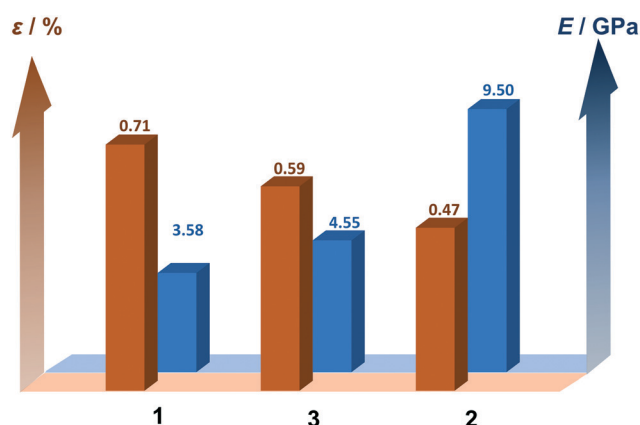


Fig. 5 A comparison of Young's moduli,  $E$ , (blue) and bending strain,  $\epsilon$ , (orange) for 1–3 reveals a trend towards a negative correlation between the two quantities.

Consequently, we have obtained in hand the whole spectrum of diverse mechanical responses (Fig. 6), going from extreme pliability (II, I), via regularly observed plasticity (III), substantial elasticity with a noticeable plastic regime close to the breakage points (1 and 3: *elastic*→*plastic*), to relatively slight elasticity with a typical brittle crystal breakage (IV, 2: slightly elastic). Subsequently, we rationalized these experimental observations against the backdrop of the calculated interaction energies as well as Young's moduli (1–3, I–IV). To help with the rationalization, the seven materials were organized into three groups according to their mechanical responses, plastically responsive materials (I–III; pale red background), materials displaying elastic responses with a slight plastic regime close to the breakage point (1 and 3, *elastic*→*plastic*; pale yellow background), and materials with sole elastic response (2 and IV, slightly elastic; pale green background).

Surprisingly, the tendency towards positive correlations between interaction energies and Young's modulus values observed for 1–3 becomes even more obvious when the whole spectrum of the mechanical observations, presented by the seven CPs, was taken into consideration (Fig. 6 bottom). More interestingly, the tendency spreads regularly over the whole range of the diverse mechanical responses presented by the seven examined materials. The most compliant materials, positioned at one end of the spectrum, displayed smaller values of Young's moduli as well as of the calculated interaction energies (for both regions C and A/D). On the other hand, the least adaptable materials, characterizing the opposite end of the spectrum, were associated with the largest values of both Young's moduli and interaction energies. These findings clearly indicated that the stiffer materials are expected to be less adaptable to applied mechanical force and that the crystal adaptability (observed for isostructural CPs) is controlled by intermolecular interactions; the stronger the interactions, the stiffer the crystals and consequently the less adaptable the crystals are to external mechanical influences.

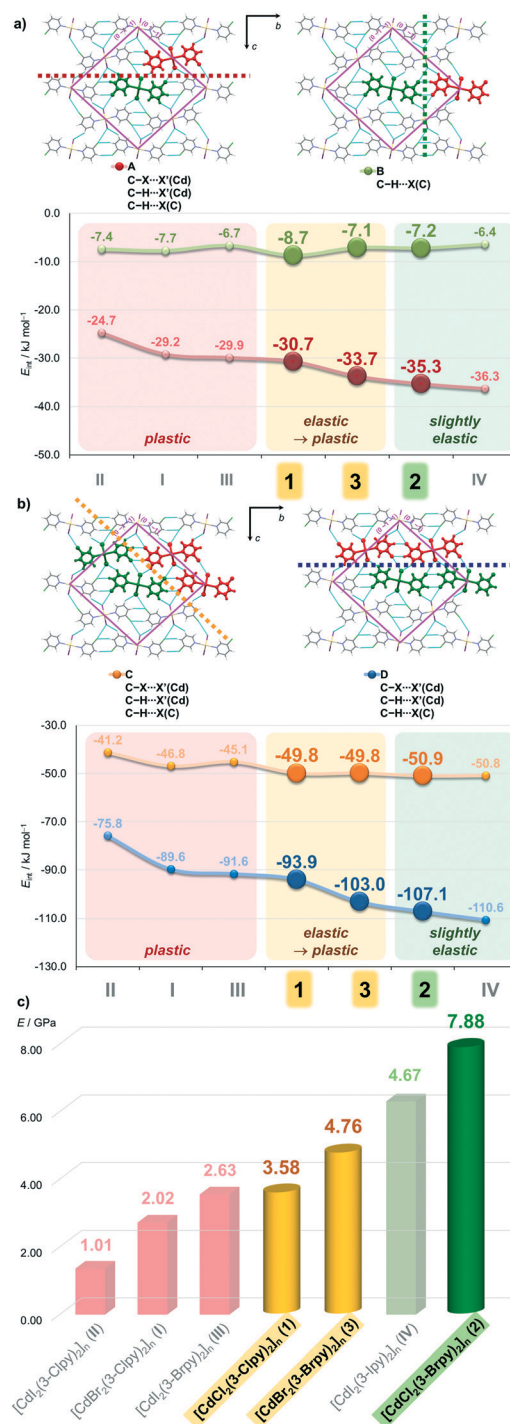


Fig. 6 (a) Single-pair and (b) double-pair of molecular fragments (red-green) marked in the isostructural compounds (1–3). Dotted lines represent the regions of intermolecular interactions parallel (orange) or diagonal (red, green, blue) to crystal faces (magenta solid lines). The M06-2X/DGDZVP interaction energies calculated for molecular interactions (A–D) between molecular fragments (red-green). The calculated energies were complemented by the analogous data taken from ref. 37. (c) The experimentally determined Young's moduli for the straight crystals of 1–3. The data were complemented by analogous ones taken from ref. 37.



## Conclusions

Having in hand crystals of a family of isostructural coordination polymers (CPs) (1–3), which displayed slight but clearly noticeable differences in their adaptability to external mechanical stimuli, enabled us to provide a deeper understanding of the relevance of intermolecular interactions in furnishing coordination polymers with a specific mechanical response (Fig. 7).

Although the differences in the mechanical behaviour (1–3) were small but visibly distinct, they were nicely supported by clear differences in the calculated interaction energies as well as by differences in Young's moduli. Moreover, the experimental findings for 1–3, together with their calculated interaction energies and Young's moduli, complemented the previously reported diversity of mechanical responses for additional isostructural CPs surprisingly well. This in turn made a whole spectrum of diverse mechanical responses which consequently allowed a straightforward rationalization of the experimental observation in the context of crystal stiffness and energetic features.<sup>37</sup> The crystal adaptability of this series of isostructural CPs to external mechanical stimuli showed to have a correlation with the strength of intermolecular interactions; the stronger the interactions, the stiffer the crystals and consequently the less adaptable the crystals are to external mechanical influences. Moreover, the interaction energies were also reflected in Young's modulus values ( $E$ ); the stronger the interactions the larger the Young's modulus values, which in turn made the crystals stiffer and consequently less tolerant to the application of the external force.

This remarkable spectrum of mechanical responsiveness of crystalline coordination polymers indicates that the mechanical properties of crystals may be much more alike to the analogous properties of other (softer) materials than was previously anticipated. Moreover, the findings provided by this isostructural family of CPs, namely the tendency towards the bending–stiffness–energy correlations, will provide engineering of crystalline materials with a desired mechanical output.

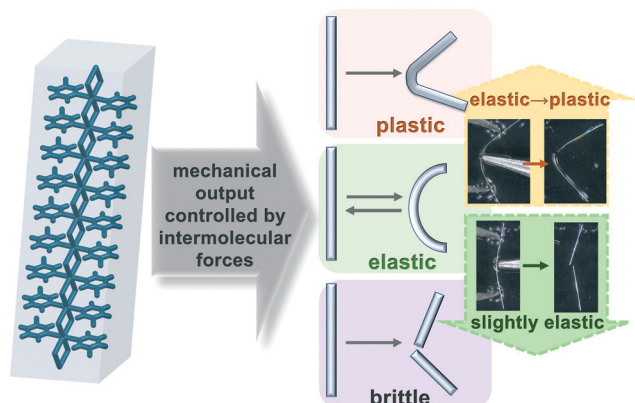


Fig. 7 Mechanical output of isostructural coordination polymers (CPs) controlled exclusively by the intermolecular interactions.

## Experimental section

### Materials

Cadmium(II) salts ( $\text{CdCl}_2 \cdot \text{H}_2\text{O}$  and  $\text{CdBr}_2 \cdot 4\text{H}_2\text{O}$ ) and the ligands, 3-chloropyridine and 3-bromopyridine, as well as solvents, were purchased from commercial suppliers and used without further purification.

### Growing crystals

Crystals of  $[\text{CdCl}_2(3\text{-Clpy})_2]_n$  (1),  $[\text{CdCl}_2(3\text{-Brpy})_2]_n$  (2), and  $[\text{CdBr}_2(3\text{-Brpy})_2]_n$  (3) were prepared by layering an aqueous solution of cadmium(II) salt with 1 mL of ethanol, and then with an ethanol solution of ligand. The resulting test tubes were sealed using parafilm and left undisturbed. After a week, a few holes were punctured in the parafilm to allow slow evaporation. White needle-like crystals of the required quality for testing mechanical properties were harvested after a few weeks.

### Crystal bending experiments and quantification

Crystal bending experiments were performed using a modified three-point bending procedure (for details see the ESI†). From several batches of each compound (1), crystals were selected, placed on a glass slide, and immersed in a small amount of paratone oil to prevent damage to the crystal by metal accessories. The crystal was held from one side with a pair of metal tweezers while the mechanical force was applied from the opposite side using a metal needle. The mechanical force was applied on both pairs of the most prominent crystal faces (the faces parallel to the elongation of the crystal) to determine the relationship between the direction of the applied mechanical force and the nature and/or extent of the mechanical response. All the bending experiments were carried out using a Dino-Lite Edge digital microscope (model AM4815ZT), and the recordings were taken and processed using DinoCapture 2.0 software (version 1.5.28.D).

The elastic responses of crystals 1–3 were quantified by calculating the bending strain ( $\epsilon$ ) from the Euler–Bernoulli equation (considering pure bending without shear component). For more details see the ESI†<sup>39</sup>

### Ductility testing

Selected, straight crystals of 1–3 were mounted on a glass slide with their ends glued with superglue. The mechanical force was applied to the mid-point of the length of the crystal, using a pair of tweezers (with their ends kept together), in steps of  $15 \mu\text{m}$  and a constant speed of  $100 \mu\text{m s}^{-1}$ . The mechanical force was applied to a crystal until its breakage.

### AFM measurements

AFM mechanical measurements were performed at room temperature on a commercial MultiMode 8 AFM instrument (Bruker). NCHV-A silicon probes (Bruker, resonance frequency

320 kHz, spring constant  $42 \text{ N m}^{-1}$ ) were used to determine the mechanical properties of the straight crystals 1–3. The deflection sensitivity of the cantilever was estimated from the slope of the loading curve obtained on a sapphire sample and the spring constant was calibrated according to the Sader method.<sup>41</sup> Reference measurements on a polystyrene standard sample (PSFILM-12M, Bruker,  $E = 2.70 \text{ GPa}$ ,  $\nu = 0.34$ ) were used to estimate the tip radius (the nominal tip radius is 8 nm and estimated tip radius values were in the range from 5 nm to 10 nm).

Freshly prepared crystals were extracted from the solution and glued in their original form on the metal disks. Force–separation curves were acquired using NanoScope software v9.7 in the force volume mode, where the matrix of  $32 \times 32$  force curves was obtained on the crystal surface. To ensure the reproducibility and statistical significance of the results the measurements were conducted on several crystal samples of each compound (1–3). Data analyses were performed using NanoScope Analysis v2.0 (Bruker). The Young's moduli of the samples were estimated from fitting individual force–separation curves on the Hertzian model ( $R^2$  were approx. 0.95).<sup>42</sup>

### Computational details

Interaction energies were calculated in Gaussian16 (ref. 43) with the M06-2X/DGDZVP method, which performs very well for the calculation of halogen-bond strengths among DFT methods with small basis sets.<sup>44</sup> All geometries were cut out from the crystal structure in Mercury<sup>45</sup> and all C–H bonds were normalized before the calculation of interaction energies for four different types of interactions (A–D). Each adjacent 1-D chain was represented as an electroneutral molecule consisting of three Cd(II) centres (see ESI† for more details). Pairwise interaction energies between selected single pairs and double pairs (depicted as red and green in Fig. 3) were calculated and corrected by basis set superposition errors (BSSE) according to the counterpoise method of Boys and Bernardi.<sup>46,47</sup> All the calculated values are divided by three to obtain the normalized interaction energies per one metal centre.

### Author contributions

M. P. and M. Đ. conceived the research and wrote the paper with the input of all authors; M. P. performed the synthesis, crystallization experiments, and mechanical measurements; I. B. and M. P. performed the AFM measurements; I. K. performed computational studies and analysed the data. All authors have given approval to the final version of the manuscript.

### Conflicts of interest

There are no conflicts to declare.

### Acknowledgements

This work has been fully supported by the Croatian Science Foundation under Project IP-2019-04-1242. The support of project CluK co-financed by the Croatian Government and the European Union through the European Regional Development Fund – Competitiveness and Cohesion Operational Programme (Grant No. KK.01.1.1.02.0016) is acknowledged.

### Notes and references

- 1 A. M. C. Coenen, K. V. Bernaerts, J. A. W. Harings, S. Jockenhoevel and S. Ghazanfari, *Acta Biomater.*, 2018, **79**, 60.
- 2 Y. Wang, L. Sun, C. Wang, F. Yang, X. Ren, X. Zhang, H. Dong and W. Hu, *Chem. Soc. Rev.*, 2019, **48**, 1492.
- 3 M. Annadhasan, S. Basak, N. Chandrasekhar and R. Chandrasekhar, *Adv. Opt. Mater.*, 2020, **8**, 2000959.
- 4 M. Annadhasan, D. P. Karothu, R. Chinnasamy, L. Catalano, E. Ahmed, S. Gosh, P. Naumov and R. Chandrasekhar, *Angew. Chem.*, 2020, **59**, 13821.
- 5 H. Souri, H. Banerjee, A. Jusufi, N. Radacsi, A. A. Stokes, I. Park, M. Sitti and M. Amjadi, *Adv. Intell. Syst.*, 2020, **2**, 2000039.
- 6 P. Naumov, S. Chizhik, M. K. Panda, N. K. Nath and E. Boldyreva, *Chem. Rev.*, 2015, **115**, 12440.
- 7 P. Naumov, D. P. Karothu, E. Ahmed, L. Catalano, P. Commins, J. M. Halabi, M. B. Al-Handawi and L. Li, *J. Am. Chem. Soc.*, 2020, **142**, 13256.
- 8 S. Das, A. Mondal and C. M. Reddy, *Chem. Soc. Rev.*, 2020, **49**, 8878.
- 9 S. Saha, M. K. Mishra, C. M. Reddy and G. R. Desiraju, *Acc. Chem. Res.*, 2018, **51**, 2957.
- 10 C. M. Reddy, R. C. Gundakaram, S. Bisavoju, M. T. Kirchner, K. A. Padmanabhan and G. R. Desiraju, *Chem. Commun.*, 2005, 3945.
- 11 C. M. Reddy, K. A. Padmanabhan and G. R. Desiraju, *Cryst. Growth Des.*, 2006, **6**, 2720.
- 12 M. K. Panda, S. Gosh, N. Yasuda, T. Mariwaki, G. D. Mukherjee, C. M. Reddy and P. Naumov, *Nat. Chem.*, 2015, **7**, 65.
- 13 G. R. Krishna, R. Devarapalli, G. Lal and C. M. Reddy, *J. Am. Chem. Soc.*, 2016, **138**, 13561.
- 14 S. P. Thomas, M. W. Shi, G. A. Koutsantonis, D. Jayatilaka, A. J. Edwards and M. A. Spackman, *Angew. Chem., Int. Ed.*, 2017, **56**, 8468.
- 15 S. Saha and G. R. Desiraju, *Chem. Commun.*, 2017, **53**, 6371.
- 16 S. Saha and G. R. Desiraju, *Chem. – Eur. J.*, 2017, **23**, 4936.
- 17 U. B. R. Khandavilli, B. R. Bhogala, A. R. Maguire and S. E. Lawrence, *Chem. Commun.*, 2017, **53**, 3381.
- 18 L. O. Alimi, P. Lama, V. J. Smith and L. J. Barbour, *Chem. Commun.*, 2018, **54**, 2994.
- 19 L. Catalano, D. P. Karothu, S. Schramm, E. Ahmed, R. Rezgui, T. J. Barber, A. Famulari and P. Naumov, *Angew. Chem., Int. Ed.*, 2018, **57**, 17254.
- 20 S. Hu, M. K. Mishra and C. C. Sun, *Chem. Mater.*, 2019, **31**, 3818.



- 21 A. Paikar, D. Podder, S. R. Chowdhury, S. Sasmal and D. Halder, *CrystEngComm*, 2019, **21**, 589.
- 22 P. Gupta, S. Allu, D. P. Karothu, T. Panda and N. K. Nath, *Cryst. Growth Des.*, 2021, **21**, 1931.
- 23 C. Cappuccino, L. Catalano, F. Marin, G. Dushaq, G. Raj, M. Rasras, R. Rezgui, M. Zambianchi, M. Melucci, P. Naumov and L. Maini, *Cryst. Growth Des.*, 2020, **20**, 884.
- 24 K. Wang, M. K. Mishra and C. C. Sun, *Chem. Mater.*, 2019, **31**, 1794.
- 25 S. Ghosh and M. C. Reddy, *Angew. Chem., Int. Ed.*, 2012, **51**, 10319.
- 26 S. Ghosh, M. K. Mishra, S. B. Kadambi, U. Ramamurty and G. R. Desiraju, *Angew. Chem., Int. Ed.*, 2015, **54**, 2674.
- 27 P. Gupta, D. P. Karothu, E. Ahmed, P. Naumov and N. K. Nath, *Angew. Chem., Int. Ed.*, 2018, **57**, 8498.
- 28 S. Saha and G. R. Desiraju, *Chem. Commun.*, 2018, **54**, 6348.
- 29 H. Liu, Z. Lu, Z. Zhang, Y. Wang and H. Zhang, *Angew. Chem., Int. Ed.*, 2018, **57**, 8448.
- 30 H. Liu, Z. Bian, Q. Cheng, L. Lan, Y. Wang and H. Zhang, *Chem. Sci.*, 2019, **10**, 227.
- 31 S. Dey, S. Das, S. Bhunia, R. Chowdhury, A. Mondal, B. Bhattacharya, R. Devarapalli, N. Yasuda, T. Moriwaki, K. Mandal, G. D. Mukherjee and C. M. Reddy, *Nat. Commun.*, 2019, **10**, 3711.
- 32 A. Worthy, A. Grosjean, M. S. Pfrunder, Y. Xu, C. Yan, G. Edwards, J. K. Clegg and J. B. McMurtrie, *Nat. Chem.*, 2018, **10**, 65.
- 33 N. Hearne, M. M. Turnbull, C. P. Landee, E. M. van der Merve and M. Redmeyer, *CrystEngComm*, 2019, **21**, 1910.
- 34 M. Đaković, M. Borovina, M. Pisačić, C. B. Åakeröy, Ž. Soldin, B.-M. Kukovec and I. Kodrin, *Angew. Chem., Int. Ed.*, 2021, **57**, 14801.
- 35 B. B. Rath and J. J. Vittal, *Chem. Mater.*, 2021, **33**, 4621.
- 36 B. Bhattacharya, A. A. L. Michalchuk, D. Silbernagl, M. Rautenberg, T. Schmid, T. Feiler, K. Reimann, A. Ghalgaoui, H. Sturm, B. Paulus and F. Emmerling, *Angew. Chem.*, 2020, **59**, 5557.
- 37 M. Pisačić, I. Biljan, I. Kodrin, N. Popov, Ž. Soldin and M. Đaković, *Chem. Mater.*, 2021, **33**, 3660.
- 38 C. Hu, Q. Li and U. Englert, *CrystEngComm*, 2003, **5**, 519.
- 39 S. Timoshenko, *Strength of materials Part 1*, D. Van Nostrand Company, New York, 1940, pp. 88–127.
- 40 C. M. Reddy, G. R. Krishna and S. Gosh, *CrystEngComm*, 2010, **12**, 2296.
- 41 J. E. Sader, J. W. M. Chon and P. Mulvaney, *Rev. Sci. Instrum.*, 1999, **70**, 3967.
- 42 H. J. Hertz, *J. Reine Angew. Math.*, 1881, **92**, 156.
- 43 *Gaussian 16, Revision C.01*, ed. M. J. Frisch, G. W. Trucks, H. B. Schlegel, G. E. Scuseria, M. A. Robb, J. R. Cheeseman, G. Scalmani, V. Barone, G. A. Petersson, H. Nakatsuji, X. Li, M. Caricato, A. V. Marenich, J. Bloino, B. G. Janesko, R. Gomperts, B. Mennucci, H. P. Hratchian, J. V.A. Ortiz, F. Izmaylov, J. L. Sonnenberg, D. Williams-Young, F. Ding, F. Lipparini, F. Egidi, J. Goings, B. Peng, A. Petrone, T. Henderson, D. Ranasinghe, V. G. Zakrzewski, J. Gao, N. Rega, G. Zheng, W. Liang, M. Hada, M. Ehara, K. Toyota, R. Fukuda, J. Hasegawa, M. Ishida, T. Nakajima, Y. Honda, O. Kitao, H. Nakai, T. Vreven, K. Throssell, J. A. Montgomery Jr., J. E. Peralta, F. Ogliaro, M. J. Bearpark, J. J. Heyd, E. N. Brothers, K. N. Kudin, V. N. Staroverov, T. A. Keith, R. Kobayashi, J. Normand, K. Raghavachari, A. P. Rendell, J. C. Burant, S. S. Iyengar, J. Tomasi, M. Cossi, J. M. Millam, M. Klene, C. Adamo, R. Cammi, J. W. Ochterski, R. L. Martin, K. Morokuma, O. Farkas, J. B. Foresman and D. J. Fox, Gaussian, Inc., Wallingford CT, 2016.
- 44 A. Siiskonen and A. Priimagi, *J. Mol. Model.*, 2017, **23**, 50.
- 45 C. F. Macrae, I. Sovago, S. J. Cottrell, P. T. A. Galek, P. McCabe, E. Pidcock, M. Platings, G. P. Shields, J. S. Stevens, M. Towler and P. A. Wood, *J. Appl. Crystallogr.*, 2020, **53**, 226.
- 46 S. F. Boys and F. Bernardi, *Mol. Phys.*, 1970, **19**, 553.
- 47 S. Simon, M. Duran and J. J. Dannenberg, *J. Chem. Phys.*, 1996, **105**, 11024.

### III

## Two-Dimensional Anisotropic Flexibility of Mechanically Responsive Crystalline Cadmium(II) Coordination Polymers

Mateja Pisačić, Ivan Kodrin, Amanda Trninić, Marijana Đaković

*Chem.Mater.* **23** (2021) 7072–7080

#### Author contributions:

**M. P.** and **M. Đ.** conceived the research and wrote the paper with the input of all authors; **M. P.** and **A. T.** performed the synthesis and crystallization experiments; **M. P.** performed structure determination and mechanical measurements; **M. P.** and **M. Đ.** performed micro-diffraction experiments; **I. K.** performed computational studies and analysed the data.

# Two-Dimensional Anisotropic Flexibility of Mechanically Responsive Crystalline Cadmium(II) Coordination Polymers

Mateja PISAČIĆ, Ivan KODRIN, Amanda TRINIĆ, and Marijana ĐAKOVIĆ\*



Cite This: *Chem. Mater.* 2022, 34, 2439–2448



Read Online

ACCESS |



Metrics & More

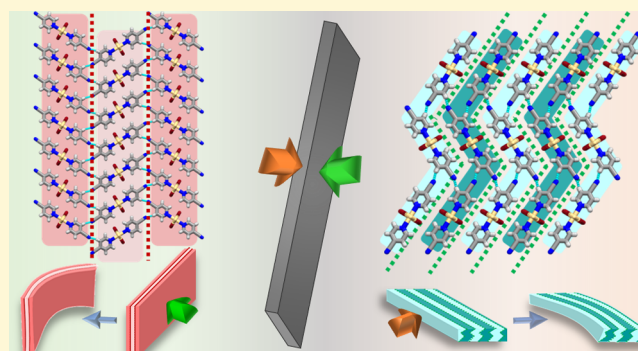


Article Recommendations



Supporting Information

**ABSTRACT:** Crystals of a family of six one-dimensional (1D) coordination polymers of cadmium(II) with cyanopyridines  $[[\text{CdX}_2\text{L}_2]_n]$ , where X = Cl, Br, or I and L = 3-cyanopyridine (3-CNpy) or 4-cyanopyridine (4-CNpy)] presented a variety of morphologies and mechanical responses with dominant two-dimensional (2D) anisotropic flexibility, which has not been previously reported. All mechanically adaptable crystals were 2D flexible and displayed a variety of direction-dependent responses; in addition to 2D isotropic flexibility observed for solely elastic materials, 2D anisotropic flexibility was noticed for both elastic and elastic  $\rightarrow$  plastic crystals. The consequences of fine and controlled structural variations on mechanical behavior were additionally explored via microfocus single-crystal X-ray diffraction and complementary theoretical studies, revealing that the relative strength and direction of the hydrogen bonding interactions were the key parameters in delivering a specific mechanical response.



## INTRODUCTION

Brittleness, a property typically associated with molecular crystalline solids, has long hampered the application of these highly ordered solid-state materials in advanced technologies.<sup>1</sup> Relatively recently, it has been demonstrated that crystalline molecular materials, although quite fragile, under certain circumstances may adapt to a variety of external stimuli (i.e., heat,<sup>2–4</sup> irradiation,<sup>5–7</sup> or pressure<sup>8–15</sup>) while maintaining their integrity, which subsequently categorized them as exceptional candidates for application in emerging technologies (i.e., optical waveguides,<sup>16</sup> electrical conductors,<sup>17,18</sup> and magnetic devices<sup>19</sup>) and introduced the exploration of crystal flexibility to the forefront of solid-state research.

Coordination polymers (CPs), in particular one-dimensional (1D) CPs, emerged as ideal model systems for exploring structural background and underlying principles that lead to flexible responsiveness and control of a targeted mechanical output of crystalline molecular solids. In the first report on the flexibility of 1D crystalline coordination polymers, we have shown that this particular class of materials is capable of displaying exceptional elasticity in response to an applied external mechanical pressure and that the extent of elastic responses could differ within a family of almost identical substances.<sup>20</sup> Moreover, the results showed that the extent of the elastic response may correlate with the importance of intermolecular interactions orthogonal to the direction of spreading of 1D polymeric chains. Furthermore, another family of closely related 1D CPs demonstrated that supramolecular interactions also have a substantial impact on plastic

deformability and that they may be critical for delivering a spectrum of variable flexible responses.<sup>21,22</sup>

In addition, two types of crystal flexibility have also been observed, 1D and two-dimensional (2D), and these were reported for both elastically and plastically bendable crystals.<sup>10,20–22</sup> For 1D flexibility, the crystals were easily bent over only one set of prominent crystal faces (viz. bending faces), and they readily broke when the force was applied to the other set of crystal faces. On the contrary, for 2D flexibility, crystals were equally easy bent over both sets of bending faces, thus displaying isotropic flexible responses. This observation urged us to explore the ability of crystals to display 2D anisotropic flexibility, i.e., being 2D flexible but presenting different extents of responses in two bending directions, as such a property might improve their application potential and performance.

With this in mind, we opted for a family of cadmium(II) coordination polymers with pyridine ligands bearing the cyano functionality. We selected two cyano derivatives, 3-cyanopyridine (3-CNpy) and 4-cyanopyridine (4-CNpy), so that we would have a sufficiently diverse set of 1D CPs to examine a

Received: January 7, 2022

Revised: February 9, 2022

Published: February 18, 2022



potential 2D anisotropy of mechanical responses, and the correlation of those with structural and energy features.

## RESULTS AND DISCUSSION

**Structural Characterization.** By combining three cadmium(II) halides ( $\text{CdX}_2$ , where  $\text{X} = \text{Cl}, \text{Br}, \text{or I}$ ) with two cyano derivatives of pyridine (3-CNpy and 4-CNpy), we were able to deliver crystals of all six CPs with the required morphology and needed quality for testing mechanical behavior, namely,  $[\text{CdCl}_2(3\text{-CNpy})_2]_n$  (1),  $[\text{CdBr}_2(3\text{-CNpy})_2]_n$  (2),  $[\text{CdI}_2(3\text{-CNpy})_2]_n$  (3),  $[\text{CdCl}_2(4\text{-CNpy})_2]_n$  (4),  $[\text{CdBr}_2(4\text{-CNpy})_2]_n$  (5), and  $[\text{CdI}_2(4\text{-CNpy})_2]_n$  (6) (Figure 1).

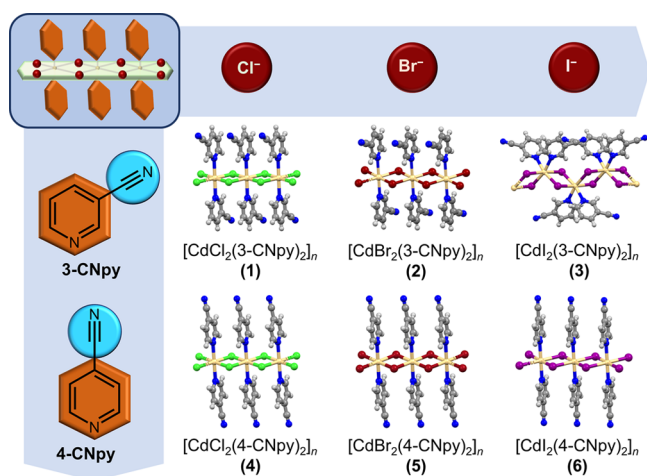


**Figure 1.** Starting ligands [3-cyanopyridine (3-CNpy) and 4-cyanopyridine (4-CNpy)] and produced 1D coordination polymers listed according to the halide anion used for building up the 1D backbone.

Structure determination revealed that all materials crystallize in the monoclinic crystal system, the chlorides (1 and 4) and bromides (2 and 5) in the  $P2_1/c$  space group and the iodide analogues in the  $I2/a$  (3) and  $C2/m$  (6) space groups. The materials (1–6) consist of the intended 1D building units, having cadmium(II) centers doubly bridged by the halide anions, and propagating in the direction of the “short” crystallographic axis (the  $a$  axis for 1–5 and  $b$  axis for 6). The octahedral geometry around the Cd(II) cations is completed by two cyanopyridine ligands bonded in the *trans* orientation in 1, 2, and 4–6 and the *cis* orientation in 3 (Figure 1).

A comparison of the relative orientation of 1D building units in the crystal packing of 1–6 revealed four different types of arrangements (Figure 2). In 1, 1D chains are arranged in a parallel fashion along the crystallographic  $c$  axis and antiparallel along the  $b$  axis, which is like the arrangement observed earlier for two other families of flexible coordination polymers.<sup>20–22</sup> The C–H $\cdots$ N hydrogen bond was found to be the only dominant intermolecular interaction (with the normalized distance  $R_{\text{HX}} < 1$ );<sup>23</sup> it links the neighboring 1D chains from antiparallel layers and runs parallel to potential bending faces (indicated by the green lines), i.e., crystal faces (011)/(0 $\bar{1}\bar{1}$ )/(01 $\bar{1}$ )/(0 $\bar{1}$ 1) (Figure 2, left column, top).

A similar arrangement of the 1D chains was found for three structurally almost identical materials, 2, 4, and 5, with an obvious difference to 1 being displayed in the tilting angle

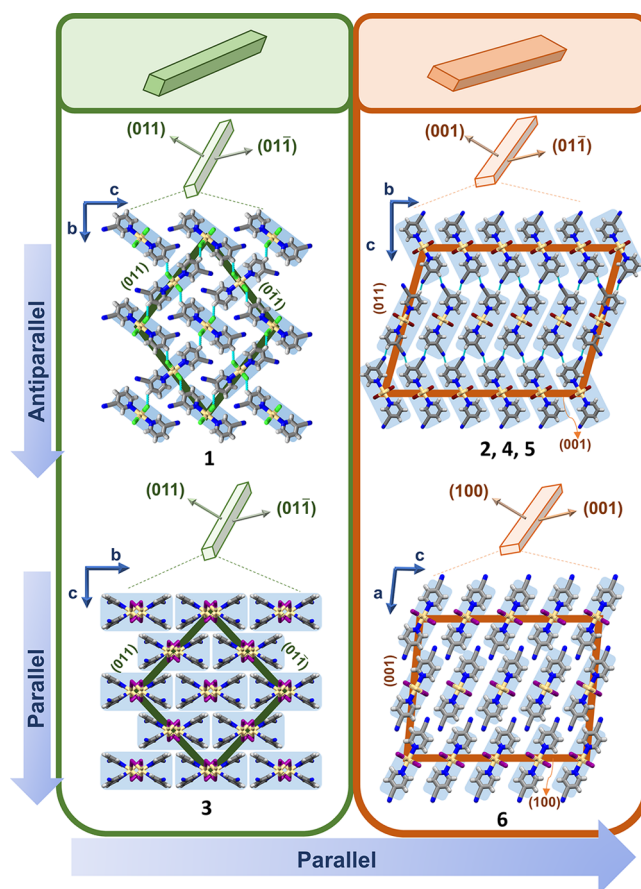


**Figure 2.** Morphologies and crystal packings of 1–6. Two equally developed pairs of prominent crystal faces were observed for 1 and 3 (left column), while differently developed ones were found for 2 and 4–6 (right column). Green (1 and 3) and red (2 and 4–6) thick lines indicate crystal faces that run along the direction of the elongation of the crystal itself. Crystal structures of 2, 4, and 5 (right column, top) are nearly identical.

between the antiparallel layers. Here, in addition to the dominant C–H $\cdots$ N interactions, which link the neighboring 1D chains from antiparallel layers, bifurcated C–H $\cdots$ X(Cd) interactions connecting the neighboring polymeric chains within the parallel 2D layers are also present (Figure 2, right column, top; Figure S2). The two interactions run parallel to the directions indicated by the orange lines representing potential bending faces, i.e., crystal faces (001)/(00 $\bar{1}$ )/(01 $\bar{1}$ )/(0 $\bar{1}$ 1). Both interactions are slightly more influential in 4 than in 2 and 5 ( $2, 0.97 < R_{\text{HX}} < 1.05$ ;  $4, 0.94 < R_{\text{HX}} < 1.04$ ;  $5, 0.95 < R_{\text{HX}} < 1.04$ ).

The 1D building units of the iodide analogues, 3 and 6, on the contrary, arrange in a parallel manner along both crystallographic axes (3,  $b$  and  $c$ ; 6,  $a$  and  $c$ ) perpendicular to the direction of the crystal elongation, i.e., short crystallographic axis (3,  $a$ ; 6,  $b$ ). In 3, the 1D chains are mutually linked via the C–H $\cdots$ N interactions in the  $b$  direction, while in 6, the only noteworthy interactions in the crystal structure are polar interactions between the cyano groups.

**Mechanical Behavior.** In addition to the diversity of arrangements of 1D building units in 1–6, a diversity of morphologies of their acicular crystals were also noticed. While crystals of 1 and 3 displayed equally developed prominent crystal faces, i.e., (011)/(0 $\bar{1}\bar{1}$ )/(01 $\bar{1}$ )/(0 $\bar{1}$ 1) (Figures S17 and



S21), a difference in the dimensions of those of 2 and 4–6, (001)/(00 $\bar{1}$ ) versus (01 $\bar{1}$ )/(0 $\bar{1}$ 1), was clearly visible (Figures S19, S23, S26, and S28 and Figure 2). Moreover, a variety of mechanical responses to external force were also observed for the six substances when their crystals were subjected to testing via a modified three-point bending procedure (Figure 3; for more details, see the Supporting Information).

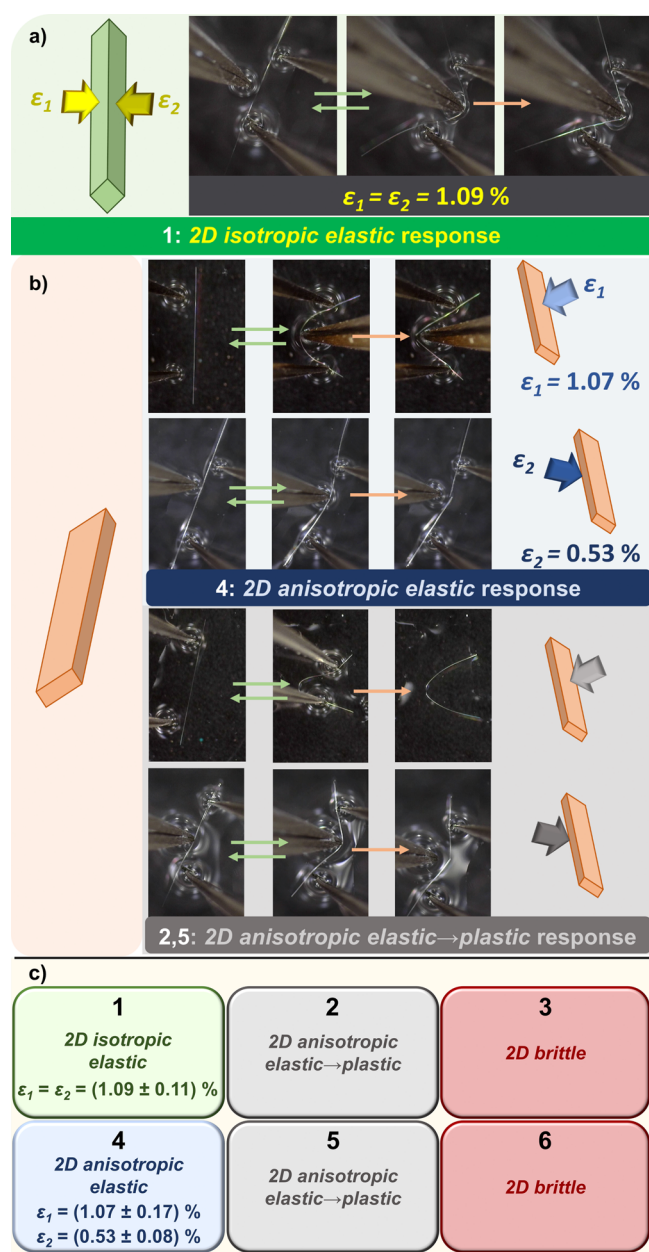


**Figure 3.** Difference in the observed mechanical response. (a) 2D isotropic elastic response of 1. (b) 2D anisotropic elastic response of 4 (light blue background) with different extents of bending in response to the application of force to faces of larger dimensions (top row;  $\epsilon_1 = 1.07\%$ ) and smaller dimensions (bottom row;  $\epsilon_2 = 0.53\%$ ). 2D anisotropic elastic  $\rightarrow$  plastic response (light gray background) of 2 and 5 displaying larger deformation when the stress is applied to faces of larger dimensions (top row) than on faces of smaller dimensions (bottom row). (c) Summary of the observed mechanical responses for crystals of 1–6 together with the bending strain values for elastically bendable crystals.

Crystals of 1 displayed typical elastic behavior. Upon application of the mechanical force, crystals bent and regained their original shape once the force was released (Movie 1). The bending–unbending cycles could be repeated a number of times, but when the maximal curvature was exceeded, the crystals broke (Figure S18). Moreover, no perceptible difference in mechanical output was observed when the force was applied to each of the two pairs of bending faces. This places crystals of 1 in the category of 2D isotropically elastic crystals. The quantification of elastic responses (for details, see the Supporting Information), using the Euler–Bernoulli equation, revealed a substantially large bending strain value ( $\epsilon = 1.09\%$ ), confirming the highly elastic flexibility of 1 (Figure S18 and Table S7). Crystals of 3, on the contrary, were not capable of tolerating external mechanical force in either of the two directions. They immediately broke, thus being classified as 2D brittle (Movie 4 and Figure S22).

As opposed to 1 and 3, crystals of 2 and 4–6, due to their differently developed pairs of potential bending faces, could be best described as very elongated plate-like crystals. Therefore, the responsiveness from both pairs was thoroughly examined and the mechanical output was carefully mapped out. Of four compounds in this group, three displayed nearly the same structure (2, 4, and 5), and we first focused on those three.

Crystals of 4 showed purely elastic responses when bent in both directions but with different extents of elasticity. The crystals were bent to a larger extent when the force was applied to the pair of larger faces [i.e., bending over the thinner bending faces, (001)/(00 $\bar{1}$ ) (Movie 5 and Figure S24)]. On the contrary, when the force was applied to the smaller crystal faces (i.e., bending over the thicker bending faces), (01 $\bar{1}$ )/(0 $\bar{1}$ 1), crystals could tolerate substantially smaller stresses while still displaying an elastic response (Movie 6 and Figure S25). The visual observations were further confirmed by quantification, and two clearly different bending strain values were obtained:  $\epsilon_1 = 1.07\%$  and  $\epsilon_2 = 0.53\%$  for bending over (01 $\bar{1}$ )/(0 $\bar{1}$ 1) and (001)/(00 $\bar{1}$ ) pairs of crystal faces, respectively (Table S8). Because crystals of 4 can be bent in two orthogonal directions with a substantial difference in the bending strain values ( $\Delta\epsilon \approx 0.5\%$ ), they were classified as 2D anisotropically elastic. Moreover, in contrast to previously reported elastic crystals with a clear distinction between the elastic terms, i.e., 1D elastic (being elastically flexible over only one set of bending faces) and 2D elastic [being elastic over both sets of bending faces but with no perceptible difference in bending extent ( $\Delta\epsilon \approx 0\%$ )], here we introduce (an)-isotropy in the 2D term to stress the difference between those two types of 2D elastic behavior, namely, 2D anisotropic elasticity and 2D isotropic elasticity.

In contrast, crystals of the bromide analogues (2 and 5), although having crystal packing almost identical to that of 4, presented somewhat different behavior. Upon exposure, crystals of both 2 and 5 readily adapted to mechanical force resembling the behavior of 4, but upon removal of the force, they could restore their original shape only partially, thus displaying a slight plastic deformation. Surprisingly, similar behavior was observed when the force was applied to both larger, (001)/(00 $\bar{1}$ ), and smaller, (01 $\bar{1}$ )/(0 $\bar{1}$ 1), bending faces but with a clear anisotropy of the extent of bending. Here as well, crystals could be bent substantially more if bent over the thinner [i.e., force exerted on the larger face, (001)/(00 $\bar{1}$ )] then over the thicker face.

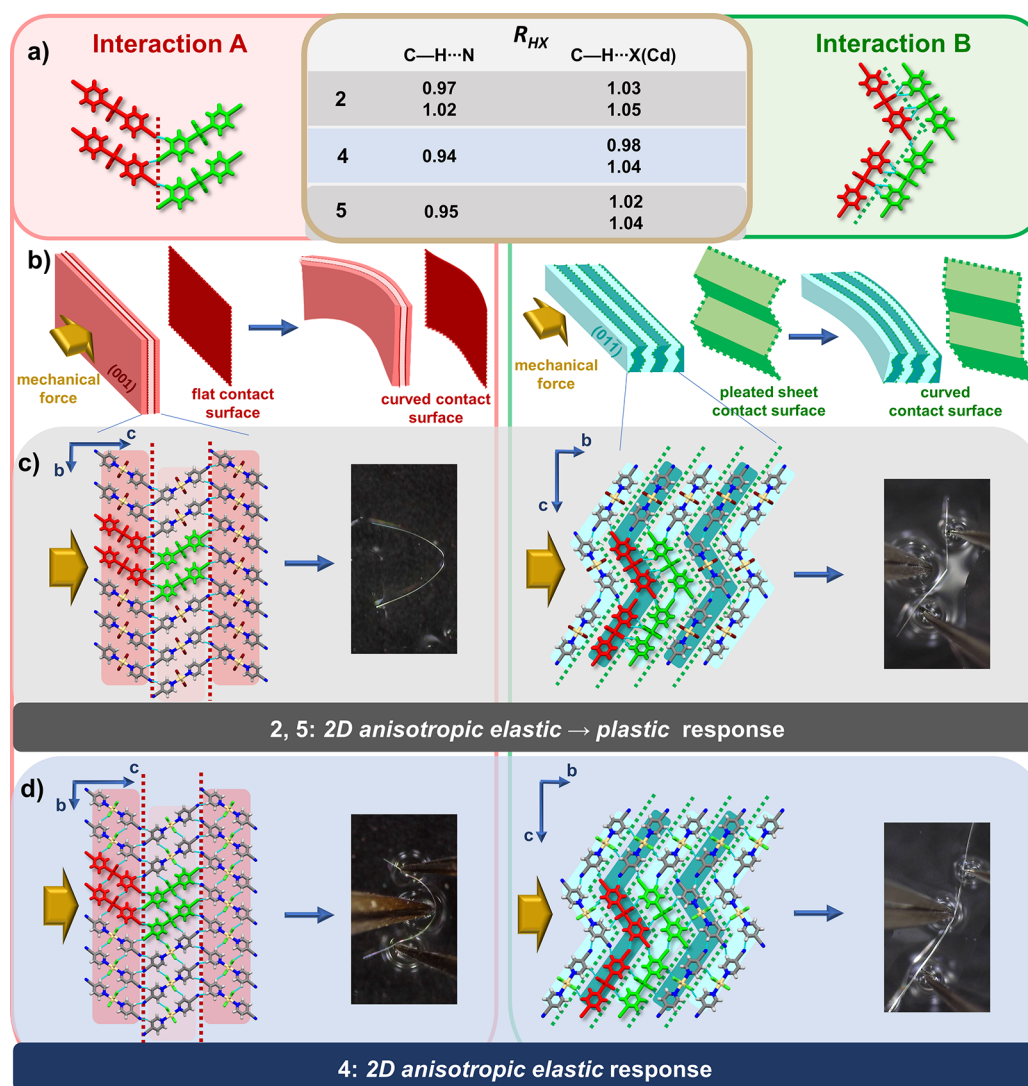


**Figure 4.** (a) Double pairs of 1D polymeric chains, with regions of weak interactions indicated as interaction A (red dotted lines) and interaction B (green dotted lines). The intermolecular interactions shorter than the sum of van der Waals radii are shown as cyan dotted lines and listed in the table with normalized distance  $R_{HX}$  for 2, 4 and 5. (b) Schematic presentation of direction dependent bending process and slicing the crystal up into 2D molecular layers parallel to the larger face (dark/pale red layers), with 2D regions of weak interactions presented as flat red contact surfaces (left), and parallel to the smaller face (dark/pale blue, zigzag layers), with 2D regions of weak interactions presented as green corrugated contact surfaces (right). (c) Crystal structure of 5 (c) and 4 (d) sliced up into 2D molecular layers parallel to crystal faces of larger dimensions face (highlighted with dark/pale red background, left) and smaller dimensions (zigzag layers, highlighted with dark/pale green background, right). Next to the highlighted molecular layers for each compound, the mechanical output of the application of the mechanical force to the respective pair of faces is presented.

Moreover, when bent over both thicker and thinner crystal faces and achieving only smaller curvatures, crystals could restore their unbent shape completely. However, with further application of the mechanical stress, crystals remain permanently deformed, and if bent even more, they finally broke (2, Movie 2 and Figure S20; 5, Movie 7 and Figure S27). When all of the observations are taken into account, it is clear that crystals of 2 and 5 can be categorized as 2D anisotropically elastic → plastic.

Finally, crystals of 6, like those of 3, showed brittle behavior when the force was applied to both pairs of prominent crystal faces (Movies 9 and 10 and Figure S29); thus, crystals of 6 were also 2D brittle.

**Structure–Mechanical Property Correlation.** Of the six examined materials, here we first focused on the three with almost identical crystal packing (2, 4, and 5) as they enabled a

correlation of fine structural details with mechanical behavior. Moreover, the three materials displayed a newly observed directional dependence of crystal adaptability on mechanical stimuli, i.e., 2D anisotropy of mechanical behavior. This was most clearly demonstrated for 4 where the difference in the extent of elasticity was confirmed by quantification ( $\epsilon_1 = 1.07\%$ , and  $\epsilon_2 = 0.53\%$ ) by which the impact of crystal dimensions was eliminated, and what in turn clearly showed that the difference in bending was primarily related to the anisotropy of the structural features in the crystal structure.

To shed more light on the origin of the observed anisotropy of mechanical output, we focused on the fine details in their supramolecular architectures, in particular the details in the regions of weaker interactions parallel to the bending faces. As crystals presented two sets of differently developed bending faces, two regions of weak interactions were identified and

indicated by the red and green dotted lines (Figure 4) and termed as interactions A (forming flat 2D planes) and interactions B (forming corrugated 2D regions), respectively.

In 2, 4, and 5, the same types of intermolecular interactions, namely, C–H...N and bifurcated C–H...X(Cd), materialized but they were of different relative importance. While in the regions parallel to the larger crystal faces only C–H...N interactions were observed (A, red dotted lines), in the regions parallel to the smaller crystal faces (B, green dotted lines) both types were present, making B regions somewhat stronger, which in turn, together with the corrugation of B, caused crystals to be less tolerable to bending over the (01 $\bar{1}$ )/(0 $\bar{1}$ 1) faces.

In addition, two types of 2D anisotropic mechanical responses were also observed within the group of the three materials (2, 4, and 5), 2D anisotropic elastic response (4), and 2D anisotropic elastic  $\rightarrow$  plastic response (2 and 5). If we further focus on the relative importance of each of the two interactions among the three materials, it is easy to notice that in 2 and 5 both interactions are less influential (being longer and less linear) than in 4, which makes layers in 2 and 5 more prone to slip over each other once the critical radius is exceeded, thus displaying elastic  $\rightarrow$  plastic behavior in contrast to solely elastic behavior of 4. This is in line with our previous findings where for the family of isostructural compounds the strength of interactions accounted for the variations in mechanical output, and where the weaker interactions allowed the slippage of neighboring slabs over each other.<sup>21,22</sup>

On the contrary, crystals of 1, while, like 4, being also pronouncedly elastic, were the only 2D isotropically responsive. Although arranged in antiparallel 2D layers as in 4, 1D building units from neighboring layers in 1 were more tilted to each other, which in turn resulted in equally developed crystal faces and an almost identical arrangement of molecular and intermolecular features parallel to bending faces, as well as in the directions of the application of force.

Finally, crystals of 3 and 6 were both 2D brittle. Unfortunately, due to the lack of materials with identical and/or similar crystal packing (as of 3 and 6) within the examined set of compounds, we were not in a position to rationalize their behavior and draw any conclusion.

**Rationalization of Mechanical Behavior against the Backdrop of Calculated Energies.** To deepen our understanding of the relationship between macroscopic responses and microscopic features, we focused solely on three materials with almost identical crystal packing, 2, 4, and 5. First, we opted to examine the strength of intermolecular interactions in two 2D regions (spreading parallel to the bending faces) indicated by red and green dotted lines (Figure 4), as these are the weakest regions in the crystal structure, and as such, they are the first barriers in preserving the crystal integrity upon its exposure to external pressure. Therefore, we calculated basis set superposition error-corrected (BSSE) interaction energies between the double pairs of adjacent molecular fragments [red and green double pairs (Figure 4); for details see Figures S30 and S31].

The interactions B (−122.7 to −160.0 kJ/mol) proved to be much stronger than the interactions A (−49.7 to 57.5 kJ/mol), as a consequence of a substantially larger contact area as well as a larger number of HBs in B than in A [three C–H...N bonds in A vs one C–H...N bond and eight C–H...X(Cd) bonds in B]. This in turn made the bending much more restrictive when

the force was applied to the smaller crystal face than to the larger one.

Furthermore, interaction energy B for the bromide analogues (2, −122.7 kJ/mol; 5, −143.7 kJ/mol) was noticeably smaller than for the chloride one (4, −160.0 kJ/mol), which made the weak regions in 2 and 5 weaker than in 4, and consequently, the adjacent domains more prone to slips over each other, thus making 2 and 5 elastic  $\rightarrow$  plastic and 4 being only elastic. On the contrary, the energies of A do not offer equally clear rationalization due to the distribution of energies being within a small energy range (−50 to −58 kJ mol<sup>−1</sup>), but rather suggesting that the concerted fashion of the interactions in both regions is most likely to be needed for the crystal to display a flexible response.

**Microfocus Synchrotron X-ray Experiments.** The crystal of 1, the only material with 2D isotropically elastic crystals, was examined by microfocus synchrotron X-ray radiation with the aim of gaining insight into the molecular-level consequences of the bending process. The crystal was mounted on a glass holder in its bent form, oriented in the way that the X-ray beam was orthogonal to the plane of the loop of the crystal, and data were collected at two points of the bent crystal, the inner and outer arc, at the region of its maximal curvature (Figure 5).

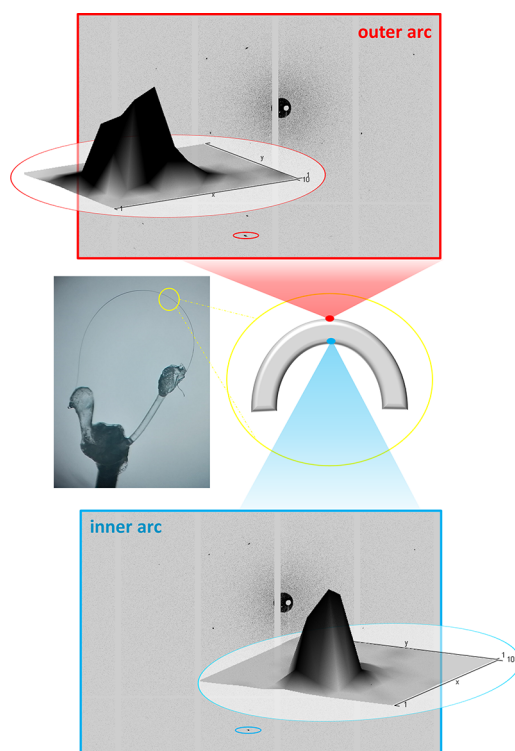


**Figure 5.** Profiles of the diffraction peaks of 1 (middle left) and the outer (top) and inner (bottom) arcs of the bent crystal.

The unit cell parameters were determined at the two points and compared with those from the straight crystal (prior bending), which confirmed that the crystal integrity was preserved, and no phase changes were introduced by bending.<sup>24</sup> The data revealed a noticeable enlargement of the *a* axis at the outer arc and its contraction at the inner arc ( $5\sigma$ ), while changes in the other unit cell parameters upon bending were less reliable ( $<3\sigma$ ). The changes in the *a* axis, in turn, indicated elongation of the Cd(II)⋯Cd(II) distances within



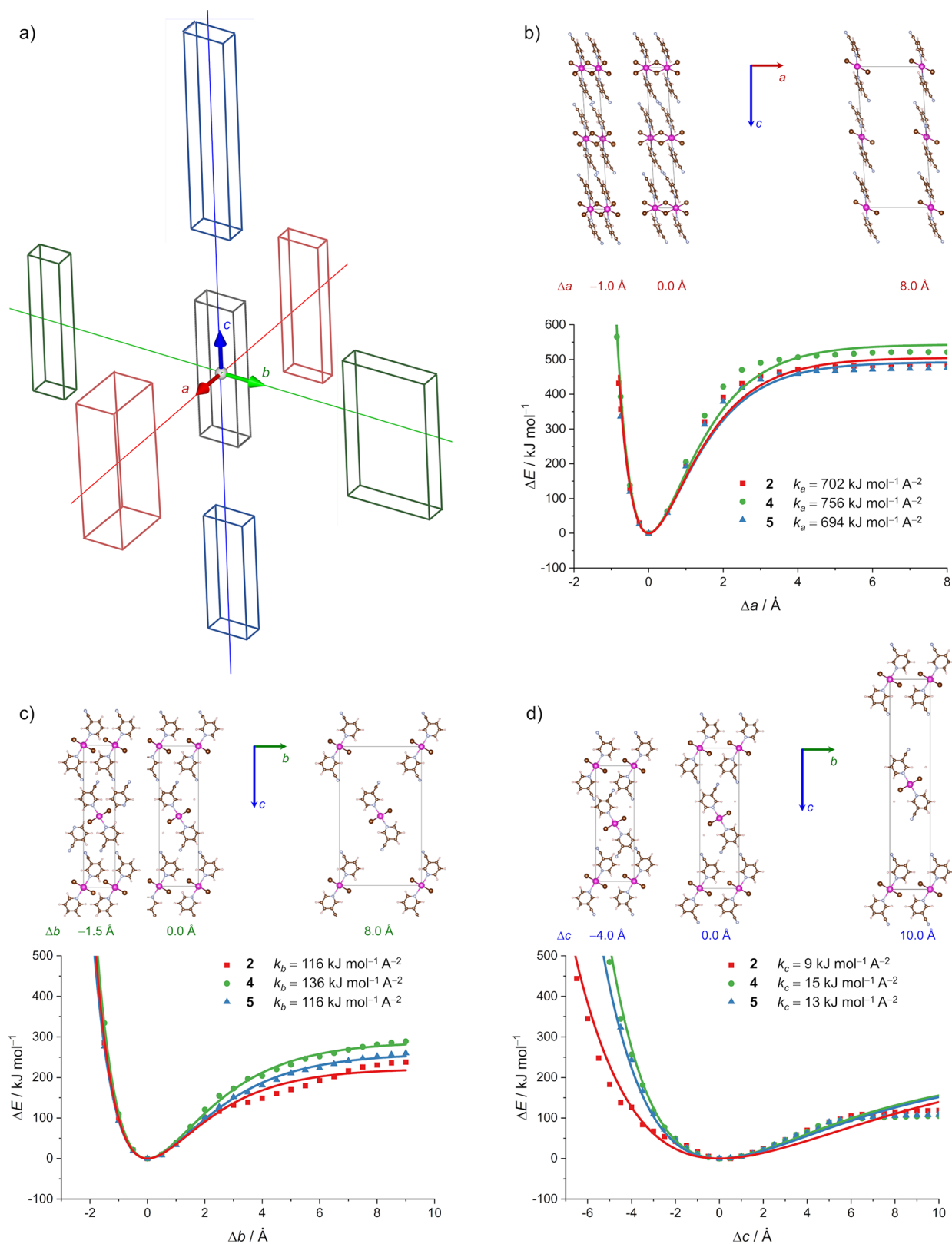


**Figure 6.** (a) Deformation of the unit cells by monodirectional stretching and shrinking along the unit cell axis. (b–d) Potential energy curves for 2 (red), 4 (green), and 5 (blue) as a function of relative deformation of the unit cell along the  $a$ ,  $b$ , and  $c$  axes. The zero values of  $\Delta a$ ,  $\Delta b$ , and  $\Delta c$  correspond to the fully optimized geometries at the PBE-D3/pob-TZVP-rev2 level of theory. The solid lines represent fits to a conventional Morse potential from which force constants  $k_a$ ,  $k_b$ , and  $k_c$  were calculated.

the 1D polymeric chains at the outer part and shortening at the inner part of the crystal. Similar shortening and elongation at the inner and outer arcs of the bent crystal, respectively, were

observed for elastically bendable crystals composed of discrete zero-dimensional (0D) metal-based building units.<sup>11</sup> However, in contrast to our materials, the distance between the



individual molecules in the 0D material was found to remain constant, while molecules rotate in the opposite directions, with respect to each other, at the two arcs of the crystal to compensate for extension and compression of the crystal parts (convex and concave) during bending. Although our findings suggest a different mechanism of elastic flexure for 1D materials (in comparison with the 0D material), they further point to the importance of concerted action of intermolecular interactions spreading in the two orthogonal directions (i.e., in regions A and B) for the crystal to display a flexible response and preserve the crystal integrity. While microfocus synchrotron experiments shed light on the molecular-level consequences of elastically bent crystals, for plastically bent crystals, where structure perturbations occur during the bending process, an alternative approach would be required, i.e., microfocus infrared spectroscopy with synchrotron radiation coupled with density functional theory (DFT) computation.<sup>25</sup>

Another interesting feature was also noticed as a consequence of bending, and it became visible upon examination of the peak profiles from two opposite parts (inner and outer part) of the bent crystal. While peaks from both parts were broadened (in comparison with the unbent crystal), broadening from the outer arc was much more pronounced than that from the inner arc (Figure 5). That in turn suggests that the bending process introduced larger distortions at the outer than at the inner region of the bent crystal. To further examine the observation, we opted for calculation of energies that would accompany distortions of the unit cells.

**Potential Energy Surface and Their Relationship with the Unit Cell Distortions.** To calculate the energy profiles that would accompany the distortions of the unit cells, we again opted for **2**, **4**, and **5** as they enabled the correlation of the results with structural features and experimental findings.

Each unit cell parameter was changed in regular increments in a separate experiment, and the three energy profiles were retrieved referring to the relative deformation of the unit cell lengths (*a*, *b*, or *c*) describing the process of extending and shrinking the unit cell axis [relative to the optimized structure corresponding to the minimum on the potential energy surface (Figure 6a); for details, see Computational Studies]. The energy profiles were then fitted to the Morse potential, which allowed us to calculate the force constants,  $k_a$ ,  $k_b$ , and  $k_c$  [along the *a*, *b*, and *c* axes, respectively (Figure 6b–d)], and to directly compare those for the three materials (**2**, **4**, and **5**) as well as to correlate them with the strength of monodirectional deformation of the unit cell along each axis. For all three materials, the calculated energy profiles indeed nicely resembled the Morse potential, which in turn also supported the smaller distortion to be more likely to materialize at the contraction part and larger distortions at the extension part of the crystal (when somewhere larger unit cell distortions materialize).

Moreover, the largest *k* values (**2**, **4**, and **5**) were, unsurprisingly, derived for the deformations along the shortest axis (*a* axis;  $k_a$ ) coinciding with the direction of spreading 1D polymeric chains. A slightly larger  $k_a$  value for **4**, in comparison with those of **2** and **5** (**2**, 702 kJ mol<sup>−1</sup> Å<sup>−2</sup>; **4**, 756 kJ mol<sup>−1</sup> Å<sup>−2</sup>; **5**, 694 kJ mol<sup>−1</sup> Å<sup>−2</sup>), reflected that it is more difficult to achieve the deformation in the direction of the *a* axis for the chloride (**4**) than for the bromide derivatives (**2** and **5**), which

is in line with the stronger Cd–X bonds in **4** (X = Cl) than in **2** and **5** (X = Br).

On the contrary, the force constants for the deformation processes along the other two directions, the *b* and *c* axes, are notably smaller due to the intermolecular interactions being the sole factors for determining the connectivity strength in those directions. The force constants  $k_b$  were larger than  $k_c$  for all three materials ( $k_b \approx 120$  kJ mol<sup>−1</sup> Å<sup>−2</sup>;  $k_c \approx 12$  kJ mol<sup>−1</sup> Å<sup>−2</sup>), pointing at the deformations along the *b* axis to be more difficult to achieve than the ones along the *c* axis. Indeed, the bending strain in **4** was 1.07% ( $\epsilon_1$ ) for applying the force to the (001)/(00 $\bar{1}$ ) pair of crystal faces, which fitted quite nicely with the lower value of the calculated  $k_c$  of 15 kJ mol<sup>−1</sup> Å<sup>−2</sup>. The bending strain was halved ( $\epsilon_2 = 0.53\%$ ) when the force was applied to the (01 $\bar{1}$ /01 $\bar{1}$ ) face, roughly corresponding to the larger  $k_b$  value of 136 kJ mol<sup>−1</sup> Å<sup>−2</sup> (as in that case the component promoting the deformation along the *c* direction also contributed, not only the one along the *b* direction).

Furthermore, somewhat larger values for both constants ( $k_b$  and  $k_c$ ) were found for **4** than for **2** and **5**, thus making **4** more prone to resist slipping of adjacent layers over each other than is the case for **2** and **5**. This finding is again quite in line with our experimental observations, where **4** was solely elastic while **2** and **5** showed elastic → plastic responsiveness.

## CONCLUSION

The family of six coordination polymers of cadmium(II) equipped with the cyanopyridine ligands provided us with a diverse data set of crystal morphologies and crystal responses that in turn yielded a newly described anisotropy in 2D flexibility of crystals. This finding prompted us to elucidate the origin of this surprising crystalline property and to rationalize it against a variety of structural, morphological, and energy features.

The six materials displayed four different arrangements of 1D building units with two different morphologies. Of six, four materials presented flexible responses, while two were brittle. All four flexible materials were 2D responsive, and their responsiveness showed a correlation with crystal morphologies; the crystals with equally developed crystal faces were 2D isotropically flexible, while materials with elongated plate-like crystals, for the first time, yielded 2D anisotropically flexible crystals, i.e., displayed a direction-dependent crystal adaptability to mechanical stimuli. More interestingly, among the three anisotropically responsive materials, a variety of responses were also observed, one material being solely elastic, while two displayed a transition from elastic to plastic behavior (elastic → plastic) at larger curvatures. The intermolecular interactions, together with structural and energy features, proved to be instrumental in delivering this assortment of crystal adaptabilities to mechanical stress. Small variations in the tilting angle between the 1D polymers from neighboring layers guided the crystal morphology, needle-like versus elongated plate-like crystal morphology, which, together with the intermolecular interactions and the energy thereof, determined the mechanical output. For a given material, the increase in the interaction energy in orthogonal directions accompanied by the corrugated arrangement of the building units proved to be critical for the weakened crystal ability to bend, which resulted in the 2D anisotropic flexibility of the crystal. On the contrary, for different materials (within the almost identical group of substances), the increase in the

interaction energies (in identical directions) was followed by an improved ability to resist plastic deformation.

This newly described 2D anisotropic mechanical responsiveness of crystals together with the findings on the origin thereof will advance the engineering and delivery of targeted mechanical responses, thus making the crystalline materials at disposal for practical applications in advanced technologies.

## EXPERIMENTAL SECTION

**Crystallization Experiments.** Crystals of compounds 1–6 were prepared by the layering technique. Cadmium(II) salt ( $\text{CdX}_2$ , 1 equiv) was dissolved in water, added to a test tube, and carefully layered with 1 mL of pure ethanol and then with an ethanol solution of the ligand (3-CNpy or 4-CNpy, 2 equiv). In a few weeks, needle-like crystals were obtained.

**PXRD.** X-ray powder diffraction experiments were performed on a Malvern Panalytical Aeris powder diffractometer under an applied voltage of 40 kV and a current of 15 mA, with Cu  $K\alpha$  radiation. The patterns were collected in the angle region between  $5^\circ$  and  $50^\circ$  ( $2\theta$ ) with a step size of  $0.02^\circ$ .

**SCXRD.** Crystals of 1–6 were mounted on a glass fiber and glued with superglue. Data were collected at room temperature, 295(2) K, on an XtaLAB Synergy-S Dualflex diffractometer equipped with a PhotonJet (Mo) microfocus X-ray source and a HyPix-6000HE hybrid photon counting (HPC) X-ray area detector. Data collection and reduction, including absorption correction, were performed using CrysAlisPro.<sup>26</sup> The structures were determined using the Olex2 interface. The starting structural model was obtained using SHELXT<sup>27</sup> and refined with the SHELXL algorithm.<sup>28</sup>

**Synchrotron Measurements: Mapping Out Slight Structural Changes.** Data were collected on the XRD1 beamline at synchrotron Elettra (Trieste, Italy).<sup>29</sup> All measurements were performed at room temperature using a wavelength  $\lambda$  of 0.7000 Å. A  $120\ \mu\text{m} \times 100\ \mu\text{m}$  X-ray beam was prealigned and masked with a pinhole being brought down to a size of approximately  $5\ \mu\text{m}$  in diameter (full width at half-maximum). The crystal was glued in a bent form on a magnetic base holder and placed on a goniometer head. The crystal was oriented in a way that the trajectory of the beam was perpendicular to the loop of the crystal. A point at the maximal curvature of the bent crystal was selected, and the crystal was positioned in two ways so that only a small portion of the outer and inner arc of the crystal was in the beam. The unit cell parameters were determined in those two positions of the bent crystal (at the outer and inner arc of a bent crystal) by collecting 12 diffraction frames with an oscillation angle of  $0.5^\circ$  (total of  $6^\circ$ ) and an exposure time of 30 s. Data reductions were performed using CrysAlisPro.<sup>26</sup> For the outer arc,  $a = 3.811(5)\ \text{\AA}$ ,  $b = 15.53(14)\ \text{\AA}$ ,  $c = 11.60(3)\ \text{\AA}$ ,  $\alpha = 90^\circ$ ,  $\beta = 91.51(8)^\circ$ ,  $\gamma = 90^\circ$ , and  $V = 687(6)\ \text{\AA}^3$ . For the inner arc,  $a = 3.770(7)\ \text{\AA}$ ,  $b = 15.62(15)\ \text{\AA}$ ,  $c = 11.59(3)\ \text{\AA}$ ,  $\alpha = 90^\circ$ ,  $\beta = 91.37(10)^\circ$ ,  $\gamma = 90^\circ$ , and  $V = 682(7)\ \text{\AA}^3$ .

**TG/DSC.** Thermal analyses were performed using a simultaneous TGA-DTA analyzer (Mettler-Toledo TGA/DSC 3+). Finely ground samples (1–6) were placed in alumina pans ( $70\ \mu\text{L}$ ) and heated in flowing nitrogen ( $50\ \text{mL min}^{-1}$ ) from room temperature to  $600\ ^\circ\text{C}$  at a rate of  $10\ ^\circ\text{C min}^{-1}$ . Data collection and analyses were performed using the program package STARE Software 15.01 (Mettler-Toledo GmbH, 2015).<sup>30</sup>

**Mechanical Adaptability Testing.** Tests of mechanical responses of prepared crystals were performed via the modified three-point bending procedure. Several crystals of each compound, from a few different batches, were selected. Each selected crystal was placed on a glass slide and immersed in a small amount of paratone oil to reduce the damage of the crystal upon the usage of metalware and to avoid crystal–surface friction. The crystal was held with a pair of metal forceps from one side, while the mechanical force was applied from the opposite side, using a metal needle. The force was applied until the crystal broke. For crystals that displayed an elastic response, the extent of the response was quantified using the Euler–Bernoulli equation.

**Computational Studies.** Periodic DFT calculations were performed for the crystal structures of coordination polymers 2, 4, and 5 in CRYSTAL17<sup>31</sup> using the PBE<sup>32</sup> functional with Grimme's D3 correction for the inclusion of weak dispersive interactions.<sup>33</sup> The revised triple- $\zeta$  basis set specifically adapted for periodic calculations, pob-TZVP-rev2, was used on all atoms.<sup>34</sup> The input files were generated by the cif2cell package.<sup>35</sup> Full optimization of atom coordinates and cell parameters was performed on the starting geometries with tighter energy convergence criteria ( $10^{-8}$ ) and root-mean-square values on gradient ( $6 \times 10^{-5}$ ) and displacement ( $1.2 \times 10^{-4}$ ). Tighter convergence on total energy ( $10^{-7}$ ) and increased truncation criteria for the calculation of Coulombs and exchange integrals (8 8 8 8 16) were set for SCF calculations. For all three compounds, the reciprocal space was sampled using  $8 \times 4 \times 1$  Pack–Monkhorst  $k$ -point mesh (the  $c$  axis was over  $26\ \text{\AA}$ ).

To rationalize the mechanical behavior of 2, 4, and 5, the potential energy surfaces associated with monodirectional deformation (stretching and/or shrinking) along the unit cell axes ( $a$ ,  $b$ , and  $c$ ) were modeled. We started from fully optimized structures and performed relaxed scan calculations. The starting geometry of each point on the energy profile was created by deformation (stretching or shrinking) of one unit cell parameter (unit cell length  $a$ ,  $b$ , or  $c$ ) at a time in increments of  $0.5\ \text{\AA}$  (smaller increments were employed around the equilibrium distance), while all other unit cell parameters were kept constant. Interatomic distances were not changed during this process. These starting geometries were then partially optimized (the unit cell parameters were fixed, while atomic positions were allowed to change), and exactly 15 optimization steps were allowed to obtain more realistic energies when compared to values obtained from single-point calculations on nonrelaxed geometries. Calculated energy values were then fitted to the conventional Morse potential function  $D_e[1 - e^{-a(X-R_e)}]$ , and the force constant was calculated as  $k = 2D_e a^2$ .

It is worth mentioning that the unit cell is not equally sensitive to the deformations along two directions, namely, the  $b$  and  $c$  directions. While the deformation along the  $b$  axis is in direct relation with the relative displacement of two neighboring polymeric chains within the unit cell (i.e., deformation of the unit cell by  $1.0\ \text{\AA}$  will increase the intrachain distance by the same amount), the deformation along the  $c$  axis and the separation of the 1D chains differ by a multiplier of 2 (a  $1.0\ \text{\AA}$  deformation of the unit cell along the  $c$  axis will separate the adjacent chains by only  $0.5\ \text{\AA}$ ) due to the presence of two 1D polymers along the  $c$  axis. Thus, the energy decreases and increases much slower when the unit cell is stretched and shrunk, respectively, by the same amount in direction  $c$  in comparison with direction  $b$ , resulting in a substantially smaller force constant value.

Interaction energies were calculated in Gaussian 16<sup>36</sup> between the selected double pairs (red-green) on fully optimized geometries obtained from periodic DFT calculations as previously described. Each adjacent 1D polymeric chain was modeled as a finite electroneutral molecule of three metal centers, and all of the calculated values were corrected by BSSEs according to the counterpoise method of Boys and Bernardi.<sup>37,38</sup> The calculated interaction energy values were divided by 3 to obtain the normalized interaction energies per metal center.

Geometries were visualized in GaussView 6<sup>39</sup> and VESTA.<sup>40</sup>

## ASSOCIATED CONTENT

### Supporting Information

The Supporting Information is available free of charge at <https://pubs.acs.org/doi/10.1021/acs.chemmater.2c00062>.

Synthetic procedures for the preparation of compounds 1–6, SCXRD results, PXRD results, TG/DTA analysis, crystal bending experiments, and computational studies (PDF)

Movie 1 (MP4)

Movie 2 (MP4)

Movie 3 (MP4)

Movie 4 (MP4)

Movie 5 (MP4)  
Movie 6 (MP4)  
Movie 7 (MP4)  
Movie 8 (MP4)  
Movie 9 (MP4)  
Movie 10 (MP4)

## AUTHOR INFORMATION

### Corresponding Author

Marijana Đaković – Department of Chemistry, Faculty of Science, University of Zagreb, 10 000 Zagreb, Croatia;  
orcid.org/0000-0001-6789-6399; Email: mdjakovic@chem.pmf.hr

### Authors

Mateja Pisačić – Department of Chemistry, Faculty of Science, University of Zagreb, 10 000 Zagreb, Croatia

Ivan Kodrin – Department of Chemistry, Faculty of Science, University of Zagreb, 10 000 Zagreb, Croatia; orcid.org/0000-0001-6353-3187

Amanda Trninić – Department of Chemistry, Faculty of Science, University of Zagreb, 10 000 Zagreb, Croatia

Complete contact information is available at:

<https://pubs.acs.org/10.1021/acs.chemmater.2c00062>

### Notes

The authors declare no competing financial interest.

## ACKNOWLEDGMENTS

This work has been fully supported by the Croatian Science Foundation under Project IP-2019-04-1242. The support of project CluK co-financed by the Croatian Government and the European Union through the European Regional Development Fund - Competitiveness and Cohesion Operational Programme (Grant KK.01.1.1.02.0016) is acknowledged. The authors acknowledge Elettra-Sincrotrone Trieste for providing beam time (Proposal 20205473) and the XRD1 beamline staff for their assistance during the experiments, in particular Maurizio Polentarutti and Giorgio Bais.

## REFERENCES

- (1) Naumov, P.; Karothu, D. P.; Ahmed, E.; Catalano, L.; Commins, P.; Mahmoud Halabi, J.; Al-Handawi, M. B.; Li, L. The rise of dynamic crystals. *J. Am. Chem. Soc.* **2020**, *142*, 13256–13272.
- (2) Liu, G.; Liu, J.; Ye, X.; Nie, L.; Gu, P.; Tao, X.; Zhang, Q. Self-Healing Behavior in a Thermo-Mechanically Responsive Cocrystal during a Reversible Phase Transition. *Angew. Chem., Int. Ed.* **2017**, *56*, 198–202.
- (3) Rath, B. B.; Gallo, G.; Dinnebier, R. E.; Vittal, J. J. Reversible Thermosolience in a One-Dimensional Coordination Polymer Preceded by Anisotropic Thermal Expansion and the Shape Memory Effect. *J. Am. Chem. Soc.* **2021**, *143*, 2088–2096.
- (4) Seki, T.; Mashimo, T.; Ito, H. Anisotropic strain release in a thermosolient crystal: correlation between the microscopic orientation of molecular rearrangements and the macroscopic mechanical motion. *Chem. Sci.* **2019**, *10*, 4185–4191.
- (5) Bushuyev, O. S.; Tomberg, A.; Friščić, T.; Barrett, C. J. Shaping Crystals with Light: Crystal-to-Crystal Isomerization and Photo-mechanical Effect in Fluorinated Azobenzenes. *J. Am. Chem. Soc.* **2013**, *135*, 12556–12559.
- (6) Nath, N. K.; Pejov, Lj.; Nichols, S. M.; Hu, C.; Saleh, N.; Kahr, B.; Naumov, P. Model for Photoinduced Bending of Slender Molecular Crystals. *J. Am. Chem. Soc.* **2014**, *136*, 2757–2766.
- (7) Yue, Y.; Norikane, Y.; Azumi, R.; Koyama, E. Light-induced mechanical response in crosslinked liquid-crystalline polymers with photoswitchable glass transition temperatures. *Nat. Commun.* **2018**, *9*, 3234.
- (8) Reddy, C. M.; Gundakaram, R. C.; Basavoju, S.; Kirchner, M. T.; Padmanabhan, K. A.; Desiraju, G. R. Structural basis for bending of organic crystals. *Chem. Commun.* **2005**, 3945–3947.
- (9) Ghosh, S.; Reddy, C. M. Elastic and Bendable Caffeine Cocrystals: Implications for the Design of Flexible Organic Materials. *Angew. Chem., Int. Ed.* **2012**, *51*, 10319–10323.
- (10) Panda, M. K.; Ghosh, S.; Yasuda, N.; Moriawaki, T.; Mukherjee, G. D.; Reddy, C. M.; Naumov, P. Spatially resolved analysis of short-range structure perturbations in a plastically bent molecular crystal. *Nat. Chem.* **2015**, *7*, 65–72.
- (11) Worthy, A.; Grosjean, A.; Pfrunder, M. C.; Xu, Y.; Yan, C.; Edwards, G.; Clegg, J. K.; McMurtrie, J. C. Atomic resolution of structural changes in elastic crystals of copper(II) acetylacetonate. *Nat. Chem.* **2018**, *10*, 65–69.
- (12) Hu, S.; Mishra, M. K.; Sun, C. C. Exceptionally Elastic Single-Component Pharmaceutical Crystals. *Chem. Mater.* **2019**, *31*, 3818–3822.
- (13) Liu, H.; Bian, Z.; Cheng, Q.; Lan, L.; Wang, Y.; Zhang, H. Controllably realizing elastic/plastic bending based on a room-temperature phosphorescent waveguiding organic crystal. *Chem. Sci.* **2019**, *10*, 227–232.
- (14) Gupta, P.; Allu, S.; Karothu, D. P.; Panda, T.; Nath, N. K. Organic Molecular Crystals with Dual Stress-Induced Mechanical Response: Elastic and Plastic Flexibility. *Cryst. Growth Des.* **2021**, *21*, 1931–1938.
- (15) Kusumoto, S.; Sugimoto, A.; Zhang, Y.; Kim, Y.; Nakamura, M.; Hayami, S. Elastic Crystalline Fibers Composed of a Nickel(II) Complex. *Inorg. Chem.* **2021**, *60*, 1294–1298.
- (16) Annadhasan, M.; Karothu, D. P.; Chinnasamy, R.; Catalano, L.; Ahmed, E.; Ghosh, S.; Naumov, P.; Chandrasekar, R. Micro-manipulation of Mechanically Compliant Organic Single-Crystal Optical Microwaveguides. *Angew. Chem., Int. Ed.* **2020**, *59*, 13821–13830.
- (17) Kwon, T.; Koo, J. Y.; Choi, H. C. Highly Conducting and Flexible Radical Crystals. *Angew. Chem., Int. Ed.* **2020**, *59*, 16436–16439.
- (18) Cappuccino, C.; Catalano, L.; Marin, F.; Dushaq, G.; Raj, G.; Rasras, M.; Rezgui, R.; Zambianchi, M.; Melucci, M.; Naumov, P.; Maini, L. Structure-Mechanical Relationships in Polymorphs of an Organic Semiconductor (C4-NT3N). *Cryst. Growth Des.* **2020**, *20*, 884–891.
- (19) Kenny, E. P.; Jacko, A. C.; Powell, B. J. Mechanomagnetism in Elastic Crystals: Insights from [Cu(acac)<sub>2</sub>]. *Angew. Chem., Int. Ed.* **2019**, *58*, 15082–15088.
- (20) Đaković, M.; Borovina, M.; Pisačić, M.; Aakeröy, C. B.; Kukovec, B.-M.; Soldin, Ž.; Kodrin, I. Mechanically Responsive Crystalline Coordination Polymers with Controllable Elasticity. *Angew. Chem., Int. Ed.* **2018**, *57*, 14801–14805.
- (21) Pisačić, M.; Biljan, I.; Kodrin, I.; Popov, N.; Soldin, Ž.; Đaković, M. Elucidating the Origins of a Range of Diverse Flexible Responses in Crystalline Coordination Polymers. *Chem. Mater.* **2021**, *33*, 3660–3668.
- (22) Pisačić, M.; Kodrin, I.; Biljan, I.; Đaković, M. Exploring the diversity of elastic responses of crystalline cadmium(II) coordination polymers: from elastic towards plastic and brittle responses. *CrystEngComm* **2021**, *23*, 7072–7080.
- (23) Lommerse, J. P. M.; Stone, A. J.; Taylor, R.; Allen, F. H. The Nature and Geometry of Intermolecular Interactions between Halogens and Oxygen or Nitrogen. *J. Am. Chem. Soc.* **1996**, *118*, 3108–3116.
- (24) Commins, P.; Karothu, D. P.; Naumov, P. Is a bent crystal still a single crystal? *Angew. Chem., Int. Ed.* **2019**, *58*, 10052–10060.
- (25) Pejov, Lj.; Panda, M. K.; Moriawaki, T.; Naumov, P. Probing structural perturbation in a bent molecular crystal with synchrotron



infrared microspectroscopy and periodic density functional theory calculation. *J. Am. Chem. Soc.* **2017**, *139*, 2318–2328.

(26) *CrysAlisPRO*; Agilent Technologies Ltd.: Yarnton, England, 2014.

(27) Sheldrick, G. M. SHELXT— Integrated Space-Group and Crystal-Structure Determination. *Acta Crystallogr., Sect. A* **2015**, *71*, 3–8.

(28) Sheldrick, G. M. A Short History of ShelX. *Acta Crystallogr.* **2008**, *A64*, 112–122.

(29) Lausi, A.; Polentarutti, M.; Onesti, S.; Plaisier, J. R.; Busetto, E.; Bais, G.; Barba, L.; Cassetta, A.; Campi, G.; Lamba, D.; Pifferi, A.; Mande, S. C.; Sarma, D. D.; Sharma, S. M.; Paolucci, G. Status of the crystallography beamlines at Elettra. *Eur. Phys. J. Plus* **2015**, *130*, 1–8.

(30) *STARe Software*, ver. 15.01; MettlerToledo GmbH: Greifensee, Switzerland, 2015.

(31) Dovesi, R.; Erba, A.; Orlando, R.; Zicovich-Wilson, C. M.; Civalieri, B.; Maschio, L.; Rerat, M.; Casassa, S.; Baima, J.; Salustro, S.; Kirtman, B. Quantum-mechanical condensed matter simulations with CRYSTAL. *Wiley Interdiscip. Rev.: Comput. Mol. Sci.* **2018**, *8*, No. e1360.

(32) Perdew, J. P.; Chevary, J. A.; Vosko, S. H.; Jackson, K. A.; Pederson, M. R.; Singh, D. J.; Fiolhais, C. Atoms, molecules, solids, and surfaces: Applications of the generalized gradient approximation for exchange and correlation. *Phys. Rev. B* **1992**, *46*, 6671–6687.

(33) Grimme, S.; Antony, J.; Ehrlich, S.; Krieg, H. A consistent and accurate ab initio parametrization of density functional dispersion correction (DFT-D) for the 94 elements H–Pu. *J. Chem. Phys.* **2010**, *132*, 154104.

(34) Vilela Oliveira, D.; Laun, J.; Peintinger, M. F.; Bredow, T. BSSE-correction scheme for consistent gaussian basis sets of double- and triple-zeta valence with polarization quality for solid-state calculations. *J. Comput. Chem.* **2019**, *40*, 2364–2376.

(35) Björkman, T. CIF2Cell: Generating geometries for electronic structure programs. *Comput., Phys. Commun.* **2011**, *182*, 1183–1186.

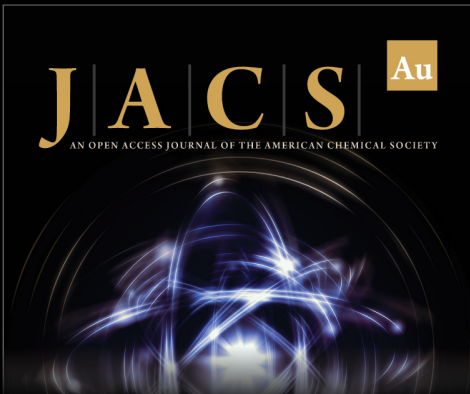
(36) Frisch, M. J.; Trucks, G. W.; Schlegel, H. B.; Scuseria, G. E.; Robb, M. A.; Cheeseman, J. R.; Scalmani, G.; Barone, V.; Petersson, G. A.; Nakatsuji, H.; Li, X.; Caricato, M.; Marenich, A. V.; Bloino, J.; Janesko, B. G.; Gomperts, R.; Mennucci, B.; Hratchian, H. P.; Ortiz, J. V.; Izmaylov, A. F.; Sonnenberg, J. L.; Williams-Young, D.; Ding, F.; Lipparini, F.; Egidi, F.; Goings, J.; Peng, B.; Petrone, A.; Henderson, T.; Ranasinghe, D.; Zakrzewski, V. G.; Gao, J.; Rega, N.; Zheng, G.; Liang, W.; Hada, M.; Ehara, M.; Toyota, K.; Fukuda, R.; Hasegawa, J.; Ishida, M.; Nakajima, T.; Honda, Y.; Kitao, O.; Nakai, H.; Vreven, T.; Throssell, K.; Montgomery, J. A., Jr.; Peralta, J. E.; Ogliaro, F.; Bearpark, M. J.; Heyd, J. J.; Brothers, E. N.; Kudin, K. N.; Staroverov, V. N.; Keith, T. A.; Kobayashi, R.; Normand, J.; Raghavachari, K.; Rendell, A. P.; Burant, J. C.; Iyengar, S. S.; Tomasi, J.; Cossi, M.; Millam, J. M.; Klene, M.; Adamo, C.; Cammi, R.; Ochterski, J. W.; Martin, R. L.; Morokuma, K.; Farkas, O.; Foresman, J. B.; Fox, D. J. *Gaussian 16*, rev. C.01; Gaussian, Inc., Wallingford, CT, 2016.

(37) Boys, S. F.; Bernardi, F. The calculation of small molecular interactions by the differences of separate total energies. Some procedures with reduced errors. *Mol. Phys.* **1970**, *19*, 553–566.

(38) Simon, S.; Duran, M.; Dannenberg, J. J. How does basis set superposition error change the potential surfaces for hydrogen bonded dimers? *J. Chem. Phys.* **1996**, *105*, 11024.

(39) Dennington, R.; Keith, T. A.; Millam, J. M. *GaussView*, ver. 6; Semichem, Inc.: Shawnee Mission, KS, 2016.

(40) Momma, K.; Izumi, F. VESTA 3 for three-dimensional visualization of crystal, volumetric and morphology data. *J. Appl. Crystallogr.* **2011**, *44*, 1272–1276.



**JACS** Au  
AN OPEN ACCESS JOURNAL OF THE AMERICAN CHEMICAL SOCIETY

Editor-in-Chief  
**Prof. Christopher W. Jones**  
Georgia Institute of Technology, USA

**Open for Submissions**

pubs.acs.org/jacsau

ACS Publications  
Most Trusted. Most Cited. Most Read.

## § 3. DISCUSSION

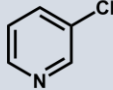
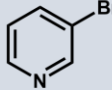
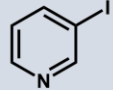
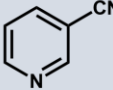
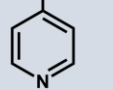
Up till now, a mechanically induced dynamic behaviour of crystalline compounds was observed primarily for the crystals of purely organic compounds. It was found that they can display a variety of mechanical responses, such as plastic and elastic bending, while some are even capable of displaying ductile and malleable behaviour comparable to metal-based materials. Also, some of the flexible organic crystals displayed other attributes of interest, such as optical transduction, electrical, and ferroelectric properties, what puts crystalline materials to the forefront of the materials for emerging technologies design.

Metal-organic crystalline coordination compounds provide a large variety of structural architectures of different dimensionalities (0D, 1D, 2D, 3D), connectivities, etc. The existence of a metal centre in the structure provides not only structural diversity, but also the opportunity to achieve functional properties of interest, such as optical, electric, and magnetic, which are in principle hardly realized in purely organic systems. Combining these with a mechanical flexibility is highly desired, however, the origin of a stress-induced responses is still quite unexplored, especially for metal-organic crystalline compounds, and we are not yet well equipped with the knowledge to deliver crystals of a desired mechanical output. Therefore, a thorough structure–property correlation must be made.

Crystalline coordination polymers, as a subgroup of metal-organic compounds, are found to be capable of displaying a variety of tuneable electronic, magnetic, and optical properties.<sup>92–95</sup> Unexpectedly, a few years ago (in 2018), it was found that one-dimensional crystalline coordination polymers of cadmium(II) halides with halopyrazine ligands ( $[\text{CdX}_2(\text{X}'\text{-pz})_2]_n$ , X, X' = Cl, Br, I) can even respond flexibly to the application of mechanical stress.<sup>73</sup> Moreover, by introducing only small structural changes, i.e. replacing an ion in the bridging between two metal centres, or a halogen atom on the ligand, the extent of elastic output can be modified. It was then realized that one-dimensional coordination polymers present as an ideal model system for a thorough and systematic correlation of structure and mechanical properties as slight structural changes can be introduced in a controlled manner. Moreover, by having one dimension prearranged – the dimension of the propagation of a polymeric chain, 1D coordination polymers serve as excellent candidates for an in-depth study of the impact of intermolecular interactions on macroscopic mechanical responses.

The research on elastically bendable coordination polymers of cadmium(II) halides with halopyrazine ligands<sup>73</sup> served as a basis that encouraged the research described in this doctoral thesis, whose main objective is to determine the pivotal structural characteristics of crystalline cadmium(II) coordination polymers to achieve adaptive properties of the desired type (elastic vs. plastic bending) and extent.

For the systematic investigation of this outstanding phenomenon, crystalline coordination polymers of cadmium(II) halides with five pyridine-based ligands (a total of 15 compounds) were prepared and thoroughly investigated within this doctoral thesis (Figure 12). The research resulted with three scientific papers in which the obtained results were described. The research results were rather intriguing, enlightening, and placed the structural background of the mechanical flexibility of crystalline compounds in a completely new perspective. Now it becomes clear that intermolecular interactions play one of the crucial roles in determining the mechanical behaviour of the crystals, but also that the behaviour of crystalline matter is much more alike to “classic” materials, and these compounds could find their place in the mechanical engineering processes in the future.

The salt \ The ligand					
	 3-Clpy	 3-Brpy	 3-Ipy	 3-CNpy	 4-CNpy
<b>CdCl<sub>2</sub></b>	$[\text{CdCl}_2(3\text{-Clpy})_2]_n$ II-1	$[\text{CdCl}_2(3\text{-Brpy})_2]_n$ II-2	$[\text{CdCl}_2(3\text{-Ipy})_2]_n$ I-4	$[\text{CdCl}_2(3\text{-CNpy})_2]_n$ III-1	$[\text{CdCl}_2(4\text{-CNpy})_2]_n$ III-4
<b>CdBr<sub>2</sub></b>	$[\text{CdBr}_2(3\text{-Clpy})_2]_n$ I-1	$[\text{CdBr}_2(3\text{-Brpy})_2]_n$ II-3	$[\text{CdBr}_2(3\text{-Ipy})_2]_n$ I-5	$[\text{CdBr}_2(3\text{-CNpy})_2]_n$ III-2	$[\text{CdBr}_2(4\text{-CNpy})_2]_n$ III-5
<b>CdI<sub>2</sub></b>	$[\text{CdI}_2(3\text{-Clpy})_2]_n$ I-2	$[\text{CdI}_2(3\text{-Brpy})_2]_n$ I-3	$[\text{CdI}_2(3\text{-Ipy})_2]_n$ I-6	$[\text{CdI}_2(3\text{-CNpy})_2]_n$ III-3	$[\text{CdI}_2(4\text{-CNpy})_2]_n$ III-6

**Figure 12.** Cadmium(II) salts and pyridine-based ligands used for the preparation of targeted crystalline coordination polymers.

### 3.1. One-dimensional coordination polymers with ligands bearing halogen functionalities for targeting the flexible response

One of the first examples of the mechanically compliant molecular crystals described a series of seven isostructural compounds of cadmium(II) halides with halopyrazine ligands, which showed a mechanically induced elastic response.<sup>73</sup> Interestingly, those crystals, although having almost identical crystal packing, showed a clear difference in the extent of the elastic bending, which was quantified by calculating the maximal bending strain,  $\varepsilon$ , that crystal can endure before the disintegration of its original shape. In all seven compounds a short “4 Å” axis was observed. Moreover, interlocking of the neighbouring polymeric chains could also be noticed, thus preventing the slippage of the domains, and allowing the elastic response. The only difference between the examined crystals was in the relative strength and importance of the supramolecular interactions. The persistent intermolecular interaction, realized in crystal structures of all seven compounds, was a C–X'...X(Cd) halogen bond. Moreover, in all crystal structures, the C–H...X and C–H...N hydrogen bonds were observed as well, with the latter being more influential.

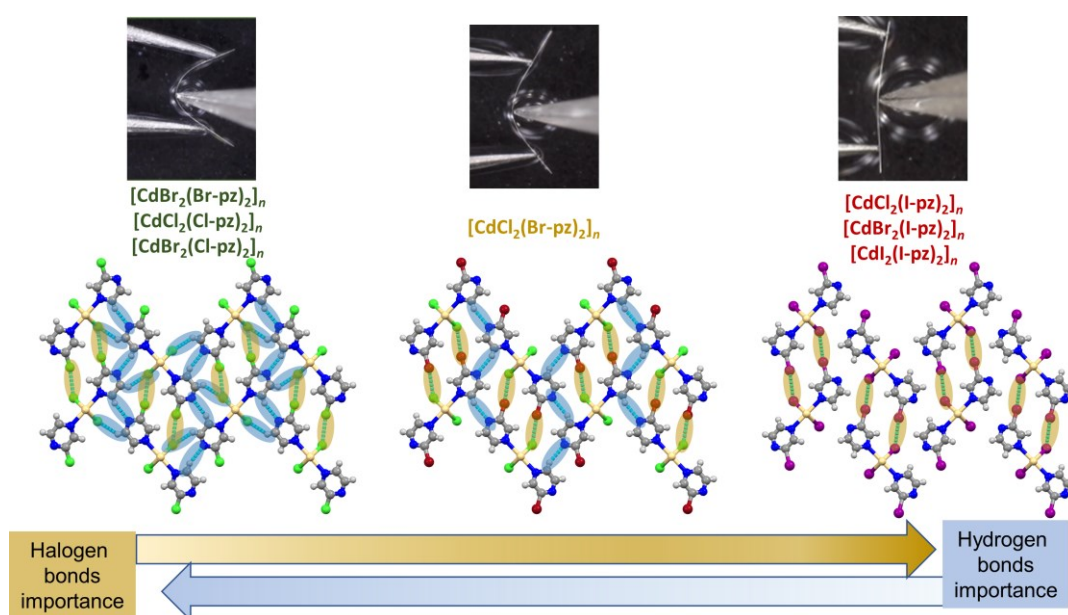


**Figure 13.** Crystals of one-dimensional coordination polymers of cadmium(II) halides with halopyrazine ligands (top), classified in the groups of highly (left), moderately (middle) and slightly (right) elastically bendable crystals, with the crystal structures of the main representatives in which hydrogen bonds are highlighted in light blue and halogen bonds in light brown.

However, the relative importance of the hydrogen and halogen bonds changed amongst the compounds and was correlated with the extent of the mechanical response. In the compounds of slightly bendable crystals, the halogen bond was dominant, while the hydrogen bond played only a supportive role. But with the increase in the elastic compliance of the crystals, the subsequent decrease in the importance of the halogen bonds in the crystal structures, followed by the concurrent increase in the strength of hydrogen bonds was observed (Figure 13).

To gain more insight into the origin of the crystals' compliance, we continued this research and opted for another group of crystalline cadmium(II) polymers by introducing a slight change in the organic ligand. Instead of the halopyrazine ligand, we chose the halopyridine ligand. In that way, we removed the hydrogen bond acceptor from the structure of the ligand (a nitrogen atom at the position 4). However, we kept a good halogen bond donor on the ligand. Even though the change sounds quite simplistic, suggesting the possible supramolecular output, the results were not obvious but, on contrary, exceptionally interesting and unexpected. These results were presented in articles **I** and **II**.

Performed synthesis resulted in crystals of all nine targeted one-dimensional polymers of a required quality for the X-ray structure analysis as well as the mechanical experiments. The obtained crystals can be divided into two subgroups regarding the morphological and crystal structure characteristics (Figure 14). The first group is composed of the crystals of  $[\text{CdCl}_2(3\text{-Ipy})_2]_n$  (**I-4**) and  $[\text{CdBr}_2(3\text{-Ipy})_2]_n$  (**I-5**). Even though these crystals crystalize in different space groups (**I-4**:  $C2/c$ , **I-5**:  $P\bar{1}$ ) the molecular arrangement is nearly identical. The arrangement of 1D polymeric chains in the crystal structures is parallel in both crystallographic directions perpendicular to the direction of an elongation of a polymeric chain ( $b$  and  $c$ , Figure 14, upper row). Moreover, their morphology is also the same, and can be described as vastly elongated plates, i.e., these crystals have different dimensions of the dominant crystal faces that run parallel to the direction of the elongation of the crystal.

The remaining seven isostructural compounds:  $[\text{CdCl}_2(3\text{-Clpy})_2]_n$  (**II-1**),  $[\text{CdBr}_2(3\text{-Clpy})_2]_n$  (**I-1**),  $[\text{CdI}_2(3\text{-Clpy})_2]_n$  (**I-2**),  $[\text{CdCl}_2(3\text{-Brpy})_2]_n$  (**II-2**),  $[\text{CdBr}_2(3\text{-Brpy})_2]_n$  (**II-3**),  $[\text{CdI}_2(3\text{-Brpy})_2]_n$  (**I-3**) and  $[\text{CdI}_2(3\text{-Ipy})_2]_n$  (**I-6**) provided acicular crystals with equally developed potential bending faces and all crystalized in the  $P2_1/c$  space group. The mutual orientation of the polymeric chains is parallel in the direction of the crystallographic axis  $b$  and antiparallel in the direction of  $c$  (Figure 14, lower row).



In all nine compounds, one-dimensional polymeric units are mutually connected via  $\text{C—H}\cdots\text{X}$  and  $\text{C—H}\cdots\text{X}'(\text{Cd})$  hydrogen and  $\text{C—X}\cdots\text{X}'(\text{Cd})$  halogen bonds, with slight differences in the relative strength in each compound. Similar types of interactions were also present in crystal structures of cadmium(II) halides with halopyrazine ligands.<sup>73</sup>

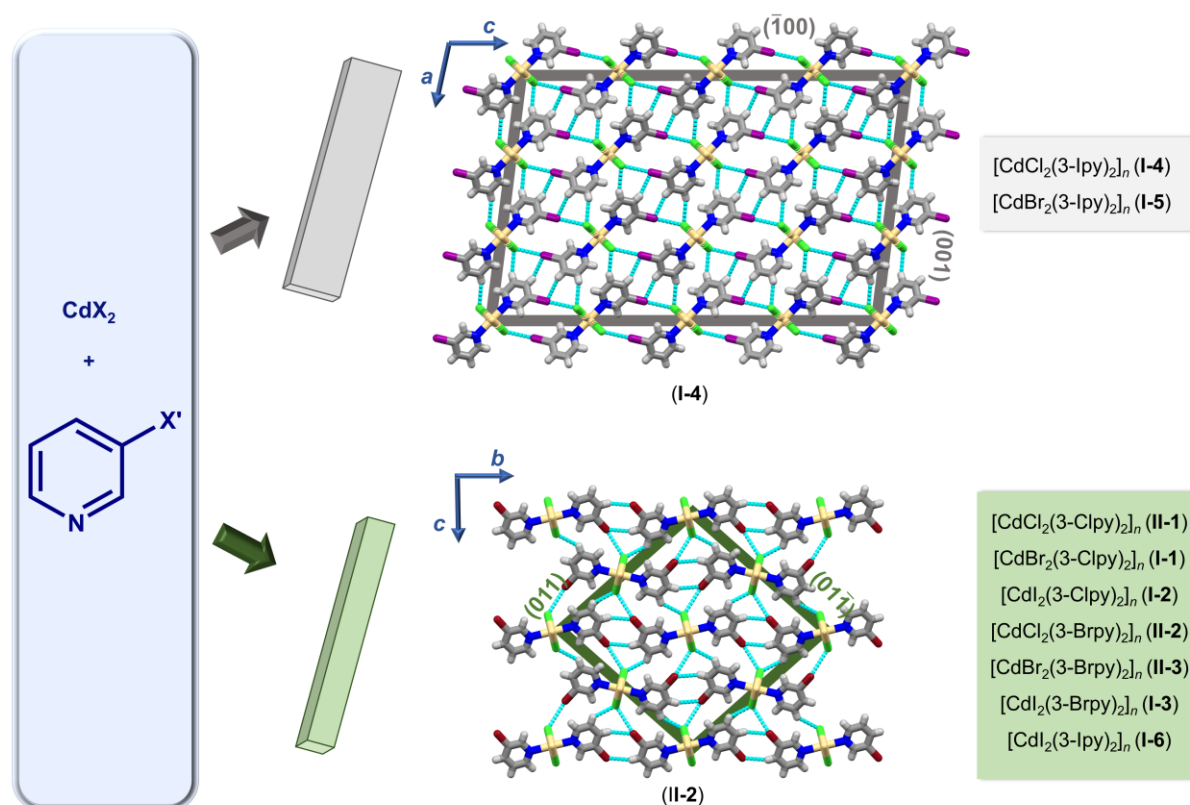


**Figure 14.** Crystals of 1D cadmium(II) halides with halopyridines classified into two groups; those with vastly elongated plate-like morphology (grey picture borders, top row) and those with equally developed bending faces (green picture borders, bottom row) with crystal packings representing each of the two groups. In **I-4**, along both crystallographic directions,  $a$  and  $c$ , 1D polymeric chains are organized in a parallel fashion, which resulted in substantially different structural arrangement in (potential) bending directions, (orthogonal to  $(100)/(00\bar{1})$  vs.  $(001)/(\bar{1}00)$ ). In **II-2**, 1D polymeric chains are arranged in a parallel fashion along the  $b$  axis and in an antiparallel fashion along the  $c$  crystallographic axis, resulting in almost identical structural arrangement in (potential) bending directions (orthogonal to  $(011)/(0\bar{1}\bar{1})$  and  $(0\bar{1}1)/(01\bar{1})$ ).

The mechanical properties of prepared compounds were firstly evaluated using the modified three-point bending technique. The selected crystals were immersed in the paratone oil, and each crystal was held from one side with a pair of forceps, while the mechanical force was applied from the opposite side with a metal needle, at the middle of the length of the crystal. The elastic response of crystals was quantified by calculating the bending strain ( $\varepsilon$ ) using the Euler-Bernoulli equation (considering only pure bending without shear component),<sup>96</sup> to compensate the elastic bending for the dimensions of the crystals (length and thickness).

Firstly, the focus will be on the group of the crystals of **I-4** and **I-5**. These crystals appeared in a morphology of vastly elongated plates, and therefore the mechanical force could have been applied in two ways, perpendicular to the faces of larger or smaller dimensions. Both crystals gave the mechanically stimulated flexible response only when the stress was applied on the pair of faces of larger dimensions, while upon the application of the stress on the faces of smaller dimension crystals readily cracked and broke. Therefore, these crystals were classified as one-dimensionally (1D) flexible (Figure 15b).

However, the type of the flexible response differed between those two compounds. Crystals of **I-4** responded with slight elastic bending ( $\varepsilon = 0.27\%$ ) and being bent over the maximum bending radius they broke (Figure 15b, upper row). Therefore, these crystals were classified as 1D elastically flexible. On the other hand, crystals of **I-5** displayed irreversible deformation when the stress was applied to the face of larger dimensions, so these crystals were categorized as 1D plastically flexible (Figure 15b, lower row).

Amongst the group of seven isostructural compounds, i.e., the ones with equally developed crystal faces, a variety of flexible responses were observed, a range from plastic over elastic→plastic, and to finally purely elastic responses (Figure 16). It was observed that all those crystals gave the same type and extent of the mechanical response, regardless of the pair of dominant crystal faces the mechanical stress was applied to, what was expected, since the crystal packing features are almost identical in potential bending directions (Figure 16a). These crystals were therefore classified as two-dimensionally (2D) responsive.

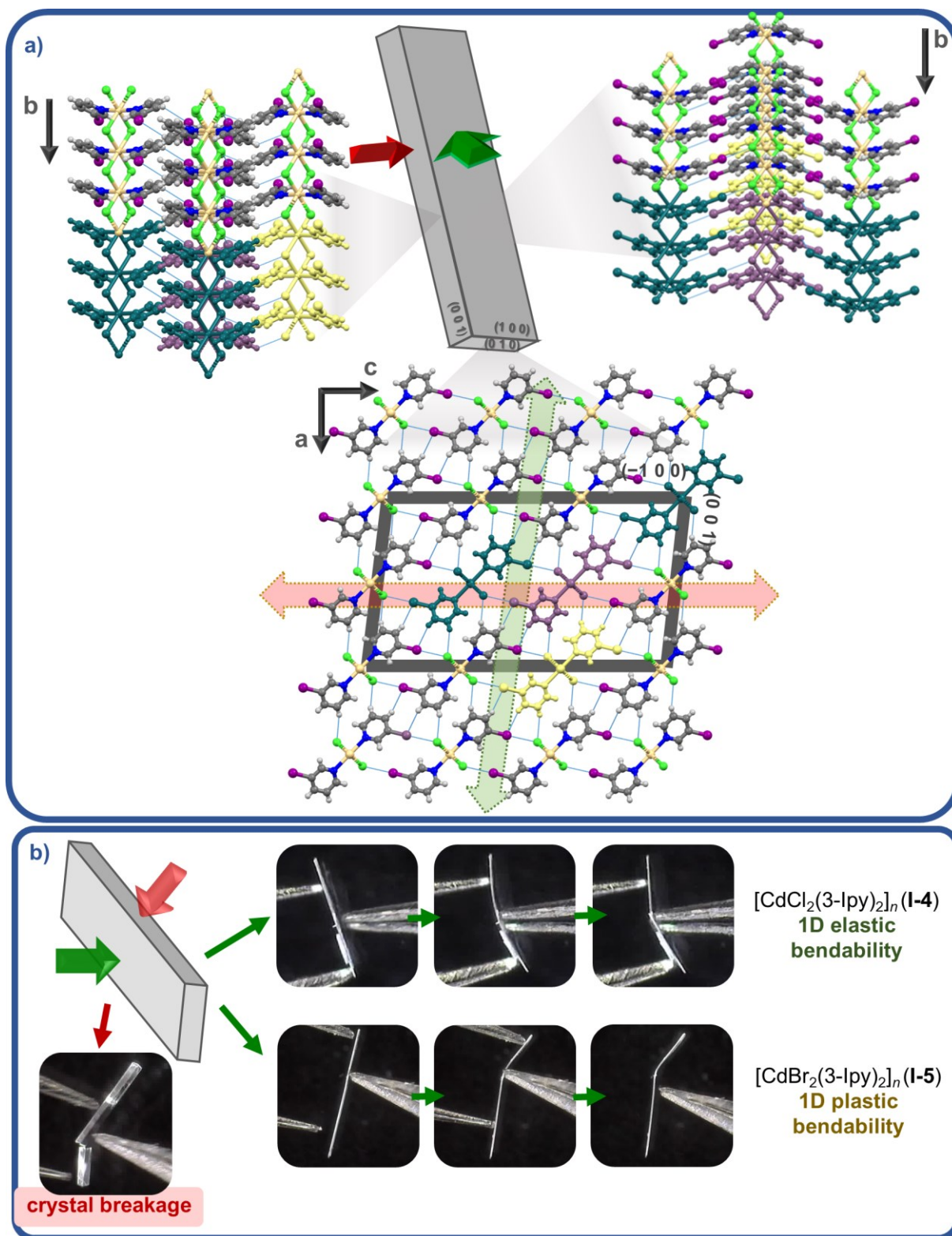


**Figure 15.** a) Crystal packing of **I-4** viewed perpendicular to crystal faces. b) One-dimensionally responsive plate-like crystals.  $[\text{CdCl}_2(3\text{-Ipy})_2]_n$  (**I-4**) displaying slight 1D elastic bending (down, left) and  $[\text{CdBr}_2(3\text{-Ipy})_2]_n$  (**I-5**) displaying plastic bending (down, right).

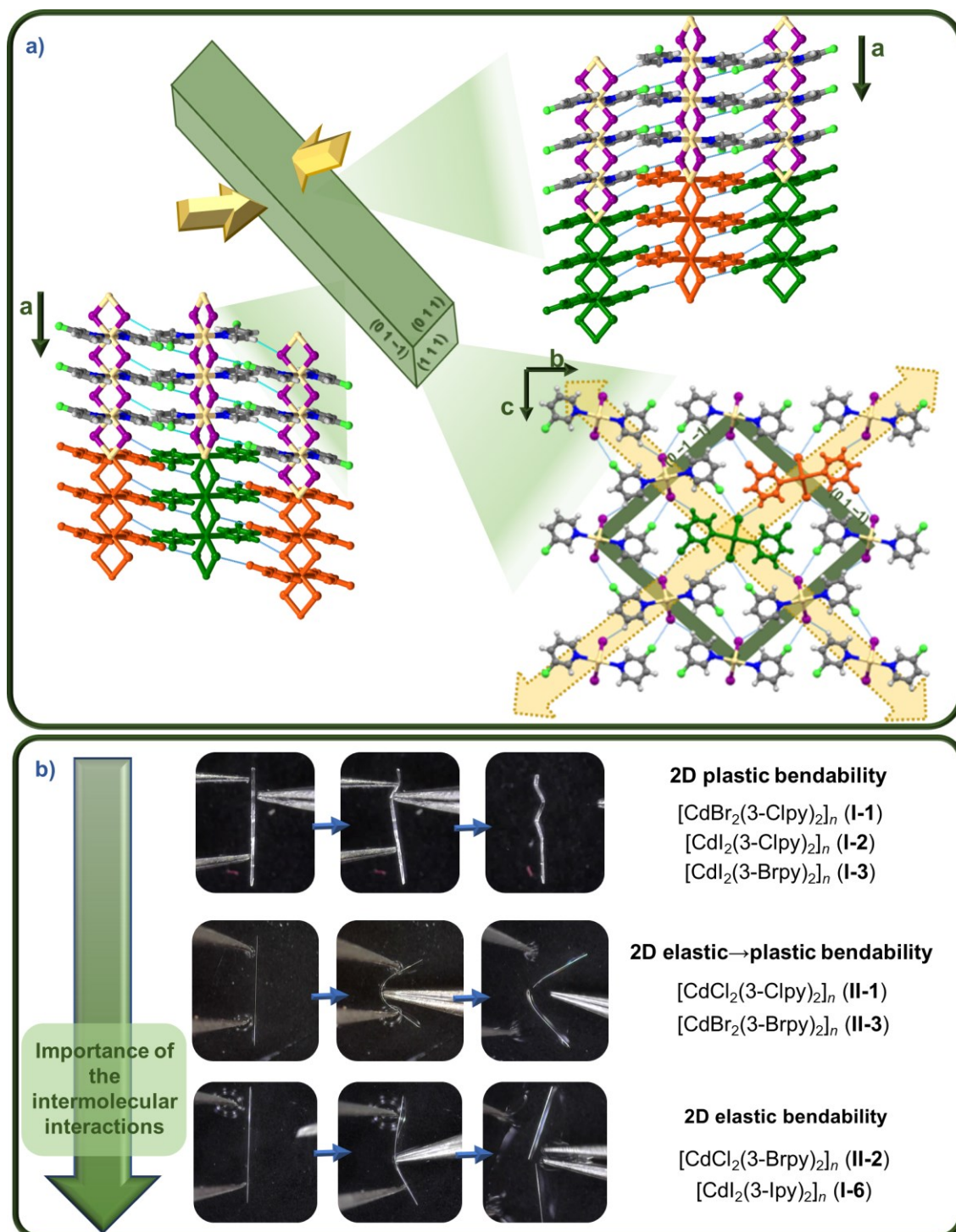


**Figure 16.** a) Crystal packing of **I-2** viewed perpendicular to (011), (01 $\bar{1}$ ) and (111) crystal faces. b) Observed mechanically induced 2D flexible responses of the isostructural compounds of cadmium(II) halides with halopyridine ligands. Crystals of **I-1–I-3** showing plasticity (upper row), **II-1** and **II-3** elastic→plastic bending (middle), while **II-2** and **I-6** displayed elastic bending with a typical brittle breakage (lower row).



Crystals of compounds **I-1–I-3** bent during the application of the mechanical force regardless of the pair of the impacted crystal faces and remained permanently deformed even with the removal of the stress, i.e., they were thus categorized as 2D plastically bendable (Figure 16b, upper row). These crystals showed to be extensively pliable that they could be deformed severely without being broken, such as plasticine. Moreover, the outstanding compliance of these crystals was further demonstrated with a modified five-point bending experiment, in which the crystals successfully overcome all barriers without being broken or damaged, and consequently, during the process being straightened out, just like a metal wire (Figure 17).

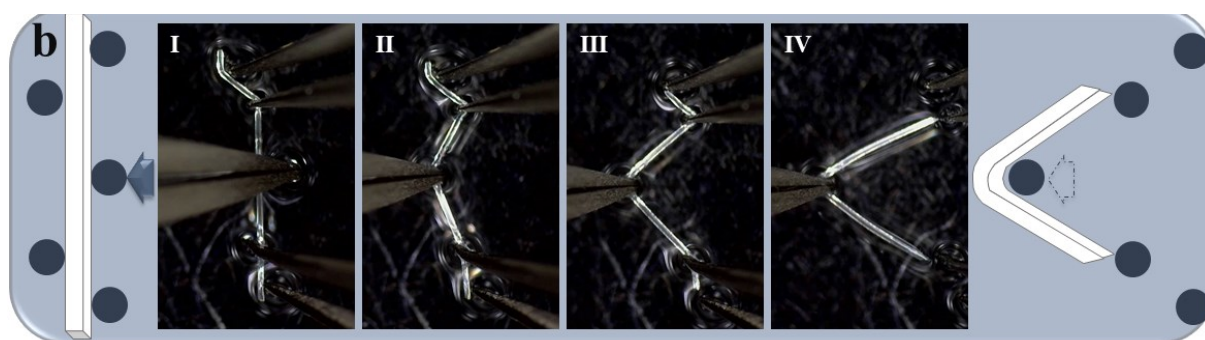


**Figure 17.** Five-point bending experiment for the crystal of **I-3**.

As opposed to **I-1–I-3**, crystals of **II-2** and **I-6** displayed purely reversible deformation, i.e. they displayed elastic response. (Figure 16b, lower row). By application of the mechanical force, crystals bent and restored their original shape completely once the mechanical force was removed. They could be repeatedly bent many times, as long as the critical radius was not exceeded – after which they broke (Figure 16b, lower row, right picture). However, these crystals could have been bent only slightly before being broken (**II-2**:  $\varepsilon = 0.47\%$ ; **I-6**:  $\varepsilon = 0.40\%$ ), and upon breakage they showed a typical brittle breakage. The broken parts of the crystal immediately straightened up and displayed elastic bending as well. The same response was observed when the mechanical force was applied to both sets of dominant crystal faces, therefore, crystals of **II-2** and **I-6** were categorized as 2D elastically bendable crystals.

Crystals of the remaining two compounds, **II-1** and **II-3**, behaved rather interestingly upon the mechanical force application, and it can be said that their mechanical output is somewhere in between elastic and plastic (Figure 16b, middle row). By exerting the mechanical force on the crystals, they behaved as a typical elastically bendable material when bent to smaller

extents, i.e. during the stress application they bent, and after releasing the stress they regained the undeformed shape. These crystals were able to tolerate larger bending extents than the crystals of **II-2** and **I-6** without being broken (**II-1**:  $\varepsilon = 0.71\%$ , **II-3**:  $\varepsilon = 0.59\%$ ). However, at higher bending strains, close to the point of breakage, these crystals became irreversibly deformed, i.e., plastically bent, while with further stress application crystals eventually broke. Interestingly, the parts of the broken crystals remained deformed in the proximity of the point of crystal breakage. Therefore, crystals which gave this type of mechanical response were classified as elastically→plastically bendable. Since these crystals gave the same type of the mechanical response regardless of the direction of the force application, i.e., when being impacted on both pairs of potential bending faces which run parallel to the direction of an elongation of a crystal itself, they were categorized as 2D elastically→plastically bendable. Hence, we can say that within this series of the isostructural compounds there is a clear difference in mechanically stimulated crystals' compliance – from being purely elastic to extensively plastic with which they resembled soft materials.

However, even more interesting results emerged from this research. Besides the difference in the extent of crystals' elastic compliance observed before,<sup>73</sup> for the first time, the variable plastic pliability amongst the group of plastically bendable crystals of **I-1–I-3** was observed too. While the crystals of **I-2** were extremely easily plastically deformable, so that it was even hard to handle them without causing a plastic deformation, crystals of **I-1** and **I-3** displayed slightly more resilient. To investigate the difference in the pliability of both elastically and plastically bendable crystals more closely, and their ductile possibilities as well, a new type of modified mechanical tensile stress experiment was performed. Crystals were mounted with their ends fixed to the glass slide using a superglue, in a way that the middle part of the crystal (that was not glued to the glass slide) stayed in the air for the impact of the oil and a glass–crystal friction on the results to be eliminated. The mechanical stress was applied with a metal forceps (with the curved ends) to the middle part of the crystal in a controlled manner, by moving in steps of 15  $\mu\text{m}$ , with a constant velocity of 100  $\mu\text{m} / \text{s}$  (Figure 18a). By comparing the obtained results, a fine difference in the mechanical responses was observed. The most pliable was the crystal of **I-2**, as it showed an exceptional compliance to tensile stress by displaying continuous plastic deformation and a flow of crystalline material, the observation that was not reported previously for the metal-organic crystals. Upon application of the mechanical force, crystal became readily plastically deformed, i.e., elongated, and with further



application of the mechanical force the elongation of the crystal could be undoubtedly observed (Figure 18b, right column). Moreover, the crystal did not break, but continued being heavily deformed, and during deformation, it could be clearly observed that the domains of the crystal slide one over another, resulting in a plastic flow of a material upon which crystal was thinned out, ending in a very tiny crystal fibres. This behaviour was previously observed only for the high symmetry metals, metal-alloys, ceramics and globular organic materials.<sup>46</sup>

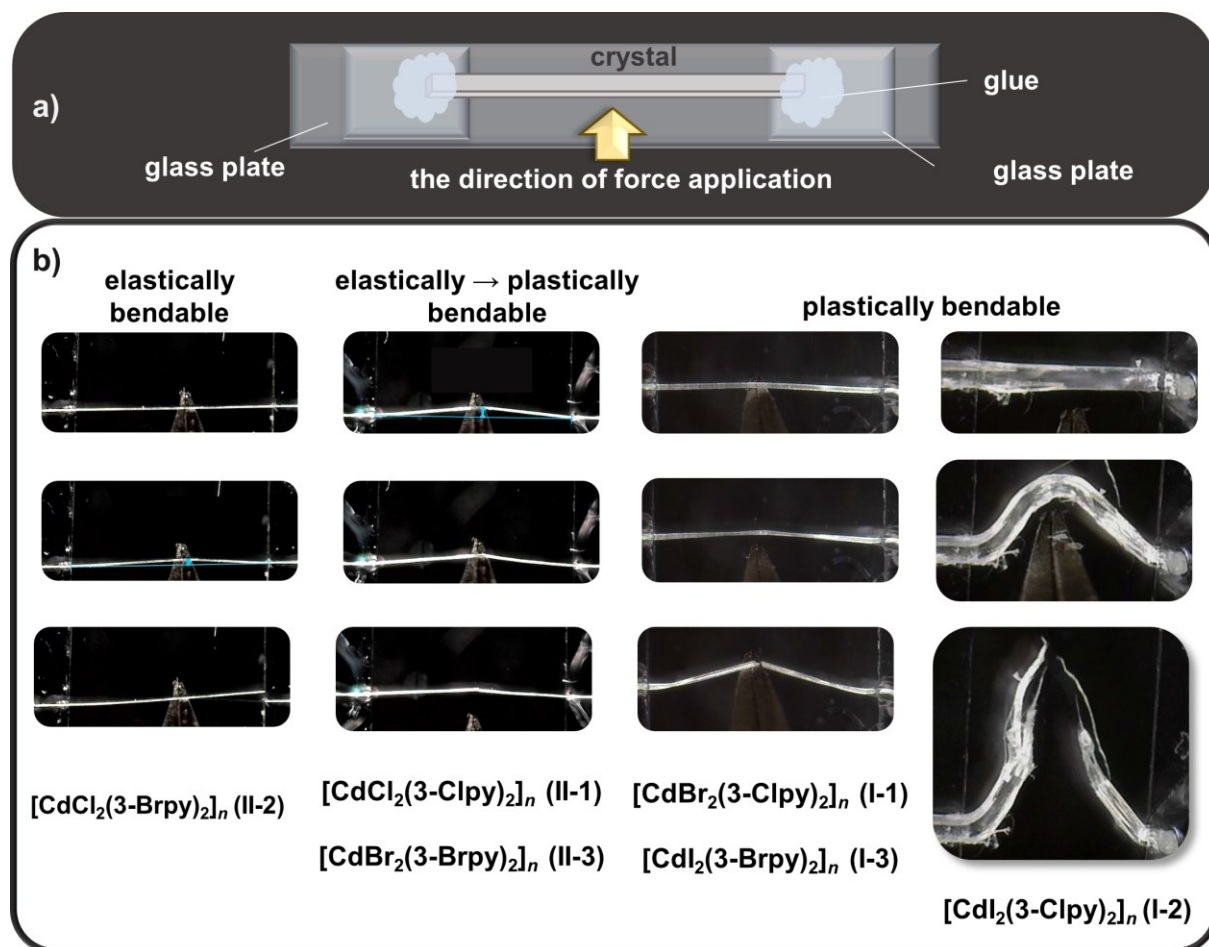


**Figure 18.** Modified tensile stress experiment. a) Experimental set-up for modified tensile stress experiment. b) Difference in the observed responses amongst elastically bendable, elastically→plastically, and plastically bendable crystals.

Somewhat less compliant were plastically bendable crystals of **I-1** and **I-3** (Figure 18b). Upon being slightly mechanically impacted, crystals stretched and suffered the irreversible deformation to a certain degree but regenerated their initial state to some extent after the

mechanical force was released. Upon further application of the stress, crystals continued to deform until they finally broke, and the broken parts of the crystal were clearly plastically deformed (in a proximity of the point where crystal was attached to the glass plate). However, in this case a thinning of the crystal was not observed, and the breakage resembled a typical brittle breakage.

The result of the ductile-testing experiment of the remaining crystals, **II-1** and **II-3**, classified as elastically→plastically bendable, and **II-2**, i.e., the elastically bendable one, were similar to some extent (Figure 18b). When being impacted slightly (the impactor moved only a small distance) the crystals stretched and recovered their original, unstretched shape completely upon the removal of the force, i.e., they displayed elastic deformation. But with further stress application, crystals of the elastically bendable compounds broke (again, with the complete restoration of the initial length; Figure 18b). On the other hand, crystals of **II-1** and **II-3** of approximately the same length and thickness, endured two times larger deformation (approx. two times larger distance impactor travelled) than the crystal of **II-2** before they broke, however the broken parts of the crystal remained slightly plastically deformed and stretched out (Figure 18b).

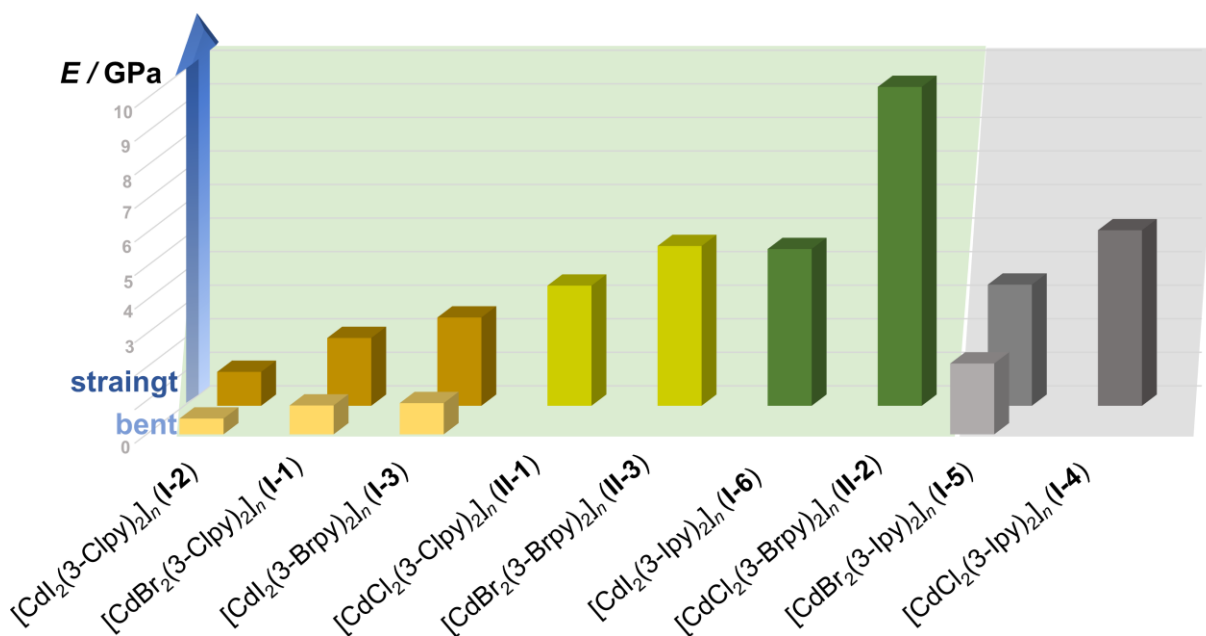


**Figure 19.** Young's moduli ( $E$ ) obtained for the straight and plastically bent crystals of one-dimensional polymers of cadmium(II) halides with halopyridine ligands.

To further investigate the observed differences in the mechanical behaviour of the crystals the local Young's moduli values of straight and plastically bent crystals (Figure 19) using the atomic force microscopy (AFM) were determined.<sup>76,97,98</sup> The lowest values of Young's moduli were obtained for the plastically bendable crystals with the most pliable crystal, **I-2**, showing the lowest value of the elastic modulus (**I-2**: 1.01 GPa; **I-1**: 2.02 GPa; **I-3**: 2.63 GPa; **I-5**: 3.61 GPa). A bit higher values of the Young's moduli were obtained for the elastically→plastically bendable crystals (**II-1**: 3.58 GPa; **I-3**: 4.55 GPa), while purely elastically bendable crystals had the highest value of the Young's modulus (**II-2**: 9.50 GPa; **I-6**: 4.67 GPa). Moreover, the Young's moduli values were lower for the plastically bent crystals (impacted at the point of the maximal curvature) in comparison to the Young's moduli values of the unbent crystals. This “softening” of the crystals that materializes with bending was also previously noticed and reported in literature for the crystals of hexachlorobenzene and was assigned to the reduction of the crystal density, packing imperfections and increased mosaicity.<sup>25</sup>

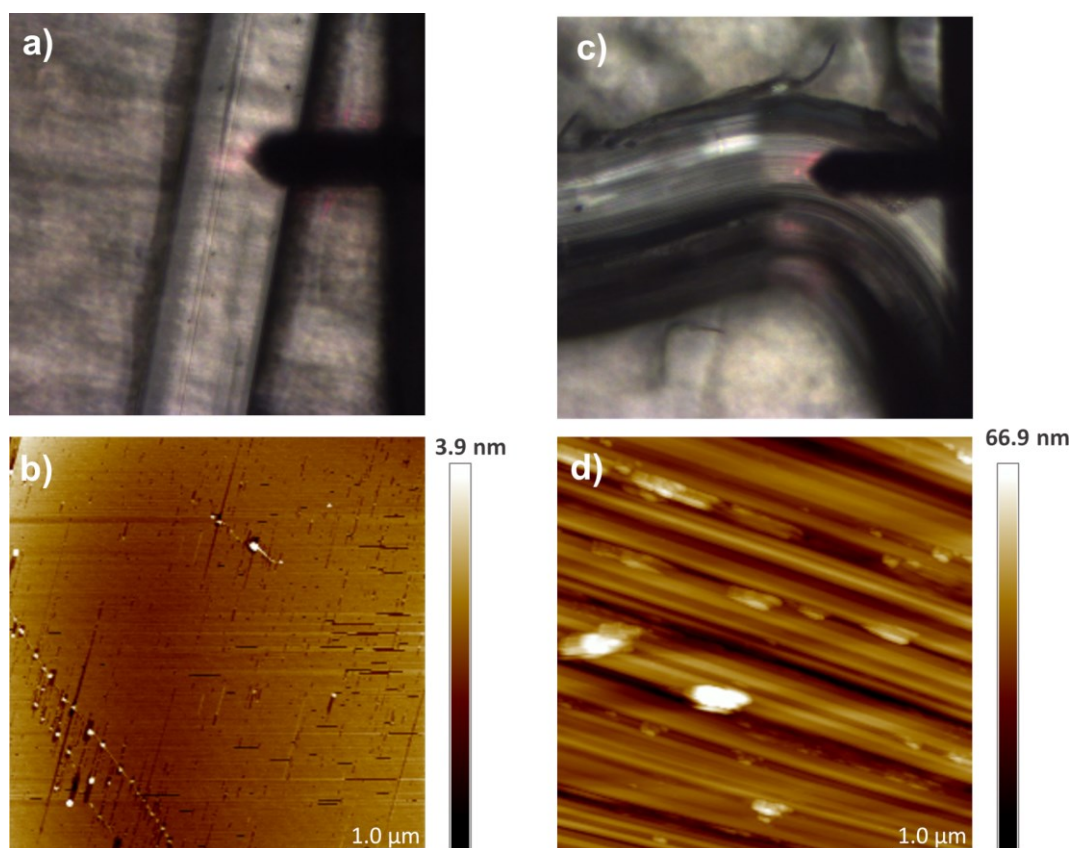


**Figure 20.** Optical microscope photograph and surface topography visualized with AFM of a straight (a, b) and bent (c, d) crystal of **I-1**, respectively.

Moreover, it was found for the plastically bendable crystals that flat surface of straight crystal (Figure 20a and b) becomes substantially striated upon bending (Figure 20c and d), what strongly suggested that during the bending neighbouring crystal domains segregate, most likely as a consequence of weakening the intermolecular interactions caused by slippage of the layers upon bending. Similar pleating of the crystal's surface was observed as well for the plastically bendable crystals of hexachlorobenzene.<sup>25</sup> Plastic bendability facilitated by gliding of the neighbouring molecular layers could have also been seen as the change of an interfacial angle at the end of a bent crystal (Figure 21b, middle). Moreover, by comparing the results obtained from micro-focus X-ray diffraction experiment on a straight and a plastically bent crystal also confirmed the proposed hypothesis. While the diffraction peaks of the undeformed crystal are sharp (Figure 21a), azimuthal elongation, i.e., broadening of diffraction peaks at the most bent part, as well as on the lateral region of the bent crystal can be observed, with the latter being more pronounced (Figure 21b).

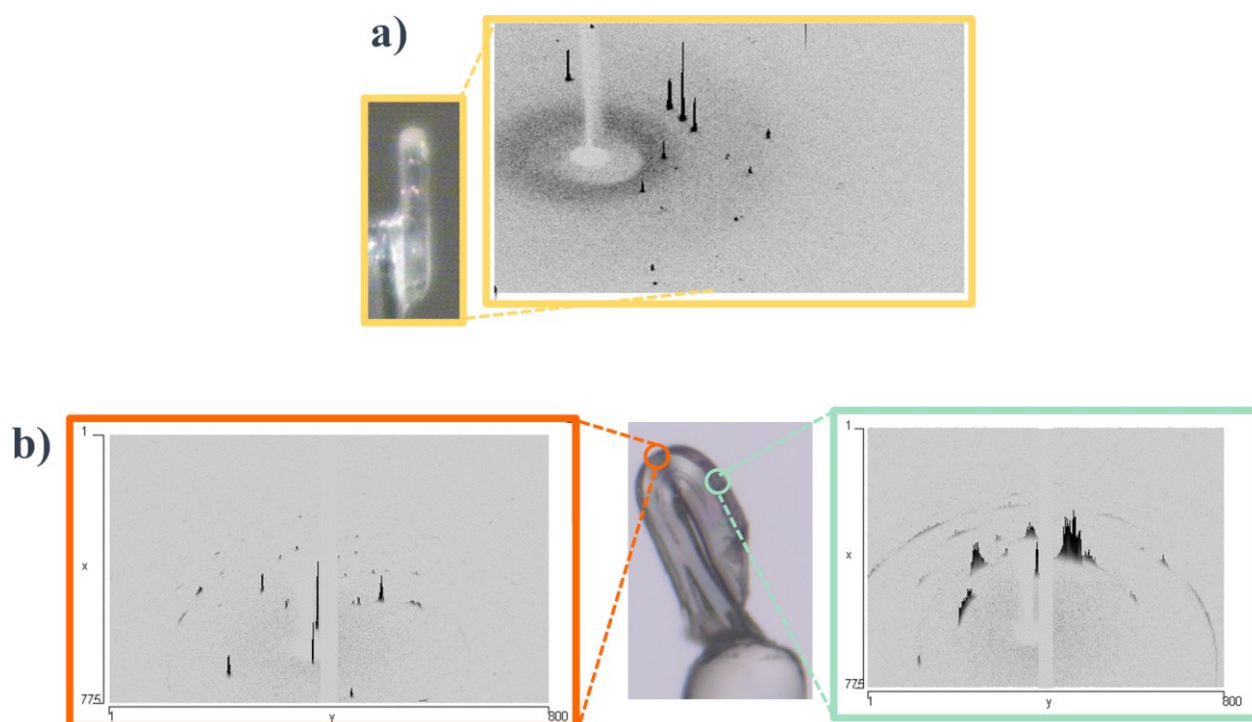


**Figure 21.** a) Undeformed crystal of **I-2** and its diffraction image comprised of sharp diffraction peaks. b) Plastically bent crystal of **I-2** (middle) and corresponding diffraction images collected on the U-turn (left, orange outline), and on the lateral part (right, pale green outline).

However, the unit cell parameters remained unchanged in comparison to the straight crystal. This suggests that during the bending, molecular layers slide one on top of other, without any deformation of a unit cell. Moreover, results suggest that the sliding of the molecular slabs is more pronounced on the lateral points of the crystal, than on the maximally bent part. This kind of diffraction peaks broadening, a so-called asterism, are typically observed because of tilts of mesoscopic, relatively defect-poor crystalline regions bounded by structural dislocations.<sup>99,100</sup> Moreover, these results are suggesting that, even upon being severely deformed, a bent crystal is still truly a crystal.<sup>101</sup>

To correlate the mechanical behaviour with the structural features, a detailed inspection of the crystal packing was performed, with a strong focus on the intermolecular interactions. In the set of seven isostructural compounds the arrangement of the building blocks (one-dimensional polymeric chains) is nearly identical. Moreover, similar types of the intermolecular interactions can be observed in all seven compounds, however, their relative importance differs amongst the compounds (regarding the normalized hydrogen/halogen bond distances,<sup>102</sup> Table 2). Therefore, the difference in crystals' compliance most probably arises from the subtle variations in the importance of the intermolecular interactions, the halogen and hydrogen bonds. While in the structure of plastically bendable crystals the halogen bond interactions are somewhat less influential, their importance (as well as the importance of hydrogen bond interactions) becomes more pronounced for achieving the elastic→plastic and purely elastic responses (Table 2). Similar trend was observed in the crystal structures of cadmium(II) halides with halopyrazine ligands,<sup>73</sup> where relative importance of halogen and hydrogen bonds played a key role in achieving different extents of elastic responses. Moreover, these results were also in line with the plastically bendable crystals of another 1D coordination polymer which showed 2D plastic response,  $[\text{ZnCl}_2(3,5\text{-Cl}_2\text{py})_2]_n$ .<sup>41</sup> In the crystal structure of this compound, only very weak intermolecular interactions were observed, similarly as in the 2D plastically bendable crystals of **I-1**, **I-2** and **I-3**, which had the weakest interactions amongst the group of seven compounds.

Similar observations can be made for the remaining two 1D flexible crystals, **I-4** and **I-5**. The intermolecular interactions in the crystal structure of the plastically bendable compound (**I-4**) are weaker than in the elastically bendable compound (**I-5**), thus allowing the slippage of the molecular layers on top of each other, consequently ending up in plastic

deformation. On the other hand, slightly stronger interactions in crystal structure of **I-5** prevent slippage mechanism and enable elastic deformation.

**Table 2.** Details on hydrogen and halogen bond geometries observed in the crystal structures of crystalline coordination polymers of cadmium(II) halides with halopyridine ligands, with the compounds arranged by the increase of the compliance (the least compliant → the most compliant) for the each group of compounds.

Compound	Hydrogen bonds			Halogen bonds		
	D—H···A	<(D—H···A) / °	$R_{\text{HA}}^*$	D—X1···X2	<(D—X1···X2) / °	$R_{\text{X1X2}}^*$
<b>I-6</b>	C1—H1···I1	136.6	<b>1.04</b>	C2—I2···I1	168	<b>0.96</b>
<b>II-2</b>	C3—H2···Br1	146	<b>1.00</b>	C2—Br1···Cl1	165	<b>0.99</b>
	C4—H3···Br1	138	<b>1.00</b>			
	C5—H4···Br2	150	<b>0.98</b>			
<b>II-3</b>	C3—H2···Br2	148	<b>1.03</b>	C2—Br2···Br1	166	<b>0.97</b>
	C4—H3···Br1	136	<b>0.98</b>			
	C5—H4···Br2	147	<b>1.04</b>			
<b>II-1</b>	C3—H2···Cl2	145	<b>1.01</b>	C2—Cl2···Cl1	164	<b>1.03</b>
	C4—H3···Cl1	136	<b>0.97</b>			
	C5—H4···Cl2	149	<b>1.03</b>			
<b>I-3</b>	C4—H3···I1	139	<b>1.00</b>	C2—Br1···I1	170	<b>0.98</b>
<b>I-1</b>	C4—H3···Br1	138	<b>0.97</b>	C2—Cl1···Br1	167	<b>1.01</b>
<b>I-2</b>	C4—H3···I1	141	<b>1.00</b>	C2—Cl1···I1	171	<b>1.02</b>
<b>I-4</b>	C4—H9···Cl1	130	<b>1.03</b>	C2—I1···Cl1	179	<b>0.92</b>
	C3—H8···I1	141	<b>1.01</b>			
<b>I-5</b>	C3—H3···I1	139	<b>1.03</b>	C2—I1···Br1	174	<b>0.92</b>
	C4—H4···Br1	163	<b>1.06</b>			

\*The normalized distance,  $R$ , defined according to Lommerse et al.<sup>102</sup>  $R_{\text{HA}} = d(\text{H}\cdots\text{A}) / (r_{\text{H}} + r_{\text{A}})$  and  $R_{\text{X1X2}} = d(\text{X1}\cdots\text{X2}) / (r_{\text{X1}} + r_{\text{X2}})$ , where  $r_{\text{H}}$ ,  $r_{\text{A}}$ ,  $r_{\text{X1}}$  and  $r_{\text{X2}}$  are the Bondi's van der Waals radii of the respective interacting halogen and hydrogen bond atoms (Cl 1.75, Br 1.86, I 1.98 Å, or H 1.20 Å).



To further support these observations, a calculation of the interaction energies was also performed. The interaction energy calculations were carried out on the molecular double pairs and in two different arrangements of the molecules, parallel and tilted to the crystal faces (Figure 22). For all compounds, the interaction energy values calculated for the regions parallel to the faces were lower, therefore clearly suggesting that these are the areas that allow the slippage of the neighboring domains during the plastic bending. Moreover, these interaction energies were lower for the plastically bendable crystals than those for the elastically bendable crystals. Calculated interaction energies also nicely followed the observed trends of the Young's moduli values and bending strain values (calculated for the elastically bendable compounds). The increase of the interaction energies is followed by the enlargement of Young's modulus values, and a concurrent decrease in the crystal's ability to adapt, i.e., enlargement of the bending strain value ( $\varepsilon$ ).

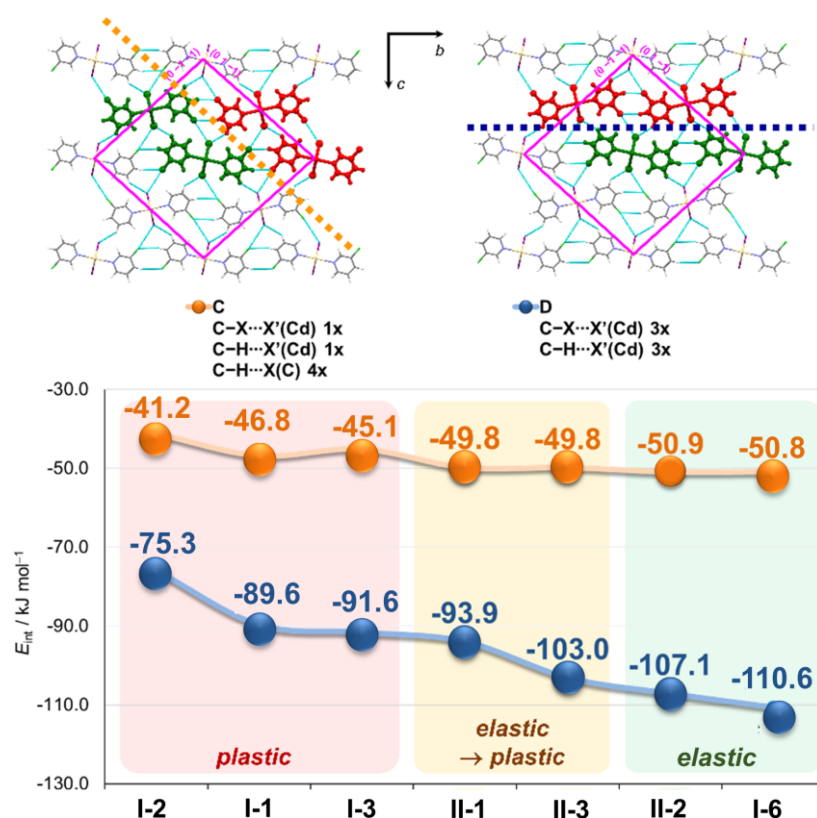


**Figure 22.** Double-pairs of molecular fragments red–green marked in the crystal packing of II-2. Dotted lines represent the regions of intermolecular interactions parallel (orange) or tilted (blue) to crystal faces (magenta solid lines). The interaction energies were calculated (M06-2X/DGDZVP) for molecular interactions (C–D) between molecular fragments (red–green).

To investigate the impact of plastic bending on thermal properties, the DSC measurements were performed. By comparison of the DSC curves obtained for the undeformed and plastically deformed crystals, it could be clearly observed that with inducing the plastic deformation crystal becomes thermally less stable, what is reflected in lowering the temperature of decomposition (Figure 23). Similar results were obtained for other plastically bent crystals where it was observed that the thermal processes such as melting or decomposition, start at a deformed part of the crystal, since that part is the “weakest link” where the structural perturbations are the most pronounced.<sup>33,35</sup>

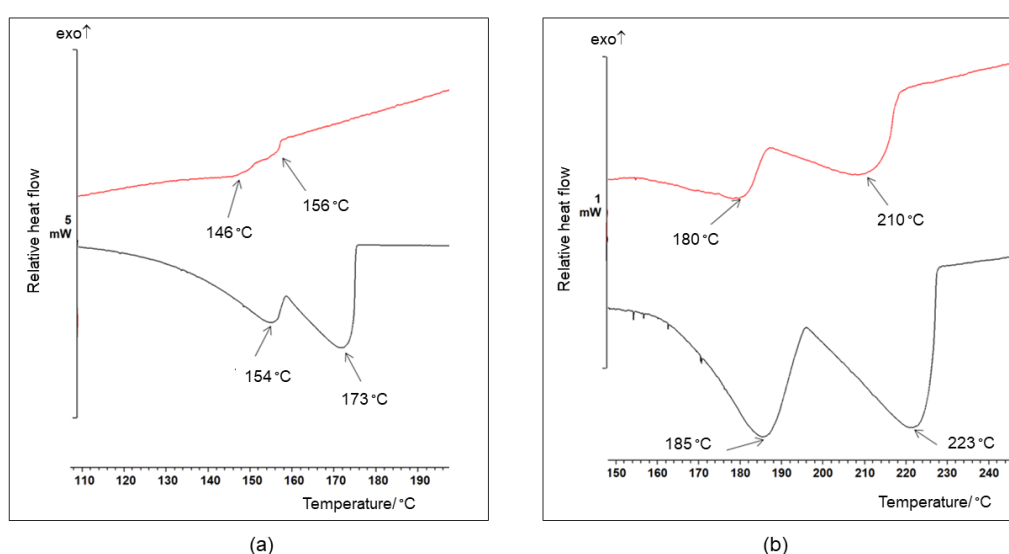


**Figure 23.** DSC curves of straight (**black**) and plastically bent (**red**) crystal of  $[\text{CdI}_2(3\text{-Brpy})_2]_n$  (**I-3**) (a) and  $[\text{CdB}_2(3\text{-Ipy})_2]_n$  (**I-5**) (b).

### 3.2. Modulating the crystalline mechanical responses through cyano functionality

To further investigate the origin of the crystalline material's ability to adapt to the external mechanical stimuli, a new series of the crystalline polymers was prepared by combining cadmium(II) halides with the cyano derivatives of pyridine, namely 3-cyanopyridine and 4-cyanopyridine:  $[\text{CdCl}_2(3\text{-CNpy})_2]_n$  (**III-1**),  $[\text{CdBr}_2(3\text{-CNpy})_2]_n$  (**III-2**),  $[\text{CdI}_2(3\text{-CNpy})_2]_n$  (**III-3**),  $[\text{CdCl}_2(4\text{-CNpy})_2]_n$  (**III-4**),  $[\text{CdBr}_2(4\text{-CNpy})_2]_n$  (**III-5**),  $[\text{CdI}_2(4\text{-CNpy})_2]_n$  (**III-6**) (Figure 24). In that way, the influence of the position of the cyano group on the morphology, mechanical properties, crystal structure and intermolecular interactions could have been monitored. The prepared compounds provided an unexpected variety of morphological, structural and mechanical responses, making this set of crystalline compounds an unprecedented pool of valuable information.

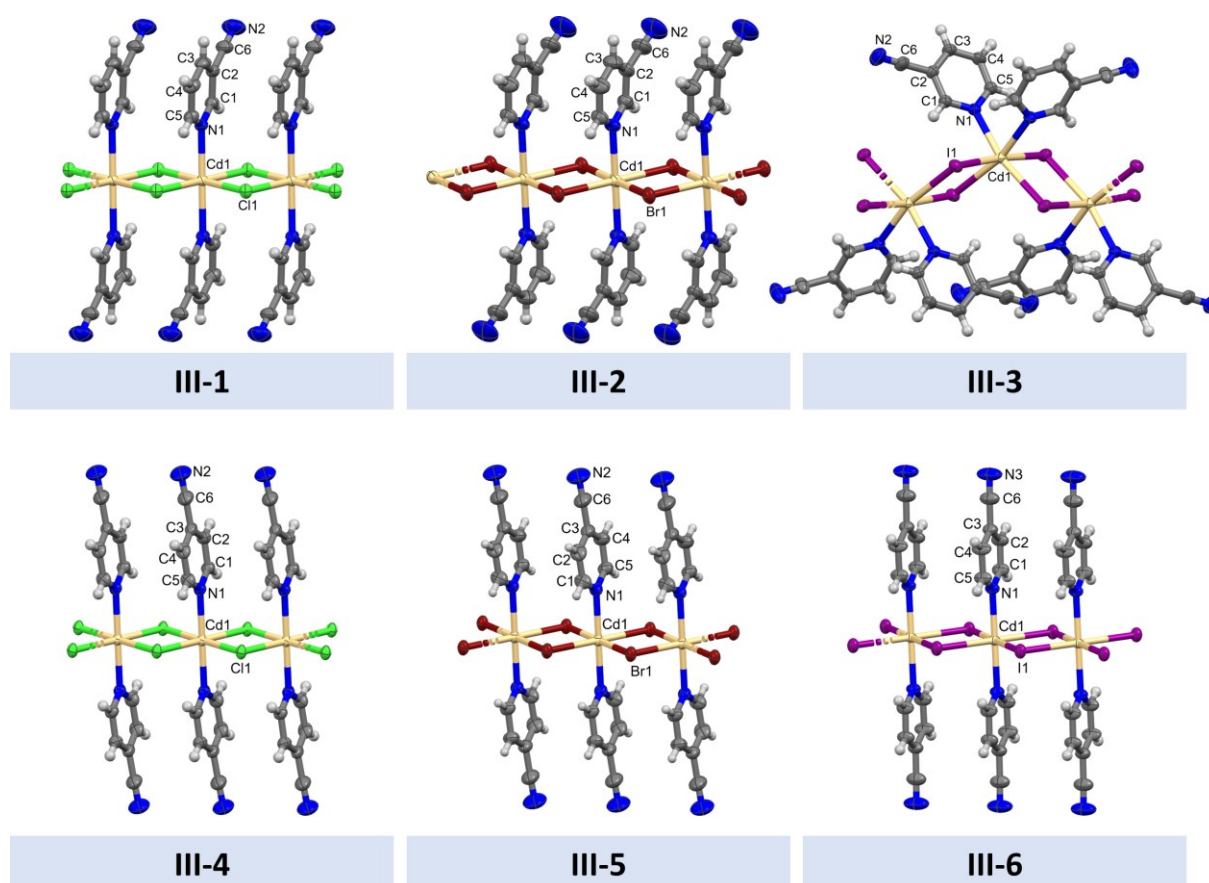


**Figure 24.** ORTEP plots of one-dimensional crystalline coordination polymers of cadmium(II) halides with 3-cyanopyridine (upper row) and 4-cyanopyridine (lower row).

The crystalline products were of elongated morphology but, as in the case of the cadmium(II) polymers with halopyridines, two types of the morphologies were observed – needles with the equally developed crystal faces, and those with clearly distinctive dimensions of the dominant crystal faces, i.e., extensively elongated plates, with the latter morphology prevailing within this set of compounds (Figure 25). The only crystals that crystallized in acicular morphology with equally developed crystal faces were the crystals of chloride and iodide compound with 3-cyanopyridine, **III-1**, and **III-3**.

The diffraction X-ray analysis showed that all prepared compounds crystallize in the monoclinic space groups ( $P2_1/c$ : **III-1**, **III-2**, **III-4**, **III-5**;  $I2/a$ : **III-3**;  $C2/c$ : **III-6**). Moreover, the structure determination revealed an unusual *cis*-geometry for **III-3**, while all other prepared compounds delivered targeted 1D polymeric chains with cyanopyridine ligands in *trans*-orientation. 1D polymeric building blocks are differently arranged in the crystal structure and provide four diverse structural arrangements.

The crystal structure (and the morphology) of **III-1** is comparable to the crystal structures of the elastically bendable crystals of cadmium(II) halides with halopyrazine ligands.<sup>73</sup> 1D polymer building units arrange parallel in the direction of crystallographic *c* axis and antiparallel in the direction of the crystallographic *b* axis, with the angle between the neighboring polymeric chains being almost 90 degrees. The mechanical response of those crystals was as well similar to those of polymers with halopyrazine ligands, crystals of **III-1** also gave elastic bending as a response to the mechanical stress. Moreover, the type and the extent of the elastic response were the same regardless of the direction of the stress application, with the bending strain value of 1.09%, therefore classifying those crystals as highly 2D isotropically elastically bendable.

Crystals of **III-2**, **III-4**, and **III-5**, were found to be of nearly identical crystal structures with each other and presented similar arrangement of the polymeric chains in crystal structure as in **III-1**, being parallel in the direction of the *b*, and antiparallel in the direction of *c* crystallographic axis. However, the orientation, and the tilting angle between the adjacent polymeric units in the direction of the *c* axis was different (i.e., larger than 90 degrees) than in the crystal structure of **III-1**, what consequently delivered a new packing type as well as morphology of a plate-like needles.

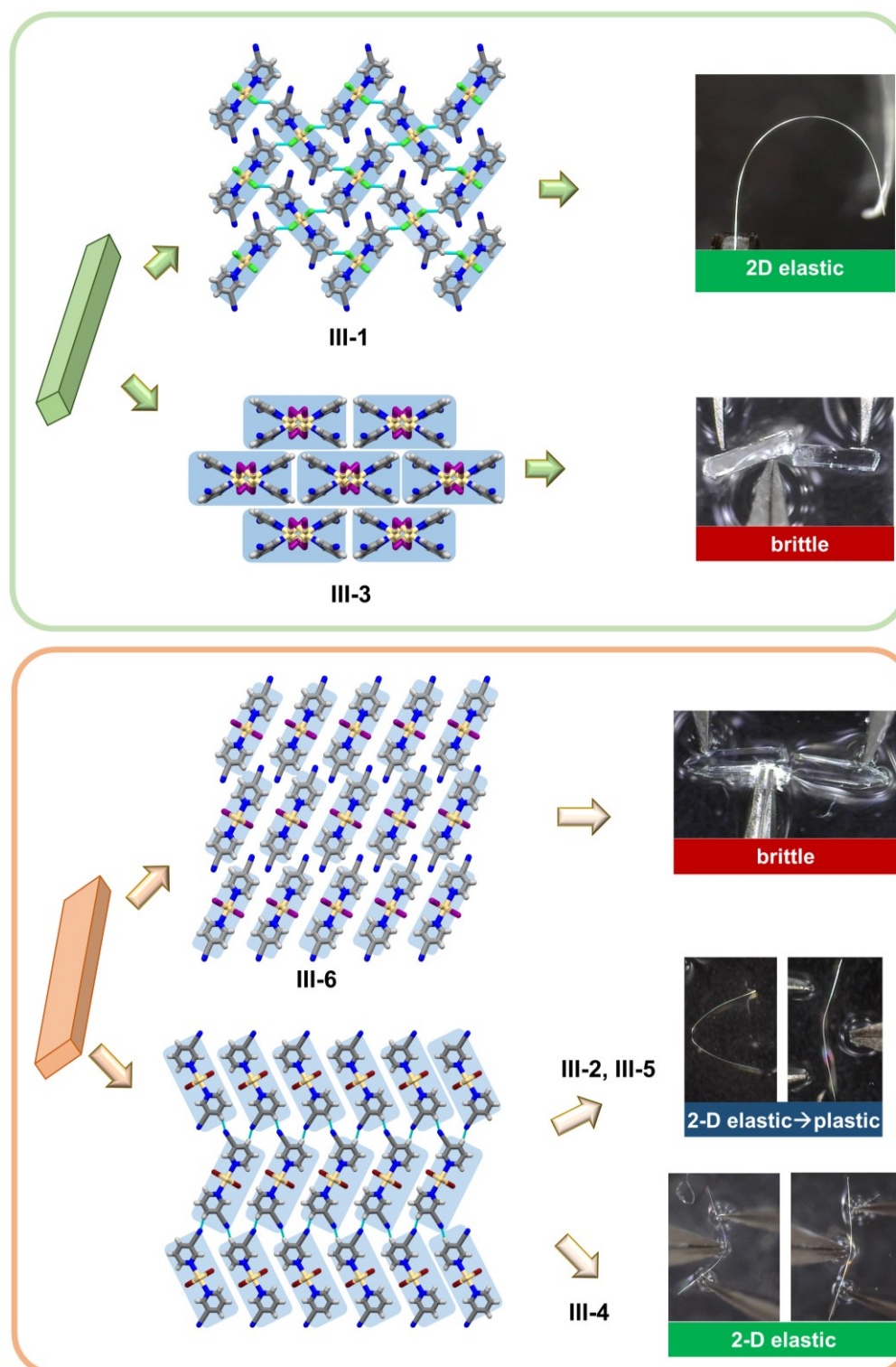


**Figure 25.** The observed morphologies, crystal packing types and mechanical responses in a family of crystalline one-dimensional coordination polymers with 3-cyanopyridine, and 4-cyanopyridine.

By probing the crystals' mechanical response, it was determined that these three compounds of almost identical crystal structure, are adaptable to the application of the outer stress. While crystals of **III-4** responded purely elastically, crystals of **III-2** and **III-5** respond elastically at smaller curvatures but at greater curvatures became slightly plastic, and then eventually broke with further application of the force, what classified them as elastically→plastically bendable. However, one important feature was observed, crystals of these plate-like crystals displayed direction-dependent responses. More precisely, since there was a noticeable distinction in the dimensions of the dominant crystal faces, the mechanical force could have been applied either on the set of larger or smaller crystal faces, and a clear difference in the mechanical responses was observed. Crystals of **III-4**, although elastically bendable over both sets of crystal faces, displayed larger extent of bending when the mechanical force was applied on the set of larger crystal faces ( $\varepsilon = 1.07\%$ ) than on the smaller one ( $\varepsilon = 0.53\%$ ). Since these crystals were two-dimensionally bendable, but with a clear difference in the extents of crystal bendability, they have been categorized as 2D anisotropically elastically bendable (Figure 26c, top). This was the first time that a difference in the crystals' mechanical pliability was reported for the two-dimensionally responsive crystals.

Similar behaviour was also observed for the crystals of bromide analogues with both organic ligands, **III-2** and **III-5**. The crystals showed elastic→plastic bending over both sets of crystal faces, but the compliance was substantially less pronounced when the mechanical force was applied on the set of smaller crystal faces as the crystal could be elastically and plastically bent to a smaller extent before breakage than on the larger one. Again, due to the difference in the extent of the mechanical response, crystals of **III-2** and **III-5** were classified as 2D anisotropically elastically→plastically bendable (Figure 26c, bottom).

To explain the difference in the type of the mechanically induced behaviour (elastic (**III-4**) vs. elastic→plastic (**III-2** and **III-5**)), and direction dependence of the bending extents, a thorough analysis of the structural features was performed from both the experimental and computational point of view (Figure 26a–b). In the crystal structures of **III-2**, **III-4**, and **III-5** similar types of hydrogen bond interactions were observed, C4–H4⋯N2, and C4–H4⋯X(Cd), and C5–H5⋯X(Cd), but their relative importance varied (concerning the normalized distance,  $R$ , defined by Lommerse et al.<sup>102</sup> and a geometrical distribution).



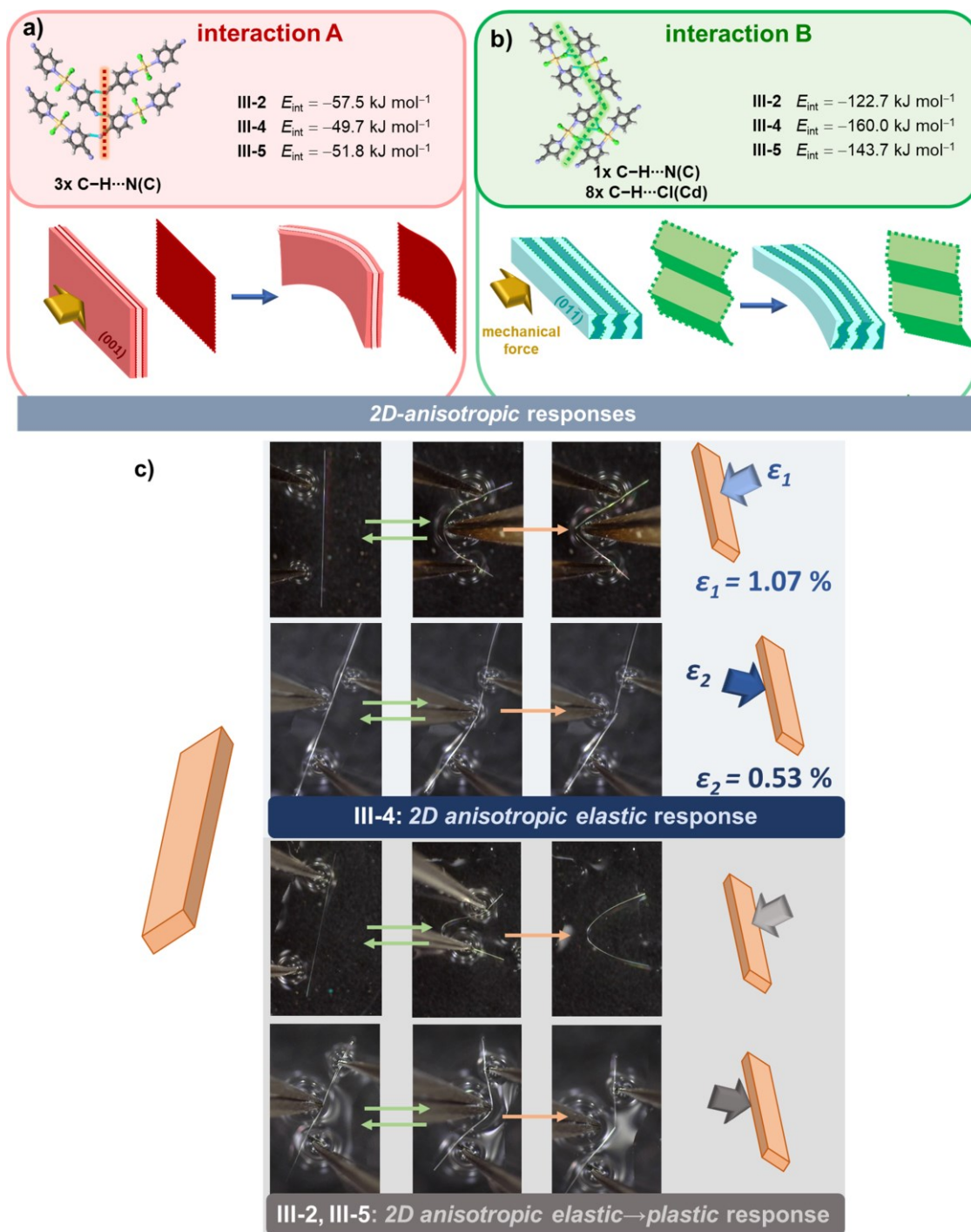


**Figure 26.** a–b) The double pairs of 1D polymeric chains, and representation of the regions of the intermolecular interactions termed as Interaction A and Interaction B, together with schematic presentation of ‘slicing up’ the crystal to the 2D molecular layers parallel to the larger (dark/pale red) and smaller (dark/pale green) crystal faces. c) 2D anisotropic elastic response of **III-4** (light blue background) and elastic→plastic response (light grey background) of **III-2** and **III-5**.

By thorough inspection of their crystal packing features, parallel to the bending faces, it was observed that crystal structures could be divided into two-dimensional molecular layers between which the planes of the intermolecular interactions are. The intermolecular interactions are also found to be the weakest link in the crystal structure, responsible for directing the mechanical response towards the specific outcome. In all three cases, parallel to the faces of larger dimensions the flat planes were defined in between which only the C–H $\cdots$ N interaction (interaction A) was observed, while parallel to the faces of smaller dimensions these plates were corrugated and the presence of both the C–H $\cdots$ N and C–H $\cdots$ X(Cd) interactions were observed (referred as interaction B). The obtained results from both the structural and calculated aspects pointed to the same conclusions. Firstly, the interactions (A and B type) in the structure of elastically bendable crystals (**III-4**) were stronger (shorter and more linear) than in the elastically $\rightarrow$ plastically bendable counterparts (**III-2** and **III-5**). These results suggest that stronger interactions guide the mechanical response towards reversible, i.e. elastic. On the other hand, weakening of the intermolecular interactions, leads to the sliding of the neighbouring domains upon mechanically induced stress, which therefore allows plastic deformation. Moreover, when comparing the strength of the intermolecular interactions in the two directions of interest, i.e., parallel to the two pairs of bending faces, it was clearly noticeable that interaction energies are substantially different. In the planes parallel to the faces of larger dimensions interactions are considerably less stabilizing ( $-49.7 - -57.5$  kJ mol $^{-1}$ ) than those parallel to the faces of smaller dimensions ( $-122.7 - -160.0$  kJ mol $^{-1}$ ). The stronger interactions together with the corrugation of the adjacent layers decrease the crystal's ability to compensate the large amounts of stress which consequently makes the crystal more prone to breakage when applying the mechanical force in that specific direction. Therefore, subtle differences in the strength of hydrogen bond interactions define the type of mechanical response.

To deepen the understanding of the observed mechanically induced crystal responses, in particular the direction-dependence, potential energy calculations were made for monodirectional distortions (shrinking or stretching in an increment of 0.5 Å) in the direction of the unit cell axes (along the *a*, *b*, or *c* axis). The fit of the obtained potential energy curves to the conventional Morse curve provided three force constants  $k_a$ ,  $k_b$ , and  $k_c$  for each compound, associated with a specific perturbation (shrinking and stretching) of the unit cell (Figure 27).

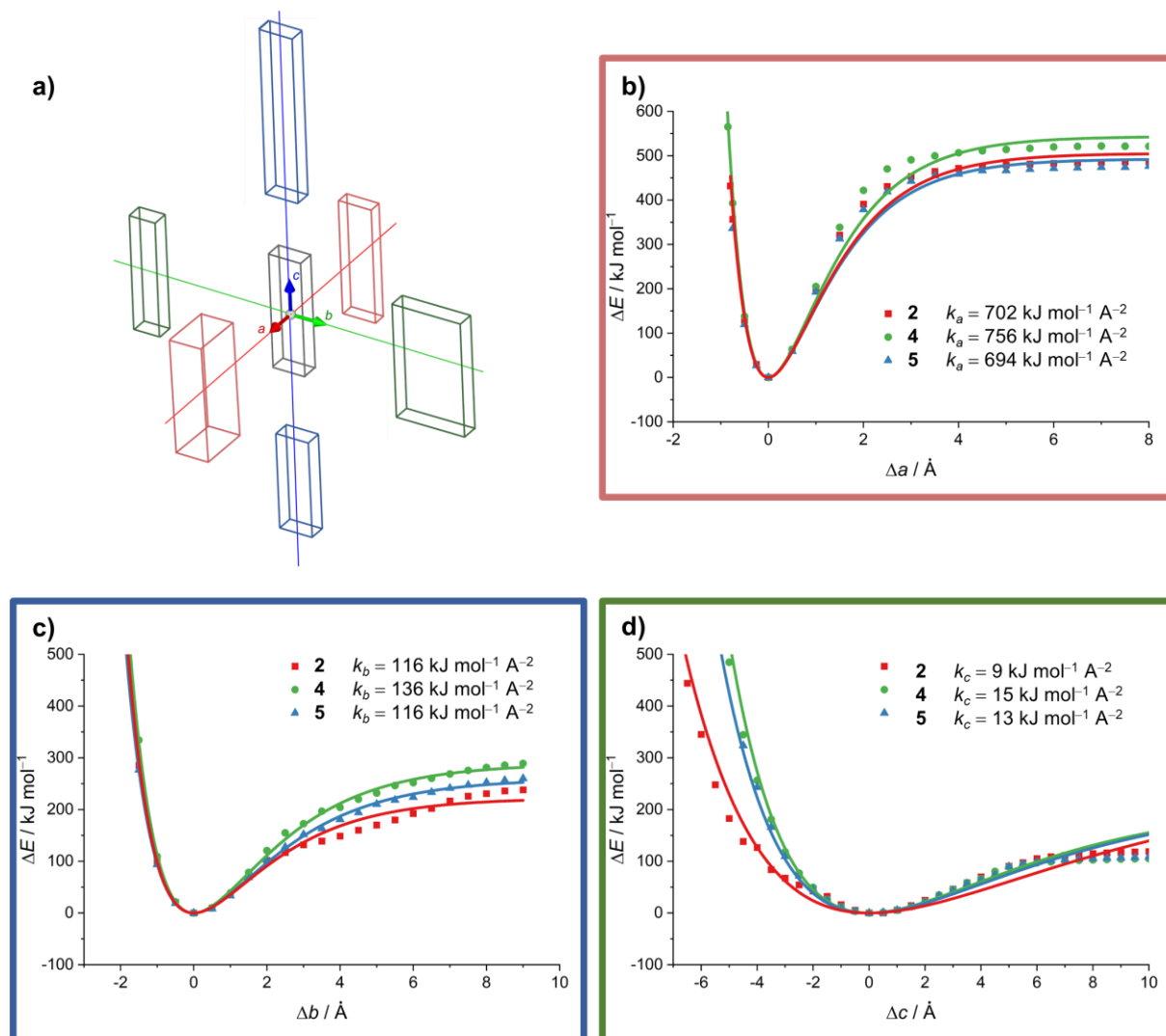


**Figure 27.** a) Schematic representation of contraction and expansion of the unit cell, along the  $a$ ,  $b$  and  $c$  axis. b–d) Potential energy curves for **III-2** (red), **III-4** (green), and **III-5** (blue) as a function of relative deformation of the unit cell along the  $a$ ,  $b$ , and  $c$  axes respectively. The solid lines represent fits to the conventional Morse potential from which the constants  $k_a$ ,  $k_b$ , and  $k_c$  were calculated.

For all three inspected materials (**III-2**, **III-4**, and **III-5**) a force constant  $k_a$ , associated to a unit cell deformation along  $a$  axis, was expectedly of the largest values amongst all three obtained force constants. This direction coincides with the direction of the propagation of the polymeric chains, therefore the deformation of the unit cell along that direction corresponds to deformation of Cd—X (X = Cl, Br) covalent bond. Moreover, the value for the chloride analogue **III-4** (756

$\text{kJ mol}^{-1} \text{ \AA}^{-2}$ ) is larger than the values for the bromide compounds, **III-2** ( $702 \text{ kJ mol}^{-1} \text{ \AA}^{-2}$ ) and **III-5** ( $694 \text{ kJ mol}^{-1} \text{ \AA}^{-2}$ ) what conveys the fact that the Cd—Cl bond is stronger than the Cd—Br bond. On the other hand, the remaining two force constants,  $k_b$ , and  $k_c$  are of substantially lower values than the  $k_a$ , as by this model, only the intermolecular interactions are affected with deformation along the  $b$  and  $c$  axes. Moreover, values of the force constants for deformation along the  $c$  axis were substantially smaller than that corresponding ones for the deformation along the  $b$  axis. However, there is a quite nice correlation between the force constant values and the mechanical behaviour of the crystals. The smaller value of the force constant is obtained along the  $c$  direction, which coincides with crystals being the most deformable perpendicularly to that direction (i.e. by applying the mechanical force on the pair of faces of larger dimensions ( $001/00\bar{1}$ ) crystals bend substantially, and upon bending most of perturbations occurs in the direction of  $c$  axis). On the other hand, crystals are less adaptable if the mechanical force is applied to a pair of smaller faces ( $011/0\bar{1}\bar{1}$ ) which can be explained by the substantially larger value of the constant  $k_b$ . However, during the application of the mechanical force on the faces of smaller dimensions, both constants,  $k_b$ , and  $k_c$  need to be taken into the account, but  $k_b$  (because of its substantially larger value) is most likely responsible for the diminished tolerance of crystal on the outer stimuli.

The similar calculations were also made for previously reported mechanically adaptable crystalline coordination polymers, the plastically bendable  $[\text{ZnCl}_2(3,5\text{-Cl}_2\text{py})_2]_n$ , and elastically crystal of  $[\text{CdBr}_2(2\text{-Clpz})_2]_n$ .<sup>76</sup> The potential energy calculations were made for the isotropic perturbations of the unit cell along the axes perpendicular to the elongation of the polymeric chain, and obtained curves were also fitted to the classical Morse curve potential, and force constants,  $k_{CP}$ , were extracted for each compound. The value of the  $k_{CP}$  for the elastically bendable compound was twice higher than the value for the plastically bendable compound. Those results suggested that in the elastically bendable crystals any deformation of the unit cell will not be favoured but rather the restoring of the equilibrium position (i.e., macroscopically observed as undeformed crystal) will most likely occur. That behaviour is facilitated by the presence of strong interactions within the crystal structure. As opposed to that, in the plastically bendable compound, lack of the strong intermolecular interactions enables the formation of stable interwoven networks because of the permanent deformation (macroscopically observed as plastic bending). In this way, the authors proposed a so-called “spaghetti” model for the plastic bending of the crystalline compounds (Figure 11c).

Similarly, to those previously reported results, larger values of the force constants for the elastically bendable **III-4**, than for the elastic→plastic adaptable crystals of **III-2** and **III-5** were obtained. These results nicely follow the observation of the stronger intermolecular interactions facilitating the elastic response of the crystalline compounds by preventing the sliding of the neighbouring slabs and allowing the crystal to restore its original position once the mechanical stress is removed. On the other hand, somewhat weaker intermolecular interactions, together with the lower values of the force constants enable the slippage of the domains in crystals of **III-2** and **III-5** at larger stresses, which macroscopically manifests as an elastic→plastic response.

Thorough inspection of the structural features and theoretical calculations provided a valuable insight into the structural requirements for achieving the specific mechanical response. However, the mechanism of the molecular movements that materialize because of bending and enable the elastic response still remained vague. To get an insight into the stress-induced events on the molecular scale, microfocus X-ray diffraction experiments on a bent crystal of the 2D isotropically elastically bendable compound, **III-1**, were performed. The diffraction images were collected at the outer, and inner arc of the bent crystal, at the point of its maximum curvature, and unit cell parameters were determined. The most pronounced difference was observed in the value of the crystallographic parameter  $a$  in comparison to the straight, undeformed crystal. While enlargement of the  $a$  axis on the outer arc suggests the stretching of the polymeric chain and extension of the Cd···Cd distance, its shortening on the inner arc indicates exactly the opposite – compression of the polymeric chains and consequently shortening of the Cd···Cd distance. This observation was in line with the previously reported microfocus experiments on the zero-dimensional elastic compound of bis(2,4-pentanedionato)copper(II), [Cu(acac)<sub>2</sub>].<sup>72</sup> Furthermore, one other interesting characteristic of the collected peaks could be noticed. The diffraction peaks collected on the outer and inner arc of the bent crystal were substantially broadened in comparison to those collected for the undeformed crystal. Moreover, broadening was more pronounced on the outer, than on the inner arc of the bent crystal, what suggested that more pronounced molecular movements occur on the outer than on the inner arc of the bent crystal. More specifically, the polymeric chain can be more stretched than compressed, which can also be concluded if observing the calculated potential energy curves (Figure 28).

The crystals of iodide analogues with both organic ligands, **III-3** and **III-6**, displayed typical brittle behaviour of the crystalline material, and were not comparable with any other compound.

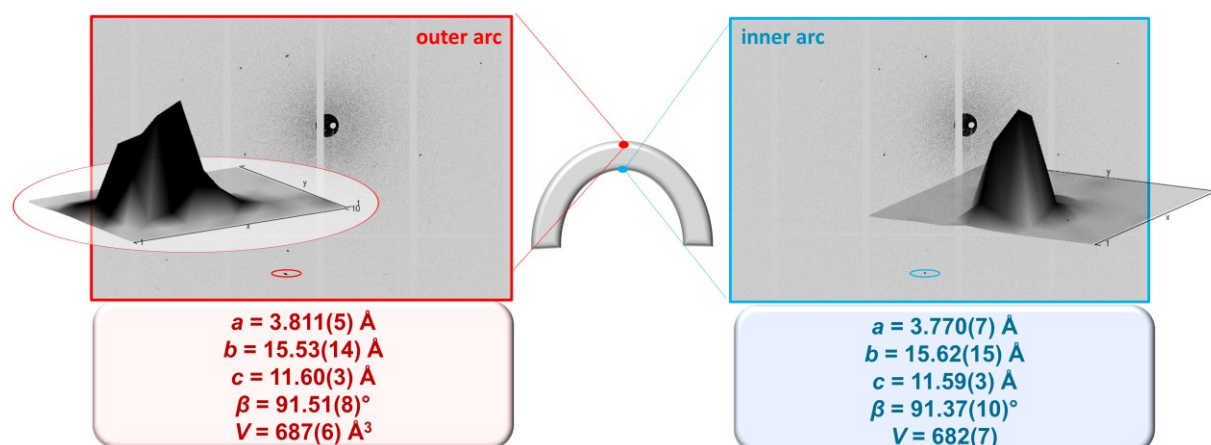


**Figure 28.** The diffraction peak profile and unit cell parameters for a bent crystal of **III-1** on an outer and inner arc.



## § 4. CONCLUSIONS AND OUTLOOK

This doctoral thesis provides a comprehensive insight into the mechanically induced flexibility of one-dimensional crystalline coordination polymers of cadmium(II) halides with pyridine-based ligands, namely 3-halopyridines, 3-cyanopyridine and 4-cyanopyridine. Here we epitomize the research findings, put them in a broader scientific context, and outline potential future research avenues of this emerging scientific field.

This thesis is based on the three original scientific papers which provided systematic research of the structure–mechanical property correlation on a series of one-dimensional crystalline cadmium(II) coordination polymers using both experimental and computational approach. Each of the three papers individually delivers plethora of valuable knowledge, complementing each other, and even more importantly, completing the part of an exciting puzzle of mechanically adaptable crystalline materials. All three papers combined provided us with a substantial amount of data to draw border conclusions on the origin of the mechanically induced flexibility of crystalline materials.

The obtained results show that introducing small changes in the structure, such as replacement of a bridging anion in a polymeric chain, or a functionality on a ligand, has a substantial impact on supramolecular arrangement, crystal morphology and most importantly, on macroscopic mechanical output. More surprisingly, on a set of isostructural compounds, obtained results showed that subtle manipulation of the structural features causes a slight change in the geometry and strength of the intermolecular interactions, which has unexpectedly major consequences on the macroscopically observed mechanical responsiveness of crystals, not only the extent but also the type of the flexible response. It was demonstrated that crystals can display the whole spectrum of mechanical bendability, from purely elastic, towards elastic→plastic, to variable plasticity, and even unprecedented ductility and flow of crystalline material, thus showing mechanical resemblance to common, widely used materials. DFT computational studies, together with the in-depth structural investigation, allowed the detection of the “weakest regions” in the crystal packing, i.e. planes of the intermolecular interactions, typically hydrogen and halogen bonds, parallel to the bending faces. These regions are considered as most likely responsible for allowing the specific crystals’ mechanical responses. A clear bending–stiffness–energy correlation was observed. With the increase of the strength

of the intermolecular interactions, decrease of the crystals' pliability followed by the increase of the stiffness is observed, which is reflected in the enlargement of Young's modulus. On the other hand, the strength of the intermolecular interactions in plastically bendable compounds is substantially lower, therefore allowing the slippage of the neighbouring domains over each other upon application of the mechanical force. The mechanism of the plastic bending by sliding of the neighbouring domains over each other was also supported by clearly visible delamination of the crystal at the kink of the plastically bent crystal, visualized by AFM surface mapping.

Furthermore, two types of mechanical bending were observed, one-dimensional (1D) and two-dimensional (2D) flexibility. However, it was noticed that the same crystal can give different extents of mechanical response depending on the direction of the force application, i.e. some of the two-dimensionally bendable crystals can display different extents of flexibility according to the pair of potential bending faces to which mechanical force is applied. These crystals were therefore classified as 2D anisotropically flexible, while those that give the same type and extent of mechanical responses are termed as 2D isotropically flexible.

Having all this in mind, in the overall intricacy of a variety of structural factors responsible for equipping crystals of metal-organic compounds with flexibility, intermolecular interactions can be recognized as one of the key parameters that need to be fine-tuned in order to deliver specific mechanical responses.

Research into the mechanical properties of molecular solids has recently become a subject of rapidly growing interest, not only in the crystallographic, but also in the wider scientific community. Flexible crystals have proven to be the materials suitable for use in many other fields such as optics, biophysics, and even pharmaceutical technology, however, their full potential has not yet been fully realized because of the lack of understanding of the origin of this amazing phenomenon. Coordination polymers of cadmium(II) halides with pyridine- and pyrazine-based ligands have proven to be mechanically adaptable crystalline materials whose mechanical response can be controlled by introducing small structural changes, which provides the basis for a detailed structure–function correlation, and consequently enlightening the still insufficiently known deformation mechanisms in crystalline materials. The ultimate scientific goal of a future work is to provide a thorough understanding the underlying structural principles not only of coordination polymers but also other classes of crystalline materials. For that, a highly interdisciplinary approach and involvement of scientists from disciplines such as crystal engineering, physics, theoretical chemistry, and many other, that will allow a systematic

evolution of this topic and finally the design and control of the mechanical properties of functional materials for various applications is required.

## § 5. LIST OF ABBREVIATIONS AND SYMBOLS

<b>I-1</b>	$[\text{CdBr}_2(3\text{-Clpy})_2]_n$
<b>I-2</b>	$[\text{CdI}_2(3\text{-Clpy})_2]_n$
<b>I-3</b>	$[\text{CdI}_2(3\text{-Brpy})_2]_n$
<b>I-4</b>	$[\text{CdCl}_2(3\text{-Ipy})_2]_n$
<b>I-5</b>	$[\text{CdBr}_2(3\text{-Ipy})_2]_n$
<b>I-6</b>	$[\text{CdI}_2(3\text{-Ipy})_2]_n$
<b>II-1</b>	$[\text{CdCl}_2(3\text{-Clpy})_2]_n$
<b>II-2</b>	$[\text{CdCl}_2(3\text{-Brpy})_2]_n$
<b>II-3</b>	$[\text{CdBr}_2(3\text{-Brpy})_2]_n$
<b>III-1</b>	$[\text{CdCl}_2(3\text{-CNpy})_2]_n$
<b>III-2</b>	$[\text{CdBr}_2(3\text{-CNpy})_2]_n$
<b>III-3</b>	$[\text{CdI}_2(3\text{-CNpy})_2]_n$
<b>III-4</b>	$[\text{CdCl}_2(4\text{-CNpy})_2]_n$
<b>III-5</b>	$[\text{CdBr}_2(4\text{-CNpy})_2]_n$
<b>III-6</b>	$[\text{CdI}_2(4\text{-CNpy})_2]_n$
<b>AFM</b>	atomic force microscopy
<b>acac</b>	2,4-pentanedione (acetylacetone)
<b>DFT</b>	density functional theory
<b>DSC</b>	differential scanning calorimetry
<b>1D</b>	one-dimensional
<b>2D</b>	two-dimensional
<b>py</b>	pyridine
<b>pz</b>	pyrazine

## § 6. REFERENCES

- [1] IUCr dictionary, accessed May 4<sup>th</sup>, 2022.
- [2] P. Naumov, S. Chizhik, M. K. Panda, N. K. Nath, E. Boldyreva, *Chem. Rev.* **115** (2015) 12440–12490.
- [3] P. Commins, I. T. Desta, D. P. Karothu, M. K. Panda, P. Naumov, *Chem. Comm.* **52** (2016) 13941–13954.
- [4] E. Ahmed, D. P. Karothu, P. Naumov, *Angew. Chem. Int. Ed.* **57** (2018) 8837–8846.
- [5] G. A. Abakumov, V. I. Nevodchikov, *Dokl. Phys. Chem.* **266** (1982) 1407–1410.
- [6] F. I. Ivanov, N. A. Urban, *React. Solids* **1** (1986) 165–170.
- [7] O. S. Bushuyev, A. Tomberg, T. Friščić, C. J. Barrett, *J. Am. Chem. Soc.* **135** (2013) 12556–12559.
- [8] O. S. Bushuyev, T. C. Corkery, C. J. Barrett, T. Friščić, *Chem. Sci.* **5** (2014) 3158–3164.
- [9] H. Koshima, N. Ojima, H. Uchimoto, *J. Am. Chem. Soc.*, **131** (2009) 6890–6891.
- [10] T. Taniguchi, J. Fujisawa, M. Shiro, H. Koshima, T. Asahi, *Chem. Eur. J.* **22** (2016) 22, 7950–7958.
- [11] T. Kim, M. K. Al-Muhanna, S. D. Al-Suwaidan, R. O. Al-Kaysi, C. J. Bardeen, *Angew. Chem.* **123** (2013) 7027–7031.
- [12] T. Kim, L. Zhu, L. J. Mueller, C. J. Bardeen, *J. Am. Chem. Soc.* **136** (2014) 6617–6625.
- [13] E. Hatano, M. Morimoto, T. Imai, K. Hyodo, A. Fujimoto, R. Nishimura, A. Sekine, N. Yasuda, S. Yokojima, S. Nakamura, K. Uchida, *Angew. Chem. Int. Ed.* **56** (2017) 12576–12580.
- [14] E. Uchida, R. Azumi, Y. Norikane, *Nature Commun.* **6** (2015) 7310: 1–7.

- [15] P. Naumov, S. C. Sahoo, B. A. Zakharov, E. V. Boldyreva, *Angew. Chem. Int. Ed.* **52** (2013) 9990–9995.
- [16] S. Chizhik, A. Sidelnikov, B. Zakharov, P. Naumov, E. Boldyreva, *Chem. Sci.* **9** (2018) 2319–2335.
- [17] Ž. Skoko, S. Zamir, P. Naumov, J. Bernstein, *J. Am. Chem. Soc.* **132** (2010) 14191–14202.
- [18] P. Gupta, D. P. Karothu, E. Ahmed, P. Naumov, N. K. Nath, *Angew. Chem. Int. Ed.* **57** (2018) 8498–8502.
- [19] B. B. Rath, M. Gupta, J. J. Vittal, *Chem. Mater.* **34** (2022) 178–185.
- [20] C.M. Reddy, S. Basavoju, G. R. Desiraju, *Chem. Commun.* **31** (2005) 2439–2441.
- [21] C. M. Reddy, R. C. Gundakaram, S. Basavoju, M. T. Kirchner, K. A. Padmanabhan, G. R. Desiraju, *Chem. Commun.* **31** (2005) 3945–3947.
- [22] C. M. Reddy, K. A. Padmanabhan, G. R. Desiraju, *Cryst. Growth Des.* **6** (2006) 2720–2731.
- [23] C. M. Reddy, M. T. Kirchner, R. C. Gundakaram, K. A. Padmanabhan, G. R. Desiraju, *Chem. Eur. J.* **12** (2006) 2222–2234.
- [24] C. M. Reddy, G. R. Krishna, S. Gosh, *CrystEngComm* **12** (2010) 2296–2314.
- [25] M. K. Panda, S. Ghosh, N. Yasuda, T. Moriwaki, G. Dev Mukherjee, C. M. Reddy, P. Naumov, *Nat. Chem.* **7** (2015) 65–72.
- [26] A. Mukherjee, G. R. Desiraju, *IUCrJ* **1** (2014) 49–60.
- [27] G. R. Krishna, R. Decarapalli, G. Lal, C. M. Reddy, *J. Am. Chem. Soc.* **138** (2016) 13561–13567.
- [28] S. P. Thomas, M.W. Shi, G. A. Koutsantonis, D. Jayatilaka, A. J. Edwards, M. A. Spackman, *Angew. Chem. Int. Ed.* **56** (2017) 8468–8472.
- [29] S. Saha, G. R. Desiraju, *J. Am. Chem. Soc.* **139** (2017) 1975–1983.
- [30] S. Saha and G. R. Desiraju, *Chem. Commun.* **53** (2017) 6371–6374.



- [31] L. Catalano, D. P. Karothu, S. Schramm, E. Ahmed, R. Rezgui, T. J. Barber, A. Famulari, P. Naumov, *Angew. Chem. Int. Ed.* **57** (2018) 17254–17258.
- [32] S. Saha and G. R. Desiraju, *Chem. Commun.* **54** (2018) 6348–6351.
- [33] L. O. Alimi, P. Lama, V. J. Smith, L. J. Barbour, *Chem. Commun.* **54** (2018) 2994–2997.
- [34] R. Devarapalli, S.B. Kadambi, C.-T. Chen, G. R. Krishna, B. R. Kammari, M. J. Buchler, U. Ramamurty, C. M. Reddy, *Chem. Mater.* **31** (2019) 1391–1402.
- [35] S. Hu, M. K. Mishra, C. C. Sun, *Chem. Mater.* **31** (2019) 3818–3822.
- [36] H. Liu, Z. Bian, Q. Cheng, L. Lan, Y. Wang, H. Zhang, *Chem. Sci.* **10** (2019) 227–232.
- [37] A. Paikar, D. Podder, S. R. Chowdhury, S. Sasmal, D. Haldar, *CrystEngComm* **21** (2019) 589–593.
- [38] N. K. Nath, P. Gupta, P. J. Hazarika, N. Deka, A. Mukherjee, G. K. Dutta, *Cryst. Growth Des.* **19** (2019) 6033–6038.
- [39] P. Gupta, T. Panda, S. Allu, S. Borah, A. Baishya, A. Gunnam, A. Nangia, P. Naumov, N. K. Nath, *Cryst. Growth Des.* **19** (2019) 3039–3044.
- [40] U. B. R. Khandavilli, M. Lusi, P. J. Frawley, *IUCrJ* **6** (2019) 630–634.
- [41] B. Bhattacharya, D. Roy, S. Dey, A. Puthuvakkal, S. Bhunia, S. Mondal, R. Chowdhury, M. Bhattacharya, M. Mandal, K. Manoj, P. K. Mandal, C. M. Reddy, *Angew. Chem. Int. Ed.* **59** (2020) 10971–10980.
- [42] S. Bhandary, A. J. Thompson, J. C. McMurtrie, J. K. Clegg, P. Ghosh, S. R. N. K. Mangalampalli, S. Takamizawa, D. Chopra, *Chem. Commun.* **56** (2020) 12841–12844.
- [43] C. Cappuccino, L. Catalano, F. Marin, G. Dushaq, G. Raj, M. Rasras, R. Rezgui, M. Zambianchi, M. Melucci, P. Naumov, L. Maini, *Cryst. Growth Des.* **20** (2020) 884–891.
- [44] J. Ravi, A. V. Kumar, D. P. Karothu, M. Annadhasan, P. Naumov, R. Chandrasekar, *Adv. Funct. Mater.* **31** (2021) 2105415, 1–10.

- [45] P. Commins, A. B. Dippenaar, L. Li, H. Hara, D. A. Haynes, P. Naumov, *Chem. Sci.* **12** (2021) 6188–6193.
- [46] A. Mondal, B. Bhattacharya, S. Das, S. Bhunia, R. Chowdhury, S. Dey, C. M. Reddy, *Angew. Chem. Int. Ed.* **59** (2020) 10971–10980.
- [47] S. Ghosh, M. C. Reddy, *Angew. Chem. Int. Ed.* **51** (2012) 10319–10323.
- [48] C.-T. Chen, S. Gosh, C. M. Reddy, M. J. Buehler, *Phys. Chem. Chem. Phys.* **16** (2014) 13165–13171.
- [49] S. Ghosh, M. K. Mishra, S. B. Kadambi, U. Ramamurty, G.R. Desiraju, *Angew. Chem. Int. Ed.* **54** (2015) 2674–2678.
- [50] S. Ghosh, M. K. Mishra, S. Ganguly, G. R. Desiraju, *J. Am. Chem. Soc.* **137** (2015) 9912–9921.
- [51] S. Saha, G. R. Desiraju, *Chem. Commun.* **52** (2016) 7676–7679.
- [52] S. Saha, G. R. Desiraju, *Chem. Eur. J.* **23** (2017) 4936–4943.
- [53] S. Saha, G. R. Desiraju, *J. Am. Chem. Soc.* **139** (2017) 1975–1983.
- [54] K. Wang, M. K. Mishra, C. C. Sun, *Chem. Mater.* **31** (2019) 1794–1799.
- [55] M. S. Kazantsev, V. G. Konstantinov, D. I. Dominskiy, V. V. Bruevich, V. A. Postnikov, Y. N. Luponosov, V. A. Tafeenko, N. M. Surin, S. A. Ponomarenko, D. Y. Paraschuk, *Synth. Met.* **232** (2017) 60–65.
- [56] H. Liu, Z. Lu, Z. Zhang, Y. Wang, H. Zhang *Angew. Chem. Int. Ed.* **57** (2018) 8448–8452.
- [57] S. Hayashi, S. Yamamoto, D. Takeuchi, Y. Ie. K. Takag, *Angew. Chem. Int. Ed.* **57** (2018) 17002–17008.
- [58] A. Ölander, *J. Am. Chem. Soc.* **54** (1932) 3819–3833.
- [59] M. A. Ferreira, M. A. Luersen, P. C. Borges, *Dental Press J. Orthod.* **17** (2012) 71–82.
- [60] N. Nayan, V. Buravalla, U. Ramamurty, *Mater. Sci. Eng. A* **525** (2009) 60–67.

- [61] A. Lai, Z. Du, C. P. Gan, A. C. Schuh, *Science* **341** (2013) 1505–1508.
- [62] S. Takamizawa, Y. Miyamoto, *Angew. Chem. Int. Ed.* **53** (2014) 6970–6973.
- [63] S. Takamizawa, Y. Takasaki, *Angew. Chem. Int. Ed.* **54** (2015) 4815–4817
- [64] Y. Takasaki, S. Takamizawa, *Nat. Commun.* **6** (2015) 8934: 1–5.
- [65] S. Takamizawa, Y. Takasaki, *Chem. Sci.* **7** (2016) 1527–1534.
- [66] S. Sakamoto, T. Sasaki, A. Sato-Tomita, S. Takamizawa, *Angew. Chem. Int. Ed.* **58** (2019) 13722–13726.
- [67] T. Sasaki, K. Nishizawa, S. Takamizawa, *Cryst. Growth Des.* **21** (2021) 2453–2458.
- [68] T. Sasaki, S. Ranjan, S. Takamizawa, *CrystEngComm* **34** (2021) 5801–5804.
- [69] S. Takamizawa, Y. Tasaki, T. Sasaki, N. Ozaki, *Nat. Commun.* **9** (2018) 3984: 1–6.
- [70] S. H. Mir, Y. Takasaki, E. R. Engel, S. Takamizawa, *Angew. Chem. Int. Ed.* **56** (2017) 15882–15885.
- [71] S. Ranjan, S. Takamizawa, *Cryst. Growth Des.* **22** (2022) 1831–1836.
- [72] A. Whorby, A. Grosjean, M. C. Pfrunder, Y. Xu, C. Yan, G. Edwards, J. K. Clegg, J. C. McMurtrie, *Nat. Chem.* **10** (2018) 65–69.
- [73] M. Đaković, M. Borovina, M. Pisačić, C. B. Aakeröy, Ž. Soldin, B.-M. Kukovec, I. Kodrin, *Angew. Chem. Int. Ed.* **57** (2018) 14801–14805.
- [74] A. J. Thompson, A. Worthy, A. Grosjean, J. R. Price, J. C. McMurtrie, J. K. Clegg, *CrystEngComm*, **23** (2021) 5731–5737.
- [75] N. K. Nath, P. Gupta, P. J. Hazarika, N. Deka, A. Mukherjee, G. K. Dutta, *Cryst. Growth Des.* **19** (2019) 6033–6038.
- [76] B. Bhattacharya, A. A. L. Michalchuk, D. Silbernagl, M. Rautenberg, T. Schmid, T. Feiler, K. Reinmann, A. Ghalgaoui, H. Sturm, B. Paulus, F. Emmerling, *Angew. Chem. Int. Ed.*, **59** (2020) 5557–5561.

- [77] B. B. Rath, J. J. Vittal, *Chem. Mater.* **33** (2021) 4621–4627.
- [78] L. Mei, S. W. An, K. Q. Hu, L. Wang, J. P. Yu, Z. W. Huang, X. H. Kong, C. Q. Xia, Z. F. Chai, W. Q. Shi, *Angew. Chem. Int. Ed.* **59** (2020) 16061–16068.
- [79] S. Kusumoto, A. Sugimoto, Y. Zhang, Y. Kim, M. Nakamura, S. Hayami, *Inorg. Chem.* **60** (2021) 1294–1298.
- [80] Z. Tang, X.-P. Sun, S.-D. Wang, X.-Y. Ji, Y. Li, Z.-S. Yao, J. Tao, *Chem. Sci. China* **65** (2022) 710–718.
- [81] P. P. Bag, M. Chen, C. C. Sun, C. M. Reddy, *CrystEngComm* **14** (2012) 3865–3867.
- [82] U. B. R. Khandavilli, M. Yousuf, B. E. Schaller, R. R. E. Steendam, L. Keshavarz, P. McArdle, P. J. Frawley, *CrystEngComm* **22** (2020) 412–415.
- [83] M. Annadhasan, S. Basak, N. Chandrasekhar, R. Chandrasekar *Adv. Opt. Mater.* (2020) 2000959: 1–30.
- [84] M. Annadhasan, D. P. Karothu, R. Chinnasamy, L. Catalano, E. Ahmed, S. Ghosh, P. Naumov, R. Chandrasekar, *Angew. Chem. Int. Ed.* **59** (2020) 13821–13830.
- [85] M. Annadhasan, A. R. Agrawal, S. Bhunia, V. V. Pradeep, S. S. Zade, C. M. Reddy, R. Chandrasekar, *Angew. Chem. Int. Ed.* **59** (2020) 13852–13858.
- [86] N. P. Thekkeppat, M. Lakshmipathi, A. S. Jalilov, P. Das, A. M. P. Peedikakkal, S. Ghosh, *Cryst. Growth Des.* **20** (2020) 3937–3943.
- [87] J. Ravi, M. Annadhasan, A. V. Kumar, R. Chandrasekar, *Adv. Funct. Mater.* (2021) 2100642: 1–9.
- [88] D. P. Karothu, G. Dushaq, E. Ahmed, L. Catalano, S. Polavaram, R. Ferreira, L. Li, S. Mohamed, M. Rasras, P Naumov, *Nat. Commun.* **12** (2021) 1326: 1–8.
- [89] V. V. Pradeep, C. Tardío, I. Torres-Moya, Ana. M. Rodríguez, A. V. Kumar, M. Annadhasan, A. de la Hoz, P. Prieto, R. Chandrasekar, *Small* **17** (2021) 2006795.

- [90] J. M. Halabi, E. Ahmed, L. Catalano, D. P. Karothu, R. Rezgui, P. Naumov, *J. Am. Chem. Soc.* **141** (2019) 14966–14970.
- [91] T. Kwon, J. Y. Koo, H. C. Choi, *Angew. Chem. Int. Ed.* **59** (2020) 16436–16439.
- [92] M. Mitsumi, K. Kitamura, A. Morinaga, Y. Ozawa, M. Kobayashi, K. Toriumi, Y. Iso, H. Kitagawa, T. Mitani, *Angew. Chem. Int. Ed.* **41** (2002) 2767–2771.
- [93] S. R. Batten, K. S. Murray, *Coord. Chem. Rev.* **246** (2003) 103–130.
- [94] G. Givaja, P. Amo-Ochoa, C. J. Gomez-Garcia, F. Zamora, *Chem. Soc. Rev.* **41** (2012) 115–147.
- [95] N. Hearne, M. M. Turnbull, C. P. Landee, E. M. van der Merwe, M. Redemeyer, *CrystEngComm* **21** (2019) 1910–1927.
- [96] Timoshenko, S. *Strength of materials*, D. Van Nostrand Company, New York, 1940.
- [97] E. H. H. Chow, D.-K. Bučar, W. Jones, *Chem. Commun.* **48** (2012) 9210–9226.
- [98] M. F. Dupont, A. Elbourne, E. Mayes, K. Latham, *Phys. Chem. Chem. Phys.* **21** (2019) 20219–20224.
- [99] P. Gay, R. W. K. Honeycombe, *Proc. Phys. Soc. A.* **64** (1951) 844–845.
- [100] S. Hameed, D. Pelc, Z. W. Anderson, A. Klein, R. J. Spieker, M. Lukas, Y. Liu, M. J. Krongstad, R. Osborn, C. Leighton, R. M. Fernandes, M. Greven, *Nat. Mat.* **21** (2022) 54–61.
- [101] P. Commins, D. P. Karothu, P. Naumov, *Angew. Chem. Int. Ed.* **58** (2019) 10052–10060.
- [102] J. P. M. Lommerse, A. J. Stone, R. Taylor, F. H. Allen, *J. Am. Chem. Soc.* **118** (1996) 3108–3116.



## § 7. CURRICULUM VITAE

Personal and contact information	
Date of birth	February 27 <sup>th</sup> , 1994
Affiliation	University of Zagreb, Faculty of Science, Department of Chemistry, Division of General and Inorganic Chemistry Horvatovac 102a, 10000 Zagreb, Croatia
Phone	+385 1 460 6305
E-mail	<a href="mailto:mpisacic@chem.pmf.hr">mpisacic@chem.pmf.hr</a>
Education	
2017	enrollement in Ph.D. program in Inorganic and Structural chemistry UniZg, Faculty of Science, Zagreb, Croatia Supervisor: Assoc. prof. Marijana Đaković
2017	Master's degree in Chemistry (mag. chem.) UniZg, Faculty of Science, Zagreb, Croatia Supervisors: Assoc. Prof. Ivana Biljan and Assist. Prof. Ivan Kodrin
2015	Bachelor's degree in Chemistry (univ. bacc. chem.) UniZg, Faculty of Science, Zagreb, Croatia Supervisor: Prof. Višnja Vrdoljak
Other education and training	
June 19–30, 2022	<i>The Zürich School of Crystallography</i> , Zürich, Switzerland
February 21–25, 2022	Workshop <i>Determination of X-ray charge density - bring your own datasets</i> Ruđer Bošković Institute, Zagreb, Croatia
April 06–14, 2019	<i>17<sup>th</sup> BCA/CCG Intensive Teaching School in X-Ray Structure Analysis</i> Trevelyan College, Durham, UK
August 18, 2019	<i>Crystal Engineering using the Cambridge Structural Database</i> Vienna, Austria
September 12–13, 2019	<i>Science communication workshop</i> Zagreb, Croatia
Scientific results	
<ul style="list-style-type: none"><li>• 10 scientific papers</li><li>• 34 conference contributions</li></ul>	

Awards	
2022	Annual Science Award of the Faculty of Science, University of Zagreb
2020	Award for the best oral presentation at the 4 <sup>th</sup> Symposium of Faculty of Science Ph.D. students
2017	The University of Zagreb Rector's award for best students' research work
2017	Award of the Department of Chemistry (Faculty of Science, University of Zagreb) for students' scientific research
Travel and other grants	
2022	IUCr Travel Award for participating in the 33 <sup>rd</sup> European crystallographic meeting (ECM33), Versailles, France
2021	IUCr Bursary Award for participating in the 25 <sup>th</sup> Congress of the International Union of Crystallography (IUCr25), Prague, Czech Republic
2019	IUCr Travel Award for participating in the 32 <sup>nd</sup> European crystallographic meeting (ECM32), Vienna, Austria
2019	Bursary for the 17 <sup>th</sup> BCA/CCG Intensive Teaching School in X-Ray Structure Analysis, Durham, UK
	University of Zagreb scholarship for Academic staff mobility
2018	Bursary for the 26 <sup>th</sup> Croatian-Slovenian Crystallographic Meeting (26CSCM), Poreč, Croatia
Organization activities and popularization of the science	
2022–	Co-chair of the GIG-01 of the ECA (European Young Crystallographers)
2022	<i>Science Slam</i> , ECM33, Versailles, France
2022	6 <sup>th</sup> Faculty of Science Ph.D. Student Symposium, Zagreb, Croatia, April 23-24, 2022
2021–now	Member of the steering committee for the organization of the <i>ECA Lunch webinars</i>
2019	Solid-State Science and Research 2019 Meeting, Zagreb, Croatia, June 27-29, 2019
2019	European Researchers' night
2018–now	Event "Chemistry Magic"
2015–2019	Department of Chemistry: Open Day
Teaching activities and mentoring	
Teaching:	<ul style="list-style-type: none"> <li>General chemistry (exercises), General chemistry laboratory 1 and 2 (laboratory exercises) and Chemistry 1 (exercises)</li> </ul>
Assistant mentor of:	<ul style="list-style-type: none"> <li>10 graduate diploma (mag. chem.) theses (8 graduated, and 2 on going)</li> <li>4 undergraduate diploma (univ. bacc. chem.) theses</li> <li>2 students awarded with the University of Zagreb Rector's award for best students' research work</li> <li>1 exchange student( through the CEEPUS network)</li> </ul>

---

**Professional memberships**

- European Crystallographic Association (ECA)
- Croatian Crystallographic Association (HKZ)
- Croatian Chemical Society (HKD)
- Società Italiana Luce di Sincrotrone (SILS)

**Scientific interests and competences**

**Scientific interests:** Crystal engineering of flexible crystalline materials, supramolecular chemistry

**Competences:** various methods of solution and mechanochemical synthesis of organic and metal-organic compounds, thermal methods (thermogravimetry, differential scanning calorimetry), variable temperature-IR spectroscopy, molecular modelling, diffraction methods (SCXRD, PXRD), the experience of working with the synchrotron radiation:

- *XRD1 beamline*, Elettra, Trieste, Italy
- *PXI beamline*, Swiss Light Source, PSI, Villigen, Switzerland
- *6-ID-D beamline*, Advanced Photon Source, Argonne National Laboratory, Lemont, Illinois, USA

**LIST OF PUBLICATIONS:**

1. P. Šutalo, **M. Pisačić**, I. Biljan, I. Kodrin, Porous Organic Polymers with Azo, Azoxy and Azodioxy Linkages: A Computational Study. *CrystEngComm*, **24** (2022), 4748-4763.
2. **M. Pisačić**, I. Kodrin, A. Trninić, M. Đaković, Two-Dimensional Anisotropic Flexibility of Mechanically Responsive Crystalline Cadmium(II) Coordination Polymers. *Chem. Mater.* **34** (2022) 2439–2448.
3. **M. Pisačić**, I. Kodrin, I. Biljan, M. Đaković, Exploring the diversity of elastic responses of crystalline cadmium(II) coordination polymers: from elastic towards plastic and brittle responses. *CrystEngComm* **23** (2021) 7072–7080.
4. **M. Pisačić**, I. Biljan, I. Kodrin, N. Popov, Ž. Soldin, M. Đaković, Elucidating the Origins of a Range of Diverse Flexible Responses in Crystalline Coordination Polymers. *Chem. Mater.* **33** (2021) 3660–3668.
5. **M. Pisačić**, I. Kodrin, N. Matijaković, N. Chatterjee, C. L. Oliver, B.-M. Kukovec, M. Đaković, Reversible Temperature-Stimulated Single-Crystal-to-Single-Crystal Conformational Polymorph Transformation in Cadmium(II) Coordination Trimer with a Water Vapor Sorption/Desorption Potential. *Cryst. Growth Des.* **20** (2020) 401–413.
6. N. Politeo, **M. Pisačić**, M. Đaković, V. Sokol, B.-M. Kukovec, Synthesis and crystal structure of a 6- chloro-nicotinate salt of a one-dimensional cationic nickel(II) coordination polymer with 4,4'- bi-pyridine. *Acta Cryst. E* **76** (2020) 599–604.
7. N. Politeo, **M. Pisačić**, M. Đaković, V. Sokol, B.-M. Kukovec, The first coordination compound of deprotonated 2-bromo-nicotinic acid: crystal structure of a dinuclear paddle-wheel copper(II) complex. *Acta Cryst. E* **76** (2020) 225–230.
8. N. Politeo, **M. Pisačić**, M. Đaković, V. Sokol, B.-M. Kukovec, The first coordination compound of 6-fluoronicotinate: the crystal structure of a one-dimensional nickel(II) coordination polymer containing the mixed ligands 6-fluoronicotinate and 4,4-bipyridine. *Acta Cryst. E* **76** (2020) 500–505.
9. K. Varga, N. Lešić, B. Bogović, **M. Pisačić**, B. Panić, I. Biljan, I. Novak, H. Vančik, Thermally-Induced Reactions of Aromatic Crystalline Nitroso Compounds. *ChemistrySelect* **4** (2019), 4709–4717.
10. M. Đaković, M. Borovina, **M. Pisačić**, C. B. Aakeröy, Ž. Soldin, B.-M. Kukovec, I. Kodrin, Mechanically Responsive Crystalline Coordination Polymers with Controllable Elasticity. *Angew. Chem. Int. Ed.* **57** (2018) 14801–14805.

---

CONFERENCE CONTRIBUTIONS:

1. L. Čolakić, **M. Pisačić**, M. Đaković, Dual stress – mechanical properties of copper(II) crystals with 3-nitropyridine, SiSK7, 22 October 2022, Zagreb, Croatia.
2. **M. Pisačić**, L. Balen, M. Đaković, A walk through the valley of weak interactions and diverse mechanical responses of crystals, ECM33, 23-27 August 2022, Versailles, France (**oral presentation**)
3. M. Đaković, **M. Pisačić**, O. Mišura, *Mechanically responsive crystals: Tuning flexibility through fine-tuning intermolecular interactions*, ECM33, 23-27 August 2022, Versailles, France (oral presentation)
4. **M. Pisačić**, B. Lovrić, M. Đaković, *Shaping crystals using mechanical force: A structural perspective on flexible crystalline coordination polymers of cadmium(II)*, 4th joint AIC-SILS, 12-15 September 2022, Trieste, Italy (**oral presentation**)
5. **M. Pisačić**, *Communicating crystallography through ECA Lunch webinars*, 4th joint AIC-SILS, 12-15 September 2022, Trieste, Italy (**oral presentation**)
6. L. Čolakić, **M. Pisačić**, M. Đaković, *Flexible crystals of cadmium(II) halides with dichloropyridine ligands*, XIV Meeting of Young Chemical Engineers, 24–25 February 2022, Zagreb, Croatia (oral presentation)
7. **M. Pisačić**, M. Đaković, *Crystalline coordination polymers on the move*, 27<sup>th</sup> Croatian Meeting of Chemists and Chemical Engineers, Veli Lošinj, 5–8 October 2021. (**oral presentation**)
8. L. Čolakić, **M. Pisačić**, M. Đaković, *Mechanical properties of crystals of cadmium(II) halides with 2,6-dibromopyrazine ligands*, Fourth symposium of supramolecular chemistry, 10 December 2021. (poster presentation)
9. M. Borovina, **M. Pisačić**, A. Husinec, V. Badurina, M. Đaković, *Investigating the Impact of Supramolecular Connectivity on Mechanical Properties of Crystals*, Fourth symposium of supramolecular chemistry, 10 December 2021. (oral presentation)
10. M. Borovina, **M. Pisačić**, A. Husinec, V. Badurina, M. Đaković, *Mechanical properties of copper(II) and cadmium(II) halides equipped with 3-nitropyridine ligands*. 27<sup>th</sup> Croatian Meeting of Chemists and Chemical Engineers, Veli Lošinj, 5–8 October 2021. (poster presentation)
11. Ž. Soldin, **M. Pisačić**, K. Zozoli, M. Đaković, *Elastically deformable crystals of Cd(II) coordination polymers*, 27<sup>th</sup> Croatian Meeting of Chemists and Chemical Engineers, 5–8 October 2021. (poster presentation)
12. **M. Pisačić**, M. Đaković, *Tuning mechanical responses of crystalline cadmium(II) coordination polymers through cyano functionality and halide anions*, XXV General Assembly and Congress of the International Union of Crystallography, Prague, Czech Republic, 14–22 August 2021. (**oral presentation**)
13. M. Đaković, **M. Pisačić**, *Variable adaptability of coordination polymers of cadmium(II) to external mechanical stimuli*, XXV General Assembly and Congress of the International Union of Crystallography, Prague, Czech Republic, 14–22 August 2021. (oral presentation)

- 
14. L. Čolakić, **M. Pisačić**, M. Đaković, *Fine-tuning of mechanical flexibility of cadmium(II) halide crystals via ligand replacement*, Solid-State Science & Research, Zagreb, 10–11 June 2021. (poster presentation)
  15. O. Mišura, **M. Pisačić**, M. Đaković, *Fine-tuning of crystal bendability of cadmium(II) one-dimensional coordination polymers via co-crystallization*, Fifth Symposium of Faculty of Science Ph.D. students, Zagreb, 25–26 April 2021. (poster presentation)
  16. **M. Pisačić**, M. Đaković: Dynamic crystals of cadmium(II) coordination compounds, *Fourth symposium of Faculty of Science Ph.D. students*, February 28<sup>th</sup>, 2020, Zagreb, Croatia (**oral presentation**)
  17. M. Đaković, **M. Pisačić**, Impact of Halides and Halogen Atoms on Mechanical Flexibility of Cd(II) Coordination Polymers., *4<sup>th</sup> International symposium on halogen bonding*, November 2–5, 2022, Stellenboch, South Africa (oral presentation)
  18. L. Čolakić, **M. Pisačić**, M. Đaković: Influence of structure on the flexibility of cadmium(II) crystals with halide and pyridinecarboxime ligands, *XIII Meeting of Young Chemical Engineers*, February, 20–21, 2020, Zagreb, Croatia (oral presentation)
  19. **M. Pisačić**, M. Đaković: Mechanically Adaptable Crystals: Impact of Supramolecular Connectivity on Crystal Flexibility, *Third symposium of supramolecular chemistry*, 4 December 2019, Zagreb, Croatia (**invited oral presentation**)
  20. L. Čolakić, **M. Pisačić**, M. Đaković, *Impact of structure on crystal flexibility of cadmium(II) compounds with halogenide and pyridinecarboxime ligands*, 6<sup>th</sup> symposium of chemistry students, 26 October 2019, Zagreb, Croatia (oral presentation)
  21. I. Biljan, I. Kodrin, **M. Pisačić**, P. Štrbac, H. Vančik, *Synthesis and characterization of new aromatic azodioxy and azo polymers*, 17<sup>th</sup> European Symposium on Organic Reactivity, 8–13 September 2019, Dubrovnik, Croatia (poster presentation)
  22. **M. Pisačić**, O. Mišura, M. Đaković: *Engineering mechanical flexibility in crystalline coordination polymers and their two-component systems*, 1<sup>st</sup> International Conference on Noncovalent Interactions, 2–6 September 2019, Lisbon, Portugal (poster presentation)
  23. **M. Pisačić**, M. Đaković: *Exceptionally flexible coordination polymers of Cd(II)*, 32nd European Crystallographic Meeting, 18–22 August 2019, Vienna, Austria (**poster presentation**)
  24. **M. Pisačić**, M. Đaković: *Structural characteristics of flexible coordination polymers of cadmium(II)*, Solid-State Science & Research 2019, June 27–29, 2019, Zagreb, Croatia (**poster presentation**)
  25. O. Mišura, **M. Pisačić**, M. Đaković, *Steric and electronic effects in formation of co-crystals in solid-state and their sustainability in solution*, Solid-State Science & Research 2019, 27–29 June 2019, Zagreb, Croatia (poster presentation)
  26. **M. Pisačić**, M. Đaković, *Understanding the role of weak interactions in responsiveness of molecular crystals to external mechanical stimuli*, 27<sup>th</sup> Slovenian-Croatian Crystallographic Meeting, 19–24 June 2019, Rogaška Slatina, Slovenia (**oral presentation**)



- 
27. M. Đaković, **M. Pisačić**, *Flexibility of crystalline matter: Crystals of coordination polymers with a variety of mechanical responses*, 27<sup>th</sup> Slovenian-Croatian Crystallographic Meeting, June 19-24, 2019, Rogaška Slatina, Slovenia (oral presentation)
28. **M. Pisačić**, M. Đaković: *Supramolecular architectures of flexible crystalline coordination polymers of cadmium(II)*, Symposium of PhD students of Faculty of Science, February 22<sup>nd</sup>, 2019, Zagreb, Croatia (**poster presentation**)
29. M. Đaković, **M. Pisačić**, N. Penić: *Crystalline coordination polymers with flexible response to applied external mechanical force*, 26<sup>th</sup> Croatian meeting of chemists and chemical engineers, 9-12 April 2019, Šibenik, Croatia (oral presentation)
30. **M. Pisačić**, M. Đaković: *Structural characteristics of crystal coordination polymers with elastic response on applying outer mechanical stress*, Second symposium of supramolecular chemistry, December 12<sup>th</sup>, 2018, Zagreb, Croatia (**poster presentation**)
31. Ž. Soldin, M. Lujanac, **M. Pisačić**, M. Đaković, *Synthesis and characterization of copper(II) and nickel(II)  $\beta$ -diketonates with pyridine-based amides*, 3<sup>rd</sup> International Congress of Chemists and Chemical Engineers of Bosnia and Herzegovina, October 19-21, 2018, Sarajevo, Bosnia and Herzegovina (poster presentation)
32. **M. Pisačić**, M. Đaković, *Understanding the role of weak interactions in responsiveness of molecular crystals to external mechanical stimuli*, 26<sup>th</sup> Croatian-Slovenian Crystallographic Meeting, June 13-17, 2018, Poreč, Croatia (**oral presentation**)
33. **M. Pisačić**, *Kinetics of dimerization of 2-nitrosopyridine and its derivatives in solid state*, 4<sup>th</sup> symposium of chemistry students, October 28, 2017, Zagreb, Croatia (**oral presentation**)
34. K. Varga, **M. Pisačić**, I. Biljan, V. Tomišić, Z. Mihalić, H. Vančik, *Behaviour of 2-nitrosopyridines in solution and in solid state*, Math/Chem/Comp 2017, June 19-24, 2017, Dubrovnik, Croatia (oral presentation)



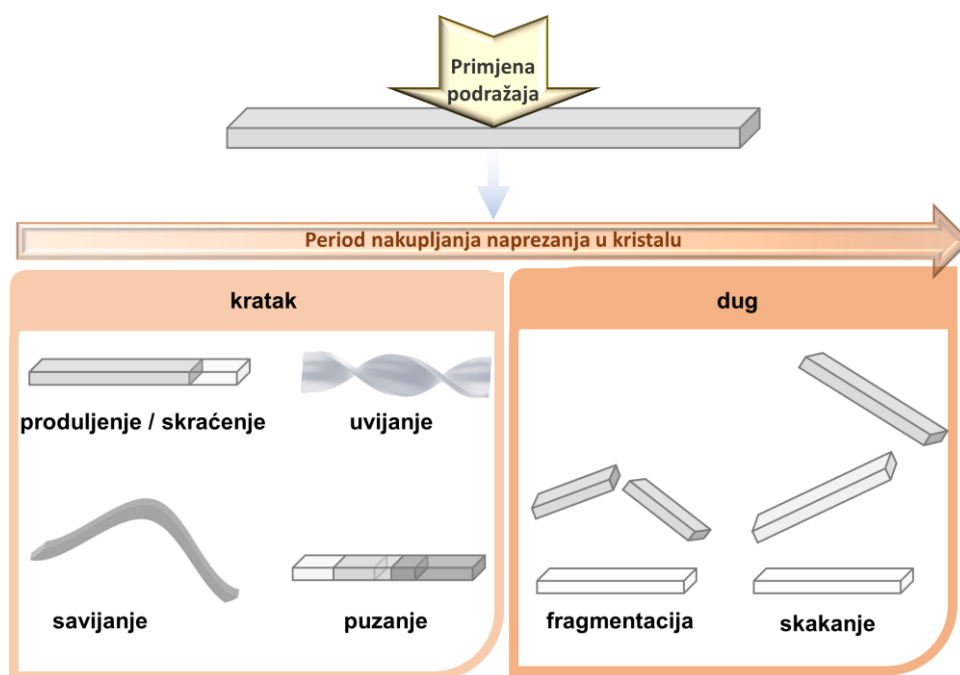
Sveučilište u Zagrebu  
Prirodoslovno-matematički fakultet  
**Kemijski odsjek**

Doktorski rad

## PROŠIRENI SAŽETAK

### Uvod

Tradicionalno poimanje kristalnih tvari krutima, lomljivima i statičnima počelo se mijenjati otkrićem kristala koji pod utjecajem vanjskih podražaja poput svjetlosti, topline i mehaničke sile, daju dinamičan odgovor.<sup>I,II</sup> Potaknuti mehanički odziv kristala može biti spor i kontroliran (savijanje ili puzanje) ili nagao (skakanje ili čak eksplozija), a način na koji će kristal odgovoriti određuje akumulacijski period naprezanja u kristalu (Slika I).



**Slika I.** Makroskopski opaženi mehanički odzivi kristala uslijed primjene vanjskog podražaja.

[I] P. Naumov, S. Chizhik, M. K. Panda, N. K. Nath, E. Boldyreva, *Chem. Rev.* **115** (2015) 12440–12490.

[II] P. Commins, I. T. Desta, D. P. Karothu, M. K. Panda, P. Naumov, *Chem. Commun.* **52** (2016) 13941–13954.

Ukoliko je akumulacijski period kratak, odnosno nastalo naprezanje se oslobađa kontinuirano, mehanički odziv će biti kontroliran, dok dugi akumulacijski period popraćen naglim oslobađanjem nakupljenog naprezanja dovodi do naglašenijih mehaničkih odziva, odnosno skakanja, fragmentacije ili čak i eksplozije kristala.

Mehanički odzivi potaknuti svjetlošću i/ili topline, poznati su već više od pola stoljeća, i relativno su dobro istraženi. Uočeno je da se primjenom svjetlosnog ili toplinskog podražaja u kristalu potiču kemijske reakcije (izomerizacija, cikloadicija i slično) ili fazna transformacija, te dolazi do nejednolikog nastajanja produkta u volumenu početnog kristala, što uzrokuje nastanak stresa u kristalu, čije oslobađanje dovodi do mehaničkog odgovora kristala.<sup>I</sup>

S druge strane, istraživanje mehanički potaknutih odziva kristala tek je u začetku, te još uvijek nije u potpunosti jasno koji strukturni preduvjeti moraju biti ispunjeni kako bi kristali bili prilagodljivi na primjenu sile. Uočeno je da se kristali mogu deformirati ireverzibilno (Slika II), odnosno, uslijed primjene sile se deformiraju te ostaju trajno deformirani čak i nakon prestanka primjene sile, pritom pokazujući plastičnu savitljivost,<sup>III, IV</sup> smicanje<sup>V</sup> ili feroelastičan odziv.<sup>VI</sup> Nadalje, deformacija može biti i reverzibilna (Slika II), odnosno kristali se deformiraju uslijed primjene sile, ali poprimaju svoj izvorni oblik nakon prestanka primjene mehaničke sile, to jest pokazuju elastično savijanje<sup>VII, VIII</sup> ili superelastičan odziv.<sup>IX</sup> Ovo područje kristalnog inženjerstva aktivno je tek dvadesetak godina, no ubrzano se razvija, te je u ovo kratko vrijeme objavljen znatan broj znanstvenih radova na temu savitljivih kristala organskog sastava.<sup>X–XII</sup>

---

[III] L. Catalano, D. P. Karothu, S. Schramm, E. Ahmed, R. Rezgui, T. J. Barber, A. Famulari, P. Naumov, *Angew. Chem. Int. Ed.* **57** (2018) 17254–17258.

[IV] L. O. Alimi, P. Lama, V. J. Smith, L. J. Barbour, *Chem. Commun.* **54** (2018) 2994–2997.

[V] C. M. Reddy, M. T. Kirchner, R. C. Gundakaram, K. A. Padmanabhan, G. R. Desiraju, *Chem. Eur. J.* **12** (2006) 2222–2234.

[VI] S. H. Mir, Y. Takasaki, E. R. Engel, S. Takamizawa, *Angew. Chem. Int. Ed.* **56** (2017) 15882–15885.

[VII] S. Ghosh, M. C. Reddy, *Angew. Chem. Int. Ed.* **51** (2012) 10319–10323.

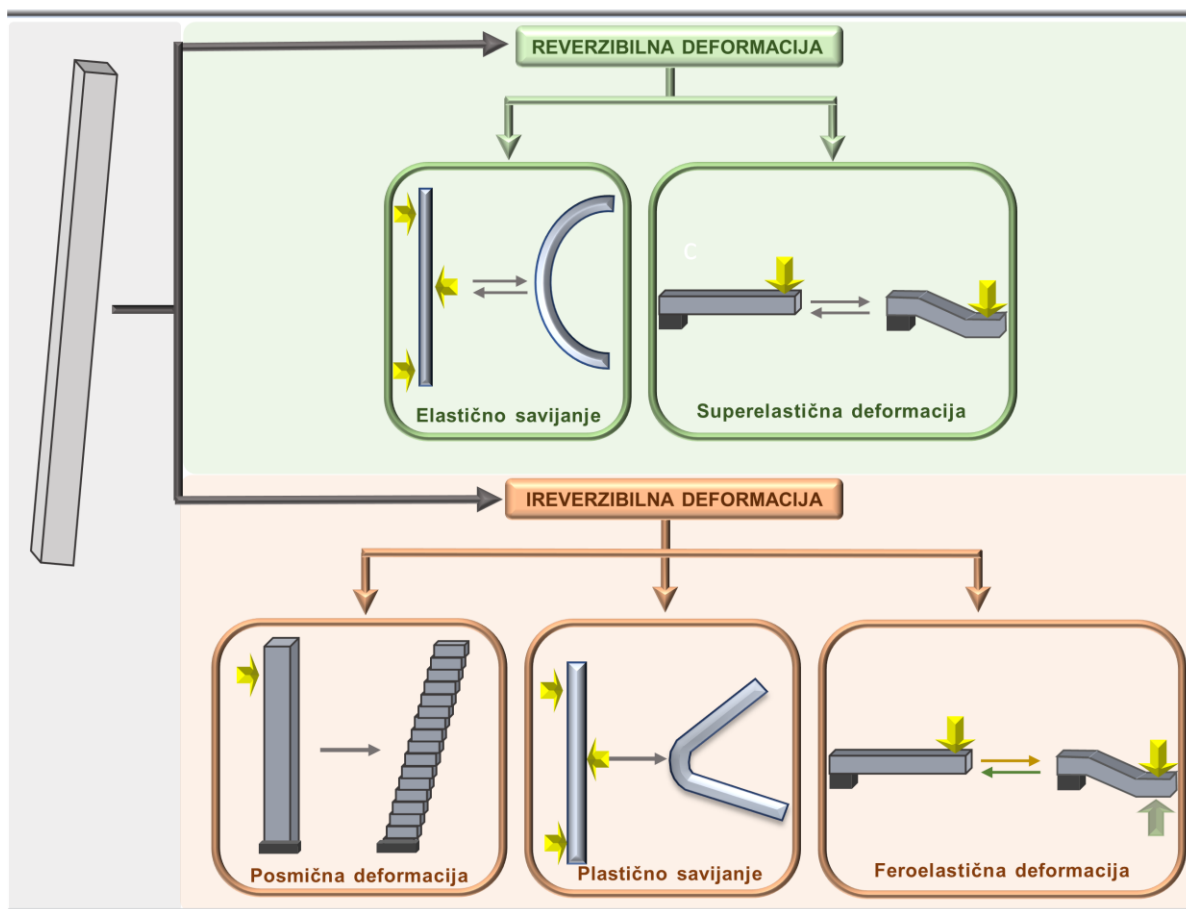
[VIII] H. Liu, Z. Lu, Z. Zhang, Y. Wang, H. Zhang, *Angew. Chem. Int. Ed.* **57** (2018) 8448–8452.

[IX] S. Takamizawa, Y. Miyamoto, *Angew. Chem. Int. Ed.* **53** (2014) 6970–6973.

[X] T. Seki, H. Ito, *Chem. Eur. J.* **22** (2016) 4322–4329.

[XI] S. Saha, M. K. Mishra, C. M. Reddy, G. R. Desiraju, *Acc. Chem. Res.* **11** (2018) 2957–2967.

[XII] E. Ahmed, D. P. Karothu, P. Naumov, *Angew. Chem. Int. Ed.* **57** (2018) 8837–8846.



**Slika II.** Vrste mehanički potaknutih odziva kristala.

Usporedbom strukturnih značajki mehanički prilagodljivih kristala organskih spojeva uočeno je da je strukturna anizotropija, odnosno postojanje područja jakih i slabih međumolekulskih interakcija u kristalu, značajka većine plastično savitljivih kristala.<sup>XI</sup> Pritom su područja slabih međumolekulskih interakcija, odnosno područja takozvanih „ravnina klizanja“, definirana kao ključan faktor za ostvarivanje plastične savitljivosti, jer omogućuju klizanje molekulskih slojeva jednih preko drugih uslijed primjene mehaničke sile, te posljedično trajnu deformaciju kristala. To je primijećeno na većem broju primjera, a jedan od glavnih predstavnika, ujedno i najistraženiji, jest kristal heksaklorbenzena.<sup>XIII, XIV</sup> S druge

[XIII] C. M. Reddy, G. R. Krishna, S. Gosh, *CrystEngComm* **12** (2010) 2296–2314.

[XIV] M. K. Panda, S. Ghosh, N. Yasuda, T. Moriwaki, G. Dev Mukherjee, C. M. Reddy, P. Naumov, *Nat. Chem.* **7** (2015) 65–72.

strane, gotovo izotropno kristalno pakiranje, u kojem su strukturni fragmenti „isprepleteni“, čime se sprječava klizanje slojeva uslijed primjene sile, uočeni su kao jedan od vrlo važnih kriterija za postizanje elastične savitljivosti organskih kristala.<sup>XI</sup> Osim toga, za neke organske kristale uočeno je da istovremeno mogu pokazivati iznimna mehanička svojstva, ali i druga svojstva od interesa, kao što su na primjer optička svojstva,<sup>XV, XVI</sup> čime se otvara mogućnost njihove potencijalne šire primjene (u proizvodnji fleksibilnih svjetlovoda i dr.).

Uvođenjem metalnog centra u organske sustave omogućuje se ostvarivanje još šireg dijapazona svojstava od interesa, poput električnih ili magnetskih, koja su teško ostvariva u organskim sustavima. Međutim, mehanička fleksibilnost uočena je u puno manjoj mjeri kod metalo–organskih sustava. Prvi primjeri mehanički savitljivih metalo–organskih kristalnih materijala objavljeni su tek 2018. godine, kada su, gotovo istovremeno, opisani elastično savitljivi kristali bis(pentan-2,4-dionato)bakra(II),<sup>XVII</sup> te serija elastično savitljivih kristala jednodimenzijskih koordinacijskih polimera kadmijevih(II) halogenida s halogenpirazinskim ligandima.<sup>XVIII</sup> Slijedila je objava još nekolicine radova koji opisuju plastično<sup>XIX–XXI</sup> i elastično<sup>XXII–XXVII</sup> savitljive kristale metalo–organskih spojeva.

---

[XV] H. Liu, Z. Lu, Z. Zhang, Y. Wang, H. Zhang, *Angew. Chem. Int. Ed.* **57** (2018) 8448–8452.

[XVI] S. Hayashi, S. Yamamoto, D. Takeuchi, Y. Ie. K. Takag, *Angew. Chem. Int. Ed.* **57** (2018) 17002–17008.

[XVII] A. Whorty, A. Grosjean, M. C. Pfrunder, Y. Xu, C. Yan, G. Edwards, J. K. Clegg, J. C. McMurtrie, *Nat. Chem.* **10** (2018) 65–69.

[XVIII] M. Đaković, M. Borovina, M. Pisačić, C. B. Aakeröy, Ž. Soldin, I. Kodrin, *Angew. Chem. Int. Ed.* **57** (2018) 14801–14805.

[XIX] N. K. Nath, P. Gupta, P. J. Hazarika, N. Deka, A. Mukherjee, G. K. Dutta, *Cryst. Growth Des.* **19** (2019) 6033–6038.

[XX] B. Bhattacharya, A. A. L. Michalchuk, D. Silbernagl, M. Rautenberg, T. Schmid, T. Feiler, K. Reinmann, A. Ghalgaoui, H. Sturm, B. Paulus, F. Emmerling, *Angew. Chem. Int. Ed.* **59** (2020) 5557–5561.

[XXI] Z. Tang, X.-P. Sun, S.-D. Wang, X.-Y. Ji, Y. Li, Z.-S. Yao, J. Tao, *Chem. Sci. China* **65** (2022) 710–718.

[XXII] L. Mei, S. W. An, K. Q. Hu, L. Wang, J. P. Yu, Z. W. Huang, X. H. Kong, C. Q. Xia, Z. F. Chai, W. Q. Shi, *Angew. Chem. Int. Ed.* **59** (2020) 16061–16068.

[XXIII] A. J. Thompson, A. Worthy, A. Grosjean, J. R. Price, J. C. McMurtrie, J. K. Clegg, *CrystEngComm* **23** (2021) 5731–5737.

[XXIV] B. B. Rath, J. J. Vittal, *Chem. Mater.* **33** (2021) 4621–4627.

[XXV] B. B. Rath, M. Gupta, J. J. Vittal, *Chem. Mater.* **34** (2022) 178–185.

[XXVI] S. Kusumoto, A. Sugimoto, Y. Zhang, Y. Kim, M. Nakamura, S. Hayami, *Inorg. Chem.* **60** (2021) 1294–1298.

[XXVII] A. J. Thompson, A. I. Chamorro Orue, A. Jayamohan Nair, J. R. Price, J. McMurtrie, J. K. Clegg, *Chem. Soc. Rev.* **50** (2021) 11725–11740.

No, već i na tom ograničenom broju primjera uočeno je da zaključci do kojih se do sada došlo o strukturnom podrijetlu mehanički potaknute savitljivosti u organskim sustavima nisu u potpunosti primjenjivi na kristale metalo–organskih sustava. Stoga je uočena potreba za detaljnom i sustavnom korelacijom strukturnih značajki i mehaničkih svojstava metalo–organskih kristala.

### **Hipoteze i ciljevi**

Cilj ovog doktorskog rada jest utvrditi koji strukturni preduvjeti moraju biti zadovoljeni kako bi kristali koordinacijskih polimera kadmija(II) imali svojstvo mehanički potaknute savitljivosti, te kako bi se ta znanja mogla iskoristiti u dizajnu kristala metalo–organskih sustava koji daju fleksibilan odziv željene vrste, ali i stupnja.

Pritom su postavljene sljedeće hipoteze:

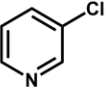
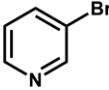
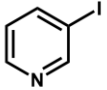
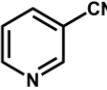
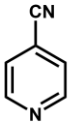
1. Postojanje područja vrlo slabih interakcija u kristalu (disperznih te slabih vodikovih i/ili halogenskih interakcija) paralelnih smjeru pružanja 1D polimernog lanca, odnosno smjeru izduženja kristala, tzv. ravnina klizanja, omogućit će plastičnu deformaciju kristala.
2. Međumolekulske interakcije (vodikove i/ili halogenske interakcije srednje do velike jakosti) podjednake jakosti u smjerovima okomitim na smjer pružanja 1D polimernog lanca, odnosno, izduženja kristala, omogućit će elastičan odziv.
3. Stupanj elastične savitljivosti kristala moguće je kontrolirati ugađanjem međumolekulskih interakcija.
4. Savijanjem kristala dolazi do malih strukturnih promjena na molekulskoj razini koja dovode do izmjene makroskopskih svojstava (na primjer termičkih svojstava).



## Rezultati i rasprava

Ovaj rad temelji se na tri izvorna znanstvena rada koja su omogućila sustavno istraživanje korelacije između strukture i mehaničkih svojstava na nizu jednodimenzijskih kristalnih koordinacijskih polimera kadmija(II), koristeći sinergiju eksperimentalnog i računalnog pristupa. Svaki od tri rada pojedinačno donosi mnoštvo vrijednih informacija, nadopunjujući tako ostale, i što je još važnije, doprinoseći ukupnom razumijevanju mehaničke fleksibilnosti kristala.

U okviru ovog istraživanja pripremljeno je i detaljno okarakterizirano petnaest kristalnih koordinacijskih polimera kadmijevih(II) halogenida s halogenskim i cijano- derivatima piridina (Slika III).

SOLI	CdCl <sub>2</sub>		CdBr <sub>2</sub>		CdI <sub>2</sub>
ORGANSKI LIGANDI					
PRIREĐENI SPOJEVI	[CdCl <sub>2</sub> (3-Clpy) <sub>2</sub> ] <sub>n</sub> (II-1) [CdBr <sub>2</sub> (3-Clpy) <sub>2</sub> ] <sub>n</sub> (I-1) [CdI <sub>2</sub> (3-Clpy) <sub>2</sub> ] <sub>n</sub> (I-2)	[CdCl <sub>2</sub> (3-Brpy) <sub>2</sub> ] <sub>n</sub> (II-2) [CdBr <sub>2</sub> (3-Brpy) <sub>2</sub> ] <sub>n</sub> (II-3) [CdI <sub>2</sub> (3-Brpy) <sub>2</sub> ] <sub>n</sub> (I-3)	[CdCl <sub>2</sub> (3-Ipy) <sub>2</sub> ] <sub>n</sub> (I-4) [CdBr <sub>2</sub> (3-Ipy) <sub>2</sub> ] <sub>n</sub> (I-5) [CdI <sub>2</sub> (3-Ipy) <sub>2</sub> ] <sub>n</sub> (I-6)	[CdCl <sub>2</sub> (3-CNpy) <sub>2</sub> ] <sub>n</sub> (III-1) [CdBr <sub>2</sub> (3-CNpy) <sub>2</sub> ] <sub>n</sub> (III-2) [CdI <sub>2</sub> (3-CNpy) <sub>2</sub> ] <sub>n</sub> (III-3)	[CdCl <sub>2</sub> (4-CNpy) <sub>2</sub> ] <sub>n</sub> (III-4) [CdBr <sub>2</sub> (4-CNpy) <sub>2</sub> ] <sub>n</sub> (III-5) [CdI <sub>2</sub> (4-CNpy) <sub>2</sub> ] <sub>n</sub> (III-6)

**Slika III.** Kadmijeve(II) soli i organski ligandi korišteni za pripravu ciljanih kristalnih koordinacijskih polimera.

Proučavani ciljani koordinacijski polimeri priređeni su klasičnom otopinskom sintezom koja je rezultirala polikristalnim produktima, dok su kristalizacijski eksperimenti s ciljem dobivanja jediničnih kristala zadovoljavajuće kvalitete za provođenje eksperimenata ispitivanja mehaničkih svojstava te karakterizaciju, provedeni tehnikom nadslojavanja, pri čemu je vodena otopina odgovarajuće kadmijeve(II) soli nadslojena etanolnom otopinom liganda. Spojevima za koje je utvrđeno da njihova molekulska i kristalna struktura nije pohranjena u kristalografskoj bazi podataka (CSD, engl. *Cambridge structural database*)<sup>XXVIII</sup> određena je molekulska i kristalna struktura iz podataka prikupljenih eksperimentima difrakcije rendgenskog zračenja u jediničnom kristalu. Svi produkti dodatno su okarakterizirani

[XXVIII] C. R. Groom, I. J. Bruno, M. P. Lightfoot and S. C. Ward, *Acta Cryst. B* **72** (2016) 171–179.

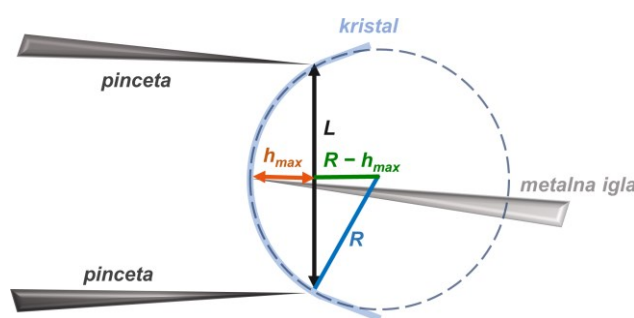
difrakcijom rendgenskog zračenja u polikristalnom uzorku, te termičkim metodama (termogravimetrijski i razlikovnom pretražnom kalorimetrijom).

Mehanička svojstva priređenih kristala ispitana su nizom dizajniranih eksperimenata koji su prilagođeni milimetarskoj skali. Odziv kristala na primjenu mehaničke sile primarno je utvrđen modificiranim eksperimentom savijanja u tri točke, pri čemu je ustanovljena vrsta mehaničkog odziva (elastična, plastična savitljivost ili lom). Za kristale koji su pokazali elastičan odziv provedena je i kvantifikacija opaženog odziva, izračunom maksimalnog naprezanja uslijed savijanja,  $\varepsilon$  (engl. *bending strain*) korištenjem Euler-Bernoulli jednadžbe (ne uzimajući u obzir komponentu smicanja) [jednadžbe 1–3], pri čemu je otklonjen utjecaj dimenzija kristala (duljine,  $L$  i debljine,  $t$ ) na savitljivost (Slika IV).<sup>XXIX</sup>

$$R^2 = \left(\frac{L}{2}\right)^2 + (R - h_{\max})^2 \quad [1]$$

$$R = \frac{\left(\frac{L}{2}\right)^2 + h_{\max}^2}{2h_{\max}} \quad [2]$$

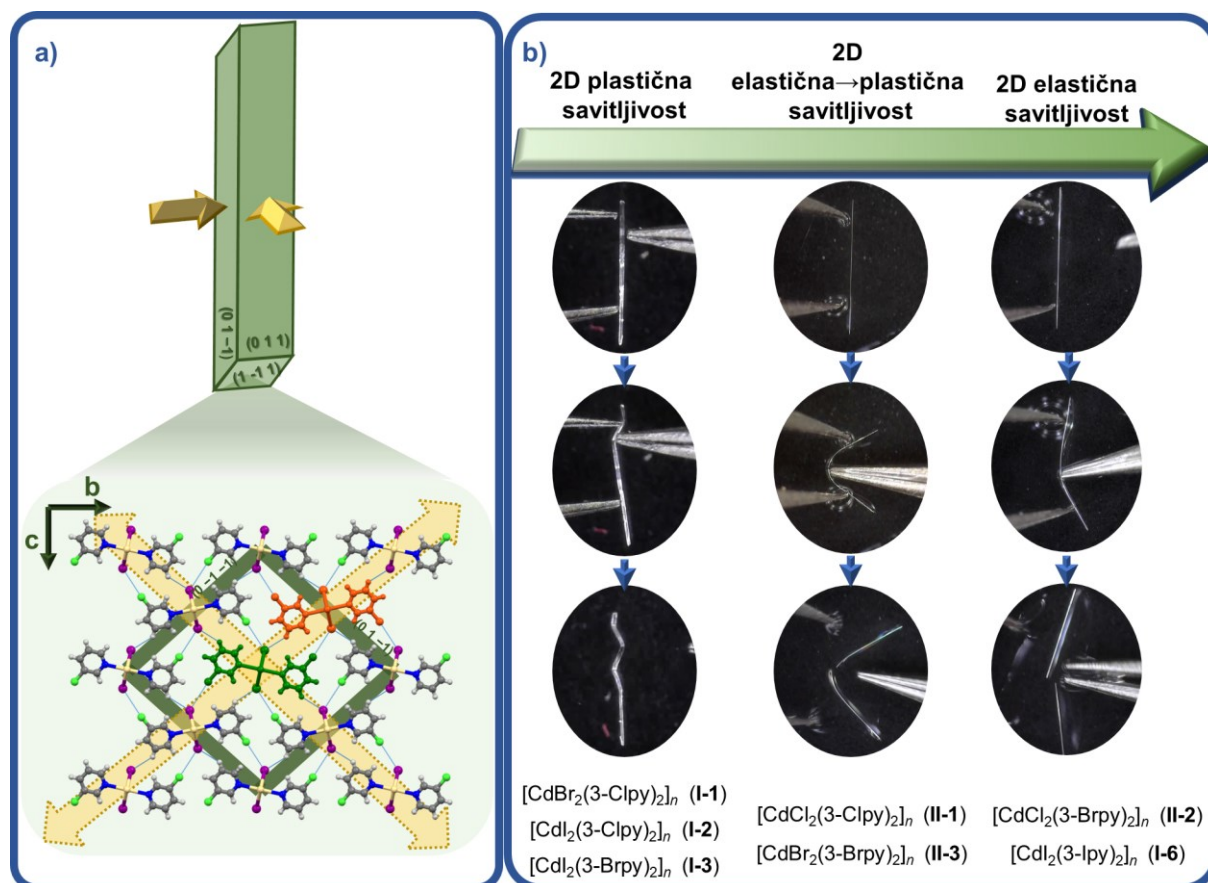
$$\varepsilon (\%) = \frac{t}{R} \cdot 100 \quad [3]$$



**Slika IV.** Shematski prikaz modificiranog eksperimenta savijanja kristala u tri točke s naznačenim geometrijskim parametrima potrebnim za izračun vrijednosti maksimalnog naprezanja prije pucanja ( $\varepsilon$ ).

[XXIX] S.Timoshenko, Strength of materials, D. Van Nostrand Company, New York, 1940.

Prva dva rada (I i II) opisuju niz od devet kristalnih spojeva s tri halogenpiridinska liganda, 3-klorpiridinom (3-Clpy), 3-brompiridinom (3-Brpy) i 3-jodpiridinom (3-Ipy):  $[\text{CdCl}_2(3\text{-Clpy})_2]_n$  (**II-1**),  $[\text{CdBr}_2(3\text{-Clpy})_2]_n$  (**I-1**),  $[\text{CdI}_2(3\text{-Clpy})_2]_n$  (**I-2**),  $[\text{CdCl}_2(3\text{-Brpy})_2]_n$  (**II-2**),  $[\text{CdBr}_2(3\text{-Brpy})_2]_n$  (**II-3**),  $[\text{CdI}_2(3\text{-Brpy})_2]_n$  (**I-3**),  $[\text{CdCl}_2(3\text{-Ipy})_2]_n$  (**I-4**),  $[\text{CdBr}_2(3\text{-Ipy})_2]_n$  (**I-5**) i  $[\text{CdI}_2(3\text{-Ipy})_2]_n$  (**I-6**). Sedam od devet priređenih spojeva (**I-1** – **I-3**, **I-6**, i **II-1** – **II-3**) kristaliziralo je u monoklinskom kristalnom sustavu u prostornoj grupi  $P2_1/c$  s gotovo identičnim uređenjem građevnih jedinki u kristalnim pakiranjima (Slika V). Nadalje, priređeni kristalni produkti kristalizirali su u obliku igličaste morfologije s jednakim dimenzijama dominantnih kristalnih ploha koje se pružaju paralelno sa smjerom izduženja kristala. Time je osiguran zadovoljavajući skup podataka za detaljno istraživanje utjecaja sustavnog uvođenja malih strukturnih promjena na makroskopska mehanička svojstva. Rezultati su pokazali da mala manipulacija strukturnim značajkama (tj. zamjena jednog atoma halogena u strukturi drugim) koja uzrokuje blagu promjenu geometrije i jakosti međumolekulskih interakcija, ima neočekivano velike posljedice na makroskopski mehanički odziv kristala; ne samo na maksimalno naprezanje nastalo uslijed svijanja koje kristal može podnijeti prije loma ( $\epsilon$ ), već i na vrstu (plastična/elastična savitljivost) fleksibilnog odgovora. Među sedam spojeva gotovo identične kristalne strukture, uočen je širok raspon mehanički inducirane fleksibilnosti kristala. Svi kristali dali su mehanički odziv neovisno o tome na koji od dva para dominantnih kristalnih ploha se mehanička sila primijenila, odnosno svi su bili dvodimenzijski (2D) fleksibilni. Kristali **II-2** i **I-6** pokazali su blagu elastičnu savitljivost s tipičnim krtim lomom i jednakim iznosom maksimalnog naprezanja prije loma,  $\epsilon \approx 0,4 \%$ , neovisno o paru dominantnih kristalnih ploha na koje se primijenila mehanička sila, odnosno 2D elastičnu savitljivost. Kristali **II-1** i **II-3** su pri manjim naprezanjima pokazali isti odziv kao i kristali **II-2** i **I-6**, odnosno elastičnu savitljivost. No, pri većim naprezanjima, a naročito pri naprezanjima blizu točke pucanja ( $\epsilon > 0,6 - 0,7 \%$ ), kristali spojeva **II-1** i **II-3** postaju plastično deformirani, nakon čega se i lome. Jednako ponašanje kristala uočeno je uslijed primjene sile na oba para kristalnih ploha, te su stoga ti kristali klasificirani kao 2D elastično→plastično savitljivi. Kristali preostala tri spoja, **I-1**–**I-3**, pokazali su plastičnu savitljivost bez obzira na par kristalnih ploha na koje se primjenjuje mehanička sila, te su stoga klasificirani kao 2D plastično savitljivi.

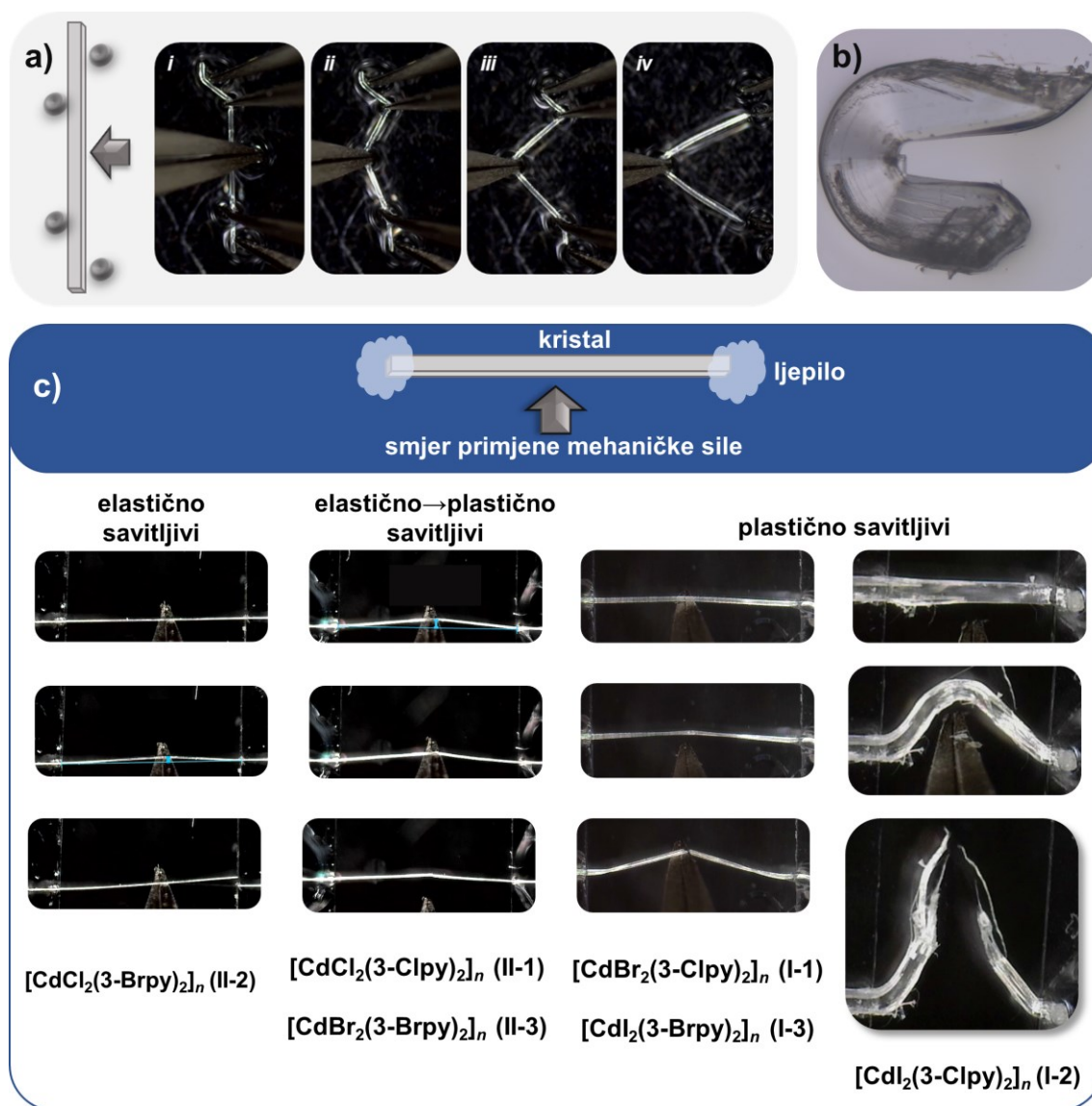


**Slika V.** a) Shematski prikaz igličaste morfologije kristala s jednako razvijenim dominantnim kristalnim plohama (gore) te pogled na kristalno pakiranje prikazano u kristalografskoj ravni  $bc$  s naznačenim plohama kristala (zelene linije) i mogućim smjerovima primjene mehaničke sile (žute strelice); b) vrste opaženih mehaničkih odziva.

Nadalje, uočena je jasna razlika u plastičnom odzivu kristala, odnosno lakoći s kojom može biti prouzročena plastična deformacija između tri spoja (I-1–I-3). Kristali sva tri spoja pokazali su se iznimno prilagodljivima na primjenu mehaničke sile tijekom modificiranih eksperimenata savijanja u tri i u pet točaka (Slika VIa), deformirajući se pritom i uspješno „prolazeći“ kroz sve postavljene prepreke bez pucanja. Kristali spoja I-2 pokazali su se najpodatnijima, odnosno, toliko plastično savitljivima da je bilo teško i rukovati s njima a da ih se pritom ne deformira plastično. S druge strane, kristali spojeva I-1 i I-3 pokazali su veći otpor na primjenu mehaničke sile, odnosno, pokazali su manju prilagodljivost.

Osim toga, provedeni su eksperimenti kojima se ispitala mogućnost kristala da izdrže vlačnu deformaciju. Eksperimentalni postav za modificirani vlačni eksperiment sastojao se od predmetnog stakalca na koje su zalijepljene dvije staklene pločice s međusobnim razmakom od

2–3 milimetra (Slika VIc). Kristali zadovoljavajuće kvalitete, debljine i duljine (malo dulji od duljine razmaka među staklenim pločicama) bili su postavljeni tako da su im krajevi položeni na staklene pločice i fiksirani trenutnim ljepilom za podlogu, čime je omogućeno da je središnji dio kristala tijekom provođenja modificiranog vlačnog eksperimenta u zraku kao mediju, kako bi se izbjegao utjecaj ulja i trenja na rezultate. Na sredinu duljine kristala primjenjivala se mehanička sila s metalnom pincetom sa savijenim vrhovima, brzinom od 100  $\mu\text{m/s}$ , u jednolikim pomacima od 15  $\mu\text{m}$  po koraku.



**Slika VI.** a) Eksperiment savijanja kristala spoja I-3 u pet točaka, b) plastično deformiran kristal spoja I-2, c) shematski prikaz modificiranog vlačnog eksperimenta te razlika u uočenoj vlačnoj deformaciji među kristalima koji su pokazali elastičan, elastično→plastičan te plastičan odziv.

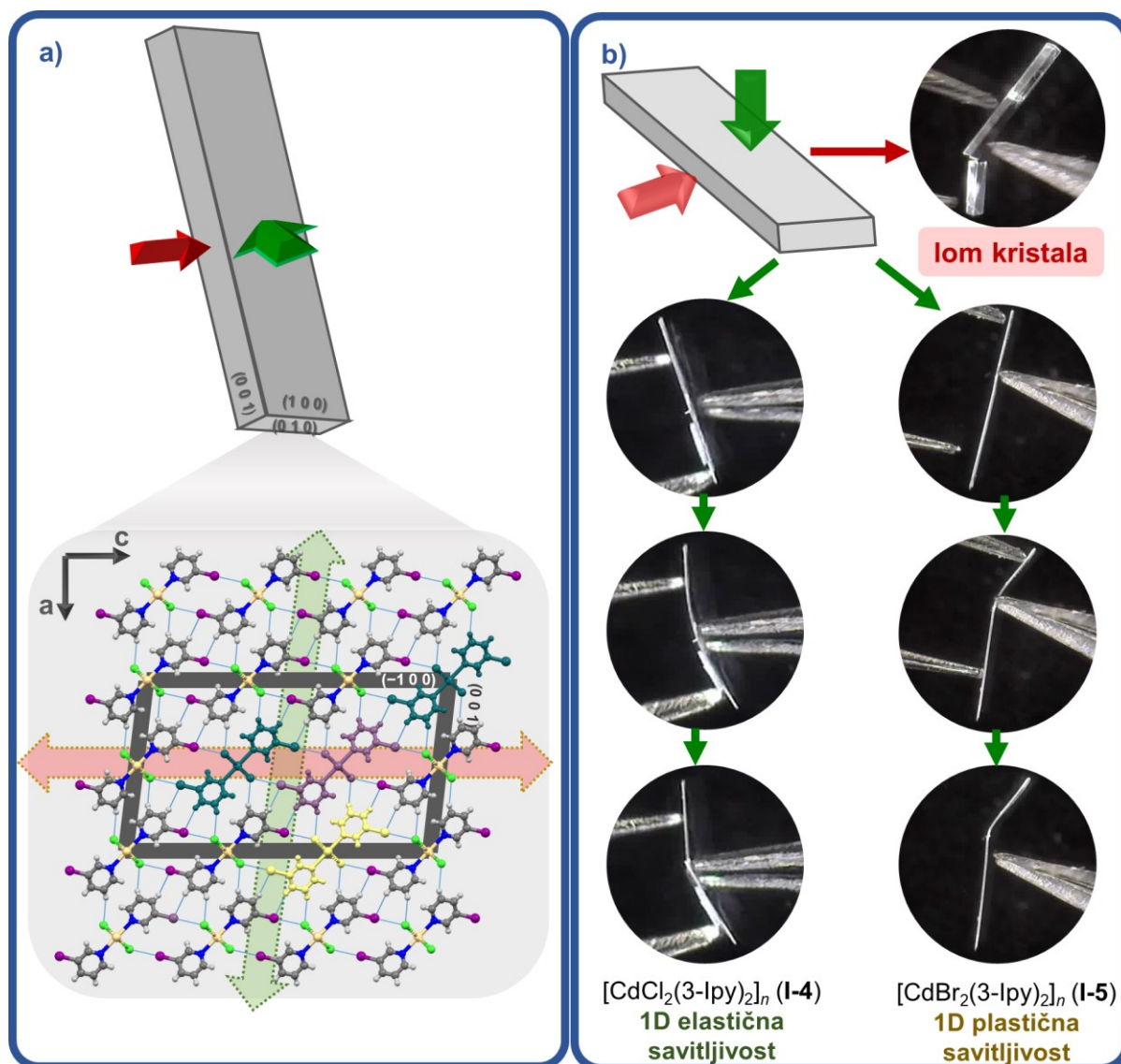
Pritom je uočena jasna razlika u vlačnoj deformaciji među elastično, elastično→plastično i plastično savitljivim kristalima. Elastično savitljivi kristali (**II-2**) pokazivali su elastičan odziv i prilikom provođenja vlačnog eksperimenta, odnosno, primjenom sile primijećeno je blago produljenje, a prestankom primjene sile vratili su se u izvorni, ravni, neproduljeni oblik. Uvođenjem daljnje vlačne deformacije, kristal relativno brzo pukne, a mjesto loma nalikuje mjestu loma tipičnog krutog kristala, te je duljina kristala očuvana (zbroj duljina dva dijela nastala lomom kristala odgovara duljini početnog kristala). Kristali koji pokazuju prijelaz iz elastične u plastičnu savitljivost, odnosno elastično→plastično savitljivi kristali (**II-1** i **II-3**) pri malim deformacijama pokazuju slično ponašanje kao i kristali elastično savitljivih spojeva. No, uvođenjem daljnje vlačne deformacije, kristali pokazuju plastičan odziv, odnosno, prestankom djelovanja sile ne vrata se u početan, nedeformirani oblik, već ostanu blago plastično deformirani. Uvođenjem daljnje deformacije kristali se slome, te pritom pokazuju krti lom, kao i u prethodnom slučaju, a dva dijela razlomljenog kristala su blago plastično deformirana (blago produljena i savijena u blizini mjesta gdje su kristali ljepilom pričvršćeni za stakalce). Kada se mehanička sila primjenjivala na plastično savitljive kristale (**I-1**, **I-2** i **I-3**), mogla se uočiti jasna razlika, dok su kristali **I-1** i **I-3** pokazivali ponašanje slično elastično→plastično savitljivim kristalima, no s većom mogućnosti vlačne deformacije prije pucanja i uočenom naglašenijom plastičnom deformacijom prije i nakon pucanja, kristali spoja **I-2** pokazali su iznimnu mogućnost vlačne deformacije i tečenja kristalnog materijala, koja je bila naročito naglašena u slučaju kristala većih dimenzija dominantnih kristalnih ploha (odnosno krupnijih kristala). Kristali spoja **I-2** pokazali su kontinuiranu, plastičnu deformaciju prilikom vlačnog naprezanja, uslijed koje je uočeno tečenje kristalnog materijala te kontinuirano stanjivanje kristala sve do potpunog diskontinuiteta kristalnog materijala. Mjesto loma kristala nije nalikovalo krtom lomu, već je bilo moguće uočiti vrlo tanke kristalne niti od kojih su neke bile približno nanometarskih dimenzija (Slika VIc, desno dolje). Takvo ponašanje materijala uobičajeno je za materijale visoke simetrije, odnosno metale, metalne legure, kompozitne materijale i organske krutine sastavljene od molekula približno okruglog oblika (engl. *globular shape*).<sup>XXX, XXXI</sup>

---

[XXX] C. L. Hom, R. M. McMeeking, *Int. J. Plast.* **7** (1991) 255–274.

[XXXI] A. Mondal, B. Bhattacharya, S. Das, S. Bhunia, R. Chowdhury, S. Dey, C. M. Reddy, *Angew. Chem. Int. Ed.* **59** (2020) 10971–10980.



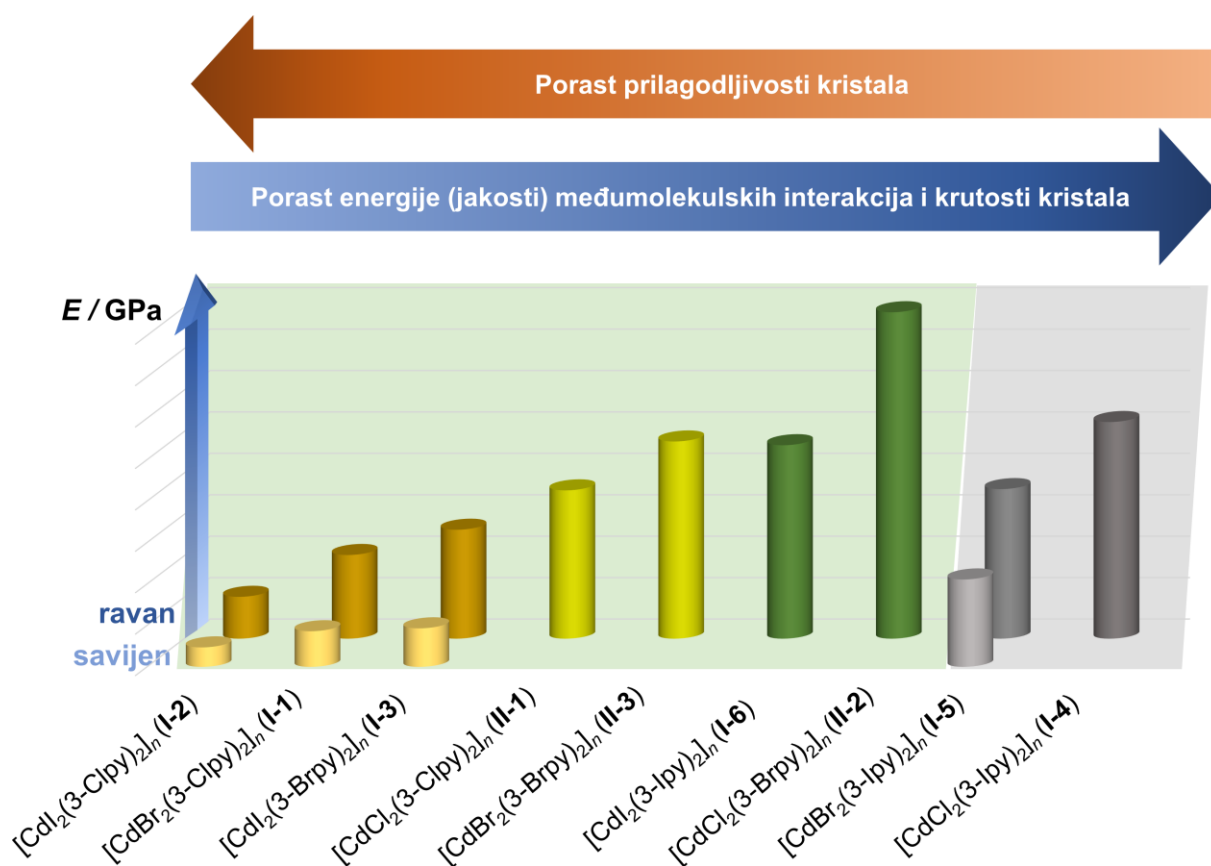


**Slika VII.** a) Shematski prikaz pločastih kristala spojeva **I-4** i **I-5** te kristalno pakiranje prikazano u  $ac$  kristalografskoj ravnini. Potencijalni smjerovi primjene mehaničke sile prikazani su zelenom, odnosno crvenom strelicom. b) Mehanički odziv kristala spojeva **I-4** i **I-5**. Kristali pokazuju kruti odziv ukoliko se mehanička sila primjeni na par ploha manjih dimenzija (smjer primjene mehaničke sile prikazan crvenom strelicom). Kristali pokazuju fleksibilan odziv ukoliko se mehanička sila primjeni na par ploha većih dimenzija (smjer primjene mehaničke sile prikazan zelenom strelicom), elastičan u slučaju spoja **I-4** i plastičan u slučaju spoja **I-5**.

Preostala dva spoja iz serije, iako su kristalizirali u različitim prostornim grupama (**I-4**:  $C2/c$ , **I-5**:  $P\bar{1}$ ) imali su vrlo slično uređenje građevnih jedinki u kristalnom pakiranju, a priređeni kristali su bili vrlo izdužene pločaste morfologije, tj. karakterizirani kristalnim plohama

različitih dimenzija koje se pružaju paralelno s izduženjem kristala (Slika VIIa). Kristali oba spoja dali su jednodimenzijski mehanički odziv – 1D fleksibilnost, odnosno pokazali su mehaničku fleksibilnost samo uslijed primjene sile na par ploha većih dimenzija, dok su primjenom mehaničke sile na par manjih ploha pokazali tipičan kruti odziv. Kristali **I-4** pokazali su blagi elastični odgovor, odnosno 1D elastičnost (Slika VIIb, lijevo), dok su kristali **I-5** bili plastično savitljivi također samo u jednoj dimenziji, to jest pokazali su 1D plastičnost (Slika VIIb, desno).

Daljnja mehanička karakterizacija uključivala je određivanje vrijednosti lokalnog Youngovog modula izvornih, nedeformiranih i plastično savijenih kristala pomoću mikroskopije atomskih sila (AFM, engl. *Atomic force microscopy*).



**Slika VIII.** Youngov modul ( $E$ ) nedeformiranih i plastično deformiranih kristala (određen u točki maksimalne savijenosti kristala) koordinacijskih polimera kadmijevih(II) halogenida s halogenpiridinskim ligandima.

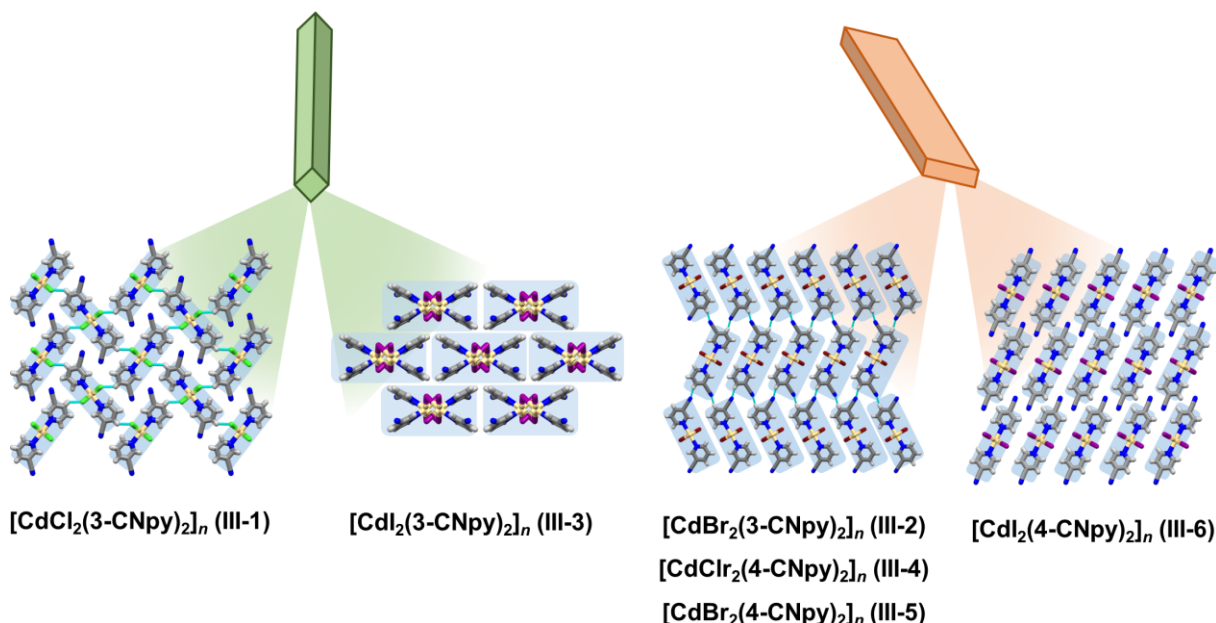
Usporedbom vrijednosti Youngovih modula elastičnosti, uočeno je da kristali koji su se pokazali najprilagodljivijima na primjenu vanjske mehaničke sile (plastično savitljivi kristali, **I-1**, **I-2**, **I-3** i **I-4**), imaju najnižu vrijednost Youngovog modula. S povećanjem krutosti kristala, povećava se i vrijednost Youngovog modula, tako da su najmanje savitljivi kristali (blago elastično savitljivi, **II-2** i **I-6**) oni s najvećom vrijednošću Youngovog modula. Nadalje, utvrđeno je da plastično savijanje uzrokuje omekšavanje kristala na savijenom dijelu, jer je dobivena vrijednost Youngovog modula niža od vrijednosti modula izvornog, nedeformiranog kristala (Slika VIII).

DFT (engl. *density functional theory*) računalne metode, zajedno s detaljnom strukturnom analizom, otkrile su područja međumolekulskih interakcija, vodikovih i halogenskih veza, paralelnih s plohama savijanja, koje su najvjerojatnije odgovorne za pojedini mehanički odziv kristala. Uočena je jasna korelacija energije interakcija, savijanja i krutosti (Slika VIII). Povećanje jakosti međumolekulskih interakcija uzrokuje smanjenje mogućnosti prilagodljivosti kristala na mehaničku silu, odnosno povećanje krutosti kristala, što se posljedično odražava u povećanju vrijednosti Youngovog modula. S druge strane, energija međumolekulskih interakcija u kristalima plastično savitljivih spojeva znatno je manja, čime je omogućeno klizanje susjednih domena uslijed primjene mehaničke sile. Mehanizam plastičnog savijanja kristala klizanjem domena, također je potvrđen i jasno vidljivim raslojavanjem kristala u točki maksimalne savijenosti plastično savijenog kristala, a raslojavanje kristala bilo je vidljivo oslikavanjem površine mikroskopom atomskih sila.

Kako bi se dodatno proširio skup podataka za korelaciju struktura–svojstvo, uvedena je modifikacija na ligandu zamjenom halogenog atoma cijano- skupinom. Uvođenje cijano-liganda, 3-cijanopiridina, odnosno 4-cijanopiridina, u strukturu jednodimenzijskih koordinacijskih polimera pružilo je raznolik skup podataka, odnosno kristalne produkte različitih molekulskih struktura, uređenja građevnih jedinki u kristalnom pakiranju, morfologija i konačno mehaničkih odgovora kristala.

Od šest pripremljenih kristalnih spojeva:  $[\text{CdCl}_2(3\text{-CNpy})_2]_n$  (**III-1**),  $[\text{CdBr}_2(3\text{-CNpy})_2]_n$  (**III-2**),  $[\text{CdI}_2(3\text{-CNpy})_2]_n$  (**III-3**),  $[\text{CdCl}_2(4\text{-CNpy})_2]_n$  (**III-4**),  $[\text{CdBr}_2(4\text{-CNpy})_2]_n$  (**III-5**),  $[\text{CdI}_2(4\text{-CNpy})_2]_n$  (**III-6**), tri su bila gotovo identičnog uređenja građevnih jedinki u kristalnom pakiranju (**III-2**, **III-4** i **III-5**), dok su preostala tri imala potpuno različito kristalno uređenje (Slika IX). Osim toga, uočene su dvije vrste igličastih morfologija, iglice s jednako razvijenim dominantnim plohama kristala i one s izrazito različitim dimenzijama kristalnih ploha koje se

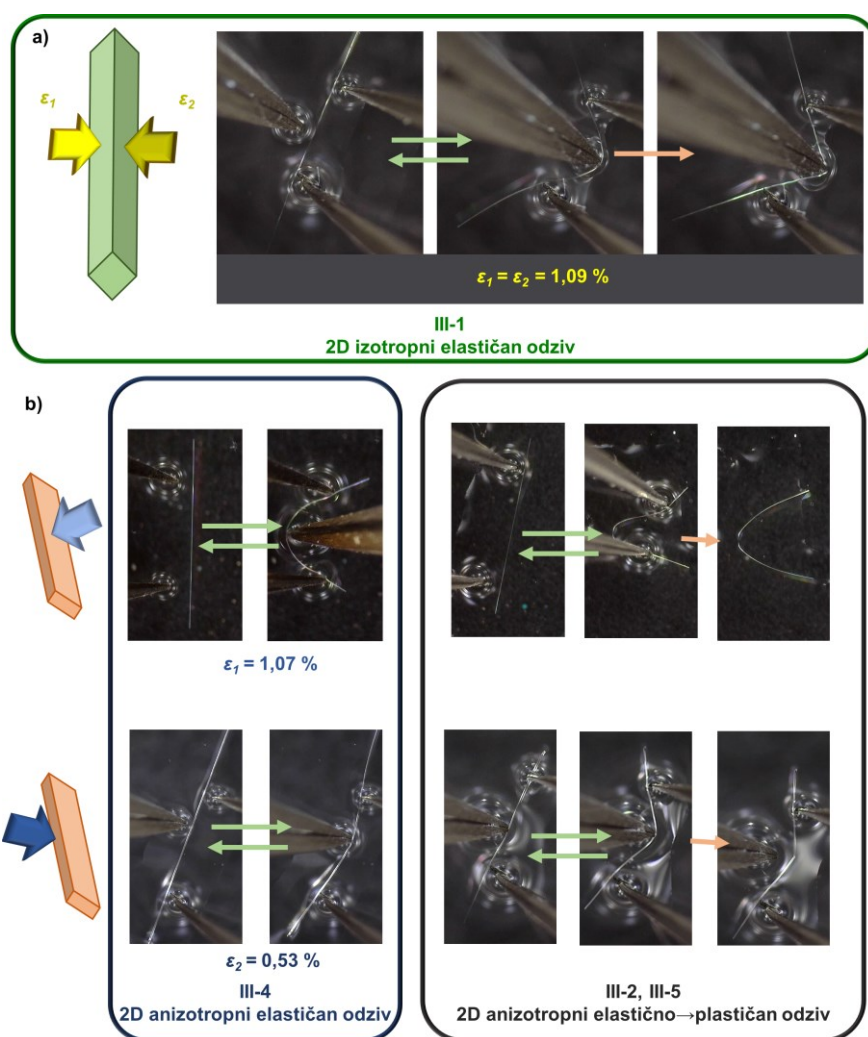
pružaju paralelno s produljenjem samog kristala, tj. morfologija nalik na vrlo izduženu pločicu, pri čemu je ta morfologija dominantno opažena među kristalima priređenih spojeva.



**Slika IX.** Morfologija kristala i kristalna pakiranja jednodimenzijskih koordinacijskih polimera kadmijevih(II) halogenida s cijanopiridinskim ligandima.

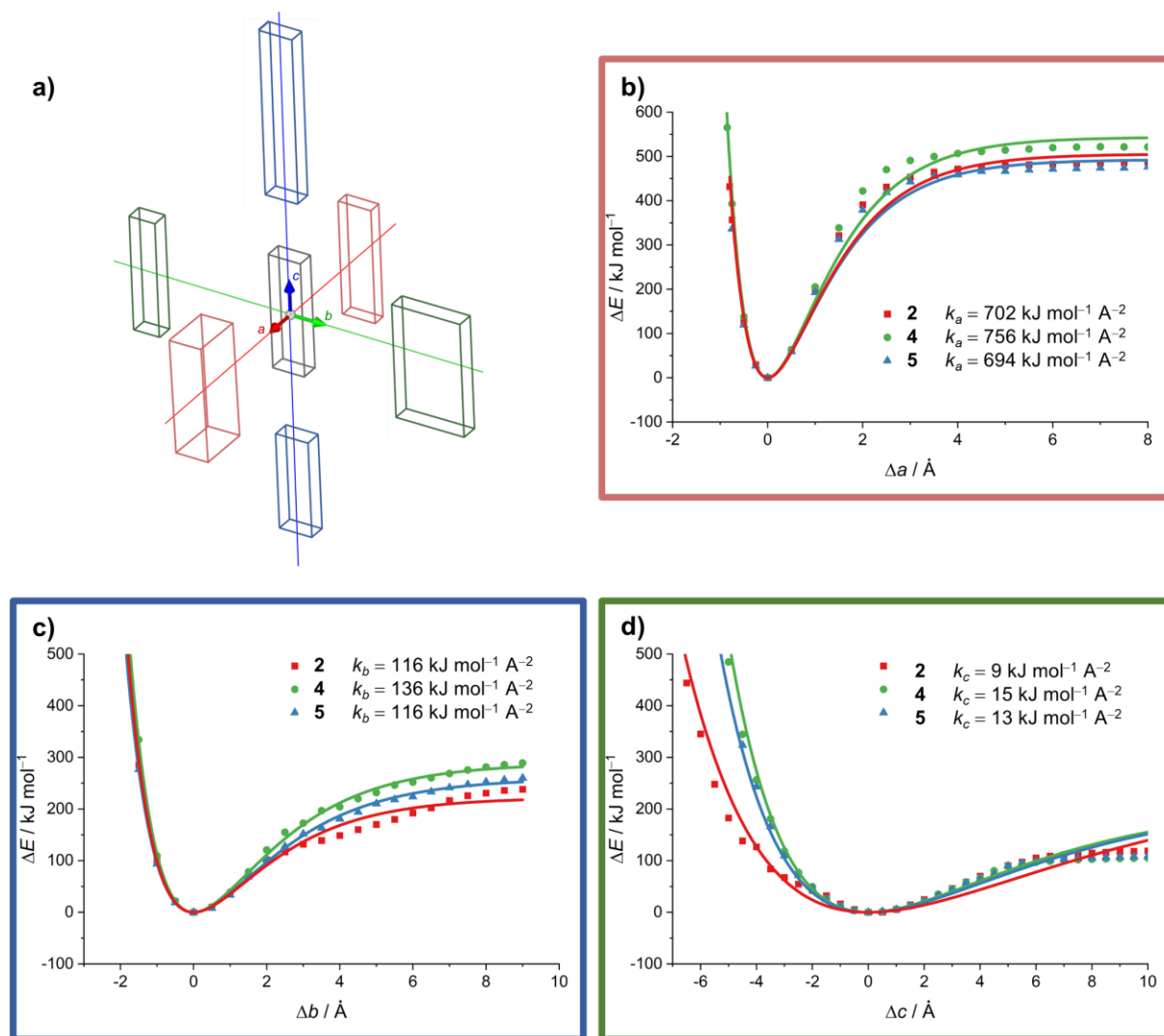
Kristali pripremljenih spojeva pokazali su različite odgovore na vanjski mehanički podražaj. Kristali jodidnih spojeva, **III-3** i **III-6** ponašali su se kao tipični krhki kristali, odnosno lomili su se prilikom primjene i najslabije mehaničke sile, bez obzira na koji par kristalnih ploha je sila bila primijenjena. Kristali **III-1** vrlo su sličnog kristalnog pakiranja i pokazuju sličan 2D elastičan odziv prethodno opisanim elastično savitljivim kristalnim koordinacijskim polimerima kadmijevih(II) halogenida s halogenpirazinskim ligandima.<sup>xviii</sup> Kristali **III-1** dali su elastičan odziv jednakog stupnja ( $\epsilon = 1,1 \%$ ) neovisno o paru ploha na koje je primijenjena mehanička sila, te je njegov odziv klasificiran kao 2D izotropan elastičan odziv (Slika Xa). S druge strane, kristali preostala tri spoja također su pokazala 2D odziv, međutim, stupanj fleksibilnog odziva razlikovao se ovisno o smjeru primjene sile, pa su ti odgovori klasificirani kao 2D anizotropni. Kristale kloridnog spoja (**III-4**) bilo je moguće jače saviti ukoliko se mehanička sila primjenjivala na plohe većih dimenzija ( $\epsilon = 1,1 \%$ ), nego na plohe manjih dimenzija ( $\epsilon = 0,53 \%$ ), te je stoga odziv tih kristala nazvan 2D anizotropan elastičan (Slika Xb, lijevo). Kristali bromidnih analoga (**III-2** i **III-5**) pokazali su međusobno slično ponašanje

uslijed primjene mehaničke sile. Pri vrlo malim deformacijama, ti kristali dali su elastičan odziv, dok su uvođenjem daljnje deformacije postali plastično deformirani, a nakon toga je došlo i do loma kristala, stoga je njihov odziv klasificiran kao elastičan→plastičnom (Slika Xb). No, uočeno je da se kristali **III-2** i **III-5** mogu jače saviti (prije nego što se slome) ukoliko se mehanička sila primjenjuje na plohe većih dimenzija, u odnosu na slučaj kad se mehanička sila primjenjuje na plohe manjih dimenzija, odnosno uočena je anizotropija u mehaničkom odzivu. Stoga su kristali spojeva **III-2** i **III-5** klasificirani kao 2D anizotropno elastično→plastično savitljivi (Slika Xb, desno).



**Slika X.** a) 2D izotropan elastičan odziv kristala spoja **III-1** sa stupnjem savitljivosti 1,09 %. b) Anizotropija mehaničkih odziva kristala spojeva **III-2**, **III-4** i **III-5**. Kristali spoja **III-4** daju različit stupanj elastičnog odziva ovisno o plohi na koju se mehanička sila primjenjuje (lijevo), odnosno 2D anizotropan elastičan odziv, dok kristali spojeva **III-2** i **III-5** pokazuju 2D anizotropan elastično→plastičan odziv (desno).

Kako bi se produbilo razumijevanje opaženih mehaničkih odziva, posebice ovisnost mehaničkog odziva o smjeru primjene mehaničke sile, provedene su računalne studije. Provedeni su izračuni energija interakcija, te su dodatno izračunate potencijalne energije za deformacije (komprimiranje i širenje) jediničnih ćelija duž smjerova kristalografskih osi iz čega su izračunate pripadajuće konstante sile,  $k_a$ ,  $k_b$  i  $k_c$  (Slika XI). Pritom je uočena korelacija između vrijednosti konstanta sile i opaženih mehaničkih odziva.



**Slika XI.** a) Shematski prikaz deformacija jedinične ćelije komprimiranjem i širenjem duž kristalografskih osi  $a$ ,  $b$  i  $c$ . Potencijalne energije za deformacije duž kristalografske osi b)  $a$ , c)  $b$  i d)  $c$ , te Morseove krivulje i izračunate pripadajuće konstante sile  $k_a$ ,  $k_b$  i  $k_c$  za spojeve **III-2**, **III-4** i **III-5**.



Očekivano, konstante sile najveće su u smjeru kristalografske osi  $a$  koja odgovara smjeru propagacije polimernog lanca, odnosno deformacija kristalografske osi  $a$  odgovara deformaciji kovalentnih veza. S druge strane, najmanja vrijednost konstante sile dobivena je u smjeru kristalografske osi  $c$ . U tom smjeru, koji odgovara smjeru primjene mehaničke sile na plohe većih dimenzija utvrđeno je da su sva tri kristala mehanički najprilagodljivija. Time se može pretpostaviti da su međumolekulske interakcije u tom smjeru najslabije, te omogućuju iznimnu prilagodljivost kristala. Nadalje, vrijednosti konstanta sile za deformaciju jedinične ćelije u smjerovima  $b$  i  $c$  su veće za elastično savitljivi kristal, nego za elastično→plastično savitljive kristale, što ukazuje da su elastično savitljivi kristali više skloni oduprijeti se klizanju slojeva jednih u odnosu na druge.

Mikrodifrakcijski eksperimenti na savijenom kristalu (**III-1**), na području maksimalne savijenosti kristala, pokazali su da dolazi do blagog širenja difrakcijskih maksimuma u usporedbi s ravnim kristalom. Nadalje, uočeno je da dolazi do povećanja vrijednosti parametra jedinične ćelije  $a$  na vanjskom luku te smanjenja na unutarnjem luku savijenog kristala. S obzirom da se smjer kristalografske osi  $a$  podudara sa smjerom u kojem se prostire jednodimenzijski polimerni lanac, rezultati sugeriraju da na vanjskom luku savijenog kristala dolazi do rastezanja, a na unutarnjem do sabijanja jednodimenzijskog polimernog lanca.

## Zaključci

Rezultati provedenog istraživanja pokazuju da uvođenje malih strukturnih promjena na molekulskoj razini ima značajan utjecaj na supramolekulsko uređenje, morfologiju kristala i naposljetku, na mehanički odgovor kristala. Uočeno je da se finim ugađanjem jakosti i usmjerenosti međumolekulskih interakcija na skupu spojeva vrlo slične strukture može kontrolirati ne samo stupanj, već i vrsta mehaničkog odziva. Pokazalo se da kristali mogu pokazati cijeli spektar mehaničke savitljivosti, od čisto elastične, elastične→plastične, do varijabilne plastičnosti, pa čak i iznenađujuće vlačne deformacije i „tečenje“ kristalne tvari. DFT računalne studije, zajedno s detaljnim strukturnim istraživanjem, omogućile su da se ustanovi koje su "najslabije karike" u kristalnom pakiranju, tj. međumolekulske interakcije, pretežno vodikove i halogenske veze, koje su najvjerojatnije odgovorne za ostvarivanje specifičnih mehaničkih odgovora kristala.

Također, uočena je jasna korelacija energije interakcija, savijanja i krutosti. Povećanje jakosti međumolekulskih interakcija u kristalnom pakiranju dovodi do smanjenja

prilagodljivosti kristala na primjenu mehaničke sile, odnosno povećanja krutosti, što se očituje u većim vrijednostima Youngovog modula elastičnosti. S druge strane, jakost međumolekulskih interakcija, u spojevima koji se plastično savijaju znatno je niža, stoga dopušta klizanje susjednih domena jedne preko druge nakon primjene mehaničke sile. Mehanizam plastičnog savijanja klizanjem domena također je potvrđen jasno vidljivom raslojavanjem kristala na savijenom dijelu plastično deformiranog kristala.

Nadalje, promatrana su dva tipa mehaničke savitljivosti, jednodimenzijska i dvodimenzijska savitljivost. Međutim, primijećeno je da isti kristal može dati različite stupnjeve mehaničkog odgovora ovisno o smjeru primjene sile, tj. dvodimenzijski savitljivi kristali mogu pokazati različite stupnjeve fleksibilnosti ovisno o smjeru primjene, odnosno paru dominantnih kristalnih ploha na koje se mehanička sila primjenjuje. Takvi kristali su stoga klasificirani kao 2D anizotropno fleksibilni, dok su oni koji daju isti stupanj i vrstu mehaničkog odgovora neovisno o paru kristalnih ploha na koje se mehanička sila primjenjuje nazvani 2D izotropno fleksibilni.

Imajući sve ovo na umu, jasno je da se u velikom broju strukturnih čimbenika koji omogućuju kristalima metalno-organskih spojeva da daju fleksibilan odziv, međumolekulske interakcije mogu prepoznati kao jedan od ključnih parametara čijim preciznim ugađanjem je moguće postići željeni, specifični mehanički odgovor.